The Design and Synthesis of Novel Heterocycles as Potential 5-HT Receptor Ligands

Grant Wishart

A Thesis submitted in partial fulfilment of the requirements of the University of Abertay Dundee for the degree of Doctor of Philosophy

The research programme was carried out in collaboration with Glaxo-Wellcome

January 1997

I certify that this thesis is the true and accurate version of the thesis approved by the examiners.

Signed .. [redacted] ..... Date ..18-3-97..

Director of Studies

DECLARATION

I hereby declare that the work presented in this thesis was carried out by me at the University of Abertay, Dundee and at Glaxo-Wellcome, Langley Court, Beckenham except where due acknowledgement is made, and has not been submitted by me for any other degree.

Signed .....[redacted]

Date .....23/1/97.....

CONTENTS

ACKNOWLEDGEMENTS

The work undertaken in this thesis was carried out in the chemistry laboratories of the School of Molecular and Life Sciences, at the University of Abertay Dundee and Glaxo-Wellcome, Langley Court, Beckenham. I thank the Research Committee of the University for the award of a Research Studentship and Glaxo-Wellcome for additional financial and scientific support.

Thanks go to Dr Neil Ringan for molecular modelling help and to the technical staff at the University of Abertay Dundee, especially Mr Stuart Nicoll, for all their help. I would also like to thank the staff at the Media Centre of the University for help in printing the molecular modelling figures.

Thanks go to all formerly of Lab No 10 of Medicinal Chemistry at the former Glaxo-Wellcome site at Beckenham. In particular Dr David Selwood, Mr Kam Jandu and to Sue Shaw for helping to make my time at Beckenham so enjoyable.

I would also like to thank those at the University of Dundee for NMR services and thanks to Dr Rob West at Glaxo-Wellcome, Stevenage for mass spectra and microanalysis.

At the University of Abertay I would also like to thank Mr Keith Sturrock for help in the laboratory and special thanks to my supervisor Dr David Bremner.

Finally I would like to thank my girlfriend Louise and son Rieve for putting up with all the late nights I have spent working on this thesis.

ABSTRACT

The seven transmembrane α-helices of the human 5-HT_{1A}, 5-$HT_{1D\alpha}$ and 5-$HT_{1D\beta}$ receptors have been modelled using the 3-dimensional coordinates of the seven transmembrane α-helices of the bacterial protein bacteriorhodopsin as a template. The probable 5-HT binding site was identified between helices 3, 4, 5 and 6. Interactions between the natural ligand 5-HT (A) and the receptor models are described in detail and the agonist binding site is further validated by the docking of four known 5-HT receptor ligands. The models are able to account qualitatively for the receptor binding affinities of the studied ligands.

Small molecule similarity studies suggest that a thieno[2,3-b]pyridine analog (B) of 5-HT could possibly act as a bio-isostere for 5-HT. This was further corroborated when (B) was docked into the 5-HT receptor models and was found to be accommodated easily in the 5-HT binding site participating in the same interactions as observed for 5-HT.

Thieno[2,3-b]pyridines similar to (B) were thus identified as synthetic target compounds. Furthermore, the models were used to provide suggestions for the design of novel, more selective, 5-HT receptor agonists.

The thieno[2,3-b]pyridine ester (C; R=CO_2Et) was reduced to the hydroxymethyl derivative (C; R=CH_2OH) but the methylthio group could not be successfully removed in the presence of the thiophene ring.

Using a different approach the thieno[2,3-b]pyridine (D; R=CO_2Me, X=CN) was synthesised as a model compound and converted through to the *t*-BOC protected amines (D, R=$NHCO_2C(CH_3)_3$, X=CN) and (D, R=$NHCO_2C(CH_3)_3$, X=$CONH_2$). The same reactions were applied to ethyl-3-(5-cyanothieno[2,3-b]

pyridin-3-yl)propanoate (E, R=CO_2Et, X=CN) but this unfortunately could not be converted through to the required *t*-BOC protected 5-HT analog (E, R=$NHCO_2C(CH_3)_3$, X=CN).

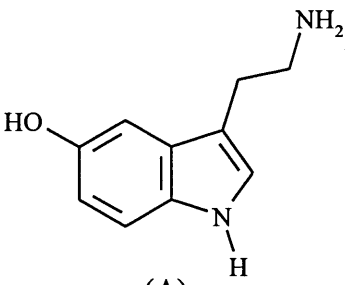

(A)

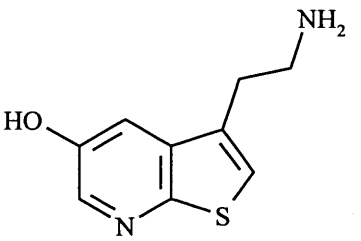

(B)

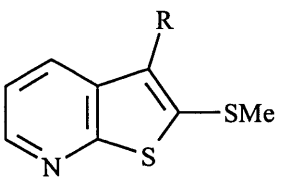

(C)

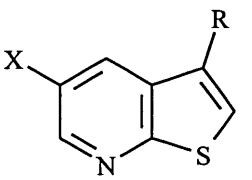

(D)

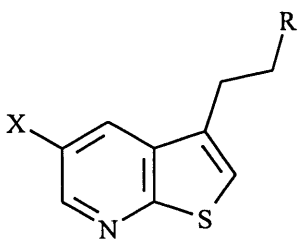

(E)

FOREWORD

Bracketed arabic numerals in the text refer to the diagrams of the molecular formulae. Arabic superscripts indicate references. The following abbreviations have been used in the text.

Å	Angstrom unit 10^{-10} m
Ac	Acetyl group CH_3CO
ADP	Adenosine diphosphate
Ar	Aryl group
t-BOC	*t*-Butoxycarbonyl group $CO_2C(CH_3)_3$
nBu	*n*-Butyl group $CH_2CH_2CH_2CH_3$
tBu	*t*-Butyl group $C(CH_3)_3$
CNS	Central nervous system
m-CPBA	*m*-Chloroperoxybenzoic acid
m-CPP	*m*-Chlorophenylpiperazine
5-CT	5-Carboxamidotryptamine
δ	Parts per million
DDQ	2,3-Dichloro-5,6-dicyano-1,4-benzoquinone
DMF	*N,N*-Dimethylformamide
DMSO	Dimethylsulfoxide
(R)-(-)DOB	(R)-(-)-1-(4-Bromo-2,5-dimethoxyphenyl)-2-aminopropane
DPPA	Diphenylphosphorylazide
E^+	Electrophile
Et	Ethyl group CH_2CH_3
fs	femtosecond 10^{-15} s
GDP	Guanosine 5'-diphosphate
GPCR	G-protein coupled receptor

G-protein	Guanine-nucleotide binding protein
GTP	Guanosine 5'-triphosphate
h	hour
[H]	Reduction
HMPA	Hexamethylphosphoric triamide
5-HT	5-Hydroxytryptamine (Serotonin)
ir	Infrared
K	degrees Kelvin
kcal	kilocalorie 4.184×10^3 Joules
K_i	Affinity constant
LC-MS	Liquid chromatography mass spectrum
(+)LSD	(+)-Lysergic acid diethylamide
Me	Methyl group CH_3
Mes	2,4,6-Trimethylbenzene
mmol	millimole 10^{-3} mol
MMPP	Magnesium monoperoxyphthalate
mp	melting point
mRNA	Messenger ribonucleic acid
MS	Mass spectrum
NADH	Nicotinamide adenine dinucleotide coenzyme I
nM	nanomolar 10^{-9} moldm^{-3}
nmr	Nuclear magnetic resonance
[O]	Oxidation
8-OH-DPAT	8-Hydroxy-2-(di-*n*-propylamino)tetralin
5-OH-TMT	5-Hydroxy-*N,N,N*-trimethyltryptamine
Ph	Phenyl group C_6H_5
PPA	Polyphosphoric acid
ps	picosecond 10^{-12} s
PTC	Phase transfer catalyst

R_f	Retention factor
RMS	Root mean square
THF	Tetrahydrofuran
tlc	Thin layer chromatography
TMEDA	*N,N,N,N*-Tetramethylethylenediamine

1 INTRODUCTION

1.1 5-HYDROXYTRYPTAMINE AND MOLECULAR MODELLING

1.1.1 Isolation of 5-hydroxytryptamine

It has been forty-seven years since Maurice Rapport crystallised the vasoconstrictor serotonin from blood serum[1] and subsequently identified this substance as 5-hydroxytryptamine[2] (5-HT, 1). Around the same time in Italy, Vittorio Erspamer and colleagues were interested in a substance known as enteramine which was present in the enterochromaffin cells of the gastrointestinal tract[3,4]. Isolation of enteramine and characterisation[5] showed it to be identical to 5-hydroxytryptamine which had been synthesised in 1951[6]. Serotonin was then discovered to be present within the mammalian central nervous system (CNS)[7] and was postulated to be an invertebrate neurohormone[8].

In the years since the mid 1950's serotonin has been studied quite extensively (over 1000 research papers on 5-HT have been published each year in the 1990's). Serotonin is now known to be an important neurotransmitter in the CNS and is present in high concentrations in the blood platelets and the enterochromaffin cells of the gastrointestinal tract. 5-HT mediates its physiological effects from the interaction with an increasing number of 5-HT receptors and has been implicated in conditions such as obesity[9], migraine[10], anxiety[11], schizophrenia[12], sleep[13] and several other processes.

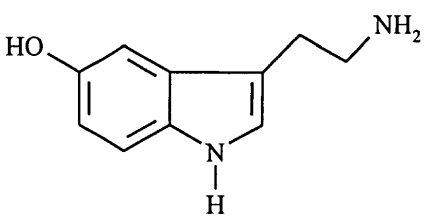

(1)

1.1.2 5-HT Receptors

Gaddum and Picarelli[14], first suggested in 1957 that there may be multiple 5-HT receptors from a study of antagonists upon a guinea pig ileum preparation. It was found that 5-HT caused contraction of the ileum by two different mechanisms, one of which was blocked by dibenzyline (D-receptors) and the other by morphine (M-receptors). This work paved the way for others and in 1979 two distinct 5-HT recognition sites were identified[15] using radioligand binding. Since these early findings numerous other 5-HT binding sites have been identified and with the development of molecular biology many 5-HT receptors have been cloned and amino acid sequences deduced. Pharmacological characterisation has allowed matching of these cloned receptors to *in vivo* 5-HT binding sites. Some excellent reviews of the molecular biology of the 5-HT receptors[16-21] and of the pharmacology of 5-HT receptors[22-25] have been published. This introduction does not try to emulate these papers but attempts to give the reader an overview of the 5-HT receptors.

The 5-HT receptors are presently classified according to Hoyer *et al.*[26] where the receptors have been divided into subfamilies dependant upon operational, transductional and structural characteristics. At present there are at least seven subtypes of 5-HT receptors, 5-HT_1 to 5-HT_7 (Table 1), some of these are already known to be heterogeneous and it is suspected that others may also be.

The 5-HT_1 family exists as at least 5 subtypes 5-HT_{1A}, 5-HT_{1B}, 5-HT_{1D}, 5-ht_{1E} and 5-ht_{1F} receptors. Lower case notation is used to denote recombinant receptors with no decisive functional data. All these receptors belong to the superfamily of receptors that interact with their secondary messenger through the activation of a guanine-nucleotide binding protein and are thus known as

G-protein coupled receptors (GPCRs). The 5-HT_1 subfamily all inhibit the enzyme adenylyl cylase (the secondary messenger) and it may be possible that some of these receptors can also interact with other secondary messengers. Genes encoding two 5-HT_{1D} receptor subtypes have been cloned and these have been designated the 5-$HT_{1D\alpha}$ and 5-$HT_{1D\beta}$ receptors[27]. The 5-$HT_{1D\beta}$ receptor is considered to be the non-rodent species homologue of the 5-HT_{1B} receptor[28] and is sometimes also referred to as a 5-HT_{1B} receptor. The receptor nomenclature of the 5-HT_{1D} receptors is known to be far from ideal[29] and a more general nomenclature has been proposed recently[30].

The 5-HT_2 receptor family is also heterogeneous and at present comprises of the 5-HT_{2A}, 5-HT_{2B} and 5-HT_{2C} receptors. All are GPCRs and are coupled preferentially to phospholipase C, hence receptor activation leads to stimulation of phosphatidyl inositol metabolism.

The 5-HT_3 receptor seems to be the odd one out as it does not belong to the GPCR family but is a ligand gated ion channel. Receptor activation leads to the opening of a transmembrane ion channel. Evidence is presently gathering that this subfamily may indeed be heterogeneous.

The 5-HT_4 receptor is positively coupled to adenylyl cylase and structurally belongs to the GPCRs. 5-ht_{5A} and 5-ht_{5B} receptors are recombinant G-protein coupled receptors with at present no transductional data or functional role hence the lower case notation. The 5-HT_6 receptor which has a similar pharmacology to the 5-HT_1 subtype, is a GPCR but shows poor structural homology to the other 5-HT receptors and is positively coupled to adenylyl cylase. Similarly the 5-HT_7 receptor is a GPCR, is positively coupled to adenylyl cylase but exhibits limited structural homology with other 5-HT subtypes.

There is also a number of 5-HT receptors that have been identified but do not satisfy the criteria for any subtype within the present classification system[26] and are known as "orphan" 5-HT receptors.

Receptor Name	Previous Name	Family	Secondary Messenger	Sequence Information
5-HT_{1A}		GPCR	- AC	421 aa human
5-HT_{1B}		GPCR	- AC	386 aa rat
5-HT_{1D}		GPCR	- AC	377 aa human 5-$HT_{1D\alpha}$ 390 aa human 5-$HT_{1D\beta}$
5-ht_{1E}		GPCR	- AC	365 aa human
5-ht_{1F}	5-$HT_{1E\beta}$, 5-HT_6	GPCR	- AC	366 aa human
5-HT_{2A}	D, 5-HT_2	GPCR	+ PI	471 aa human
5-HT_{2B}	5-HT_{2F}	GPCR	+ PI	479 aa rat
5-HT_{2C}	5-HT_{1C}	GPCR	+ PI	458 aa human
5-HT_3	M	Ligand gated ion channel		487 aa mouse ion channel unit
5-HT_4		GPCR	+ AC	Splice variants rat 407aa 5-HT_{4L} rat 397aa 5-HT_{4S}
5-ht_{5A}	5-$HT_{5\alpha}$	GPCR	Unknown	357 aa mouse, rat
5-ht_{5B}	5-$HT_{5\beta}$	GPCR	Unknown	370 aa mouse 371 aa rat
5-HT_6		GPCR	+ AC	437 aa rat
5-HT_7		GPCR	+ AC	448 aa mouse 446 aa g-pig

- AC negatively coupled to adenylyl cylase, + AC positively coupled to adenylyl cylase, + PI positively coupled to phospholipase C.

Table 1 5-HT Receptor Subtypes

Many compounds have been evaluated for biological activity at the 5-HT receptors and many high affinity agonists and antagonists are known. Due to the great wealth of information on 5-HT receptor ligands the subject is not reviewed here but the reader is directed to the reviews of 5-HT receptors[16-26]. In the 1990's there has been a massive increase in 5-HT receptor research and this has been attributed to the increasing number of receptors and hence possible drug targets. One of the main areas of 5-HT related research has been that of migraine headache where many of the major pharmaceutical companies have been competing to develop compounds with antimigraine efficacy.

1.1.3 5-HT and migraine

Migraine headache affects many people causing considerable misery and disruption to everyday life for sufferers. 5-HT has long been associated with the pathophysiology of migraine headache and in 1960 it was discovered[31] that intravenous injection of 5-HT relieved migraine. Furthermore, 5-HT metabolites have been identified in the urine of patients during a migraine attack[32]. The use of 5-HT to treat migraine is unfortunately littered by unwanted side effects such as nausea and faintness[33] however a number of other 5-HT related drugs have been used in the fight against migraine.

Prophylactic agents that are available which reduce the frequency and severity of attack include pizotifen, cyproheptadine and methysergide[34] which all show antagonistic activity at the 5-HT_2 receptors. It is conceivable that these drugs may exert their effects centrally[33] possibly via the 5-HT_{2C} receptor since all these compounds show high affinity for this subtype and the 5-HT_{2C} receptor agonist *m*-chlorophenylpiperazine (*m*-CPP) has been found to trigger migraine like headaches in humans[35]. Ergot compounds such as ergotamine (2) and dihydroergotamine (3) which are 5-HT_1 agonists are known to relieve migraine

in 70% of patients and are used as abortive antimigraine therapies[36]. However chronic side effects have been experienced by patients.

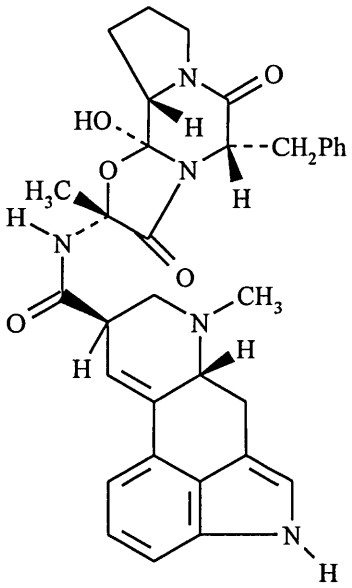

(2)

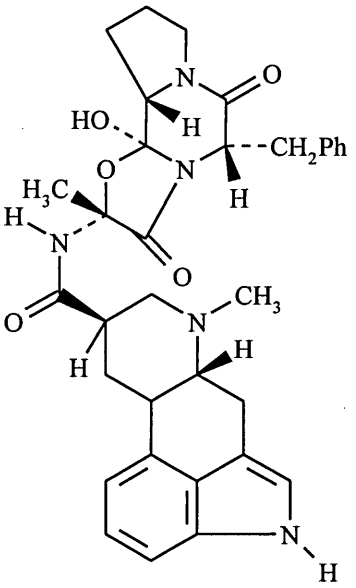

(3)

The discovery of sumatriptan[37,38] (GR43175) (4) which was described as a novel selective agonist at 5-HT_{1LIKE} receptors in dog saphenous vein heralded a major breakthrough in the understanding and treatment of migraine. A review of the discovery of sumatriptan has been published by Oxford[39].

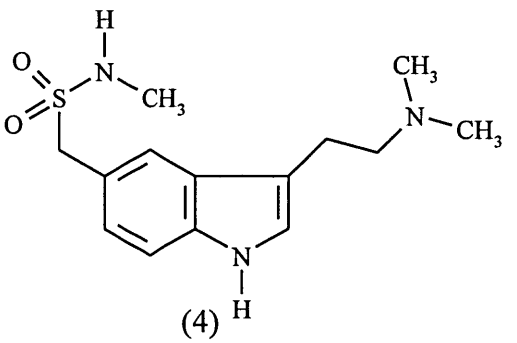

(4)

Sumatriptan was shown to be effective in acute treatment of migraine[40] and was found to bind with high affinity to 5-HT_{1D} sites with a moderate 5-fold selectivity over 5-HT_{1A} sites and was essentially inactive at numerous other

neurotransmitter binding sites[41]. Comparison of the pharmacology of sumatriptan with that of dihydroergotamine showed both compounds shared affinity for 5-HT_{1A} and 5-HT_{1D} sites and suggested that the 5-HT_{1D} receptors may play an important role in migraine relief[42]. This claim was disputed[43] due to the inability of metergoline, a putative 5-HT_1/5-HT_2 antagonist, to block the effects of sumatriptan on the dog saphenous vein. This was resolved when it was found[44] that metergoline acted as a partial agonist at cloned 5-$HT_{1D\beta}$ receptors[45]. This could explain the actions of metergoline on the dog saphenous vein and it was further suggested[44] that sumatriptan may well exert its therapeutic effects by interaction with the 5-$HT_{1D\beta}$ receptor.

The cloning of two subtypes of the 5-HT_{1D} receptor took the debate one step further since sumatriptan showed high binding affinity at both the cloned 5-$HT_{1D\alpha}$ and the 5-$HT_{1D\beta}$ receptors[27]. Therefore a number of questions had to be answered such as, if sumatriptan elicits its pharmacological effects through a 5-HT_{1LIKE} receptor, is there a common receptor pathway and does it correspond to the 5-HT_{1D} receptors, and if so could it be the 5-$HT_{1D\alpha}$ or the 5-$HT_{1D\beta}$ receptor.

Further studies of the potencies of agonists on the canine coronary artery and saphenous vein[46] gave a relative order of potencies that was consistent with a 5-HT_{1D} receptor and confirmed the presence of 5-HT_{1D} mRNA. The authors concluded that the dog saphenous vein contains a 5-HT_{1DLIKE} receptor but this cannot be proved until more selective 5-HT_{1D} agents become available. This may also provide an explanation as to why sumatriptan may cause symptoms related to coronary artery constriction. Just as the site of action of sumatriptan has been debated the mechanism of action has also led to great debate[47,48]. Two mechanisms of action have been proposed, a vascular mechanism and a neurogenic mechanism, both believed to be peripheral since sumatriptan crosses

the blood brain barrier poorly[49,50]. The vascular theory suggests that sumatriptan acts on postjunctional receptors and constricts cerebral arteries which have dilated during migraine. The neurogenic theory proposes that antimigraine drugs could block the release of pro-inflammatory neurotransmitters from trigeminovascular nerve endings within the meninges by the stimulation of presynaptic autoreceptors.

Rebeck *et al.*[51] have demonstrated the presence of 5-$HT_{1D\alpha}$ receptor mRNA in guinea pig trigeminal ganglia and human post-mortem trigeminal ganglia and propose that the development of selective 5-$HT_{1D\alpha}$ agonists may lead to antimigraine therapies with a reduced risk of side effects such as stroke. It has also been shown[52] that in human and bovine cerebral arteries the 5-$HT_{1D\beta}$ receptor gene is present and this receptor may mediate the cerebral vascular action of sumatriptan.

Summarising, two mechanisms have been proposed for the mode of action of sumatriptan each implying the involvement of a different receptor. A vascular mechanism has been postulated, possibly mediated through a 5-$HT_{1D\beta}$ receptor. A neurogenic mechanism has also been postulated, possibly involving the 5-$HT_{1D\alpha}$ receptor. It is not known which mechanism is of primary importance. It may also be possible that these antimigraine drugs may induce their effects through a different receptor (5-HT or otherwise). The whole issue has been twisted a little further by the discovery of 311C90[53] (5), a 5-HT_{1D} agonist which is known to activate trigeminovascular neurons both centrally and peripherally[54]. This has been compared to sumatriptan which is thought to have only peripheral effects and adds the possibility that central activity may be advantageous in the treatment of migraine. An excellent review on the involvement of 5-HT in migraine has recently been published[55].

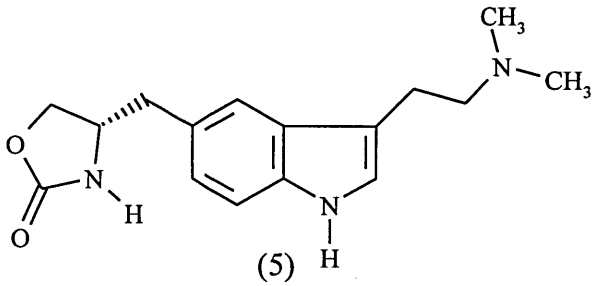

(5)

The potential "blockbuster" status of sumatriptan has prompted many of the major pharmaceutical companies to develop other indole type compounds with antimigraine potential. Merck, Sharp and Dohme have developed L694,247[56,57] (6) and MK-0462[58,59] (7). SmithKline Beecham have been studying conformationally restricted 5-HT_{1D} agonists[60] and Pfizer also have been looking at conformationally restricted compounds[61,62]. Several other laboratories have also been active in studying 5-HT_{1D} receptor agonists[63-68]. It has therefore became apparent that to aid a better global understanding of antimigraine drugs there is a need for more selective ligands.

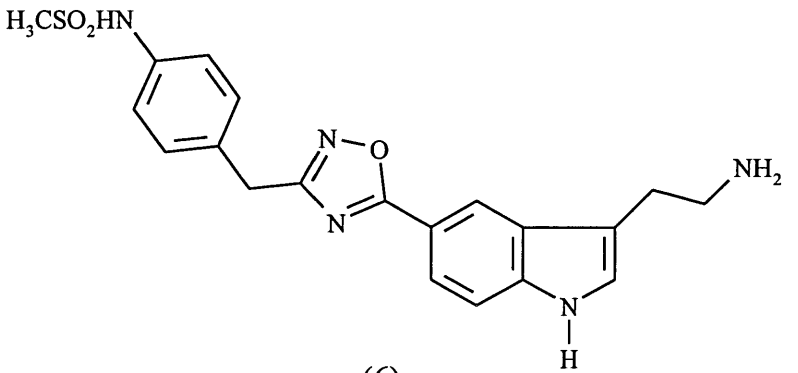

(6)

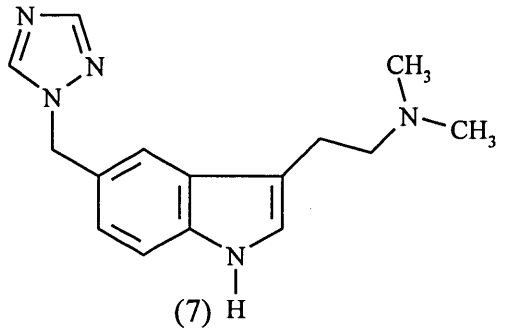

(7)

The use of molecular modelling has played an important part in rational drug design by using receptor mapping and structure affinity type studies. If the binding of agonists to the 5-HT receptors can be rationalised this will prove an invaluable tool in designing selective ligands. This project attempts to construct useful molecular models of the human 5-HT_{1D} receptors. Through a study of the binding site of these receptor models it may be possible to design and subsequently synthesise new heterocyclic ligands to probe the binding site further and possibly improve receptor selectivity. The 5-HT_{1D} receptors and indeed all 5-HT receptors except 5-HT_3 belong to the GPCR superfamily. Therefore it is pertinent to this study to discuss the structure and modelling of GPCRs.

1.1.4 Structure and modelling of GPCRs

1.1.4.1 G-protein coupled receptor activation

The family of receptor proteins that interact with guanine-nucleotide binding proteins (GPCRs) is extremely diverse and covers sensory, small molecule, peptide and glycoprotein hormone receptors. Each of these integral membrane receptors has a common structure of seven putative membrane spanning α-helices (see section 1.1.4.2) and upon agonist activation the receptor interacts with its respective secondary messenger via a heterotrimeric G-protein.

The G-proteins belong to the large family of GTPase proteins and consist of α, β and γ subunits. Upon activation of a GPCR the activated receptor interacts with the GDP bound inactive form of G_α leading to the exchange of GDP for GTP and resulting in the dissociation of G_α from both $G_{\beta\gamma}$ and the receptor. G_α-GTP can then interact with the respective secondary messenger (in some cases $G_{\beta\gamma}$ can also interact with the secondary messenger). The system returns to the inactive state when the bound GTP is hydrolysed back to GDP by the

intrinsic GTPase activity of the G_α subunit. The α, β and γ subunits of the G-protein then reassociate and the system is ready to be activated once again. At present the α, β and γ protein families consist of 18, 5 and 7 distinct multiple subunits respectively[69,70] and the crystal structures of some of these subunits have been elucidated[71-73].

1.1.4.2 Structure of GPCRs

The first GPCR to be studied in any great detail was the visual pigment rhodopsin. Rhodopsin is the photoreceptor membrane protein of rod cells in the vertebrate retina and is made up of a protein structure covalently attached to an 11-cis retinal chromophore. Light activation of the chromophore initiates a cascade of events sending electrical impulses to the brain. Bovine rhodopsin was the first GPCR to be completely sequenced in 1982[74] and this was followed by human rhodopsin in 1984[75]. Analysis of the protein sequences[74,75] showed the presence of seven areas of high hydrophobicity. Biophysical and biochemical experiments have led to the deduction that the receptor contains seven transmembrane regions that were likely to be antiparallel α-helices. This work has been covered in three extensive reviews[76-78] and allowed the proposal of 2-dimensional models for rhodopsin[79].

The availability of a low resolution 3-dimensional structure of the transmembrane protein bacteriorhodopsin[80] allowed the work to be taken one step further. Although bacteriorhodopsin is not a GPCR it does have similarities to rhodopsin in that both consist of seven transmembrane helices and both bind a retinal chromophore to a lysine residue upon putative helix 7. However there is no sequence homology between the two proteins. Findlay and Pappin[77] used the low resolution structure of bacteriorhodopsin in combination with structural predictions[81] and the proposed helix connectivity of Engelman *et al.*[82] to

construct the first, albeit crude, molecular model of the GPCR rhodopsin. The model showed that the likely ligand binding site was based within the transmembrane core region, with acidic residues being possible candidates as counterions for the positively charged Schiff's base attachment between the retinal chromophore and a lysine residue on helix 7.

Around the same time in 1986 the cloning and amino acid sequence of the β_2-adrenergic receptor which binds R-(-)-adrenaline (8) and R-(-)-noradrenaline (9) as the natural agonists was reported[83]. This was the first neurotransmitter GPCR to be sequenced. Analysis of the receptor sequence also predicted that the protein consisted of seven hydrophobic stretches of 20-25 amino acids (the putative seven transmembrane helices) and exhibited significant sequence homology to the rhodopsin sequences[83].

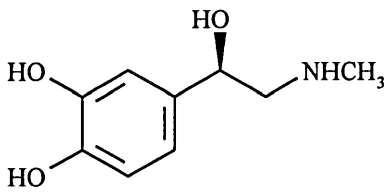

(8)

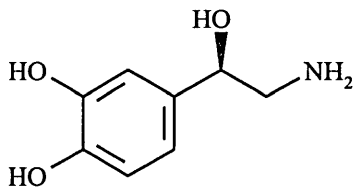

(9)

Many subsequent biochemical experiments took place upon the β-adrenergic receptors. Deletion mutagenesis indicated that the ligand binding site was in the transmembrane area of the receptor[84] and further mutations showed that an aspartate residue on helix 2 had no effect on antagonist binding but reduced agonist binding[85]. Mutation of an aspartate residue of helix 3 showed significantly decreased agonist and antagonist binding and it was thus proposed that this residue may interact with the cationic amine of the natural agonist[85]. It was later found that the aspartate residue of helix 2 is conserved in almost all GPCRs whereas the aspartate of helix 3 is only conserved in all cationic amine neurotransmitter GPCRs. A 2-dimensional model, which was similar to that of

rhodopsin[79], of how the receptor was arranged in the membrane was then proposed[86] and consisted of seven transmembrane antiparallel α-helices with an extracellular N-terminus and cytoplasmic C-terminus. The N-terminus is known to be glycosylated[86,87] and the C-terminal region can be phosphorylated[86].

From a structural viewpoint Dohlman *et al.*[88] studied the similarities of the postulated structures of rhodopsin and the β_2-adrenergic receptor suggesting roles for transmembrane proline residues and that the third intracellular loop may be involved in G-protein coupling. The role of the third intracellular loop in G-protein coupling was confirmed later in 1987 from deletion mutagenesis studies[89].

In 1988 the studies of the β-adrenergic receptors continued and in a review[90] of the work carried out in the previous year it was speculated[90] that a rhodopsin-like structure was increasingly likely to be the case for the β-adrenergic receptors. Further mutagenesis of the aspartates on helices 2 and 3[91] allowed the authors to propose an overlapping but not identical binding site for agonists and antagonists. It was proposed[91] that in the agonist binding site the protonated amine of the ligand interacts with the aspartate of helix 3 and the aromatic moiety lies between helices 3, 4, 5, 6 and 7. The conserved aspartate of helix 2 was thought to play a role in maintaining the agonist bound conformation[91]. Studies of chimeras of the β_1/β_2 adrenergic receptors have revealed that helix 4 participates in ligand specificity and helices 6 and 7 play a role in antagonist selectivity[92].

Work with peptide antibodies convinced Wang and co-workers[93] of the helical model and the authors speculated that this structure may be true for all membrane proteins belonging to the GPCR family. Using mutagenesis and chemical modification it was demonstrated[94] that for the β_2-adrenergic receptor

the *meta*-hydroxyl of catecholamine agonists hydrogen bonds with SER204 of helix 5 and the *para*-hydroxyl similarly hydrogen bonds with SER207 also of helix 5. A topological model of the β_2-adrenergic receptor agonist binding site was then proposed[94] (Figure 1). Evidence was also accumulating for the role of a putative disulfide bond between cysteines on extracellular loops 1 and 2 respectively[95]. This structural work on the adrenergic receptors has been reviewed[96-98] covering the majority of the experiments leading up to the proposed topology of the receptors in greater detail than is presented here. The conclusions of the adrenergic receptor studies has been the acceptance of the general assumption that the GPCRs encode a family of receptors whose membrane structure consists of seven antiparallel α-helices with extracellular N-terminus and cytoplasmic C-terminus. The structure and function of GPCRs in general has been reviewed[99-101].

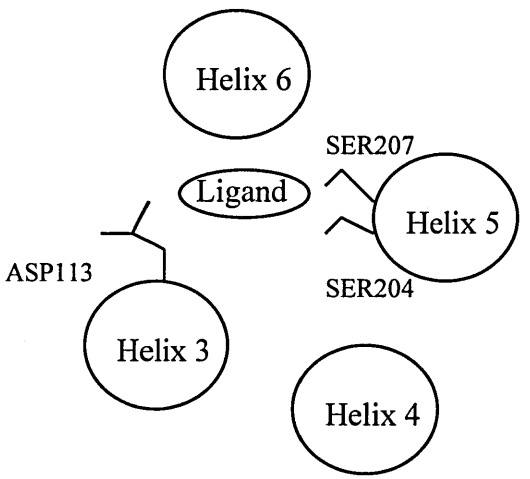

Figure 1 Model of the β_2-adrenergic receptor viewed from outside the cell

During the work on the adrenergic receptors a new GPCR was cloned[102] which had significant sequence homology with the β_2-adrenergic receptor and was later identified as the human 5-HT_{1A} receptor, the first 5-HT receptor to be cloned and sequenced[103].

The amount of published work on the GPCRs since that first bovine rhodopsin sequence[74] has been phenomenal with over 700 (including species variants) GPCR sequences known.

1.1.4.3 Mutation studies of the 5-HT receptors

There is also some limited mutagenesis data available for the 5-HT receptors which has greatly aided the modelling of these receptors. The 5-HT receptors are classed as belonging to the cationic amine neurotransmitter receptors, so called, since at physiological pH the natural agonist is characterised as having a protonated amine moiety and also includes adrenergic, muscarinic, dopaminergic and histamine receptors. This protonated amine group is generally thought to interact with an acidic residue of the receptor and this interaction is believed to be the primary interaction point of 5-HT receptor ligands with the receptors.

As with the β-adrenergic receptors[85,91] two primary agonist binding sites have been proposed, the conserved aspartates of helices 2 and 3. Mutation of these residues to asparagine in the 5-HT_{1A} receptor[104] ASP82-ASN and ASP116-ASN gave a 60-100 fold decrease in affinity for 5-HT and it was suggested that both these residues may take part in agonist binding. Mutations of the same residues of the 5-HT_{2A} receptor[105] ASP120-ASN and ASP155-ASN indicated similar results. The ASP120-ASN mutant showed a decreased and GTP-insensitive binding of agonists. Reduced binding affinity of agonists and antagonists was also observed for the ASP155-ASN mutant, however GTP sensitivity was retained. The results prompted the proposal that the aspartate of helix 3 was required for high affinity binding probably acting as a counterion for the protonated amine moiety and that the aspartate of helix 2 was necessary for allosteric activation of the G-protein.

Helix 5 mutants of the 5-HT_{1A} receptor SER198-ALA and THR199-ALA[104] both exhibited a significant decrease in agonist affinity and for the THR200-ALA mutant the binding of agonists was not even detectable. A mutant of the human 5-HT_{2A} receptor SER242-ALA[106] (which does not correspond to the above serine or threonine residues of the 5-HT_{1A} receptor) was found to alter the pharmacology of the receptor to that of the rat 5-HT_{2A} receptor. The inverse of this mutation has also been studied[107]. Mutation of ALA242-SER of the rat 5-HT_{2A} receptor resulted in a receptor which was similar to the 5-HT_{2A} human receptor.

Mutations of helix 6 have centred around two conserved phenylalanine residues. Mutation of PHE339-LEU and PHE340-LEU in the 5-HT_{2A} receptors have been investigated[108]. The PHE340-LEU mutation abolished the binding of agonists and some ergot derivatives but did not affect the 5-HT antagonist ketanserin (10) whereas the PHE339-LEU mutation only influenced ketanserin binding.

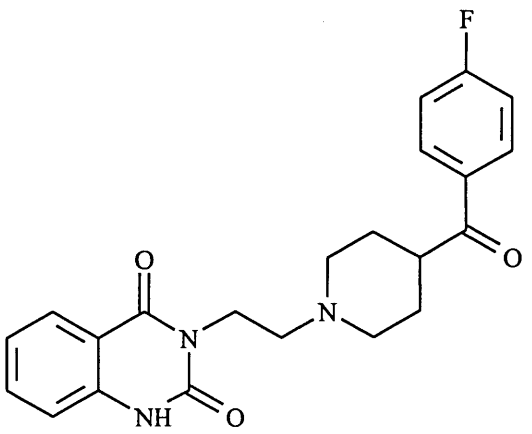

(10)

The majority of the mutagenesis studies on helix 7 have been concerned with the residue equivalent to ASN385 of the 5-HT_{1A} receptor. Mutation of this residue of the 5-HT_{1A} receptor to valine[109] resulted in a receptor with a significant

decrease in affinity for the aryloxyalkylamine β–adrenergic antagonists e.g. S-(-)-propranolol (11) but only slightly altered the affinities of other 5-HT receptor agonists and antagonists. The human 5-HT_{1D} receptors have a threonine residue in the corresponding position and mutation of this in the $5\text{-HT}_{1D\beta}$ receptor to asparagine (THR355-ASN) resulted in a receptor pharmacology that resembled the rodent 5-HT_{1B} receptor. This mutant receptor had a higher affinity for the aryloxyalkylamine β–adrenergic antagonists and a lower affinity for sumatriptan[110-112]. A further publication[113] demonstrated that mutation of this threonine residue of the $5\text{-HT}_{1D\alpha}$, $5\text{-HT}_{1D\beta}$ and 5-ht_{1E} receptors and the corresponding alanine of the 5-ht_{1F} receptor to asparagine increased the affinity for the β–adrenergic antagonists by 100-1000 fold without changing the affinity for 5-HT.

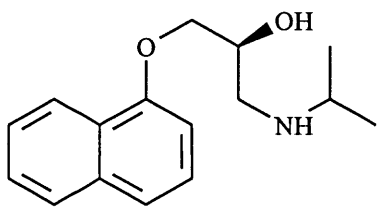

(11)

Other helix 7 residues of the 5-HT_{1A} receptor have been mutated[114]. Mutation of ASN396 to alanine, valine or phenylalanine decreased the binding affinity of the 5-HT_{1A} selective agonist 8-hydroxy-2-(di-*n*-propylamino)tetralin (8-OH-DPAT, 12) but the conserved change to glutamine had little effect. In addition, mutations of SER391 and SER393 to alanine were studied[114]. The changing of SER391 had no effect but the SER393-ALA mutant reduced ligand binding. The authors then proposed[114] that ASN396 may have either a structural role or a direct ligand binding role and SER393 may interact with the hydroxyl group of 8-OH-DPAT.

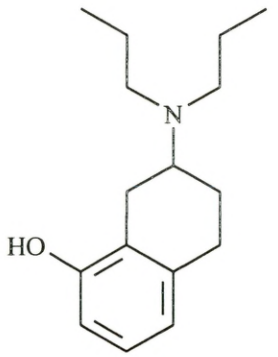

(12)

Deletion mutants of the 5-HT_{2A} receptor have shown no loss of biological activity upon removal of the N-terminal and the majority of the C-terminal domains[115]. 5-HT_{2A} and 5-HT_{2C} chimeric receptors have also been studied and it was discovered that structurally diverse 5-HT_{2A} antagonists utilise distinct regions of the 5-HT_{2A} receptor when binding[116]. The mutagenesis work on the 5-HT receptors up to 1993 has been reviewed[117,118].

The growing wealth of mutation data available for the 5-HT receptors and indeed GPCRs in general leads to the temptation of assuming that any change in binding affinity associated with a mutant receptor implies a direct ligand interaction with the mutated residue. However this is not necessarily true and a change in affinity may be the result of a conformational change in the protein. Nevertheless the mutation work has been extremely useful, not only in aiding the modelling of these receptor but in the overall understanding of ligand binding and signal transduction of GPCRs.

1.1.4.4 Approaches to modelling GPCRs

With the advent of molecular modelling in the 1980's there has been a great interest in constructing molecular models of G-protein coupled receptors. These models have been created for two reasons; to aid our understanding of the

requirements for ligand binding with a view to rational drug design, and perhaps more importantly, to allow the design of new experiments to investigate further the structure function relationships of these receptors.

At present there are no 3-dimensional crystal structure coordinates available for any G-protein coupled receptor. This has therefore rendered the molecular modelling of these GPCRs generally difficult and certainly quite speculative. As described previously biochemical and biophysical experiments have led to the conclusion that GPCRs are composed of seven helices.

The bacterial membrane protein bacteriorhodopsin has been the focus of many structural studies which resulted in the publication of a low resolution electron density map in 1975[80] showing seven transmembrane domains believed to be α-helices. Despite its name, bacteriorhodopsin is not a GPCR and is functionally unrelated to the GPCR rhodopsin and hence exhibits very little sequence homology with rhodopsin. A higher resolution structure of bacteriorhodopsin was revealed some 15 years later[119] providing atomic coordinates of the membrane portion of the protein. At that time Henderson and Schertler discussed the similarities of bacteriorhodopsin and rhodopsin[120]. Although both proteins are certainly functionally different similarities do exist. Both proteins are activated by a light induced isomerisation of a retinal chromophore attached covalently to a lysine residue on putative helix 7. Both proteins also consist of seven antiparallel transmembrane α-helices with extracellular N-terminus and intracellular C-terminus leading to the proposal[120] that GPCRs and bacteriorhodopsin may share the same topology (Figure 2).

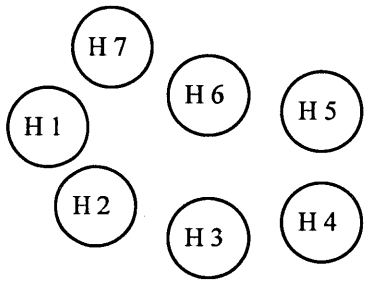

Figure 2 Representation of the topology of bacteriorhodopsin as viewed from the extracellular surface

In 1993 a significant breakthrough came[121] when 2-dimensional crystals of bovine rhodopsin were obtained and a low resolution projection density map was calculated. This demonstrated experimentally for the first time the proposed seven helical structure of rhodopsin. On comparison with bacteriorhodopsin, the rhodopsin map was found to be less elongated and the helices were tilted differently. The projection map however provided no evidence of helix order and connectivity, thus Baldwin[122] studied the alignment of 204 GPCR sequences. Transmembrane helices were identified and plotted around helical wheels which were arranged to give an arrangement where each helix is adjacent in 3-dimensions to the helix next to it in the amino acid sequence, and the helices run clockwise as viewed from the cytoplasmic side. This arrangement was shown to be similar to that of the rhodopsin map[121] and allowed the tentative identification of peaks from that map, concluding that although rhodopsin shows a similar structure to bacteriorhodopsin there are definitely differences. It has been speculated[123] that the differences could be attributed to a 15^{o} rotation around the axis perpendicular to the seven helices passing through helix 3 and that this may be caused by differences in crystallisation.

A low resolution 3-dimensional structure of bovine rhodopsin was then determined[124] in 1995. This allowed the identification of four of the seven α-helices where the remaining three were unresolved but it does correspond well

with the work of Baldwin[122] and is certainly different from bacteriorhodopsin. A 2-dimensional projection map of frog rhodopsin has also been calculated[125] and this shows a very similar structure to that of bovine rhodopsin[121] and puts the speculation[123] regarding differences in crystallisation into grave doubt. It is also worth noting that in 1996 a revised set of bacteriorhodopsin coordinates were made available[126] where the position of the fourth helix has been modified.

For most molecular models of GPCRs the starting point has been the sequence alignment of the GPCRs which when combined with hydropathy analysis (e.g. Kyte and Doolittle[127]) has allowed the identification of the seven membrane spanning helices. From this common starting point some models have used a "de novo" approach where no assumptions of the helix arrangements have been made, however by far the majority of GPCR models have used the 1990 3-dimensional coordinates of bacteriorhodopsin[119] either by attempting to align the GPCR sequence with bacteriorhodopsin or by using the arrangement of helices as a template. More recently (1993 onwards) some models have utilised the bovine rhodopsin 2-dimensional map[121] and Baldwin's helix assignments[122], claiming that bacteriorhodopsin is not similar enough to the GPCRs to warrant its use in GPCR molecular modelling.

The following sections discuss some of these models with particular attention being paid to the 5-HT receptor models. In the cationic amine neurotransmitters it is generally thought, from mutagenesis[85,91,104,105], that the protonated amine group will interact with the aspartate residue of helix 3 which is only conserved in the cationic amine receptors. Therefore virtually all cationic amine neurotransmitter receptor models have used this residue as a counterion for the protonated amine during initial docking studies of agonists. The models will be discussed according to the research group which produced them and it will

become apparent that many research groups have changed their modelling strategy between publications.

1.1.4.5 Early models

The first published molecular model of any GPCR[77] used the low resolution structure of bacteriorhodopsin[80] to produce a 3-dimensional model of rhodopsin[77]. Other early (pre-1990) models have been limited to the β_2-adrenergic receptors. Single helix models have been studied for the β_2-adrenergic receptor[128-130]. The low resolution map of bacteriorhodopsin[80] was also used for a seven helix model of the β_2 receptor[131] however the sequence of helices ran clockwise from the extracellular surface which was later proven to be incorrect[119].

1.1.4.6 Models from the University of Leeds

With an ever increasing number of GPCRs being sequenced a discriminating fingerprint of the GPCR sequences was developed[132] which could identify and align the GPCRs from primary structure analysis. This approach afforded a sequence alignment of GPCRs which was used to construct molecular models[133] based upon the original rhodopsin molecular model[77]. GPCR models developed from the 1990 bacteriorhodopsin structure using Fourier transforms[134] have also been published. In 1993 the low resolution map of rhodopsin[121] was used to construct a modified 3-dimensional rhodopsin model[135] which was to aid protein engineering studies. This model was extrapolated to other GPCRs including the adrenergic, muscarinic and neurokinin receptors[135] using the discriminating fingerprint approach[132,136] to align the sequences, and the Fourier transform techniques developed by Donnelly *et al.*[137] to predict which face of each helix is lipid accessible.

By 1994 the fingerprint methodology had been used to locate and align 393 GPCR sequences[138] and a more detailed discussion of this GPCR modelling work was published[139]. The predicted seven α-helices were identified, helices 1, 2 and 7 were superimposed directly onto the equivalent helices of bacteriorhodopsin[119] and helices 3, 4, 5 and 6 were positioned according to the density map of rhodopsin[121] using interactive graphics. The helix connectivity of Baldwin[122] was assumed, which is the same as that of bacteriorhodopsin[119]. The internal faces and relative depths of each helix were determined from the Fourier transform work of Donnelly *et al.*[137,140]. A detailed model of the β_2-adrenergic receptor[139] was then described. The adrenaline binding site was found to be between helices 3, 5, 6 and 7 with the cationic amine forming an ion pair with the aspartate of helix 3 and the catechol hydroxyl groups hydrogen bonding with the serines of helix 5. The binding site model of the β_2-adrenergic receptor was subsequently used to study other GPCR binding sites.

For the 5-HT receptors it was proposed[139] that the indole N-H of 5-HT could interact with a serine or cysteine residue on helix 3 for the 5-HT_2 and 5-HT_1 subtypes respectively. The hydroxyl group formed a hydrogen bond to the serine/threonine residue on helix 5 which corresponds to one of the important serine residues that bind the catecholamines in the β_2-adrenergic receptor. The same modelling procedure was again used to construct a neurokinin NK_2 receptor model[141]. Donnelly and Findlay have also published a brief review[142] of some of the modelling procedures that have been applied to GPCRs discussing in particular the use of the bacteriorhodopsin structure[119] and the rhodopsin density map[121].

A homology model of the muscarinic M_1 receptor[143] has been described using the early rhodopsin model[77]. The docking of agonists and antagonists prompted

the proposal[143] that antagonists interact with an aspartate of helix 3 and block the entrance to the central cleft of the receptors. Agonists similarly are thought[143] to bind to this residue then move down the central cleft to interact with the aspartate of helix 2 and in some way induce a conformational change of the receptor. This proposal has been updated[144] more recently.

1.1.4.7 Models from the University of Tromsø, Norway

The group of Dahl, Edvardsen and Sylte[145,146], in Norway, first produced a dopamine D_2 receptor model in 1990. Transmembrane helices, identified by hydrophobicity, were assumed to be 27 amino acids in length and were arranged in a circular antiparallel sequence running clockwise as viewed from outside the cell (opposite to that of bacteriorhodopsin). Molecular dynamics simulations were then used to study the interactions of dopamine within the receptor model.

The same modelling procedures were applied to the 5-HT_{1A} and 5-HT_{2A} receptors, studying the potential binding modes of some antipsychotic drugs[147]. By 1992 the models were modified[148], still using a circular arrangement of α-helices, however the helices were now ordered anticlockwise as viewed from outside the cell. This was applied to the 5-HT_{2A} receptor investigating the dynamics and electrostatics of the binding of 5-HT and the 5-HT_2 receptor antagonist ritanserin (13)[148].

It was found[148] that the protonated amine of 5-HT could interact with the conserved aspartate on helix 2 and other residues situated upon helices 1, 3, 5 and 7 whereas ritanserin formed strong interactions with the aspartates on helices 2 and 3. A more detailed model of the 5-HT_{1A} receptor was later published[149] again using the anticlockwise arrangement of helices. From molecular dynamics simulations of 5-HT and other active compounds at this receptor the 5-HT

binding site was proposed to include residues on helices 1, 2, 3 and 7 most notably the aspartate of helix 2 but not the aspartate of helix 3. The aromatic moiety of 5-HT could form interactions with residues on helix 7 with the conserved tyrosine residue stacking against the phenyl ring of the ligand.

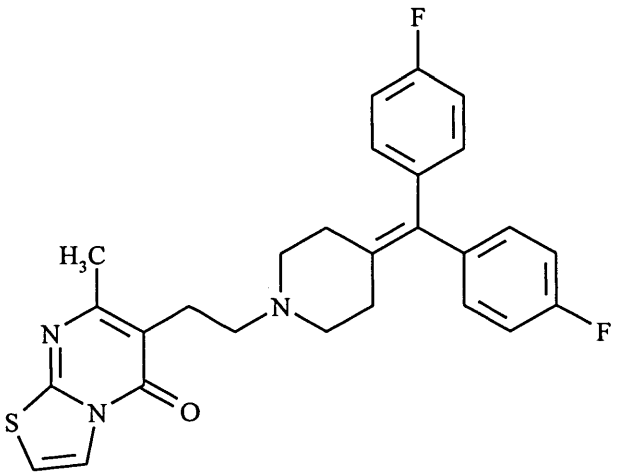

(13)

A similar process was used[150] to study the interactions of the 5-HT_2 receptor antagonist ketanserin (10) with the 5-HT_{2A} receptor. The protonated piperidine ring could interact with the aspartate of helix 3 and favourable interactions were observed with residues upon the other six helices. The aspartates of helices 2 and 3 were mutated on the model to asparagine and the mutant models exhibited a significant decrease in interaction energy between the ligand and receptor.

The models were modified once again in 1996 using the electron density map of bovine rhodopsin[121] and the helical arrangement proposed by Baldwin[122], and the interactions of some derivatives of 8-OH-DPAT with the 5-HT_{1A} receptor were described[151]. The ligands were docked in order to form interactions between the protonated amine of the ligand and the aspartate residue of helix 3. Following dynamics simulations, agonists were found to interact with both aspartates on helices 2 and 3 whereas antagonists did not show any interaction with the helix 2 aspartate.

A similar description of the interactions of ketanserin, ritanserin and 5-HT with the 5-HT_{2C} receptor has been published[152]. 5-HT was found to interact with the aspartate of helix 3 and some helix 7 residues via the protonated amino sidechain. The indole N-H could interact with a serine residue of helix 3 and the hydroxyl group could hydrogen bond to a serine of helix 5 and an asparagine near the extracellular end of helix 6. It was further suggested that the structural differences of the antagonists ketanserin and ritanserin afforded non-identical overlapping binding sites. Differences in binding affinity between the two antagonists were proposed to arise from interactions with cysteine and serine residues on helices 7 and 3 respectively.

It has become increasingly evident that the dynamical simulations described by this group[145-152] have implied that a relatively high number of residues are involved in ligand binding without much consistency between the different 5-HT receptor subtypes. This may be attributed to the dynamical approach adopted and this particular approach to modelling GPCRs has been described, by other workers in this area as rather ambitious[142].

1.1.4.8 GPCR Modelling at Marion Merrell Dow

Much of the pioneering modelling work in the last six years has been carried out by Marcel Hibert and co-workers at Marion Merrell Dow in Strasbourg. The group constructed molecular models of many GPCRs using the high resolution structure of bacteriorhodopsin[153-157]. Their modelling procedure used hydropathy indices and sequence alignments to identify the seven transmembrane α-helices. Transmembrane domains 3, 6 and 7 were positioned according to low sequence homology with the corresponding helices of bacteriorhodopsin. At this point it is worth noting that the alignment of helix 3

was changed, without reason, between the 1991 models[153,154] and the more recent models[156,157]. The remaining helices 1, 2, 4 and 5 were orientated to allow conserved and charged amino acids to protrude into the central core of the receptor to give a similar overall structure to that of bacteriorhodopsin.

Energy minimisation and ligand - receptor docking then provided some remarkable results for the cationic amine receptors. The cationic head group of the ligands could interact with the aspartate residue on helix 3 and the ion pair was stabilised by a surrounding pocket of aromatic residues. The conserved aspartate of helix 2 was postulated to play an allosteric role. The catecholamines dopamine, adrenaline and noradrenaline could form hydrogen bonding interactions with two serines upon helix 5 (one serine is mutated for cysteine in the α_2-adrenergic receptor) at their respective receptors.

Models of the 5-HT_{2A} receptor have also been described in some detail however only one of the serine residues is present on helix 5 (threonine for 5-HT_1 subtype) and this could interact with the hydroxyl group of 5-HT. The indole N-H was found to hydrogen bond with a serine on helix 4 and the aromatic portion of the ligand could interact with conserved phenylalanines on helices 5 and 6. It was also proposed that conserved tryptophan and tyrosine residues on helices 6 and 7 respectively can form hydrogen bonds with the conserved aspartate of helix 3 in the inactivated receptor and it was further suggested that upon ligand binding a conformational change would be induced involving one or both of these residues possibly leading to signal transduction.

This ligand activation process was updated[158] where it was suggested that the tyrosine of helix 7 can interact with both important aspartate residues of helices 2 and 3 ensuring a connection between the upper ligand binding region of the receptor and the lower G-protein coupling region of the receptor. More recently

detailed models using the same modelling procedures have been published for the transmembrane domains of peptide receptors[159,160] and glycoprotein hormone receptors[161]. An overview of the group's modelling of GPCRs has also been published[162].

In 1995 the original models were updated to account for the electron density footprint of bovine rhodopsin[121]. Dismissing their own speculative viewpoint that the differences between bacteriorhodopsin and rhodopsin could be accounted for by a 15° tilt of the projection map[123], the original models were modified to obtain a "perfect match" of calculated electron density with that of rhodopsin[163]. This produced structurally similar models which differed mainly in the tilt of specific helices. No revised binding site models were described for any of the 5-HT receptors but the authors claimed that the models are "qualitatively excellent", identifying the correct ligand binding sites and accounting for the gathering wealth of experimental data relating to ligand binding studies.

Due to the static nature of the models the more subtle interaction differences between ligands could not be accounted for and it was suggested that it would be very difficult for those who are attempting to construct quantitatively useful models. The rhodopsin approach has since been used to produce molecular models (including loop regions) of the V_{1A} vasopressin receptor[164,165].

1.1.4.9 The models of Glennon and Westkaemper

Glennon and Westkaemper originally constructed single helix models[166] which examined the interactions of various ligands with models of helices 2 and 3 of the 5-HT_{2A}, 5-HT_{2C} and 5-HT_{1A} receptors. Docking was performed, permitting the protonated amine of the ligand to interact with the important

aspartates of both helices. From the calculated interaction energies it was demonstrated that the ligand - helix 3 complex was more favourable than the helix 2 complex and it was therefore concluded that the aspartate of helix 3 was important for binding. The single helix models proved to be a springboard towards more detailed receptor models[167].

Models of the 5-HT_{2A}, 5-HT_{2C} and 5-HT_{1A} receptors were built[167] using an alignment with bacteriorhodopsin. The alignment by helix centres was similar to that of Hibert *et al.*[154] and was used directly without helical translation or rotation. Models of the 5-HT_{2A}, 5-HT_{2B} and 5-HT_{2C} were subsequently presented in much greater detail[168]. Helical centres were aligned and graphically evaluated with the best alignment of the centres used for the ligand docking experiments. The interactions of the agonists 5-HT (1), (+)LSD (14) and (R)-(-)DOB (15) were assessed.

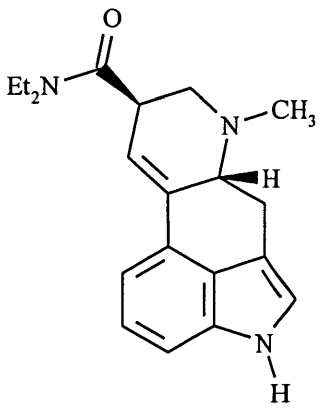

(14)

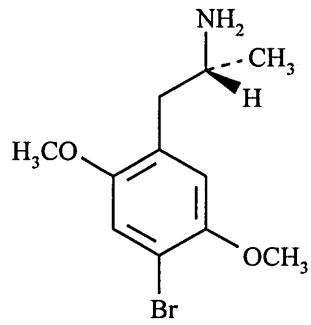

(15)

It was found that[168] the indole ring of 5-HT interacted with hydrophobic and aromatic residues of helices 4, 5 and 6, an ion pair was formed with the aspartate of helix 3, and the 5-HT hydroxyl group hydrogen bonded with the serine residue of helix 5. (+)LSD binds similarly to 5-HT but (R)-(-)DOB was able to interact in two distinct manners both maintaining the aspartate - amine ion pair,

and characterised by the position of the methoxy groups. Preliminary results of this study have also been published[169].

The 5-HT_{2A} receptor model was used in a mutagenesis study[170] correlating the binding affinities of simple ergolines (e.g. ergonovine (16)) and ergopeptines (e.g. ergotamine (2)) with respect to mutations of PHE340 and PHE339 of helix 6.

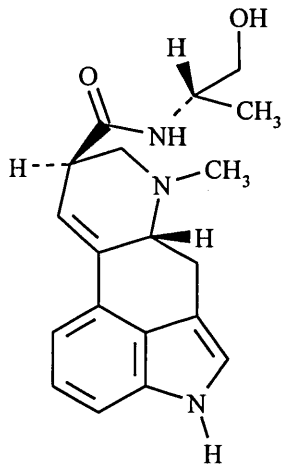

(16)

The binding of all simple ergolines was decreased by the non-conserved mutation of PHE340 and unaffected by PHE339 mutations. This is in contrast to the binding affinities of the ergopeptines which were unaffected by either mutation. These findings were supported by the molecular models which show that simple ergolines can interact with PHE340, but because of their more sterically demanding C-8 position, the ergopeptines could not adopt the orientation observed for the ergolines and are too far away to interact with either phenylalanine.

Further models of the 5-$HT_{1D\alpha}$, 5-$HT_{1D\beta}$ and 5-HT_{1B} receptors were published in an overview of 5-HT_{1D} receptors[171]. These models were used to

discuss non-conserved residues in the possible binding site and the importance of a threonine residue of helix 7 was suggested. When this residue is mutated to asparagine as is observed for the 5-HT_{1A} and 5-HT_{1B} receptors the mutant receptors show a dramatic increase in affinity for the β_2-adrenergic receptor antagonists[110-113] which may be indicative of a ligand receptor hydrogen bond interaction. This point has been investigated further[172].

Mutation of THR355 of the 5-$HT_{1D\beta}$ receptor to ASN increased the affinity for the β_2-adrenergic antagonist (-)-propranolol (11)[172]. The previously constructed 5-$HT_{1D\beta}$ model was used to create the mutant model[171]. (-)-Propranolol was docked into both the wild type and mutant models with the naphthyl ring towards helices 1, 2 and 7 and the protonated amine of the ligand interacting with the aspartate of helix 3. The models suggested that the threonine of the wild type 5-$HT_{1D\beta}$ receptor can interact with the ether oxygen but not the hydroxyl group of the ligand. The mutant receptor model showed a different picture, both oxygens of the ligand could form hydrogen bonds with the asparagine sidechain suggesting that both these hydrogen bonds are crucial for the high affinity binding of (-)-propranolol. This has been further supported[172] by binding studies of analogs of (-)-propranolol that lacked either one or both of the oxygens.

1.1.4.10 The 5-HT_{1D} receptor models of Smolyar and Osman

The mutation of THR355 of the human 5-$HT_{1D\beta}$ receptor to asparagine alters the pharmacology of the receptor to that of the rodent 5-HT_{1B} receptor[110-112] and this resulted in a 5 to 15 fold decrease in affinity for sumatriptan. Smolyar and Osman[173] have addressed this point by investigating the interactions of sumatriptan (4) with the human 5-HT_{1D} receptors. The 5-$HT_{1D\alpha}$ receptor was modelled using the general topology of bacteriorhodopsin and sumatriptan was

docked into the model, creating the protonated amine - aspartate helix 3 interaction and so that the sulfone group was near to the threonine residue (THR342 for 5-$HT_{1D\alpha}$). The complex was refined by energy minimisation and subjected to a dynamics simulation.

Sumatriptan was found to be surrounded by 14 residues and the aspartate - amine ion pair was maintained. Interactions with the residues were monitored throughout the simulation and it was observed that the threonine residue had turned away from the ligand and formed a hydrogen bond with the helical backbone. This change of interaction prompted the authors to propose[173] that this hydrogen bond stabilises the ligand - receptor complex. Mutation of the threonine residue to asparagine would not allow this stabilisation and hence would alter the affinity of sumatriptan. It was further suggested[173] that this indirect effect is totally different from the change in binding affinity observed with some β_2-adrenergic antagonists where the large increase in affinity accompanied by the THR-ASN mutation suggests a direct effect of the residue. Osman has also co-authored a series of papers modelling the thyrotropin releasing hormone[174-177] using Baldwins analysis of sequences[122].

1.1.4.11 Models from Uppsala University and Astra pharmaceuticals

Nordvall and Hacksell[178] initially modelled the muscarinic M_1 receptor based upon the bacteriorhodopsin structure[119]. A strict alignment with bacteriorhodopsin was applied which was derived from assessing the feasibility of several different alignments using experimental data and analysis of conserved and hydrophobic amino acids. The process rejected all but one of the alignments studied therefore this was used to model the receptor. The model was used to investigate the interactions of some muscarinic agonists and later, to construct D_{2A} and D_3 dopamine receptor models[179].

A 5-HT_{1A} receptor model[180] was used to account for the binding differences over the dopamine D_{2A} receptor of (R)-11-hydroxy-10-methylaporphine (17). The models suggest that the ligand can be accommodated at the 5-HT_{1A} receptor with the protonated amine - aspartate helix 3 ion pair and aromatic interactions between the substituted phenyl ring of the ligand and a phenylalanine of helix 6. The C-10 methyl group was found to be accommodated by a lipophilic pocket which is not present in the D_{2A} receptor and the methyl group thus caused steric repulsion. The increased van der Waals contact surface for (17) at the 5-HT_{1A} receptor was thought to account for its higher affinity for the 5-HT_{1A} receptor over the D_{2A} receptor. A similar approach has been used[181] to study the human galanin receptor.

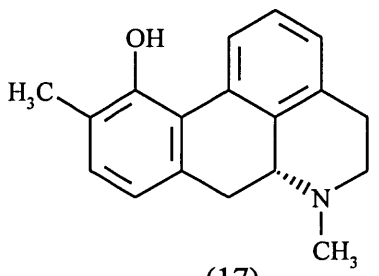

(17)

1.1.4.12 The contribution of Harel Weinstein's group

The group headed by Harel Weinstein has been one of the most significant contributors to modelling and simulations of GPCRs in the 1990s. The first computational simulation of 5-HT receptor activation was published[182] in 1990 and did not use a molecular model of the receptor but a hypothetical model based upon the protein actinidin. After the publication of the bacteriorhodopsin structure[119] a controversial alignment[183] of GPCR helices with bacteriorhodopsin was proposed. The assumption that the sequential order and packing arrangement of GPCRs is the same as bacteriorhodopsin was

questioned. It was proposed[183], from low sequence homologies, that GPCR sequences could be aligned with bacteriorhodopsin when the sequential order of these helices is ignored.

A further publication[184] discussed some of the criteria used in GPCR modelling. The "positive-inside" rule was described where positively charged lysine and arginine residues are found at the cytoplasmic ends of the helices interacting with the phospholipid head groups of the lipid bilayer. This work[183,184] later aided Zhang and Weinstein[185] in modelling the 5-HT_{2A} receptor. Full details of the modelling procedure were not given but a topological template different from bacteriorhodopsin (Figure 3) was used where the relative positions of the transmembrane helices differed from the more conventional models.

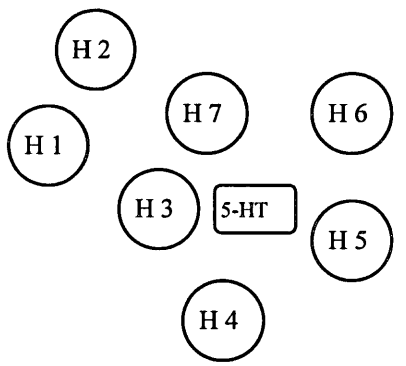

Figure 3 Representation of Zhang and Weinstein's[185] 5-HT_{2A} receptor model viewed from the extracellular side

The ligand binding site incorporated the aspartate of helix 3 and residues of helices 5, 6 and 7 with a serine residue of helix 7 forming a hydrogen bond with the hydroxyl group of 5-HT. It was further discovered during molecular dynamics simulations of the receptor complexed with various ligands, agonists would induce conformational changes in the backbone of helices 5 and 6 but an

antagonist would not. A partial agonist studied, induced a change that was intermediate of the above extremes. It was therefore concluded that the induced change may be responsible for signal transduction.

Following the publication of the low resolution rhodopsin map[121], Zhang and Weinstein[186] stated that their model of the 5-HT_{2A} receptor has the same shape as the rhodopsin map. Previous work[185] was then extended to study the conformational changes induced by ligands which belong to diverse structural families[186]. Correlation was found between ligand binding affinities and the ligand - helix 7 interaction energy, which was improved by adding the interaction energies between helix 7 and the other helices of the receptor. Furthermore it was proposed[186] that a primary event in signal transduction could be the development of an angular force acting upon helix 7 which is induced by agonist binding.

The dynamics trajectories of the 5-HT_{2A} receptor were subsequently used[187] to investigate the ligand-induced conformational changes of the transmembrane domains. An algorithm was developed which treated the ligand induced movement of the helices as rigid domain movements. Results demonstrated that an agonist-induced torque upon helix 7 exerts movement of helix 6 which is directly attached to the large intracellular loop that is involved in G-protein coupling. Helix 4 was also affected which in turn moved helix 5 which is also connected to the third intracellular loop. When partial agonists were studied movements were still induced but by a smaller magnitude and antagonists exerted a torque opposing the movement of the helices.

A double mutant[188] of the 5-HT_{2A} receptor has been studied where the conserved aspartate of helix 2 was mutated to asparagine resulting in loss of receptor coupling. The reciprocal mutation of a conserved asparagine of helix 7

to aspartate restored this loss of function, albeit lower than the wild type receptor. It was proposed that the restoration of function by the double mutant was due to the direct interaction of the two residues probably by a hydrogen bond. The model of Zhang and Weinstein[185] was used[188] to construct the mutant models and results from ligand receptor binding interactions appeared to be consistent with the hydrogen bond theory.

The implications from the receptor - ligand simulations described previously[185,187] were used[189] to probe the 5-HT_{2A} agonist binding site by mutagenesis. Mutation of SER159 of helix 3 to alanine resulted in an 18 fold decrease in 5-HT binding affinity but unaffected (+)LSD (14). The mutation of the same residue to cysteine gave only a 3 fold decrease in 5-HT binding affinity with again having no effect on (+)LSD. The 5-HT_{2A} receptor model[185,187] was used[189] to show that the protonated amine of 5-HT can, additionally, form a hydrogen bond with this serine residue but the ring embedded nitrogen of (+)LSD cannot form such an interaction.

Differences in helix 5 between the 5-HT_{2A} and 5-HT_{2C} receptors have also been investigated[190]. Mutations of the equivalent residues SER242-ALA for the 5-HT_{2A} receptor and ALA222-SER for the 5-HT_{2C} receptors were studied. Ergoline compounds with high affinity for the wild type 5-HT_{2C} receptor now had a higher affinity for the mutant 5-HT_{2A} receptor and *vice versa.* Indoleamines behaved differently and the 5-HT_{2A} mutation decreased their binding affinity but the 5-HT_{2C} mutation did not alter indoleamine binding affinity. These results were shown[190] to be consistent with the models. Ergoline compounds that are N-1 unsubstituted (e.g. (+)LSD (14)) have a free N-H available for hydrogen bonding hence the higher affinity at receptors with a serine residue. Ergoline compounds that are substituted at the N-1 position prefer the hydrophobic alanine residue of the 5-HT_{2C} wild type receptor.

Models using the conventional order of transmembrane helices have also been published for the gonadotropin-releasing hormone receptor[191,192] and the cannabinoid CB_1 receptor[193]. The entire process of modelling GPCRs has been reviewed[194] however receptor binding sites are not discussed.

1.1.4.13 The 5-HT_{1A} and 5-HT_{2A} models of Taylor and Agarwal

Contrary to the controversial alignment of Pardo *et al.*[183] it has been hypothesised[195] that any sequence homology between GPCR helices and bacteriorhodopsin may be explained by the process of gene duplication. The bacteriorhodopsin structure[119] was used to produce homology models of the 5-HT_{1A} and 5-HT_{2A} receptors[196]. The agonist binding process proposed is similar to that of Saunders[144]. An agonist initially interacts with the aspartate of helix 3 then moves down the cleft to form similar interactions with the aspartate of helix 2. This second residue is antagonist inaccessible and hence differences between agonists and antagonists can be accounted for[196].

1.1.4.14 The step by step procedure of Henri Moereels

Henri Moereels found that modelling GPCRs using bacteriorhodopsin was unsuccessful and decided to use a step by step procedure to model the 5-HT_{2A} receptor[197]. Starting with 5-HT the way in which the hydroxyl group of the ligand could interact with helix 5 in isolation was examined. The energy minimised complex was used to model the interaction of 5-HT with helix 5 of the other 5-HT receptors which all showed a hydrogen bond between the hydroxyl group and a serine/threonine residue of helix 5. The relevance of this hydrogen bond was then discussed and the possibility of adding other helices to the model was mentioned. A similar model has been studied for the dopamine

D_2 receptor[198]. This model looks at the interactions between the natural agonist and helices 3, 4 and 5 of the receptor with particular attention being paid to the roles of serine residues upon helix 5 and potential disulfide bonds.

1.1.4.15 Miscellaneous 5-HT receptor models

When studying the 5-HT receptor binding affinities of N-hydroxytryptamine derivatives some of the 5-HT receptors were modelled[199] based upon the methods of Hibert[154,156]. The models were used[199] to explain why N-hydroxytryptamine was moderately selective for the 5-HT_{2C} receptor. The models suggested that at the 5-HT_{1A} receptor the aspartate of helix 3 interacted with the protonated amine of the ligand and an asparagine residue of helix 7. The equivalent residue to the asparagine of the 5-HT_{2C} receptor is a valine which leaves the aspartate residue of helix 3 with a free oxygen which hydrogen bonds with the N-hydroxy group of the ligand in addition to the interaction with the protonated amine. This greater stabilisation is said to account for the differences in binding affinity.

The 5-HT_{1A} receptor has also been modelled[200] using a sequence alignment with bacteriorhodopsin. The agonist binding site was determined by a three point interaction of the agonists, with the aspartate of helix 3 and THR200 and SER199 of helix 5. The selectivity of 8-OH-DPAT (12) is accounted for by the hypothesis that one of the bulky *n*-propyl groups can form lipophilic interactions with small hydrophobic residues between helices 3 and 4 which are not present in the other 5-HT receptors. The aryloxypropanolamine antagonist binding site also involved the aspartate of helix 3 but the aromatic moiety was in the region of helices 1, 2 and 7. The model was further used in a study of structure-affinity relationships of arylpiperazines at the 5-HT_{1A} receptor[201].

Höltje had originally built a two helix model of the 5-HT_{2A} receptor using helices 2 and 3[202]. This was recently updated[203] when a binding site model of the 5-HT_{2A} receptor around the antagonist ketanserin (10) was constructed. It was proposed[203] that the fluorobenzoyl moiety of the antagonist takes part in a charge transfer complex with an electron rich tryptophan residue and that the purpose of the carbonyl group of the ligand is to render the phenyl ring electron deficient and not to act as a hydrogen bond acceptor. This possibility was confirmed from modelling the interactions of ketanserin with a truncated tryptophan residue. A carboxylate anion was then positioned to interact with the protonated nitrogen and the binding site model was completed by the addition of hydrophobic residues. Interaction energies of ligands within this model correlated well with binding affinities and this correlation was improved when a correction was made to account for the charge transfer complex.

A remarkable success in the prediction of affinities of new compounds has been claimed[203] and the model has been further modified by the addition of a serine and a phenylalanine residue to account for agonists. A full molecular model of the 5-HT_{2A} receptor is now being constructed[203] using bacteriorhodopsin. Ketanserin has been docked into the initial model using the developed binding site as a guide and refinement of the ketanserin - receptor complex has resulted in a binding site comparable to the predicted binding site model[203].

Friedrich Rippmann has used a sequence alignment with bacteriorhodopsin to model GPCRs in particular the 5-HT_{1A} receptor[204-206]. Some 5-HT agonists have been docked into the aspartate helix 3 binding site and their affinities have been accounted for but a detailed publication of this model is lacking.

A collaboration between some of the more prominent workers in GPCR modelling and research has provided a greater insight into the possible mode of

interaction of a number of ligands at the 5-HT receptors[207]. A multiple sequence alignment of many GPCRs has been used to correlate binding affinities of ligands with the variability of amino acid residues. Therefore without even building a model the residues that may confer specificity can be identified for the 5-HT receptors. Results indicated that the ASN/THR/VAL residue of helix 7 gave a 100 % correlation with the binding affinities of the aryloxypropanolamine β-adrenoceptor antagonists. The difference in 5-HT receptor affinity of 5-carboxamidotryptamine (5-CT, 18) could be attributed to the presence or absence of a proline residue at the extracellular end of helix 6. This residue could induce kinking in the helix allowing the ligand to form a hydrogen bond with the unsatisfied backbone carbonyl of the residue directly below the proline. The proline residue is only present in the 5-HT_{1A}, 5-HT_{1B}, 5-HT_{1D}, 5-ht_5 and 5-HT_7 receptors and hence these have high affinity for 5-CT. The remaining 5-HT receptors do not have this residue and hence exhibit low affinity for 5-CT. Other ligands have also been studied however results have not been as clear cut as the examples cited[207].

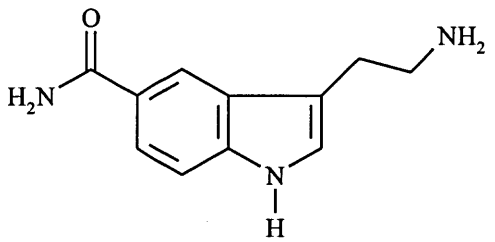

(18)

1.1.4.16 The "de novo" approach of Lybrand

"De novo" modelling of GPCRs has been studied extensively by Lybrand[208,209]. Contrary to the template approaches using bacteriorhodopsin or rhodopsin no assumptions were made upon the helix packing arrangement. The β_2-adrenergic receptor including the loop regions was modelled[208,209]

from analysis of many possible packing arrangements of the transmembrane domains. This provided two favourable models, one similar to bacteriorhodopsin with the helices running anticlockwise sequentially as viewed from the extracellular surface and the other where the helices were arranged sequentially in a clockwise direction viewed from the extracellular surface (mirror image of bacteriorhodopsin). This latter model was favoured since it accounted for the stereoselectivity of adrenaline.

The models have been further studied[210] using molecular dynamics simulations in *vacuo*, in *vacuo* with a bilayer model, and using a bilayer model which accounts for solvent effects. The motions of the loop regions in the bilayer model simulations were found to be unrealistic and it was suggested that this approach may only be useful for modelling the helical domains of the receptor. A discussion of the pitfalls of GPCR modelling has also been published[211].

1.1.4.17 The EMBL models

The lack of any real sequence homology between bacteriorhodopsin and the GPCRs was side-stepped by Cronet, Sander and Vriend[212]. Assuming that bacteriorhodopsin and the GPCRs have the same overall topology, the β_2-adrenergic receptor sequence was fitted to bacteriorhodopsin according to the preferred environment of the amino acids of the α-helices. This threading algorithm was used to model the β_2-adrenergic receptor giving reasonable agreement with experimental data. A more conventional approach was then adopted[213] using a modified GPCR alignment with bacteriorhodopsin to model many GPCRs. These models have been made publicly available in the "7TM" database[214]. Further publications have discussed the possible role in signal transduction of the arginine residue of the conserved DRY motif at the cytoplasmic end of helix 3[215] and a brief review of GPCR modelling[216].

1.1.4.18 A threading approach to GPCR modelling

The general arrangement of the helices of bacteriorhodopsin[119] was used initially[217] to model the human C5a receptor. More recently a threading method of modelling GPCRs[218] similar to the method of Cronet *et al.*[212] but based upon interaction energies has been used. The seven identified hydrophobic domains were taken one by one, threading the region through the corresponding helix of bacteriorhodopsin. Each alignment was scored upon sidechain interaction energies and evaluated with respect to structure function data.

In a subsequent publication[219] the same group investigated their models more extensively using experimental data in an effort to reduce the uncertainty associated with the models. From their model of rhodopsin, the glutamic acid residue of helix 3 was too distant to act as a counterion for the Schiff base of the retinal binding site. This was overcome by moving helix 7 towards the cytoplasm since moving helix 3 would have disrupted the disulfide bond between the cysteine at the extracellular end of helix 3 and the cysteine in the loop between helices 4 and 5. The new orientation of helix 7 conformed to the experimental data and additionally a conserved asparagine of helix 7 could interact with the important aspartate of helix 2. It was concluded that in the light of the low resolution map of rhodopsin[121], bacteriorhodopsin[119] is still a good template for modelling GPCRs.

1.1.4.19 The "heuristic direct" method

An Italian group have developed a "heuristic-direct" approach to quantitative structure-activity relationships. Models of some of the cationic amine

neurotransmitter receptors have been made and agonists, antagonists and partial agonists have been docked into the models. Correlations were studied between ligand receptor interactions and experimentally determined binding affinities and efficacies. This approach has been applied to the M_1 muscarinic[220,221] and α_1-adrenergic[222] receptors.

These bacteriorhodopsin based models were updated[223] using the GPCR topography of Baldwin[122]. The authors modelled the hamster α_{1B}-adrenergic receptor in the first instance and then used this model as a template for other receptors. The bacteriorhodopsin based models, the rhodopsin based models and bacteriorhodopsin were all subjected to molecular dynamics simulations[223]. It was found that the bacteriorhodopsin based GPCR model and the rhodopsin based GPCR model, after dynamics, gave similar refined models, which were noticeably different from the bacteriorhodopsin structure before and after dynamics.

The rhodopsin derived models were then used to model the rat muscarinic M_3 receptor correlating ligand binding affinities with ligand receptor interaction energies[224]. A dynamics study of the possible mode of signal transduction of the α_{1B}-adrenergic and the muscarinic M_3 receptors was performed, suggesting that movement of the arginine residue of the conserved DRY motif at the intracellular end of helix 3 may be an important step in signal transduction[225].

1.1.4.20 The unconventional binding site models of the dopamine receptors

Almost all the models of the cationic amine receptors have described the agonist binding site as involving the aspartate of helix 3 and residues of helices 4, 5, 6 and possibly 7. Charles Hutchins at Abbot Laboratories has questioned the validity of this binding site model[226]. Using the low resolution

bacteriorhodopsin map[80] and the connectivity of Engelman *et al.*[82] a model was made of the dopamine D_2 receptor. Site directed mutagenesis of the cationic amine neurotransmitter receptors has implicated the aspartate residues of helices 2 and 3 in agonist binding[85,91,104,105] and Hutchins has paid particular attention to this.

Dopamine was docked into the receptor model to interact, forming an ion pair, with the aspartate of helix 3. The aspartate of helix 2 was found to act as a hydrogen bond acceptor to one of the hydroxyl groups and the ligand was orientated vertically within the binding cleft between helices 2, 3, 6 and 7. The model was modified to account for the 1990 bacteriorhodopsin structure[119] and a dopamine D_1 receptor model was built using the D_2 model[226]. The interactions of many ligands with the binding site model have been studied. Antagonists have been shown to occupy the same binding site as the agonists but do not interact with the aspartate of helix 2 and partial agonists are proposed to bind in several orientations with only one of these activating the receptor.

1.1.4.21 Automated GPCR modelling

An automated method for modelling seven helix transmembrane receptors has been presented[227]. Numerous structural constraints were applied and the authors were able to produce a bacteriorhodopsin model from the low resolution density map[80] and a rhodopsin model from its density map[121]. The rhodopsin model has been used to assign helices to the density map and is consistent with the work of Baldwin[122]. It is intended[227] that future versions of the algorithm will incorporate proline induced kinks into the helical models.

An alternative automated GPCR modelling approach[228] has also been presented. The program incorporates hydropathy analysis, moment

vectors[137,140] and helical wheels to model GPCRs upon known templates. The program has additionally been used to study the solvation of GPCRs.

1.1.4.22 Miscellaneous GPCR models

A sequence alignment of bacteriorhodopsin with adenosine receptors was used to create a receptor model for the adenosine A_1 receptor in order to study ligand receptor binding[229]. Similar models have also been described for adenosine A_{2A}[230] and A_3[231] receptors. A review of adenosine A_1 receptor modelling and drug design is also available[232].

Analysis of sequence variability of the opsin family was used to model rhodopsin[233] without using any template. This gave a good agreement with the bovine rhodopsin footprint[121]. A model of bovine rhodopsin has also been described[234,235] which used the helical axis positions of bacteriorhodopsin[119] to position the helices of rhodopsin. Numerous other bacteriorhodopsin derived models have been published since 1990[236-238].

The β_2-adrenergic receptor model of Lewell[236] was interesting as she proposed that the classical β_2-adrenergic antagonists could bind between helices 1, 2, 3, 6 and 7 creating an overlap with the agonist binding site which involved residues on helices 3, 4, 5 and 6. Dopamine receptor models have been reported[239,240]. The model of Teeter *et al.*[240] was very meticulous suggesting that the differences in the electron density maps of bacteriorhodopsin and rhodopsin may evolve from differences in state (active versus inactive).

The olfactory OR5 receptor and the interactions of an odour molecule with the receptor were modelled[241]. Bacteriorhodopsin derived models of the β_1-

adrenergic[242], M_1-muscarinic[243], B_2 bradykinin[244] and AT_1 angiotensin[245] receptors have also been published.

A most stimulating bacteriorhodopsin based model of the β_3-adrenergic receptor has been published[246] using a similar modelling procedure to that of Trumpp-Kallmeyer *et al.*[156]. Additionally, available crystal structure coordinates of GTPases were used to model[246] the G_s G-protein that interacts with the β_3-adrenergic receptor. The C-terminus of G_s was docked against the C-terminus and third intracellular loop of the β_3 receptor. Analysis of the complex of the α-subunit of G_s with the receptor showed general agreement with experimental data.

When discussing GPCR work mention must be made of the contribution of Thue Schwartz in Copenhagen. Although primarily concerned with mapping peptide GPCR binding sites through mutagenesis, he has constructed real 3-dimensional models and molecular graphics models of some peptide receptors[247] using the electron density map of rhodopsin[121]. From this work, the common theory of a GPCR being activated by an agonist key is challenged, and it was suggested that an agonist may only need to stabilise the receptor in the activated state to allow G-protein interaction and signal transduction[248].

1.1.5 5-HT receptor agonists and bio-isosterism

The predominant chemical class of full 5-HT_1 agonists has been the indole derivatives such as 5-HT (1), sumatriptan (4) and 5-CT (18) however exceptions such as the aminotetralin 8-OH-DPAT (12) which is a selective 5-HT_{1A} agonist[23] do exist. The chemistry and biological activity of indole compounds with respect to 5-HT receptors has been studied extensively and in recent years

much work has been undertaken in synthesising indoles with high 5-HT_{1D} receptor affinity[57,58,60-68].

Instead of looking at this extensively studied class it is proposed that it may be possible to replace the indole nucleus of 5-HT like compounds with a thiophene containing moiety, in particular a thieno[2,3-b]pyridine ring system. The thieno[2,3-b]pyridines have been of interest to the workers of the University of Abertay Dundee for the last ten years and novel preparative routes to these compounds have been developed[249-251].

The concept of bio-isosteric replacement is well known[252,253] and traditionally thiophene rings have been used as bio-isosteres of phenyl rings in known active compounds[254-256]. In the indole series benzo[b]thiophene-3-acetic acid, an analog of the plant growth hormone indole-3-acetic acid shows retention of biological activity albeit lower than the parent indole compound[254]. Some patents of indole compounds relating to 5-HT receptor research have also subsumed their benzo[b]thiophene counterparts[257]. Thienopyridines themselves are known as quinoline and isoquinoline isosteres and medicinal chemists have exploited this in drug design (see section 1.2.6). No references to thienopyridines as analogs of 5-HT have been found during the research for this project, however there is the possibility of thieno[2,3-b]pyridine analogs of 5-HT agonists showing similar biological activity[258].

This project therefore aims to construct molecular models of the 5-HT receptors that may be involved in migraine headache. The agonist binding site will be identified and validated by the docking of some known 5-HT receptor agonists. The possibility of thieno[2,3-b]pyridine analogs of 5-HT acting as 5-HT receptor agonists will be assessed and the models can be further used to provide suggestions to improve 5-HT receptor selectivity. Target thieno[2,3-b]pyridine

compounds identified from molecular modelling as potential 5-HT receptor agonists will then be synthesised and tested for biological activity. Since the project deals with the synthesis of novel thieno[2,3-b]pyridines the chemistry of these compounds must be discussed.

1.2 THE CHEMISTRY OF THIENO[2,3-B]PYRIDINES

1.2.1 Introduction to thienopyridines

There are six possible thienopyridine ring systems and these can be classed into two groups: those that are analogs of quinoline, the [b] fused systems (19-21), and those that are analogs of isoquinoline, the [c] fused systems (22-24). In contrast to the quinolines and isoquinolines, thienopyridines do not occur widely in nature and have only been found in the basic extracts of shale oil of high sulfur content[259]. The first synthesis of a thienopyridine was by Steinkopf[260,261] in 1912.

The parent thieno[2,3-b]pyridine (19) was obtained in low yield from the reaction of the tin double salt of 2-aminothiophene with glycerol in a Skraup type synthesis. Following these papers, work on thienopyridines was almost non-existent until the 1950's. Chemists then became interested in thienopyridines for two different reasons. From a chemical viewpoint thienopyridines were interesting compounds since they contained a fused system of a π-excessive ring (thiophene) and a π-deficient ring (pyridine) and from a pharmacological viewpoint they could be considered as potential bio-isosteres of biologically active quinoline and isoquinoline compounds.

The chemistry of thienopyridines has been reviewed previously[262-265] and it is therefore not the purpose of this study to give a full thienopyridine chemistry review but to give merely an overview. Since the present study has concentrated only upon the [2,3-b] isomer this section will only discuss the important synthetic routes to, and the reactions of, thieno[2,3-b]pyridines.

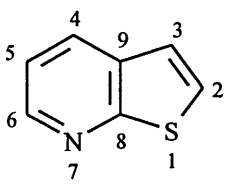
[2,3-b] (19)

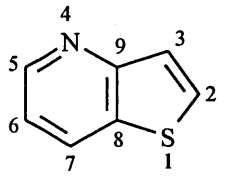
[3,2-b] (20)

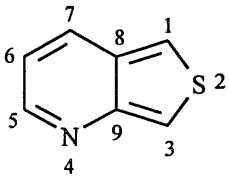
[3,4-b] (21)

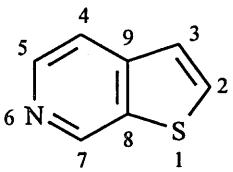
[2,3-c] (22)

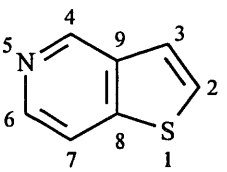
[3,2-c] (23)

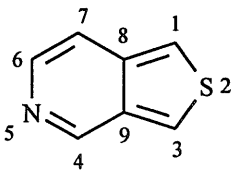
[3,4-c] (24)

1.2.2 Synthesis of thieno[2,3-b]pyridines from thiophene precursors

1.2.2.1 Skraup synthesis

Due to the notorious instability associated with aminothiophenes the more stable hexachlorostannate double salt of 2-aminothiophene (25) was reacted[260,261] with glycerol to give a low yield of the parent thieno[2,3-b]pyridine (19) [Scheme 1].

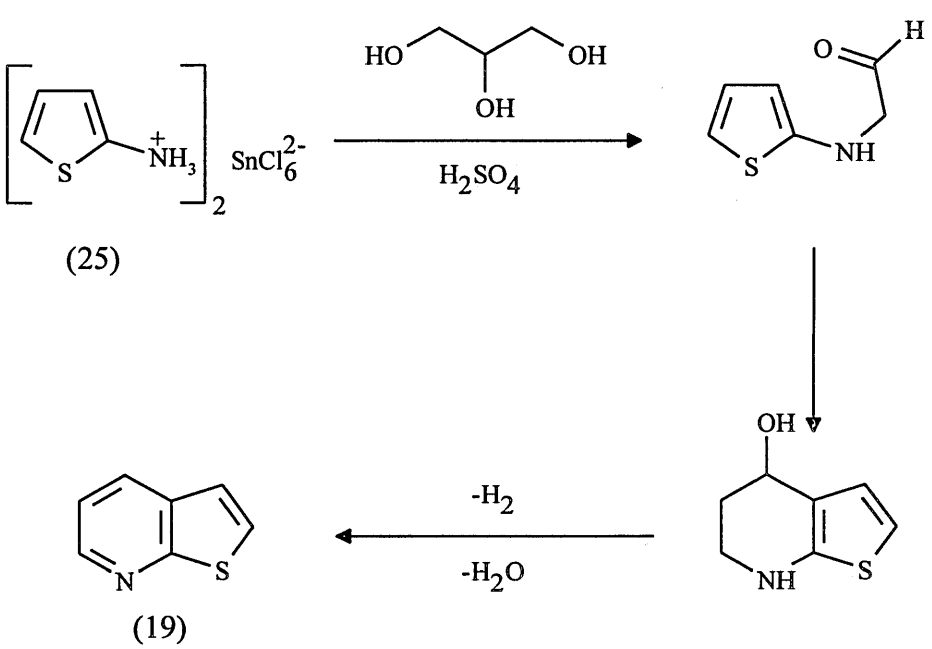

(25)

(19)

[Scheme 1]

In a variation of this reaction, Russian workers[266] used Friedel-Crafts conditions to prepare 4-methylthieno[2,3-b]pyridine (26) from reaction of the 2-aminothiophene double salt (25) and methyl vinyl ketone.

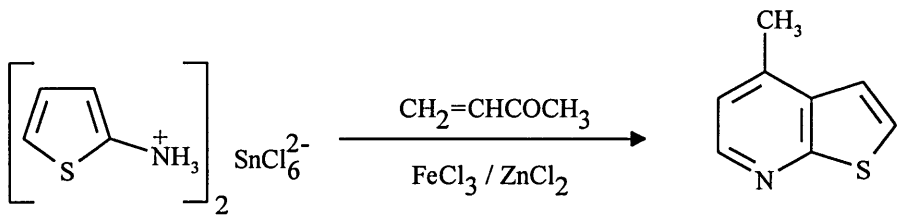

(25) (26)

When this reaction was repeated[267] by others, results were obtained that were inconsistent with the original report wherein the reaction afforded not only 4-methylthieno[2,3-b]pyridine (26) but also the 6-methyl isomer.

1.2.2.2 Reactions of aminothiophenes with 1,3-dicarbonyl compounds

The 2,4-dimethylquinoline isostere, 4,6-dimethylthieno[2,3-b]pyridine (27) was synthesised[268] in 80% yield from the reaction of (25) with acetylacetone.

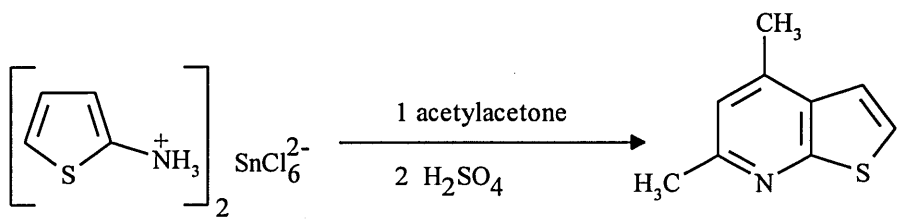

(25) (27)

The cyclisation step could also be effected by the use of zinc chloride or phosphorus pentoxide in xylene. The same reaction has also been reported by Abramenko[269].

Acetals and ketals of 1,3-dicarbonyl compounds have similarly provided thieno[2,3-b]pyridines in moderate yields. Thieno[2,3-b]pyridine (19) was

prepared[267] from the reaction of malondialdehyde tetraethylacetal with the tin salt (25).

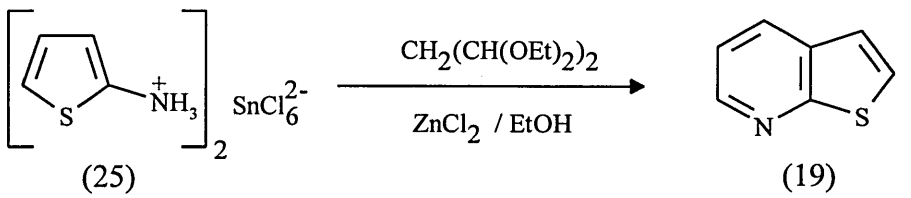

(25) (19)

The mechanism was presumed to be a stepwise process of hydrolysis of the acetal followed by Schiff base formation with the amine salt and dehydrative cyclisation. Thieno[2,3-b]pyridines were also prepared[267] from reactions of 2-aminothiophene with acetylacetone and 3-methylpentan-2,4-dione. It was also demonstrated[267] that a deactivating 2-acetyl group on the thiophene ring does not prevent cyclisation and 2-acetylthieno[2,3-b]pyridine could be prepared using malondialdehyde tetraethylacetal in 10% yield. This reaction was repeated with acetylacetone to give 2-acetyl-4,6-dimethylthieno[2,3-b]pyridine (28) in 42% yield.

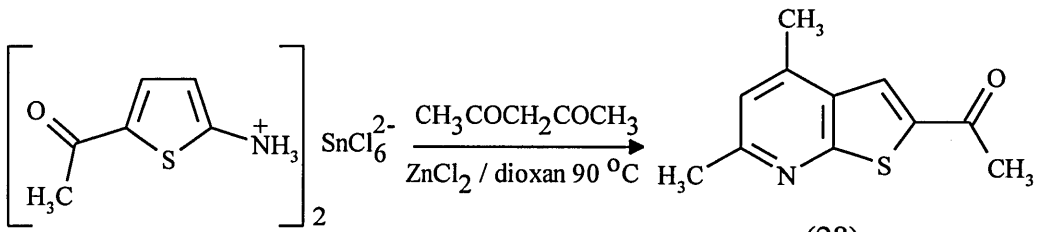

(28)

When the 2-aminothiophene salt (25) was heated with excess acetoacetaldehyde dimethylacetal in ethanolic hydrochloric acid, acetone was liberated and thienopyridine (29) was isolated as the main product (32%) with only 2-5% of 4- and 6-methyl thieno[2,3-b]pyridines formed. The mechanism of the reaction has been proposed [Scheme 2][267].

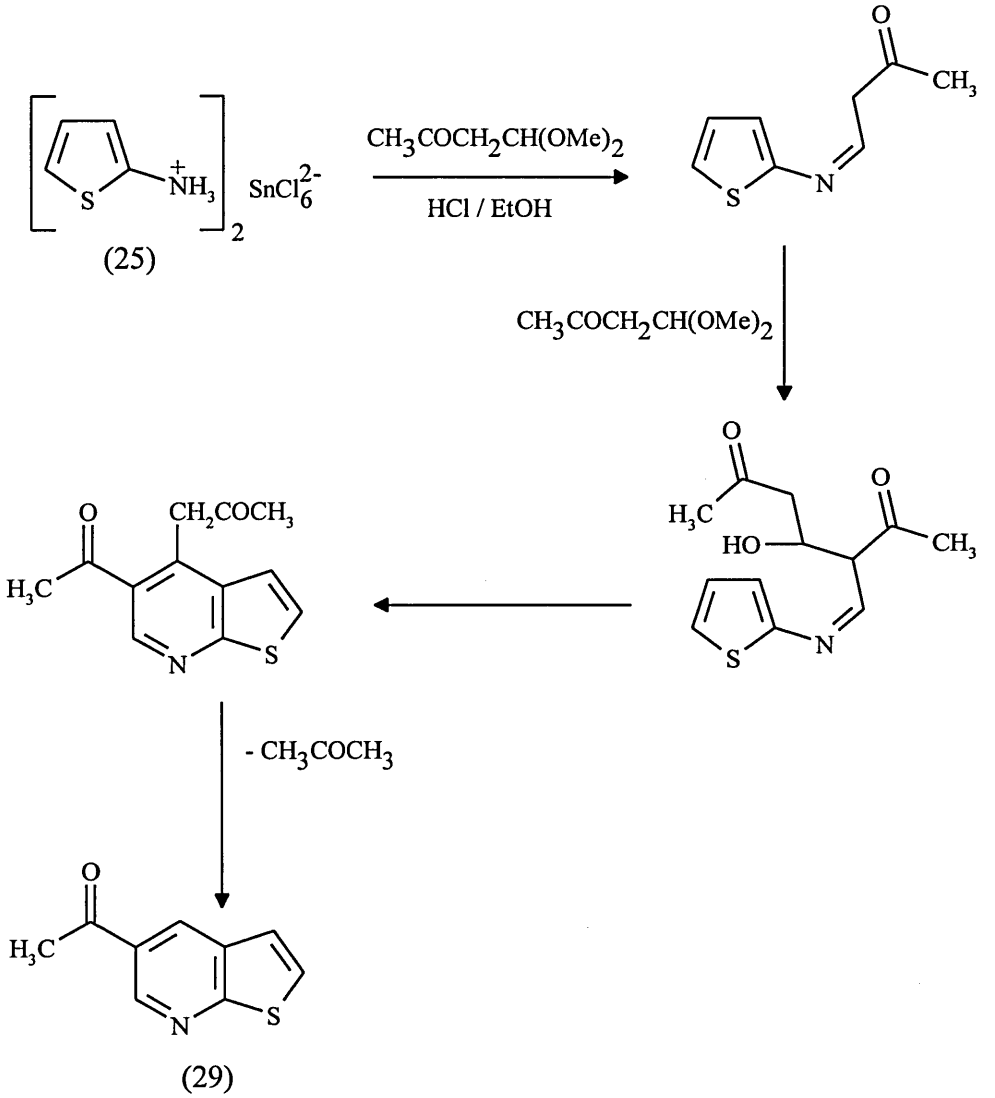

[Scheme 2]

The isolated products from this reaction differed quite considerably from the findings of Zhiryakov and Abramenko[270] who claimed that the only product isolated from the reaction of (25) with acetoacetaldehyde diethylacetal was 6-methylthieno[2,3-b]pyridine.

In a study designed to synthesise annelated models of NADH[271], thienopyridines (31) and (32) were prepared from 2-nitro-4-acetylthiophene (30) giving a 3:7 ratio of compounds (31):(32) in 50% overall yield [Scheme 3].

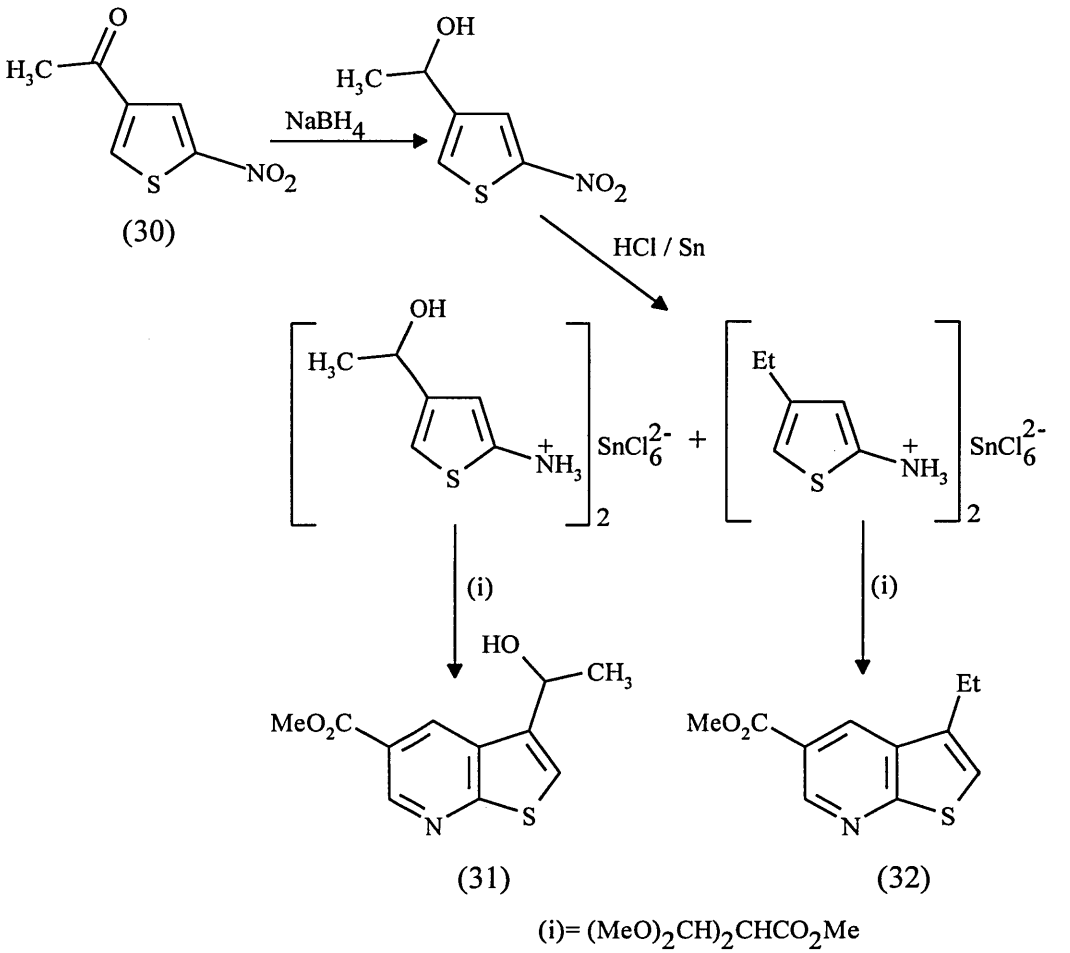

[Scheme 3]

However due to the difficulty in preparing malondialdehyde derivatives the enolate derivative 3,3-dimethoxy-2-formylpropionitrile sodium salt was reacted[271,272] with the tin salts of 2-aminothiophene, 2-aminothiophene-4-carboxylic acid and 2-aminobenzo[b]thiophene to give the corresponding thieno[2,3-b]pyridines in good yields [Equation 1].

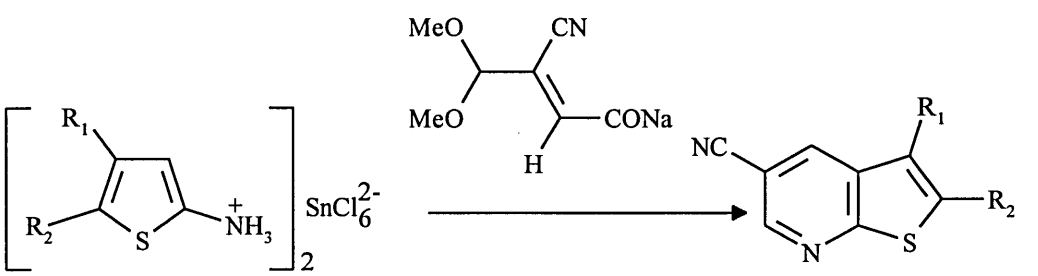

[Equation 1]

1.2.2.3 Cyclisation of 2-amino-3-carbonylthiophenes

The first application of this Friedlander type synthesis to thieno[2,3-b]pyridines was in the synthesis[273] of 6-phenylthieno[2,3-b]pyridine (34) from 2-nitrothiophene-3-carboxaldehyde (33) [Scheme 4].

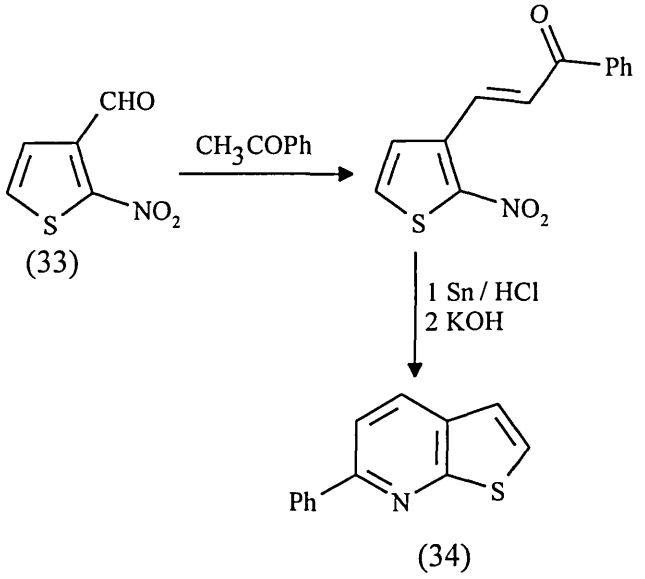

[Scheme 4]

This methodology was then adopted[274] to synthesise substituted thienopyridines [Equation 2]

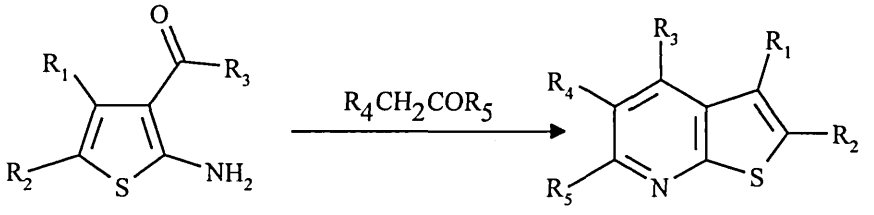

[Equation 2]

The Vilsmeier reaction has been utilised[275,276] to convert various 2-acylthienylamines into the 3-formyl derivatives which were cyclised by compounds containing an active methylene group [Scheme 5].

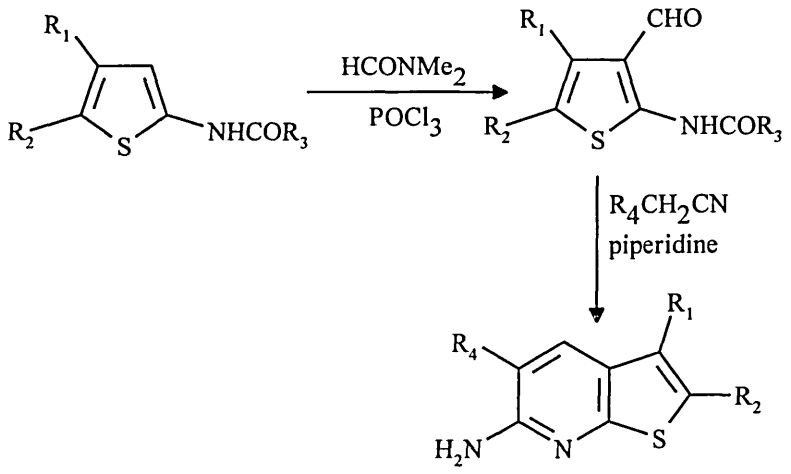

[Scheme 5]

Schäfer and co-workers had made use of a conventional approach initially[277] then in a variation 1,1-dimethylthio-2-nitroethylene was used as the cyclising agent[278] [Equation 3].

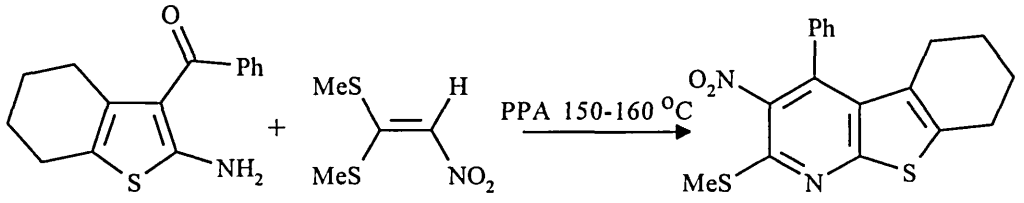

[Equation 3]

1.2.2.4 Base catalysed cyclisation of thiophene amides

In a novel variant of Camp's quinoline synthesis, the thienopyridone (36) was prepared[279] from the cyclisation of chloroacetylchloride with the aminothiophene-2-carboxylate derivative (35) [Scheme 6].

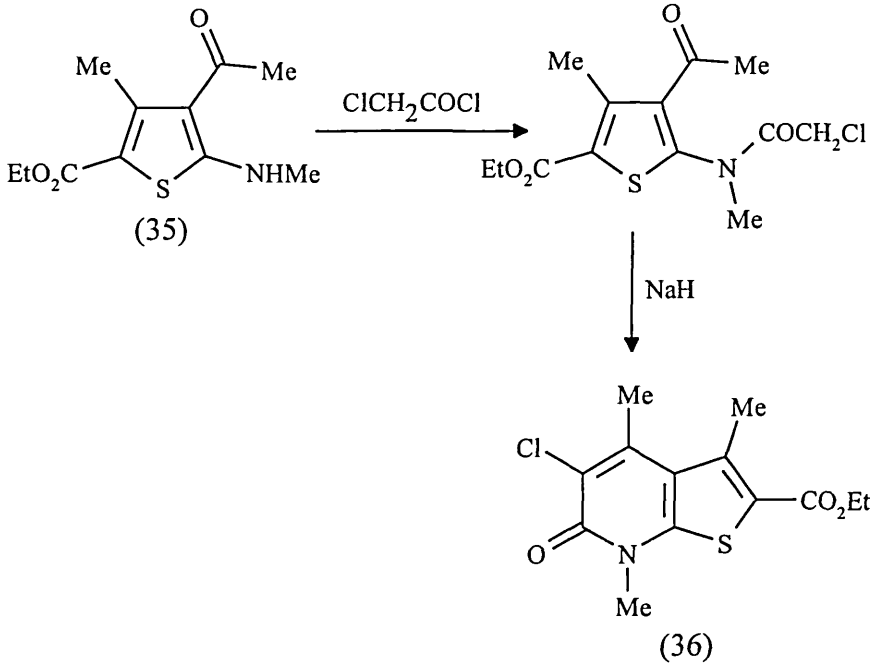

[Scheme 6]

Michael adducts (37) have also been shown[280] to undergo base catalysed cyclisation to give thienopyridine (38).

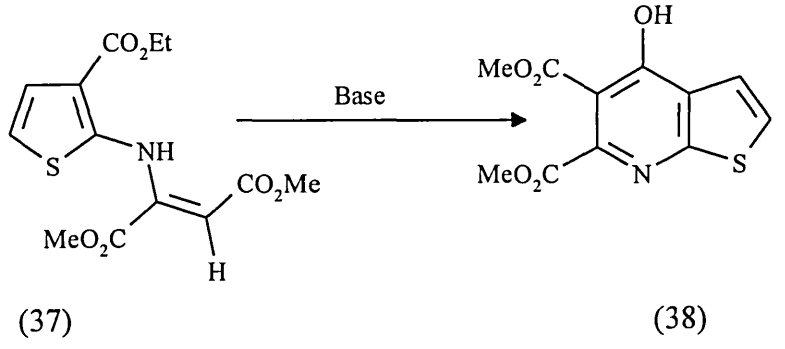

4,6-Bis(dimethylamino)thieno[2,3-b]pyridines (40) have been synthesised[281] via a hexamethylphosphoric triamide induced ring closure of 2-acetamido-3-thiophenecarboxylates (39).

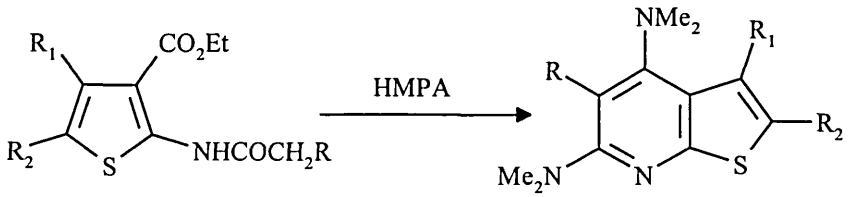

(39) (40)

When R_1=H reaction yields were a moderate 35-48% but fell dramatically to 10% if R_1 was a methyl or methylene group. The effect was even more pronounced when R_1=Ph whereupon no thienopyridine was isolated. It was proposed[281] that this was caused by steric hindrance at the 3 position which would inhibit cyclisation.

Furthermore, it was found[282] that reaction of substituted 2-amino-3-cyanothiophene (41) with ethyl aminocrotonate in the presence of catalytic amounts of p-toluenesulfonic acid afforded high yields of 2-[N-(3'-ethoxycarbonyl-2'-propenylamino)]-3-cyanothiophenes (42) which could be converted in high yield to the corresponding thienopyridine (43) [Scheme 7].

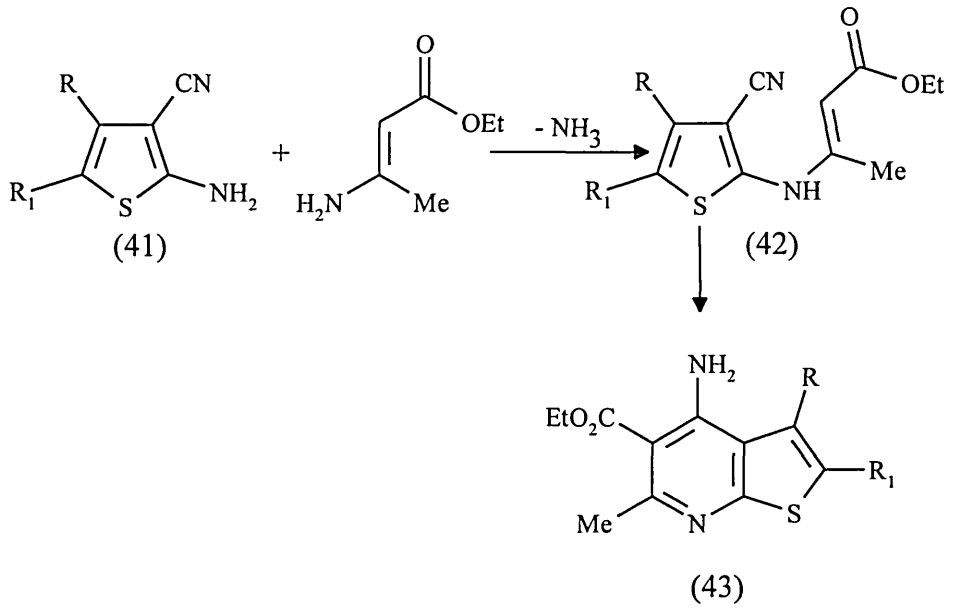

[Scheme 7]

When studying the reactivities of 4,6-dichlorothieno[2,3-b]pyridines, ethyl-4,6-dichlorothieno[2,3-b]pyridine-5-carboxylate (46) was synthesised[283] in three steps from ethyl-2-aminothiophene-3-carboxylate (44) via the thienopyridone (45) [Scheme 8].

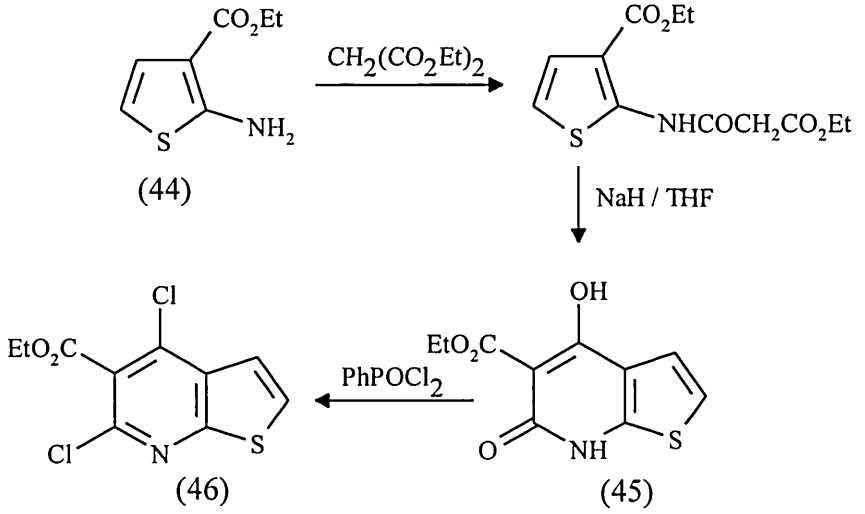

[Scheme 8]

1.2.2.5 Gould-Jacobs synthesis of thieno[2,3-b]pyridines

The first reported[284] application of the Gould-Jacobs synthesis to thienopyridines was the treatment of the tin salt of 2-aminothiophene (25) with ethoxymethylene derivatives of various active methylene compounds. Thermal cyclisation of the intermediates afforded the thieno[2,3-b]pyridines (47) [Scheme 9].

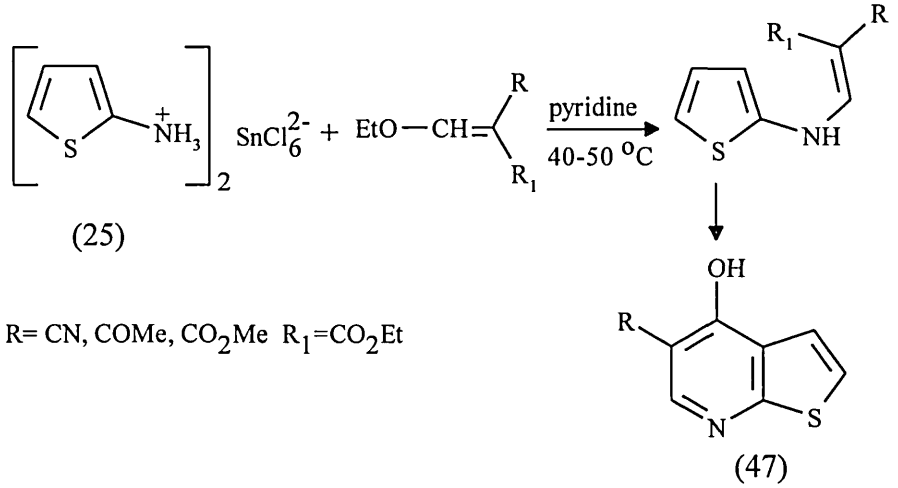

[Scheme 9]

In an attempt[285] to synthesise thienopyridine isosteres of the antibacterial agent nalidixic acid, a Gould-Jacobs condensation of substituted 2-aminothiophenes (48) with diethylethoxymethylene malonate was used to give the intermediate (49) which was thermally cyclised to the desired thieno[2,3-b]pyridines (50) [Scheme 10].

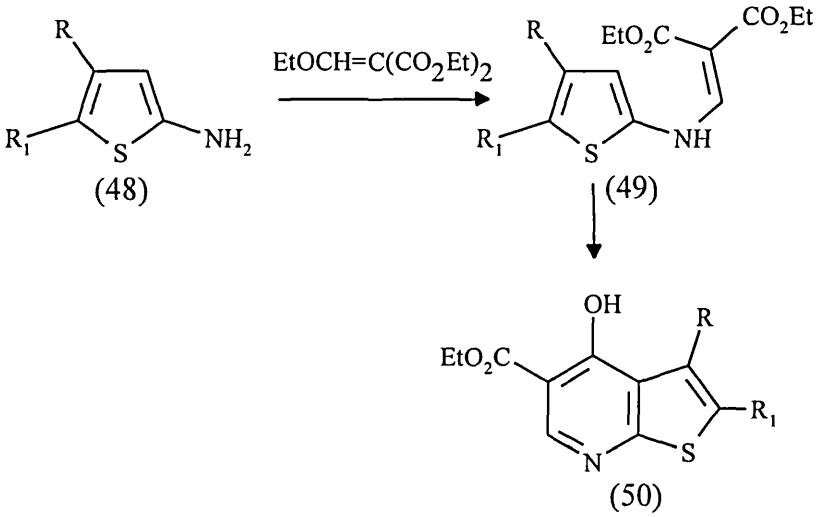

[Scheme 10]

In a related cyclisation step conducted in phosphoryl chloride the 4-chlorothienopyridine (51) was formed[286] in 55% yield.

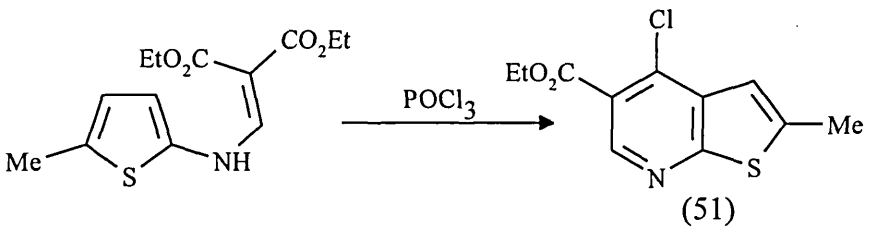

Enamines have also been cyclised[287] to thienopyridines using $AlCl_3$.

1.2.2.6 Vilsmeier reactions

The Vilsmeier-Haack reaction has been used[288] in the synthesis of 6-chlorothieno[2,3-b]pyridines (53) and 5-formyl-6-chlorothieno[2,3-b]pyridines (54) from 2-acetamidothiophenes (52).

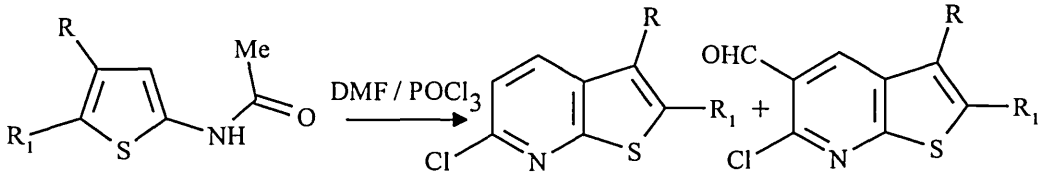

The conditions of this reaction were studied in order to optimise the yields of (53) and (54)[289]. Prolonged heating with a 3:1 ratio of $POCl_3$:DMF gave compounds (53) optimally in 66-80% yield whereas formation of (54) was maximised using a 7:3 ratio of $POCl_3$:DMF. The pathways of formation of both products have also been proposed[289,290] [Scheme 11, Scheme 12]. The principal difference between the two routes is that in the synthesis of (54), the ring and the sidechain both undergo formylation prior to cyclisation whereas in the synthesis of (53) only the thiophene ring is formylated prior to cyclisation.

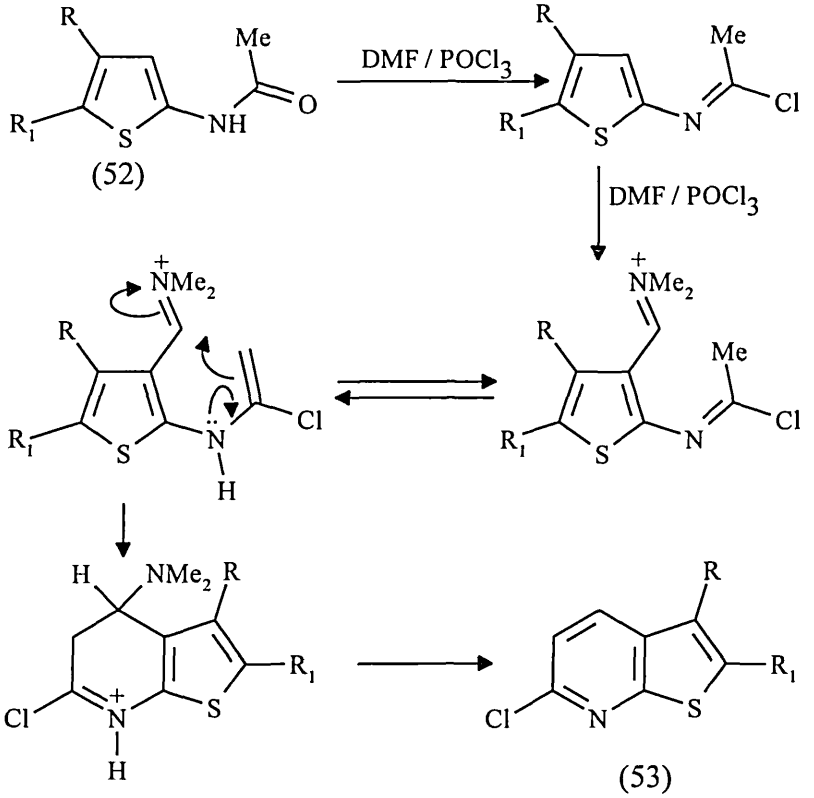

[Scheme 11]

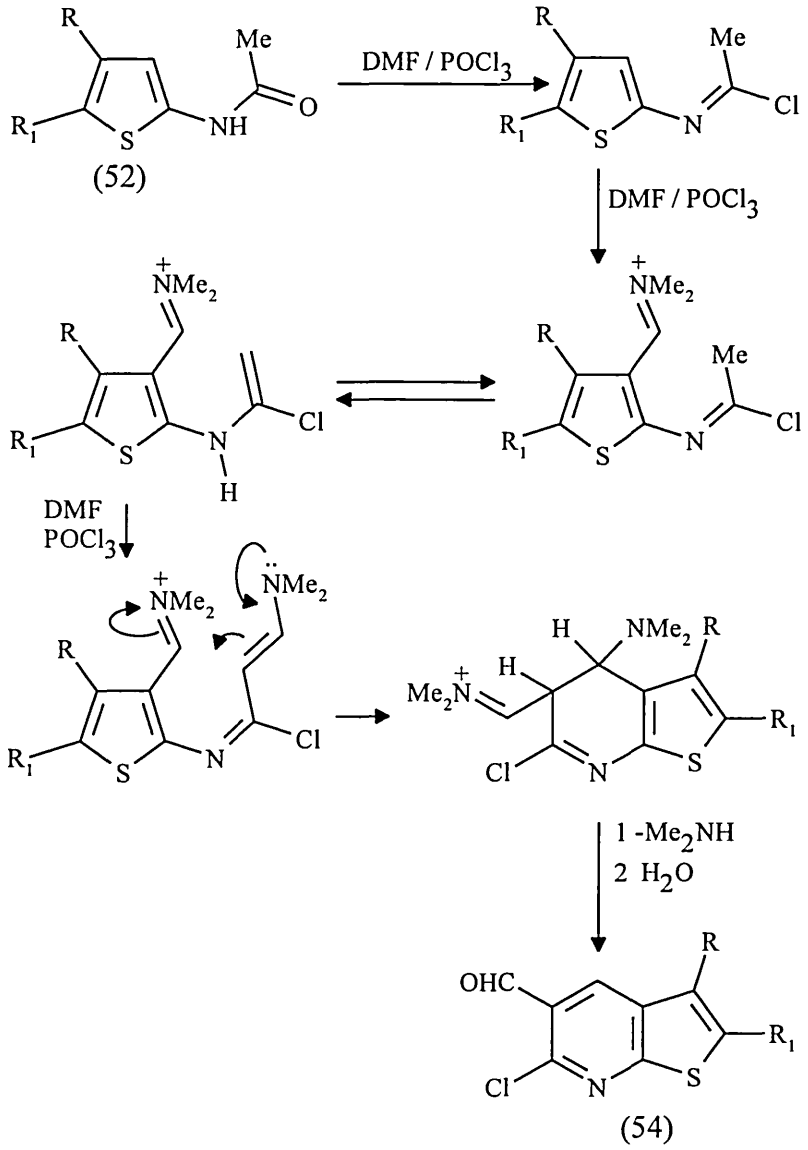

[Scheme 12]

1.2.3 Synthesis of thieno[2,3-b]pyridines from pyridine precursors

1.2.3.1 Early synthesis

The first report of this type of synthesis was by Koenigs and Geisler[291] in 1924 who claimed that 3-hydroxythieno[2,3-b]pyridine was formed from treatment of 2-pyridylthioacetic acid with acetic anhydride. This was questioned by Chichibabin[292] who showed that the product obtained was different from an

authentic sample of 3-hydroxythieno[2,3-b]pyridine (56) prepared from 3-carbomethoxy-2-chloropyridine (55) [Scheme 13].

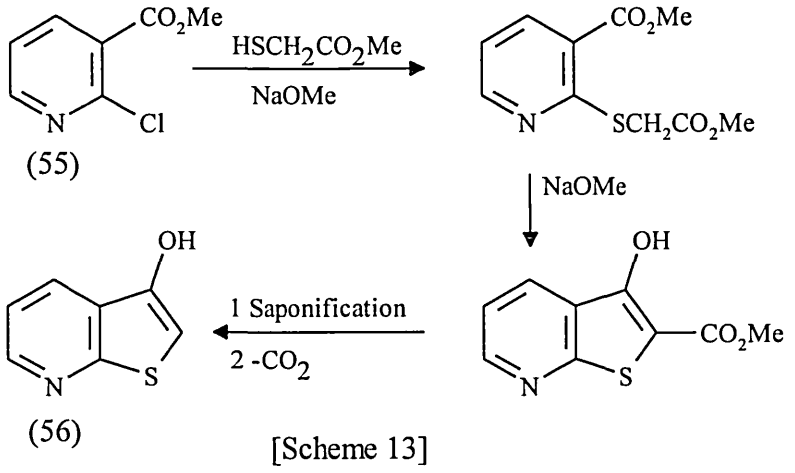

[Scheme 13]

The true structure of Koenig's product was later identified[293] as (57).

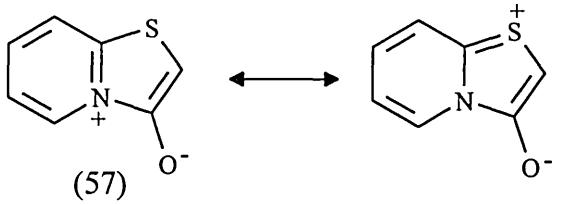

1.2.3.2 Synthesis from 2-halo-3-cyanopyridine derivatives

It was reported[294,295] that reaction of 2-chloro-3-cyanopyridine (58) with ethyl mercaptoacetate and base gave the thieno[2,3-b]pyridine (59) [Scheme 14]. The reaction is thought to proceed via nucleophilic displacement of the chlorine by ethyl mercaptoacetate followed by base promoted intramolecular cyclisation. Compound (59) has also been prepared[296] using a variation of this reaction. Highly substituted derivatives have been synthesised[297-299] using similar methodology.

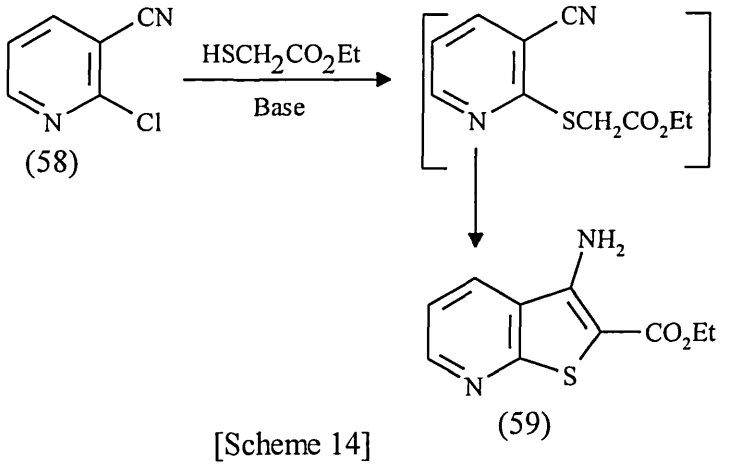

[Scheme 14]

1.2.3.3 Synthesis from substituted pyridine-2-thiols

The synthesis[270] of thienopyridine (61) from reaction of thiol (60) with chloroacetic acid followed by cyclisation and acetylation has been described [Scheme 15].

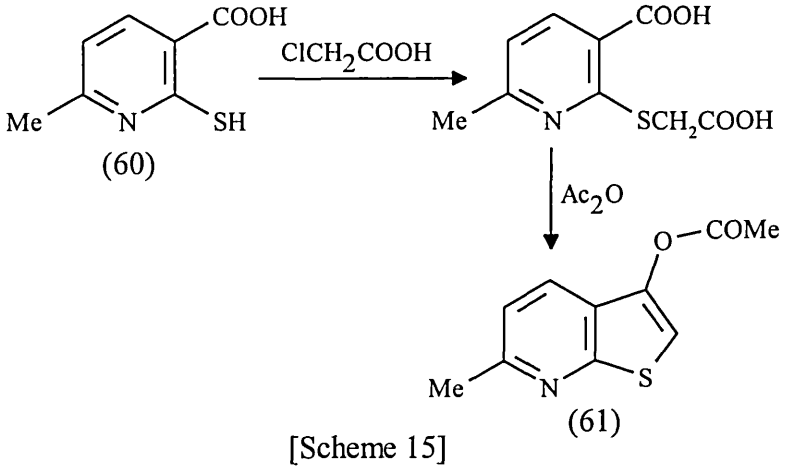

[Scheme 15]

The general reaction between substituted pyridine-2-thiols and halogen compounds with an activated methylene has been used as a popular route to thieno[2,3-b]pyridines[249,300-306] [Scheme 16]. Initial nucleophilic attack by the sulfur affords the activated sulfide which cyclises to the thienopyridine in good yields.

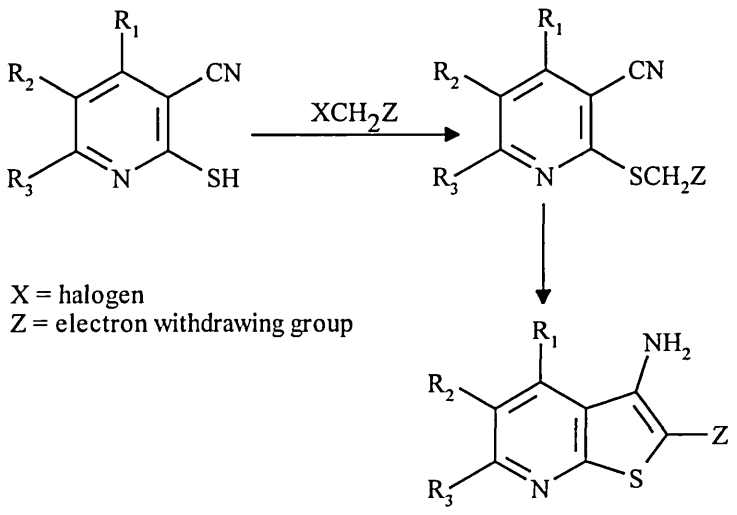

[Scheme 16]

A variation of this reaction was utilised[307] where 2,6-dimethylthiopyridine-3-carboxaldehyde (62) was reacted with chloroacetic acid to afford the thieno[2,3-b]pyridine (63) as a potential antiviral agent.

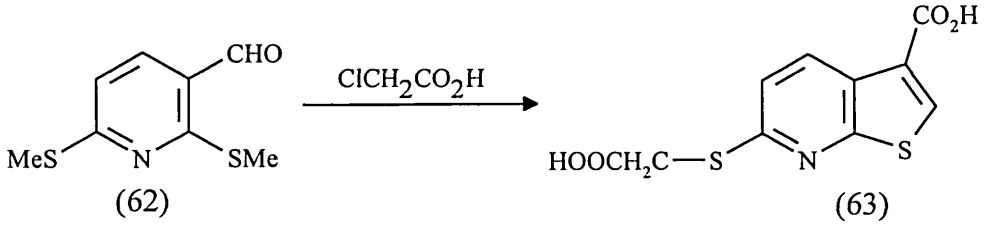

(62) (63)

1.2.3.4 Synthesis from pyridine thiones

There is probably more literature published on this synthetic route to thieno[2,3-b]pyridines than any other. The pyridine-2-thione is alkylated by compounds that contain a halogen atom adjacent to an active methylene group, then undergoes cyclisation to give the thieno[2,3-b]pyridine. Russian workers[308-322] have published a number of papers on the use of this method to prepare substituted thienopyridines [Equation 4].

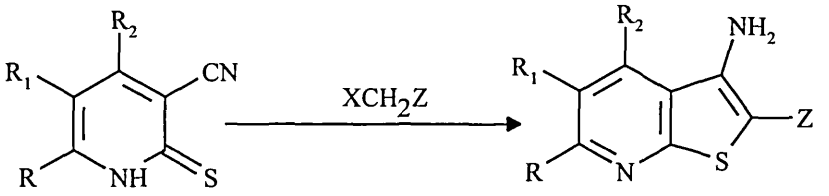

X = halogen
Z = COAr, CO_2R_3, CO_2H, $CONH_2$, CN

[Equation 4]

Thiolate salts (64) have also been alkylated[323,324] by active methylene compounds and cyclised to give substituted 3-aminothieno[2,3-b]pyridines (65) [Scheme 17].

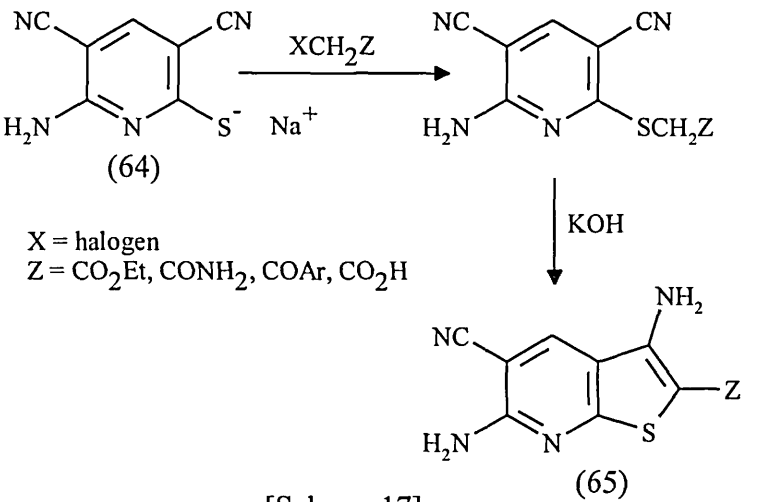

X = halogen
Z = CO_2Et, $CONH_2$, COAr, CO_2H

(65)

[Scheme 17]

Numerous other publications on the preparation of thieno[2,3-b]pyridines from pyridine thiones are available[325-332]. For example, alkylation[329] of 3-cyanopyridin-2(1H)-thione (66) with phenacyl bromide followed by spontaneous cyclisation afforded the thieno[2,3-b]pyridine (67) in 45-90% yield.

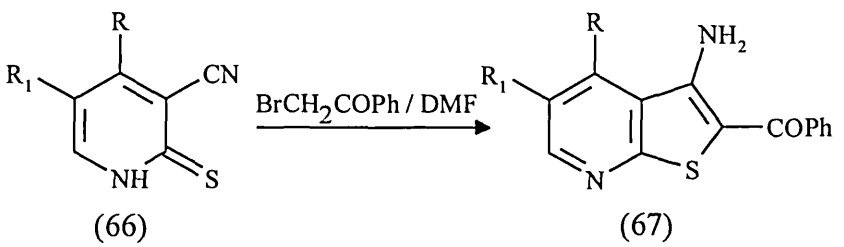

(66) (67)

In a variation[333] the thione (68) was reacted with an α-bromocarbonyl compound in the presence of potassium hydroxide to give the S-alkylated derivatives which cyclised in high yields by intramolecular aldol condensation.

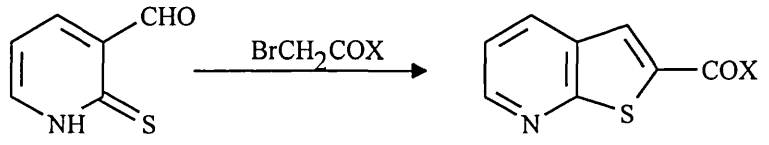

(68)

X = OEt, Ar

1.2.3.5 Synthesis from *ortho* halogenated pyridine derivatives containing an active methylene group

Thieno[2,3-b]pyridines have been prepared from the reaction of phenylisothiocyanate and carbon disulfide with *ortho* halogenated pyridine derivatives containing a methylene group activated by a nitrile or ester[250,251]. Reaction of (69a-c) with carbon disulfide in the presence of base followed by quenching with methyl iodide afforded the 2,3 substituted thieno[2,3-b]pyridines (70a-c) in 36-43% yield.

(69a-c) (70a-c)

a R=CO_2Et, b R=CO_2Me, c R=CN

The reaction is thought to proceed via base removal of the methylene protons followed by formation of a ketene dithioacetal dianion. One of the thiolate

anions displaces the halogen and the other is alkylated with methyl iodide [Scheme 18].

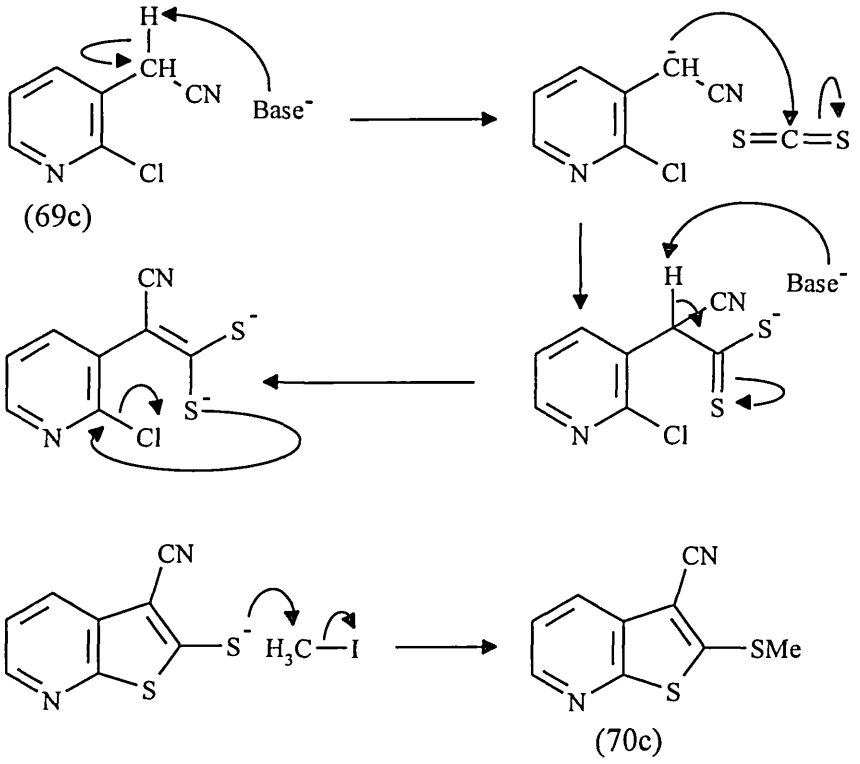

[Scheme 18]

Alkylation of the thiolate anion has also been achieved using ethyl chloroacetate[251]. The reaction of pyridines (69a-c) with phenylisothiocyanate also resulted[251] in the synthesis of thieno[2,3-b]pyridines in moderate yields. The thienopyridines however were not alkylated by the methyl iodide present, but did protonate when poured onto water.

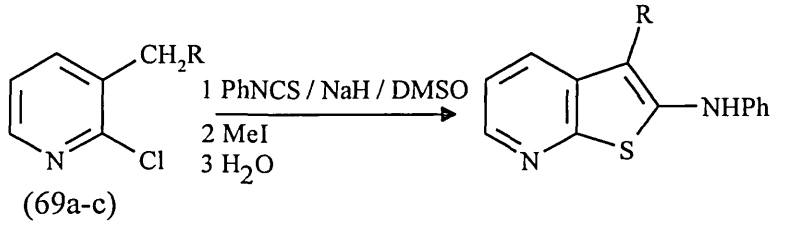

a R=CO_2Et, b R=CO_2Me, c R=CN

1.2.4 Miscellaneous preparations

Klemm and McCoy[334] reported the reaction of 3-vinylpyridine (71) with hydrogen sulfide at 630 °C to give a low yield of the parent thieno[2,3-b]pyridine (19) and thieno[3,2-c]pyridine (23).

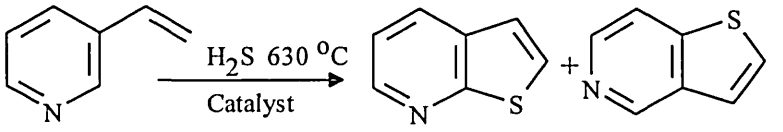

(71) (19) (23)

The reaction with 2-methyl-5-vinyl pyridine (72) also produced thienopyridines in low yields. The mechanism of the reaction was postulated to involve a non-catalytic thermal process whereby free radical substitution into the pyridine ring predominates at the α position.

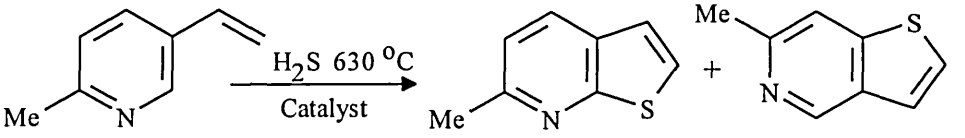

(72) 2.2% 0.3%

The synthesis[335] of 2,2-diphenyl-2,3-dihydrothieno[2,3-b]pyridine (74) from 2-mercapto-3-(2-hydroxy-2,2-diphenylethyl)pyridine (73) was achieved by the treatment of (73) with cold concentrated sulfuric acid.

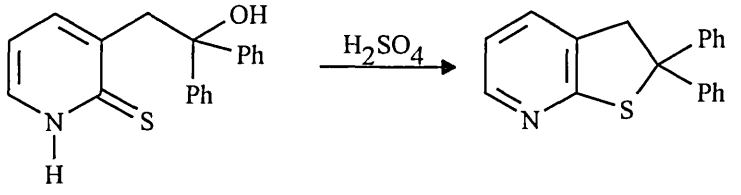

(73) (74)

The pyridinium salt (75) has been cyclised to thieno[2,3-b]pyridine derivative (76) from reaction with methylthioglycollate[336].

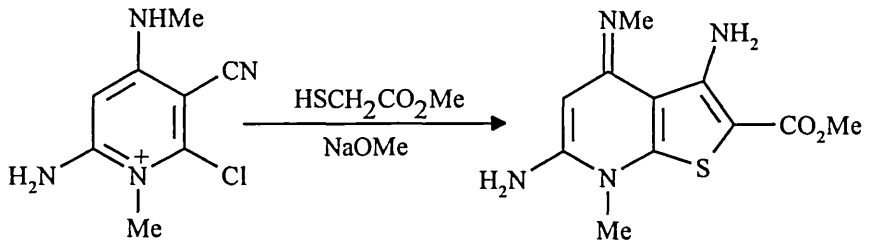

(75) (76)

After refluxing pyridin-3-ylpropiolic acid (77) in thionyl chloride a low yield of 2-carboethoxy-3-chlorothieno[2,3-b]pyridine (78) was isolated[337]. It was proposed[337] that the reaction may take place by the formation of a pyridinium salt between (77) and thionyl chloride which undergoes an addition reaction on the triple bond to give a sulfur containing intermediate which cyclises via nucleophilic attack onto the pyridine ring.

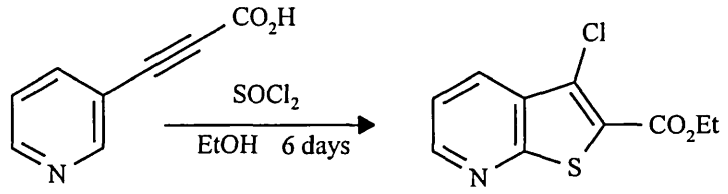

(77) (78)

Furthermore it was discovered[338] that reaction of the phenylethynylpyridine (79) with sodium hydrosulfide prepared *in situ* from the saturation of a solution of sodium ethoxide in ethanol with hydrogen sulfide, afforded 2-phenylthieno[2,3-b]pyridine (80) in 69% yield.

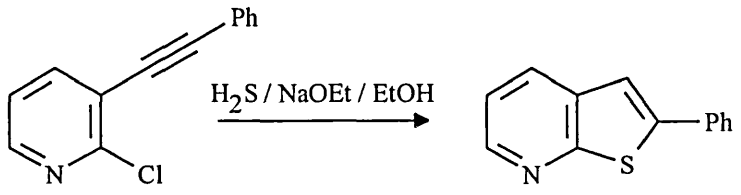

(79) (80)

A most interesting synthesis of thienopyridines from an intramolecular Diels-Alder reaction has been described[339,340]. Substituted 3-thio 1,2,4-triazenes (81) reacted intramolecularly with electron rich dienophiles to give thienopyridines (82) [Scheme 19]. When the starting triazene was oxidised to the sulfoxide (83) with *m*-chloroperoxybenzoic acid, cyclisation took place spontaneously to give the thienopyridine-S-oxide derivatives which could be converted to the thienopyridines (82) [Scheme 20].

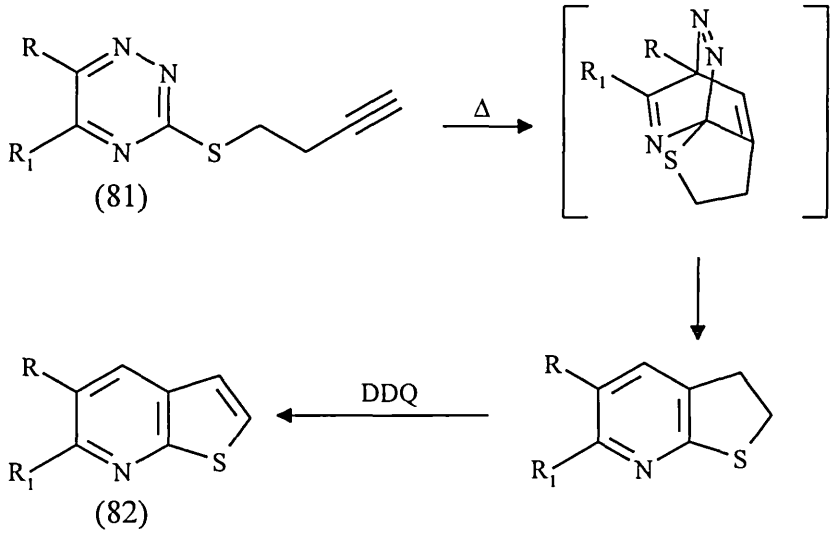

[Scheme 19]

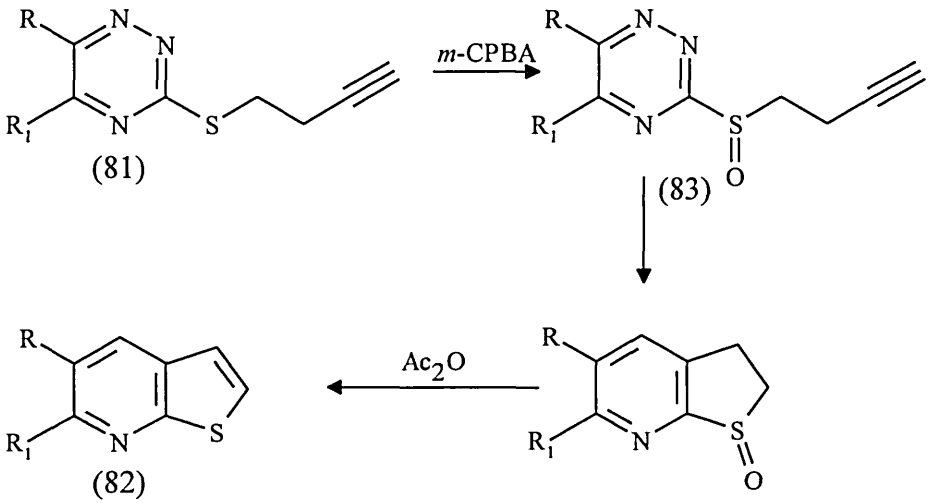

[Scheme 20]

1.2.5 Reactions of thieno[2,3-b]pyridines

1.2.5.1 Electrophilic substitution

Electrophilic substitution of thieno[2,3-b]pyridine (19) was predicted[267] to occur at the C-3 position rather than the C-2 position. The reaction of (19) with deuterated sulfuric acid at 98.5 ^{o}C gave fastest exchange at the C-3 position[267,341]. Bromination of (19) with bromine in carbon tetrachloride[267] led to the 2,3-dibromo derivative (84) in low yield.

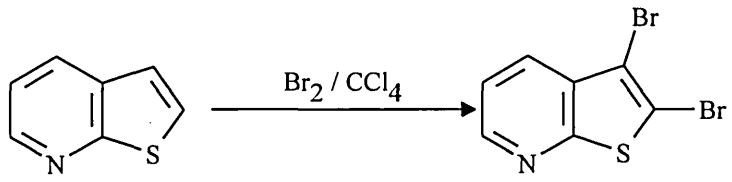

(19) (84)

Monohalogenated thienopyridines (85a-c) have been prepared[342] in 27-40% yields from (19) by reaction with elemental halogen and silver sulfate in the presence of sulfuric acid. Compound (85b) could also be prepared[342] in improved yield (57%) in non-acidic, non-aqueous conditions from reaction of (19) with dry bromine in chloroform in the presence of a buffer. When chlorine gas was bubbled through a solution of (19) in a chloroform/water mixture, two products were isolated which were identified as the monochloro (85a) and dichloro (86) thieno[2,3-b]pyridines.

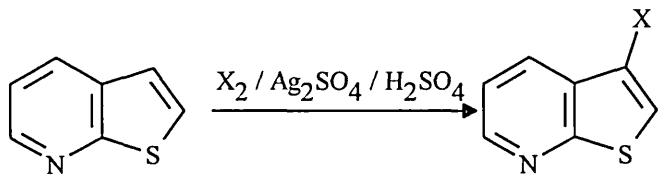

(19) (85a-c)

a X=Cl, b X=Br, c X=I

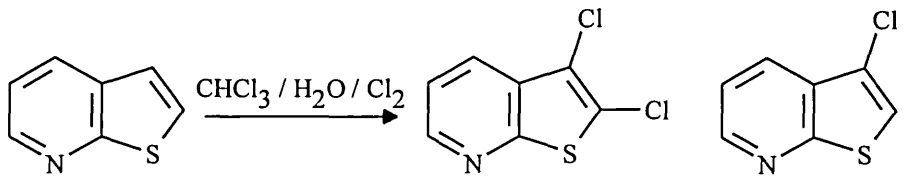

(19) (86) 40% (85a) 27%

Nitration of the halogenated thienopyridines (85a-c) gave[342] the 2-nitro-3-halothieno[2,3-b]pyridines (87a-c) in 22-47% yields. Nitration[343] of the parent compound (19) and 5-ethylthieno[2,3-b]pyridine[344] under mixed acid conditions have also been reported. Nitration occurred at the C-3 positions in yields of 55 and 53% respectively.

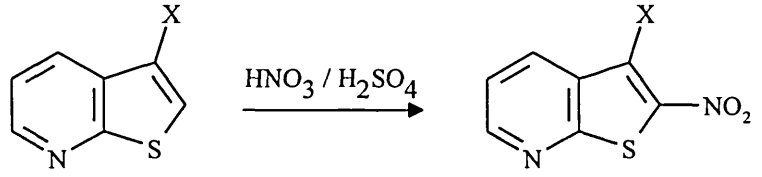

(85a-c) (87a-c)

a X=Cl, b X=Br, c X=I

It was also found that the nitration[288] of 2-bromo-6-chlorothieno[2,3-b]pyridine (88) gives the 3-nitro derivative (89) in 96% yield.

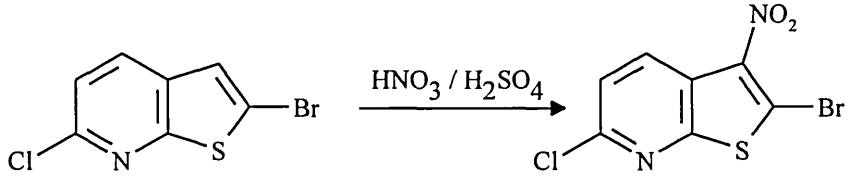

(88) (89)

Electrophilic substitution reactions of hydroxythienopyridines and thienopyridones have been studied[345]. 4-Hydroxythieno[2,3-b]pyridine (90) reacts with bromine in acetic acid and with diethylamine/formaldehyde to give substitution in the pyridine ring but treatment with nitric acid at 100 ^{o}C afforded 2-nitro-4-hydroxythieno[2,3-b]pyridine (91) as the major product [Scheme 21].

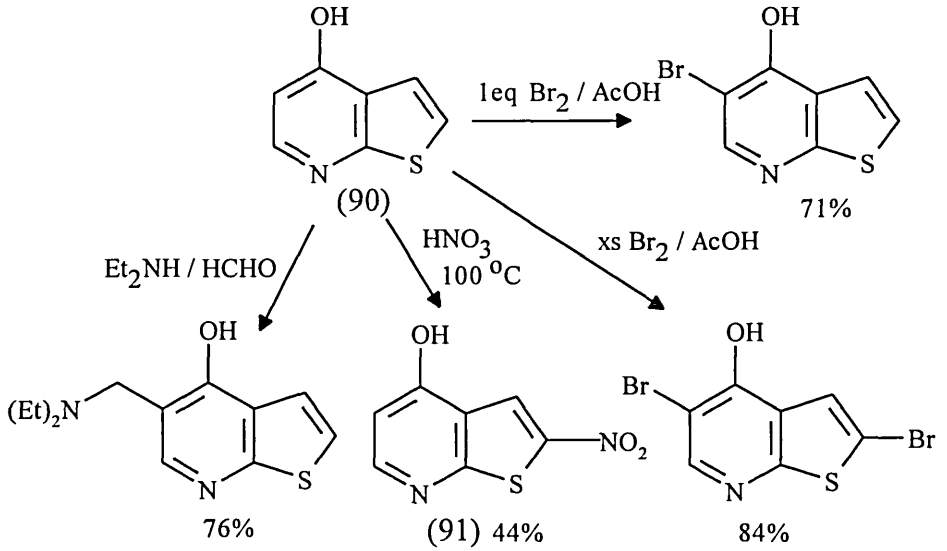

[Scheme 21]

7-methylthieno[2,3-b]pyridin-4(7H)-one (92) was subjected to the same reactions[345] giving a similar substitution pattern.

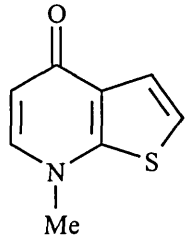

(92)

Reaction of the hydroxythieno[2,3-b]pyridone (93) with bromine in acetic acid gave the 2-bromo compound (94) but reaction with other electrophiles resulted in decomposition products only[345].

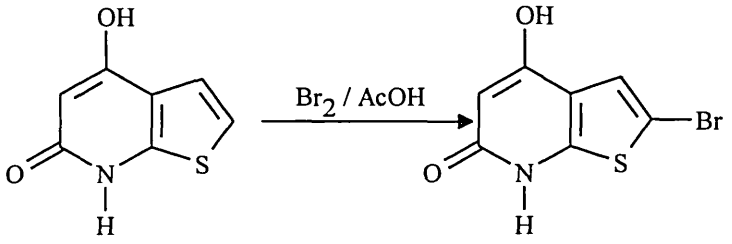

(93) (94)

1.2.5.2 Nucleophilic substitution

There is not a great deal of literature on the nucleophilic substitution reactions of thieno[2,3-b]pyridines. The only reactions published for the unsubstituted parent compound (19) are those with alkyl lithium reagents[267]. Treatment of (19) with *n*-butyllithium at 25-35 °C followed by loss of lithium hydride gave the 6-*n*-butyl derivative (95) in 47% yield. Reaction of (19) with methyllithium at lower temperatures however afforded only 25% of 6-methylthieno[2,3-b] pyridine and 75% of starting material. It was proposed[267] that the recovered starting material was the result of metalation at the position *ortho* to the sulfur atom which competes with the nucleophilic reaction and appears to be favoured at lower temperatures.

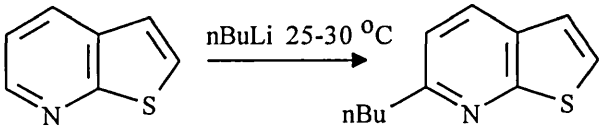

(19) (95)

Reaction of both 3-bromothieno[2,3-b]pyridine[342] and 5-bromothieno[2,3-b] pyridine[346] with copper (I) cyanide in refluxing DMF gave 3-cyanothieno[2,3-b]pyridine (45%) and 5-cyanothieno[2,3-b]pyridine (29%) respectively. The copper promoted nucleophilic substitution of the 6-chloro group of (96) has also been investigated[347]. Heating 6-chlorothieno[2,3-b]pyridine (96) with excess γ-diethylaminopropylamine and a small amount of copper powder in a sealed tube at 168 °C afforded the 6-substituted thienopyridine (97) in 58% yield.

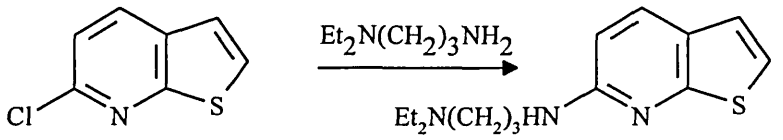

(96) (97)

Similarly nucleophilic substitution reactions of 2-bromo-6-chlorothieno[2,3-b]pyridine (88) have been reported[348]. Replacement of the 6-chloro group was easily achieved with thiophenol or piperidine.

Nucleophilic substitutions of some highly substituted thieno[2,3-b]pyridones have also been described[283] (see section 1.2.2.4, Scheme 8). Treatment of (46) with one equivalent of ethoxide in ethanol gave nucleophilic substitution at the pyridine C-4 position. When excess ethoxide was used substitution occurred at the C-4 and C-6 positions. A similar substitution pattern was observed for 4,6-dichlorothieno[2,3-b]pyridine. It was concluded[283] that unlike their 2,4-dichloroquinoline isosteres 4,6-dichlorothieno[2,3-b]pyridines undergo nucleophilic substitution almost exclusively at the C-4 position.

It was found that some nitrogen nucleophiles but not oxygen nucleophiles can displace[251] the thiomethyl group of (70c).

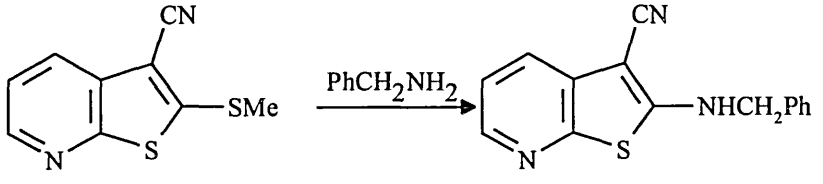

(70c)

The thiomethyl group of compound (70c) was oxidised[251] to the sulfoxide and sulfone, and reactivities of the three compounds with the anion of diethylmalonate were compared. The sulfide (70c) did not undergo nucleophilic

substitution but both the sulfoxide and the sulfone did with the latter being the most reactive.

1.2.5.3 Metalation of thieno[2,3-b]pyridines

It was originally reported[267] that reaction of thieno[2,3-b]pyridine with methyllithium at -25 °C gave a mixture of 25% of 6-methylthieno[2,3-b]pyridine and 75% of starting material. The high return of starting material was believed to come from the hydrolysis during work-up of 2-lithiothieno[2,3-b]pyridine. This was further corroborated by repetition of the reaction and hydrolysis first with deuterium oxide and then water which gave approximately equal amounts of the 2-D and 2-H compounds. Further reactions[349] of thieno[2,3-b]pyridine (19) with *n*-butyllithium and *N,N,N,N*-tetramethylethylenediamine (TMEDA) also gave 2-lithiothieno[2,3-b]pyridine (98) which upon reaction with DMF afforded the formyl derivative (99) in 66% yield [Scheme 22].

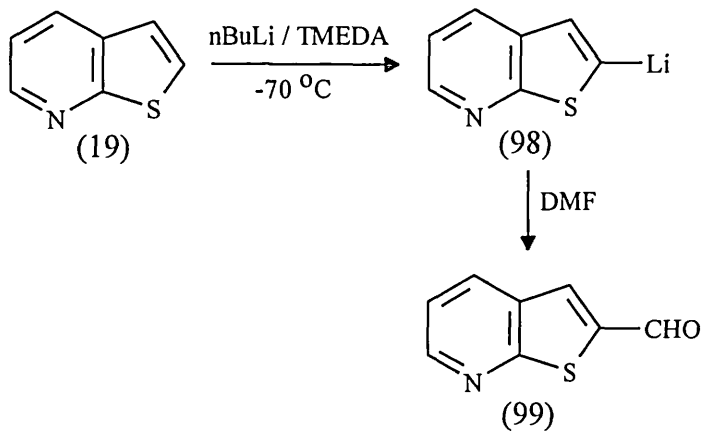

(19) (98) (99)

[Scheme 22]

3-Lithiated derivatives have been prepared[349] from lithium - halogen exchange reactions between 3-bromothieno[2,3-b]pyridine (85b) and *n*-butyllithium at -70 °C. Reactions of 3-lithiothieno[2,3-b]pyridine (100) with a number of carbonyl compounds have been described [Scheme 23].

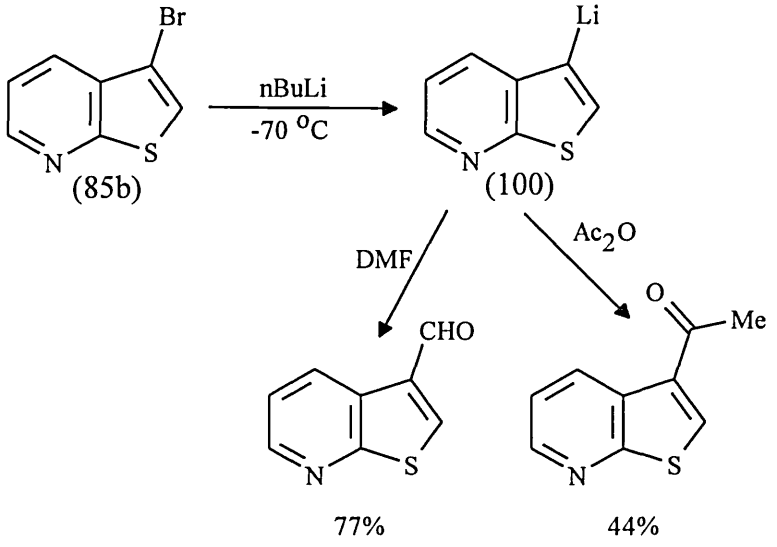

[Scheme 23]

The lithiation of 2-bromo-6-chlorothieno[2,3-b]pyridine (88) has been studied[288,348]. Reaction of (88) with *n*-butyllithium at -70 °C gave 2-lithio-6-chlorothieno[2,3-b]pyridine (101) which was reacted with several electrophiles [Scheme 24].

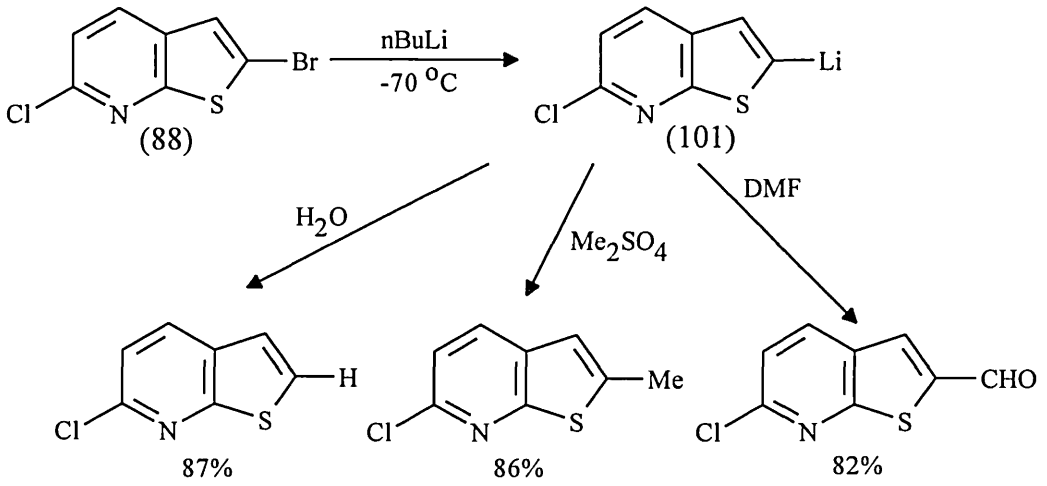

[Scheme 24]

1.2.5.4 Oxidation of thieno[2,3-b]pyridines

The oxidation of thieno[2,3-b]pyridines to their respective N-oxide derivatives has been achieved using 30% hydrogen peroxide in glacial acetic acid[350], *m*-chloroperoxybenzoic acid[351] and magnesium monoperoxyphthalate[352,353].

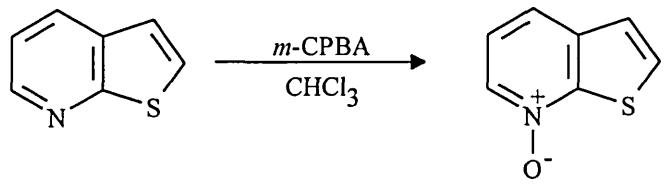

(19) (102)

The attempted[354] S-oxidation of thieno[2,3-b:4,5-b']dipyridine (103) in aqueous acetonitrile with an equimolar amount of iodobenzene dichloride gave a low yield of the sulfoxide (104). However the parent thieno[2,3-b]pyridine (19) gave a mixture of chlorinated products. Compound (103) was converted to the sulfone in 41% yield[354] by bubbling chlorine gas through a solution of (103) in carbon tetrachloride, followed by hydrolysis. Thieno[2,3-b]pyridine-1,1-dioxide (105) was synthesised[355] from reaction of (19) with sodium hypochlorite and dilute hydrochloric acid.

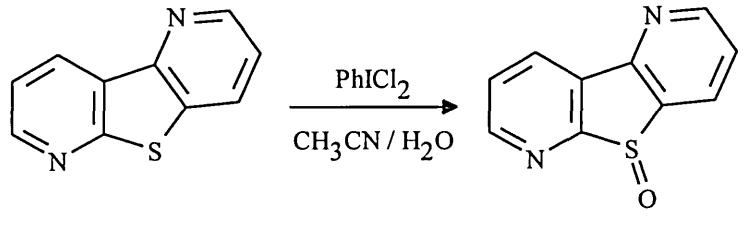

(103) (104)

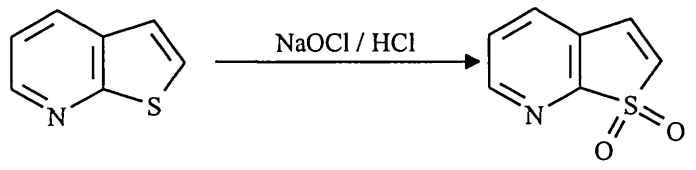

(19) (105)

1.2.5.5 Reactions of thieno[2,3-b]pyridine-7-oxides

Thieno[2,3-b]pyridine-7-oxide (102) has been nitrated by two methods[350]. Reaction with nitric acid and sulfuric acid at 90-120 °C gave 4-nitrothieno[2,3-b]pyridine-7-oxide (106) but nitration with nitric acid and glacial acetic acid gave 5-nitrothieno[2,3-b]pyridine-7-oxide (107) [Scheme 25]. It was proposed that the mechanism involved "normal" electrophilic attack of nitronium ions onto unprotonated starting material (102) to give (106). For the nitric/acetic acid reaction the concentration of nitronium ions was thought to be greatly reduced and a mechanism involving cations obtained from the protonation of water, nitric acid and acetic acid was suggested.

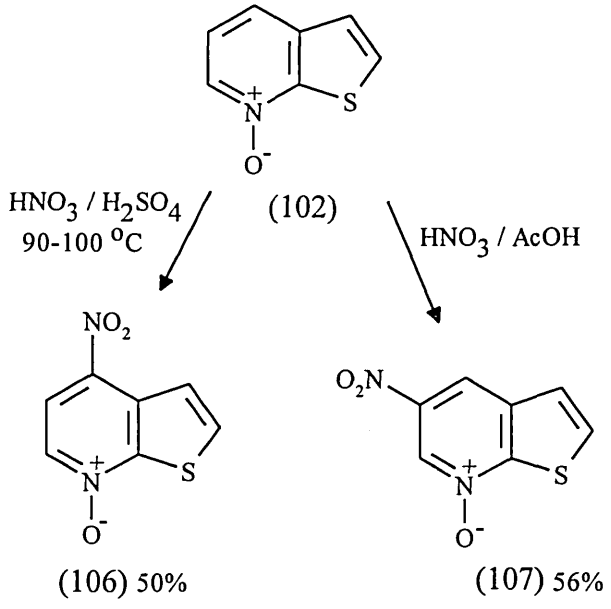

[Scheme 25]

Nucleophilic substitution reactions of thieno[2,3-b]pyridine-7-oxides have also been described. Reaction of (102) with phosphoryl chloride[356] gave two products (96) and (108) arising from α and γ substitution of the pyridine ring.

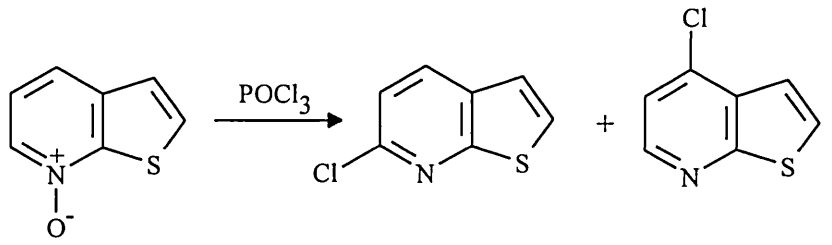

(102) (96) 31% (108) 54%

Reaction of (102) with acetic anhydride[356] followed by hydrolysis afforded the thienopyridone (109) and 5-hydroxythieno[2,3-b]pyridine (110).

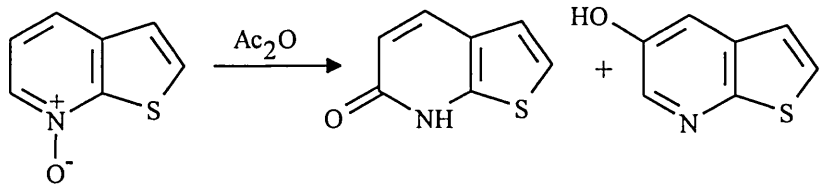

(102) (109) 13% (110) 4%

Nucleophilic substitution of 4-nitrothieno[2,3-b]pyridine-7-oxide (106) with acetyl chloride afforded the 4-chloro N-oxide (111) in 81% yield[350] which was further substituted with various nitrogen nucleophiles [Scheme 26].

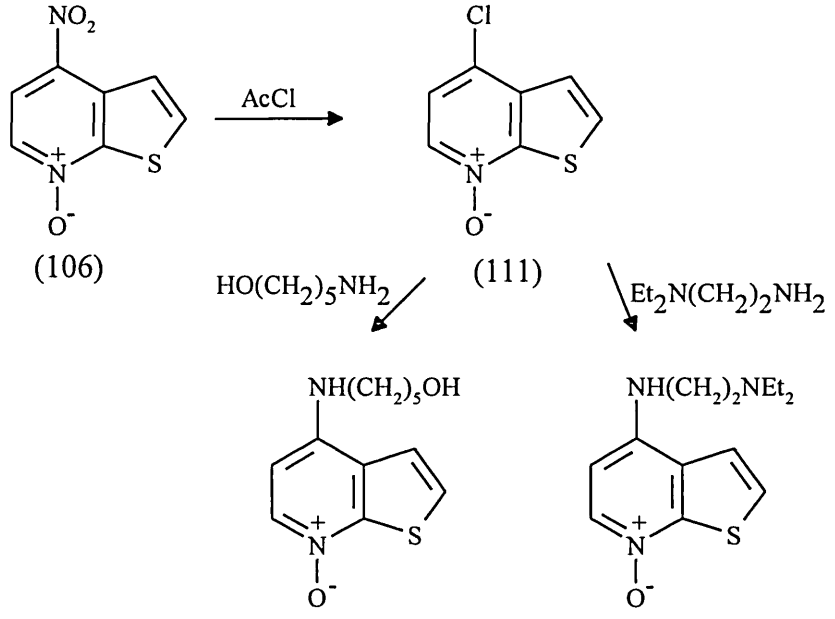

(106) (111)

[Scheme 26]

It was found[357] that thieno[2,3-b]pyridine-7-oxides reacted under Reissert-Henze conditions to introduce a cyano group at the pyridine α position [Equation 5]. The reaction was attempted with 5-nitrothieno[2,3-b]pyridine-7-oxide and gave only a small amount of 6-cyanothieno[2,3-b]pyridine but the 4-nitro isomer (106) reacted in a refluxing chloroform/water mixture to give 6-cyanothieno[2,3-b]pyridine (112) and 4-chloro-6-cyanothieno[2,3-b]pyridine (113).

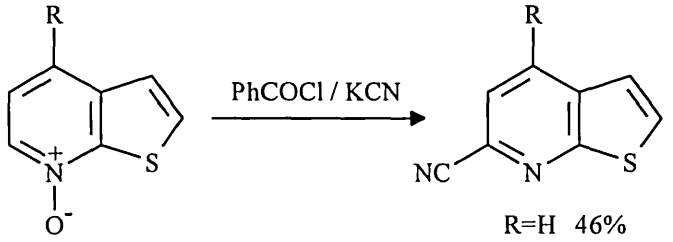

[Equation 5]

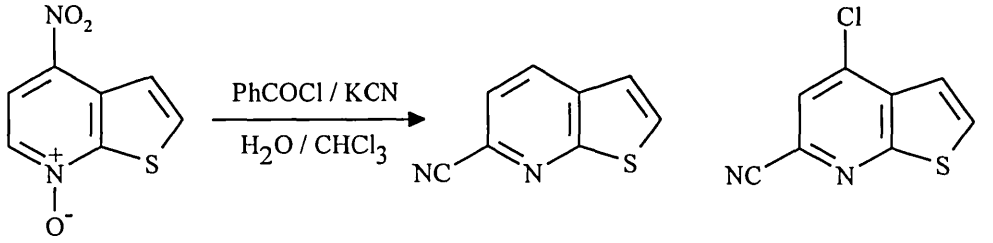

(106) (112) 51% (113) 46%

Attempted modification of this reaction[352] using potassium thiocyanate and benzoyl chloride gave only (114) in 2% yield.

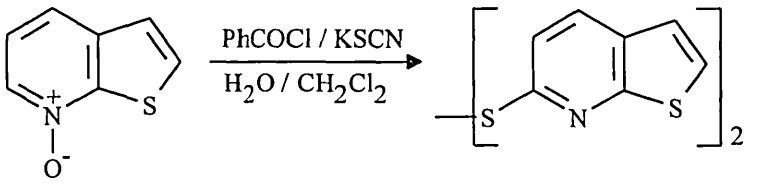

(102) (114)

Thieno[2,3-b]pyridine-7-oxide (102) also gave γ substitution upon reaction with benzoyl chloride and enamines of cyclohexanone followed by hydrolysis[358].

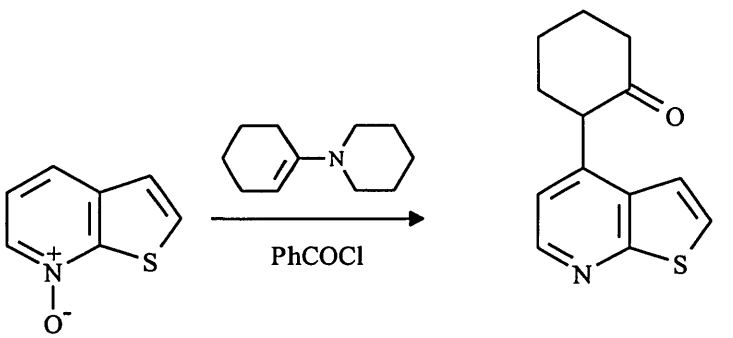

(102)

Furthermore, reaction of (102) with ethyl cyanoacetate in the presence of acetic anhydride[358] afforded a compound which could be best explained by the resonance structures (115) and (116). This compound has been used as an acylating agent for amines[351].

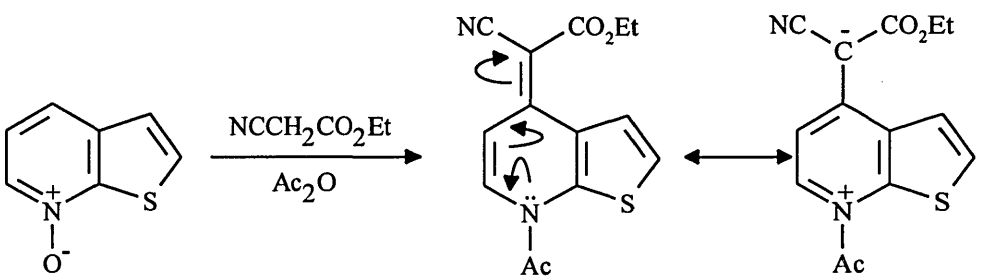

(102) (115) (116)

1.2.5.6 Reactions of thieno[2,3-b]pyridine sulfones

The only reported reactions of thieno[2,3-b]pyridine sulfones are Diels-Alder reactions. Sulfone (105) acts as a typical dienophile and undergoes reaction with anthracene and other dienes[355,359].

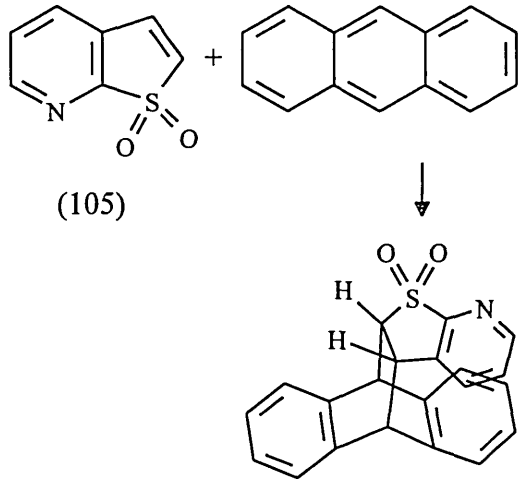

(105)

1.2.5.7 Aminothieno[2,3-b]pyridines

5-Aminothieno[2,3-b]pyridine (117) was reported[346] to undergo diazotisation reactions typical of primary aryl amines to yield various 5-substituted thieno[2,3-b]pyridines [Scheme 27].

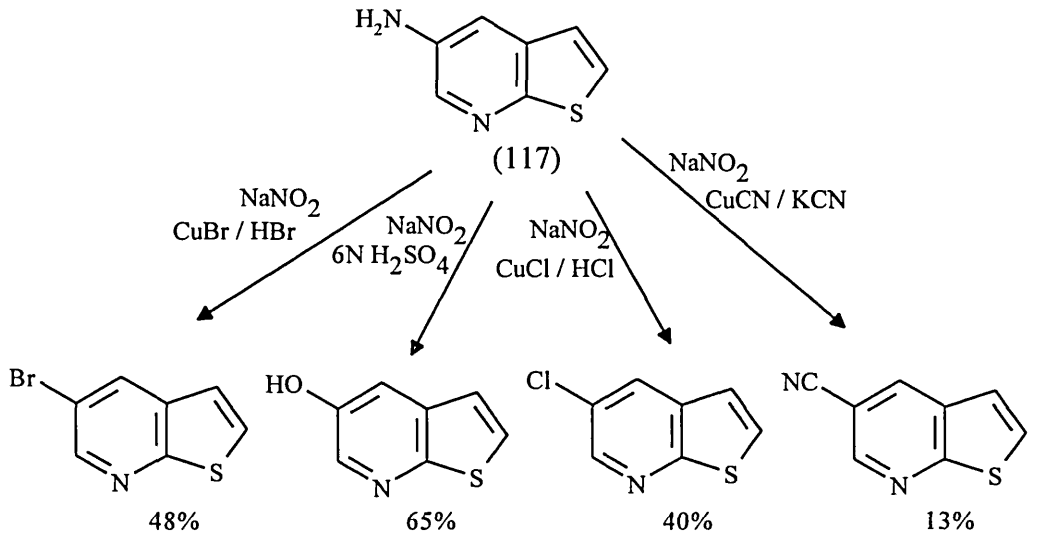

[Scheme 27]

Compound (117) also reacts[346] with aldehydes to give Schiff's bases where the C=N function could be reduced to the secondary amine. This work was extended[350] to 4-aminothieno[2,3-b]pyridine (118) which could be prepared

from the reduction of 4-nitrothieno[2,3-b]pyridine-7-oxide (106) with iron and glacial acetic acid. No reaction of (118) with aldehydes was observed using the above conditions. This was attributed to the decreased nucleophilic character of the amino group due to resonance stability of (118) which is not possible for (117). Schiff's bases were only obtained from reaction in refluxing xylene with a molecular sieve [Scheme 28].

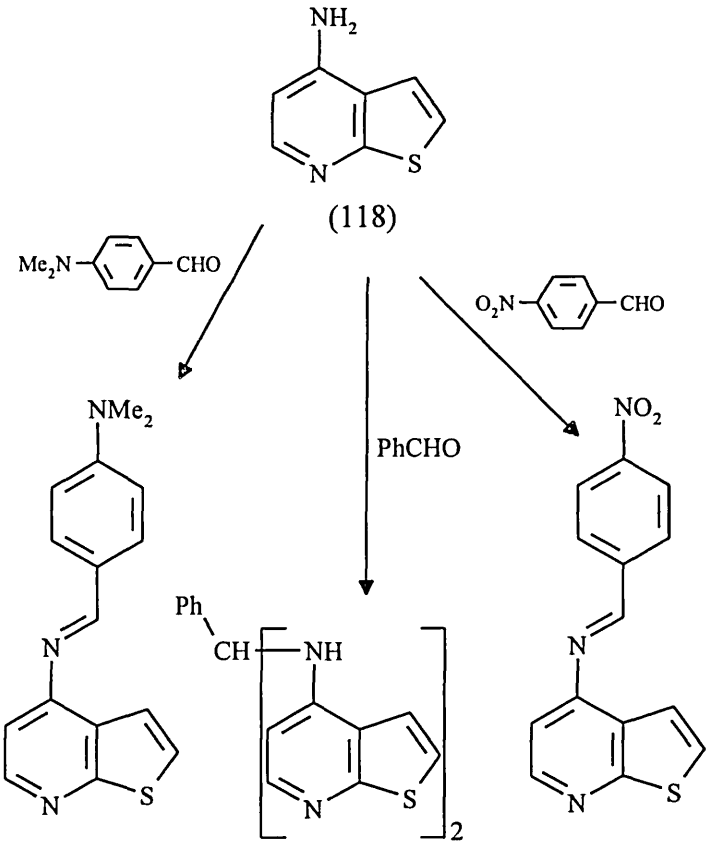

[Scheme 28]

Amino groups attached directly to the thiophene ring of thieno[2,3-b]pyridines generally yield unstable compounds as the free base. The N-acetyl derivatives however are stable and some have been prepared[360] [Equation 6, Equation 7].

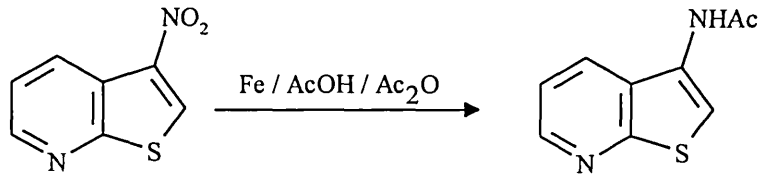

[Equation 6]

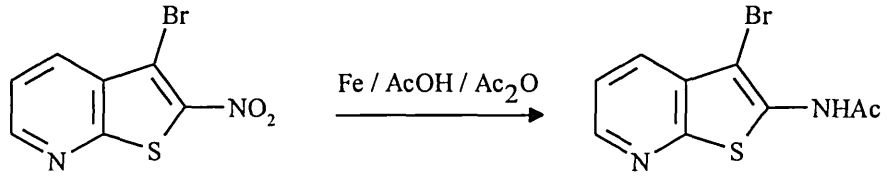

(87b)

[Equation 7]

It was found[361] that diazotisation of ethyl 3-aminothieno[2,3-b]pyridine-2-carboxylate (59) followed by hypophosphorus acid-mediated reduction gave ethyl thieno[2,3-b]pyridine-2-carboxylate (119).

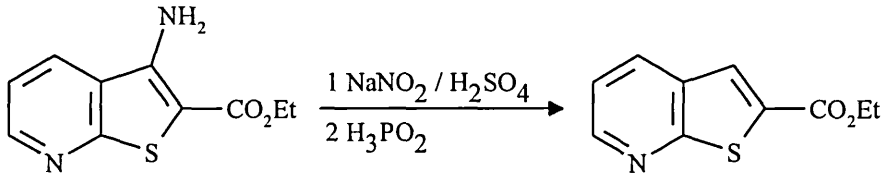

(59) (119)

1.2.5.8 Miscellaneous reactions

4,6-Dimethylthieno[2,3-b]pyridine (27) was characterised by preparing[268] the dibenzylidene derivative (120) which was formed readily from reaction of (27) with two equivalents of benzaldehyde and a small amount of zinc chloride.

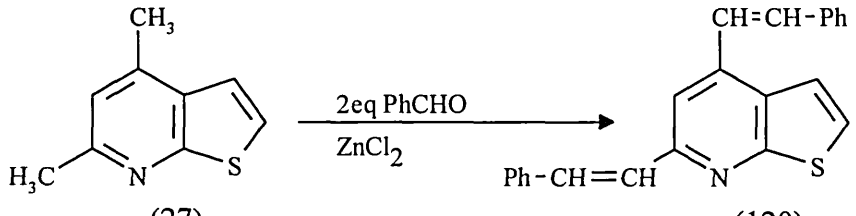

(27) (120)

Furthermore, reaction[346] of 5-bromothieno[2,3-b]pyridine (121) with potassium amide in liquid ammonia gave 40% of 4-aminothieno[2,3-b]pyridine (118) and 0-13% of the 5-amino isomer (117). It was proposed that the reaction involved an intermediate thienopyridyne.

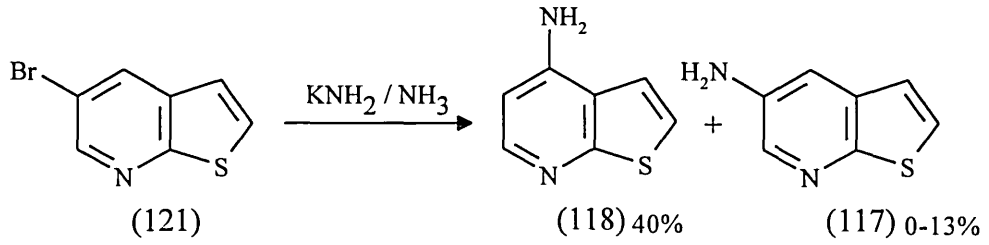

(121) (118) 40% (117) 0-13%

Diazepines have been synthesised[362] from 4,6-dimethylthieno[2,3-b]pyridine (27). For example, treatment of (27) with O-mesitylsulfonylhydroxylamine (H_2NO_3SMes) gave the N-amino compound (122) in 94% yield. This could be reacted with ethyl chloroformate in the presence of alkali to give the N-acylimide (123) which could be irradiated to afford diazepines (124) and (125) [Scheme 29].

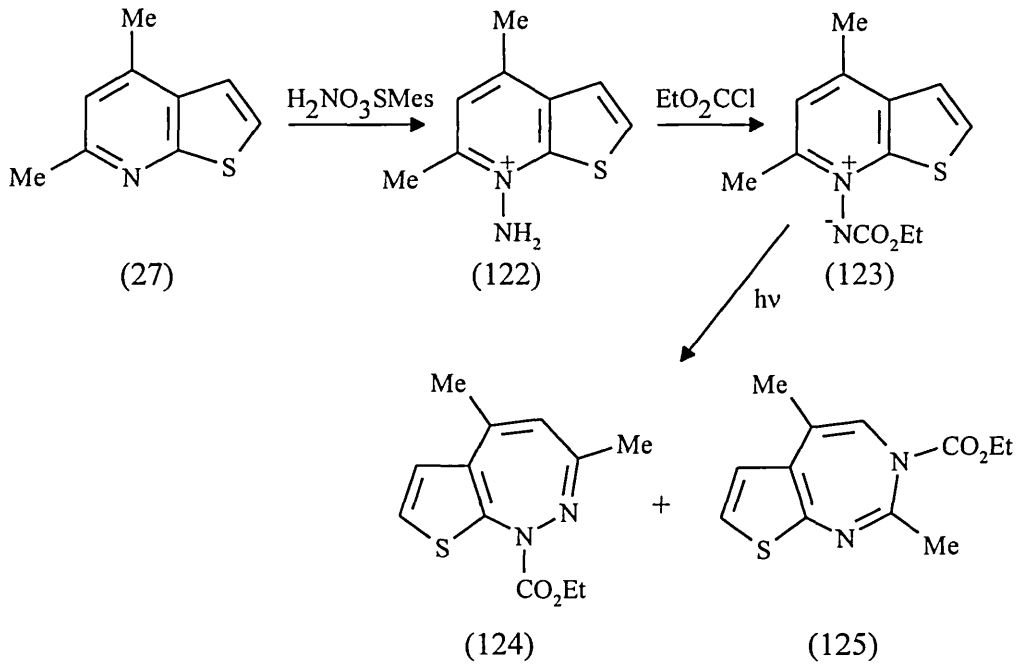

(27) (122) (123) (124) (125)

[Scheme 29]

There is also a great wealth of literature describing the synthesis of tricyclic compounds containing the thieno[2,3-b]pyridine moiety however this is well beyond the scope of this introduction.

1.2.6 Thienopyridines as pharmacological agents

Although there does not appear to be much literature on thieno[2,3-b]pyridines as pharmacological agents there are however several [2,3-c], [3,2-c] and [3,2-b] derivatives with known biological activity. The tetrahydrothieno[3,2-c]pyridines ticlopidine[363,364] (126) and clopidogrel[365] (127) are powerful inhibitors of platelet aggregation. The mechanism of action of these drugs is not entirely understood but they are believed to interfere with ADP induced platelet aggregation[366].

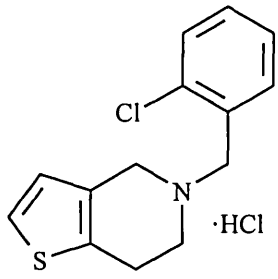

(126)

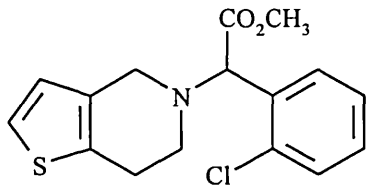

(127)

The tetrahydrothieno[2,3-c]pyridine (128) and other tetrahydrothienopyridine derivatives have been identified as selective dopamine D_1 receptor agonists[367,368].

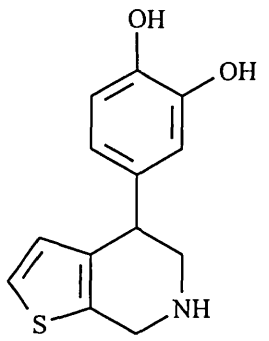

(128)

A series of substituted 4-aryltetrahydrothieno[2,3-c]pyridines (129) have shown potential as antidepressants inhibiting the uptake of noradrenaline and 5-HT[369].

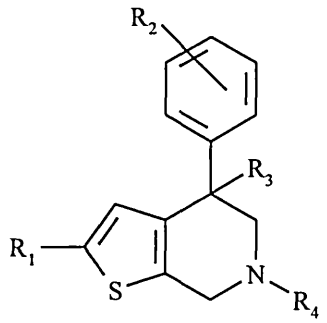

(129)

Thienopyridine arylpiperazine derivatives e.g. (130) have exhibited high affinities for the 5-HT_1 and 5-HT_2 subtypes but low dopamine D_2 receptor affinity[370] and may be useful as antipsychotic agents.

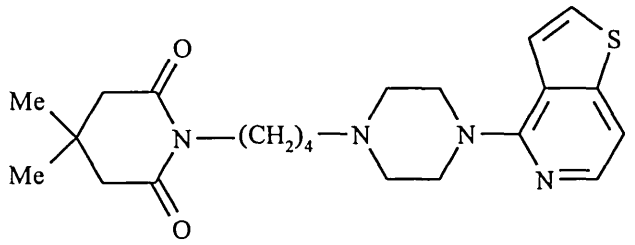

(130)

The fully aromatic thieno[3,2-b]pyridine (131) has been discovered as a leukotriene D_4 receptor antagonist which was as equally potent as its quinoline isostere[371].

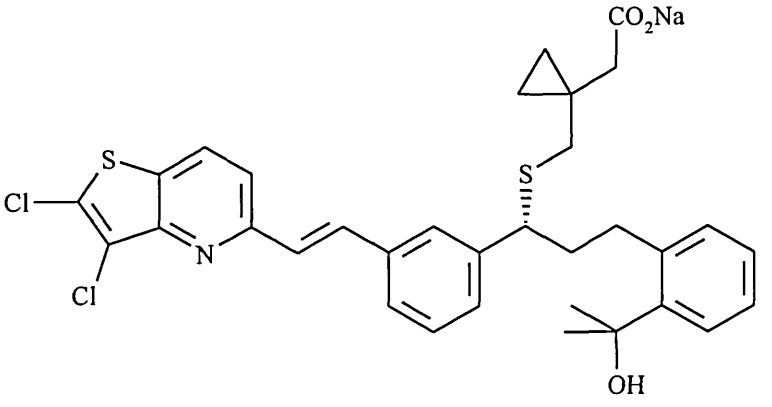

(131)

2 Molecular Modelling: Methods and Discussion

2.1 METHODS

2.1.1 Approach to modelling the 5-HT receptors

In 1993 when this project was initiated the rhodopsin projection map[121] was not available and only the coordinates of the transmembrane α-helices of bacteriorhodopsin[119] were obtainable. It was therefore assumed that the 5-HT receptors have a suitably similar overall topology to bacteriorhodopsin to warrant the use of the aforementioned coordinates as an initial, but not strict template to model the 5-HT receptors. Even today we still believe that the use of bacteriorhodopsin coordinates is a superior method to that based on the rhodopsin low resolution data and will continue to be so until high resolution coordinates of rhodopsin are published. If, or when, this happens the question will then be: are the 5-HT receptors similar enough to rhodopsin to warrant the use of the rhodopsin coordinates in a homology model of the 5-HT receptors?

The approach therefore adopted within this project was to use the bacteriorhodopsin coordinates as a template upon which the α-helices of the 5-HT receptors could be arranged prior to any refinement. In the first instance, the human 5-HT_{1A} receptor was modelled as a prototype since there is a greater wealth of experimental data and binding affinity data available for the 5-HT_{1A} receptor compared to all the remaining 5-HT_1 receptors. This prototype was used as the starting point for the models of the 5-$HT_{1D\alpha}$ and 5-$HT_{1D\beta}$ receptors which may be involved in migraine headache. There are some limitations to this approach and certain assumptions had to be made which will be discussed where appropriate.

This study did not attempt to create the "perfect" GPCR model but instead to obtain experimentally relevant molecular models of the 5-HT_{1A}, 5-$HT_{1D\alpha}$ and 5-$HT_{1D\beta}$ agonist binding sites which are qualitatively useful.

2.1.2 Sequence alignment

The amino acid sequences of the cloned human 5-HT_{1A}, 5-$HT_{1D\alpha}$, 5-$HT_{1D\beta}$, 5–ht_{1E}, 5-ht_{1F}, 5-HT_{2A} and 5-HT_{2C}[27,102,103,372-380] receptors were extracted from the Swissprot database and read into the InsightII[381] molecular modelling package. The bacteriorhodopsin[119] sequence was also obtained in a similar way. No satisfactory sequence alignment was observed between the 5-HT receptors and bacteriorhodopsin due to the very low sequence similarity. The 5-HT receptors were then aligned using the multiple alignment option of the homology module of InsightII[381] and the Dayhoff PAM 120 evolutionary scoring matrix[382]. This resulted in a sequence alignment showing seven distinct regions of high sequence homology undoubtedly corresponding to the seven α-helices of the receptors (Figure 4).

2.1.3 Hydrophobicity analysis

In addition to being comprised of conserved amino acids, the transmembrane domains are known to be hydrophobic in nature and hence an analysis of hydrophobicity should provide further evidence to assist in the identification of the α-helices.

Hydrophobicity profiles were calculated for each of the 5-HT receptors using the combined hydrophobicity scale of Kyte and Doolittle[127] with a window size of 5 residues and a hydrophobicity threshold of 0. These parameters were found to be the optimal values based on hydrophobicity analysis of the bacteriorhodopsin

```
A:                                                  mdvlspgqgnnttsppapfetggnttgisdvtvsyqvitslllgtlifcavlg
B:                                               msplnqsaeglpqeasnrslnatetseawdprtlqalkislavvlsvitlatvls
C:                                    meepgaqcappppagsetwvpqanlssapsqncsakdyiyqdsislpwkvllvmllalitlattls
D:                                                                mnitnctteasmairpktitekmlicmtlvvittlttll
E:                                                               mdflnssdqnltseellnrmpskilvsltlsglalmttti
F: meilcedntslssttnslmqlnddtrlysndfnsgeantsdafnwtvdsenrtnlscegclspsclsllhlqeknwsalltavviiltiag
G:                              mvnlrnavhsflvhligllvwqcdisvspvaaivtdifntsdggrfkfpdgvqnwpalsiviiiimtigg


A: nacvvaaialerslqnvanyligslavtdlmvsvlvlpmaal-yqvlnkwtlgqvtcdlfialdvlcctssilhlcaialdrywaitdpid
B: nafvlttilltrklhtpanyligslattdllvsilvmpisia-ytithtwnfgqilcdiwlssditcctasilhlcvialdrywaitdale
C: nafviatvyrtrklhtpanyliaslavtdllvsilvmpistm-ytvtgrwtlgqvvcdfwlssditcctasilhlcvialdrywaitdave
D: nlavimaigttkklhqpanylicslavtdllvavlvmplsii-yivmdrwklgyflcevwlsvdmtcctcsilhlcvialdrywaitnaie
E: nslviaaiivtrklhhpanylicslavtdflvavlvmpfsiv-yivreswimgqvvcdiwlsvditcctcsilhlsaialdryraitdave
F: nilvimavslekklqnatnyflmslaiadmllgflvmpvsmltilygyrwplpsklcavwiyldvlfstasimhlcaisldryvaiqnpih
G: nilvimavsmekklhnatnyflmslaiadmlvgllvmplsllailydyvwplprylcpvwisldvlfstasimhlcaisldryvairnpie


A: yvnkrtprraaalisltwligflisip-pmlgwrtped-rsdpdactiskdh-gytiystfgafyipllllmlvlygrifraarfrirktvk
B: yskrrtaghaatmiaivwaisicisip-plf-wrq-akaqeemsdclvntsqisytiystcgafyipsvlliilygriyraarn-rilnpp
C: ysakrtpkraavmialvwvfsisislp-pff-wrq-akaeeevsecvvntdhilytvystvgafyfptlllialygriyvearsrilkqtp
D: yarkrtakraalmiltvwtisifismp-plf-wrshrrlspppsqctiqhdhviytiystlgafyiplilililyyriyhaaks---lyqk
E: yarkrtpkhagimitivwiisvfismp-plf-wr--hqgtsrddeciikhdhivstiystfgafyiplalililyykiyraaktlyhkrqa
F: hsrfnsrtkaflkiiavwtisvgismpipvfglq-ddskvfkegsclladdn--fvligsfvsffipltimvity----------------
G: hsrfnsrtkaimkiaivwaisigvsvpipviglrdeekvfvnnttcvlndp--nfvligsfvaffipltimvity----------------


A: kvektgadtrhgaspapqpkksvngesgsrnwrlgveskaggalcangavrqgddgaalevievhrvgnskehlplpseagptpcapasfe
B: slygkrfttahlitgsagss-lcslnsslheghshsagsplffnhvkikladsalerkri--------------------------------
C: nrtgkrltraqlitdspgstssvtsinsrvpdvpsesgspvyvnqvkvrvsdallekkkl--------------------------------
D: rgssrhlsnrstdsqnsfasckltqtfcvsdfstsdpttefekfhasir-------------------------------------ippf
E: sriakeevngqvllesgekstksvstsyvlekslsdpstdfdkihstvr-------------------------------------slrs
F: ----------------------------------------------fltikslqkeatlcvsdlgtraklasfsflpqsslsseklfqrsih
G: ------------------------------------cltiyvlrrqalmllhghteeppglsldflkcckrntaeeensanpnqdqnarr


A: rknernaeakrkmalarerktvktlgiimgtfilcwlpffivalvlpfcessc--hmptllgaiinwlgysnsllnpviyayfnkdfqnaf
B: ------------saarerkatkilgiilgafiicwlpffvvslvlpicrdsc--wihpalfdfftwlgylnslinpiiytvfneefrqaf
C: ------------maarerkatktlgiilgafivcwlpffiislvmpickdac--wfhlaifdfftwlgylnslinpiiytmsnedfkqaf
D: dndldhpgerqqisstrerkaarilglilgafilswlpffikelivgl----siytvssevadfltwlgyvnslinpllytsfnedfklaf
E: efkhekswrrqkisgtrerkaattlglilgafvicwlpffvkelvvnv---cdkckiseemsnflawlgylnslinpliytifnedfkkaf
F: repgsytgrrtmqsisneqkackvlgivfflfvvmwcpffitnimavickescnedvigallnvfvwigylssavnplvytlfnktyrsaf
G: rkkkerrprgtmqainnerkaskvlgivffvflimwcpffitnilsvlcekscnqklmekllnvfvwigyvcsginplvytlfnkiyrraf


A: kkiikckfcrq
B: qkivpfrkas
C: hklirfkcts
D: kklircreht
E: qklvrcrc
F: sryiqcqykenkkplqlilvntipalaykssqlqmgqkknskqdakttdndcsmvalgkqhseeaskdnsdgvnekvscv
G: snylrcnykvekkppvrqiprvaatalsgrelnvniyrhtnepviekasdnepgiemqvenlelpvnpssvvserissv
```

A human 5-HT_{1A}, B human 5-$HT_{1D\alpha}$, C human 5-$HT_{1D\beta}$, D human 5-ht_{1E}, E human 5-ht_{1F}, F human 5-HT_{2A}, G human 5-HT_{2C}

Figure 4 Sequence alignment of the human 5-HT receptors

sequence and then cross-referencing the hydrophobic regions with the α-helices of the experimentally derived 3-dimensional structure[119].

The hydrophobicity profiles of the 5-HT receptors readily indicated six distinct hydrophobic regions corresponding well with the first six regions of high sequence conservation. These motifs were identified as transmembrane helices 1 to 6. Helix 7 was less well defined from the hydrophobicity profiles but the sequence alignment allowed the identification of helix 7 on the strength of its high sequence identity (Figure 5).

It is noted that there are sequence gaps in two of the identified transmembrane domains. Insertions and deletions are unlikely in structurally conserved regions. The gaps however occur towards the C-terminus of both helices and may result from an incorrect local alignment or overestimation of the lengths of the α-helices. Nevertheless these discrepancies will have very little bearing upon the agonist binding site of the 5-HT_1 receptors.

2.1.4 Helical wheel analysis

The identified α-helices were plotted around helical wheels at intervals of 100^{o} using the GCG program Helicalwheel[383]. The helical wheels for each receptor were arranged upon the template of bacteriorhodopsin. The rotational position of each helix was evaluated according to four factors.

1 Hydrophilic and charged groups were directed towards the central cleft away from the hydrophobic environment of the lipid membrane.

	HELIX 1	HELIX 2
A	VITSLLLGTLIFCAVLGNACVVAAIA	YLIGSLAVTDLMVSVLVLPMAAL-YQV
B	ISLAVVLSVITLATVLSNAFVLTTIL	YLIGSLATTDLLVSILVMPISIA-YTI
C	VLLVMLLALITLATTLSNAFVIATVY	YLIASLAVTDLLVSILVMPISTM-YTV
D	MLICMTLVVITTLTTLLNLAVIMAIG	YLICSLAVTDLLVAVLVMPLSII-YIV
E	ILVSLTLSGLALMTTTINSLVIAAII	YLICSLAVTDFLVAVLVMPFSIV-YIV
F	NWSALLTAVVIILTIAGNILVIMAVS	YFLMSLAIADMLLGFLVMPVSMLTILY
G	NWPALSIVIIIIMTIGGNILVIMAVS	YFLMSLAIADMLVGLLVMPLSLLAILY

	HELIX 3	HELIX 4
A	VTCDLFIALDVLCCTSSILHLCAIAL	AAALISLTWLIGFLISIP-PML
B	ILCDIWLSSDITCCTASILHLCVIAL	AATMIAIVWAISICISIP-PLF
C	VVCDFWLSSDITCCTASLIHLCVIAL	AAVMIALVWVFSISISLP-PFF
D	FLCEVWLSVDMTCCTCSILHLCVIAL	AALMILTVWTISIFISMP-PLF
E	VVCDIWLSVDITCCTCSILHLSAIAL	AGIMITIVWIISVFISMP-PLF
F	KLCAVWIYLDVLFSTASIMHLCAISL	AFLKIIAVWTISVGISMPIPVF
G	YLCPVWISLDVLFSTASIMHLCAISL	AIMKIAIVWAISIGVSVPIPVI

	HELIX 5	HELIX 6
A	YTIYSTFGAFYIPLLLMLVLY	KTLGIIMGTFILCWLPFFIVALVLPF
B	YTIYSTCGAFYIPSVLLIILY	KILGIILGAFIICWLPFFVVSLVLPI
C	YTVYSTVGAFYFPTLLLIALY	KTLGIILGAFIVCWLPFFIISLVMPI
D	YTIYSTLGAFYIPLTLILILY	RILGLILGAFILSWLPFFIKELIVGL
E	STIYSTFGAFYIPLALILILY	TTLGLILGAFVICWLPFFVKELVVNV
F	FVLIGSFVSFFIPLTIMVITY	KVLGIVFFLFVVMWCPFFITNIMAVI
G	FVLIGSFVAFFIPLTIMVITY	KVLGIVFFVFLIMWCPFFITNILSVL

	HELIX 7
A	LGAIINWLGYSNSLLNPVIYAY
B	LFDFFTWLGYLNSLINPIIYTV
C	IFDFFTWLGYLNSLINPIIYTM
D	VADFLTWLGYVNSLINPLLYTS
E	MSNFLAWLGYLNSLINPLIYTI
F	LLNVFVWIGYLSSAVNPLVYTL
G	LLNVFVWIGYVCSGINPLVYTL

A human 5-HT_{1A}, B human 5-$HT_{1D\alpha}$, C human 5-$HT_{1D\beta}$, D human 5-ht_{1E},

E human 5-ht_{1F}, F human 5-HT_{2A}, G human 5-HT_{2C}

Figure 5 The seven α-helices of the human 5-HT receptors

2 Highly conserved residues were directed towards the central cleft, these residues are likely to be involved in the receptor activation process or in maintaining the receptor structure.

3 Residues proposed to be involved in ligand binding from mutagenesis data (section 1.1.4.3) were directed towards the central cleft.

4 Proline residues in transmembrane helices prefer to pack against the protein interior or against other helices[384].

These rules were adhered to as strictly as possible, however, it became unavoidable that the criteria could not be met at all times. This resulted in several serine and threonine residues packing against other helices or the membrane. It is also appreciated that although the helical wheel arrangements give a good 2-dimensional representation of the receptors they cannot account for any distortions of the helical backbone caused by proline residues.

2.1.5 Modelling of the α-helices

The individual α-helices of the 5-HT_{1A}, 5-$HT_{1D\alpha}$ and 5-$HT_{1D\beta}$ receptors were constructed using the biopolymer module of InsightII as right-handed α-helices with dihedral angles of Φ=-65°, Ψ=-40° and ω=180°. As previously mentioned several of the helices contain proline residues which tend to induce kinking of the α-helical backbone. It is thought that this distortion may be an important structural feature of these receptors and thus should be incorporated into the models.

Proline induced kinks were therefore introduced according to the work of Polinsky *et al.*[385] who studied the minimum energy conformations of the α-helical peptide ALA_8-LEU-PRO-PHE-ALA_8 at a dielectric constant of 4.0.

The C-terminus of each helix was capped with an N-methyl group and the N-terminus of each helix with an acetyl group. Lysine, arginine, aspartic acid and glutamic acid residues were all assumed to be charged. The potential types and partial charges were all fixed using the set of rules accompanying the CVFF forcefield[386] as supplied with Discover[387]. Each individual helix was subjected to 200 steps of steepest descent energy minimisation without using cross-terms followed by 1000 steps of conjugate gradient energy minimisation using cross-terms. All minimisations and subsequent minimisations were performed with a dielectric constant of 4.0 using the CVFF forcefield. The dielectric constant of 4.0 was chosen to simulate the hydrophobic environment of the receptor.

The mean RMS deviation of the helical backbones between minimised and non-minimised helices was 0.998 Å. In all cases helix 4 was observed to deviate slightly more than the other helices and this was attributed to the PRO-PRO motif causing backbone conformational change.

2.1.6 Modelling the 5-HT_{1A} receptor

The seven energy minimised α-helices of the 5-HT_{1A} receptor were superimposed onto the bacteriorhodopsin template. The direction of the sidechain of the first residue of each 5-HT_{1A} receptor helix, as identified from the helical wheels (section 2.1.4), was matched with the first residue of the corresponding bacteriorhodopsin helix whose sidechain pointed in the same direction. This resulted in an initial alignment of the 5-HT_{1A} receptor backbone

with that of bacteriorhodopsin and allowed the superposition of the backbone atoms of the 5-HT_{1A} receptor onto the backbone atoms of bacteriorhodopsin.

This initial crude molecular model was then refined. Some of the helices were rotated about their helical axis to obtain a model that was totally consistent with the helical wheel projections. Translation of helices was also applied to improve interhelical sidechain interactions. The sidechain conformations of the residues were checked with reference to the standard rotamer library as supplied with the homology module of InsightII to ensure no sidechains existed in unlikely high energy conformations. The loop and terminal domains were not modelled due to the extreme uncertainty of their conformation. Additionally it is believed[84] that the agonist binding site of the cationic amine neurotransmitter receptors is within the transmembrane core.

The receptor model was then energy minimised for 1000 iterations of steepest descent followed by 2000 iterations of conjugate gradient minimisation; all backbone atoms were fixed during the simulation. This was followed by a molecular dynamics simulation of 10 ps initialisation and 100 ps simulation at 310 K with a time step of 1 fs; again with backbone atoms fixed. Non-bonded cutoffs were applied at 12 Å for both the dynamics and minimisation steps. The simulation period was divided into 10 ps intervals and average conformations over these periods were calculated. Finally the average conformations were energy minimised for 1000 steps of steepest descent followed by 2000 steps of conjugate gradient again using 12 Å cutoffs and fixed backbone atoms. The resulting minimum energy conformation was retained for the modelling of ligand receptor interactions.

2.1.7 Modelling the 5-$HT_{1D\alpha}$ and 5-$HT_{1D\beta}$ receptors

There were at least three possible methods by which the 5-$HT_{1D\alpha}$ and 5-$HT_{1D\beta}$ receptors could be modelled.

1. The 5-$HT_{1D\alpha}$ and 5-$HT_{1D\beta}$ receptor helices could be superimposed onto the backbone of bacteriorhodopsin and the receptor models could be built in the same manner as the 5-HT_{1A} receptor.

2. Homology models of the 5-$HT_{1D\alpha}$ and 5-$HT_{1D\beta}$ receptors could be constructed using the exact backbone of the previously constructed 5-HT_{1A} receptor model. The sequence alignment of the 5-HT receptors could be used to graphically mutate the 5-HT_{1A} receptor model into the required 5-HT_{1D} receptor sequence.

3. The 5-HT_{1A} receptor model could be used as the template upon which the α-helices of the 5-HT_{1D} receptors could be superimposed.

Method 1 could have possibly resulted in 5-HT_{1D} receptor models that were quite distant in terms of backbone atom deviation from the 5-HT_{1A} receptor model. Method 2 would give the impression of forcing the backbone of the 5-HT_{1D} receptor models to adopt the exact conformation of the 5-HT_{1A} receptor model. Therefore the method of choice was option 3.

The transmembrane helices of the 5-$HT_{1D\alpha}$ and 5-$HT_{1D\beta}$ receptors were superimposed onto the corresponding helices of the 5-HT_{1A} receptor model using their backbone atoms. Sidechain conformations were checked with the supplied rotamer library and the models were subjected to an identical minimisation and dynamics protocol as described for the 5-HT_{1A} receptor

model in section 2.1.6. The RMS gradient of the minimised receptor models was less than 0.001 kcal/Å. The RMS deviations in backbone structures were calculated (Table 2) and were found to be consistent with the sequence alignment, in that the 5-$HT_{1D\alpha}$ and 5-$HT_{1D\beta}$ receptors show greater similarity with each other rather than with the 5-HT_{1A} receptor.

Receptor	Backbone RMS deviation (Å)
5-HT_{1A} / 5-$HT_{1D\alpha}$	0.77
5-HT_{1A} / 5-$HT_{1D\beta}$	0.76
5-$HT_{1D\alpha}$ / 5-$HT_{1D\beta}$	0.42

Table 2 Backbone RMS deviations between the 5-HT receptor models

2.1.8 Ligand - Receptor complexes

2.1.8.1 5-Hydroxytryptamine

5-HT (1) was assembled within InsightII, the ethylamine sidechain was protonated and CVFF forcefield potential types and partial charges were assigned. The molecule was then energy minimised to a gradient of less than 0.001 kcal/Å to give the two global minimum energy conformations previously calculated[258]. These were named 5-HT(A) and 5-HT(B) (Figure 6).

The two conformations of the ligand were docked into the 5-HT_{1A} and 5-HT_{1D} receptor models in a variety of positions allowing the protonated amine group to interact with the helix 3 aspartate residue which protrudes into the central cleft of the models. The hydroxyl group of 5-HT was positioned in such a way so it could potentially interact with a number of serine or threonine residues upon helices 4, 5 and 6. Sidechain conformations of the receptor model were again cross-referenced with the rotamer library to ensure no sidechains were trapped in

unlikely high energy conformations. The ligand receptor complexes were then energy minimised for 1000 iterations of steepest descent followed by 2000 iterations of conjugate gradient minimisation. Cutoffs were applied at 12 Å and the receptor backbone atoms were fixed in position.

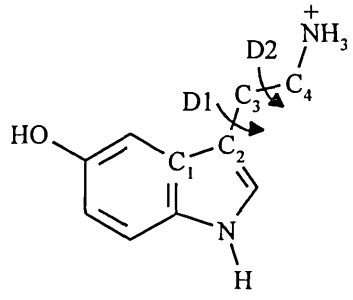

Conformation	D1 (C1-C2-C3-C4)	D2 (C2-C3-C4-N)
5-HT (A)	80.33°	-178.40°
5-HT (B)	-80.33°	178.40°

Figure 6 The global minimum energy conformations of 5-HT

2.1.8.2 8-Hydroxy-2-(di-*n*-propylamino)tetralin

8-Hydroxy-2-(di-*n*-propylamino)tetralin (8-OH-DPAT, 12) is a selective 5-HT_{1A} receptor agonist[388,389] (Table 3). Although both enantiomers of (12) exhibit similar high affinity binding at the 5-HT_{1A} receptor it is known that only the R enantiomer is a full agonist, the S enantiomer being a partial agonist[390]. Therefore this study is concerned only with (R)-8-OH-DPAT (Figure 7).

The tetralin ring structure was built and energy minimised within InsightII yielding two distinct ring conformations. These conformations were found to be consistent with conformations found for the tetralin ring moiety within the CSSR database[393,394]. The required substituents were added, the molecules

were protonated and partial charges assigned. Conformational analysis was performed at 30° increments around the five rotatable bonds as illustrated in Figure 7.

Ligand	Binding Affinity (pK_i)		
	5-HT_{1A}[a]	5-$HT_{1D\alpha}$[b]	5-$HT_{1D\beta}$[b]
5-HT	8.38	8.41	8.37
8-OH-DPAT	8.61	6.92	6.59
5-CT	9.53	9.15	8.80
5-OH-TMT	6.70[c]	na	na
Sumatriptan	6.62	8.47	8.11

(a) 5-HT_{1A} binding data from reference 391, (b) 5-HT_{1D} binding data from reference 27, (c) 5-OH-TMT data from reference 392, na no data available

Table 3 Binding affinity data for compounds to be docked into receptor models

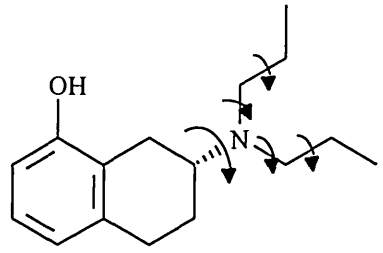

Figure 7 The five rotatable bonds of (R)-8-OH-DPAT

Each conformer was energy minimised to an RMS gradient of less than 0.001 kcal/Å. The lowest energy conformation for each ring conformation was retained and named 8-OH-DPAT(I) and 8-OH-DPAT(II) (Figure 8) with the latter being the global minimum energy conformation by 3 kcal/mol. Both conformations were docked into the 5-HT_{1A} and 5-HT_{1D} receptor models by superposition of the phenol moiety of 8-OH-DPAT onto that of 5-HT in the final energy minimised 5-HT receptor complexes. The 8-OH-DPAT receptor

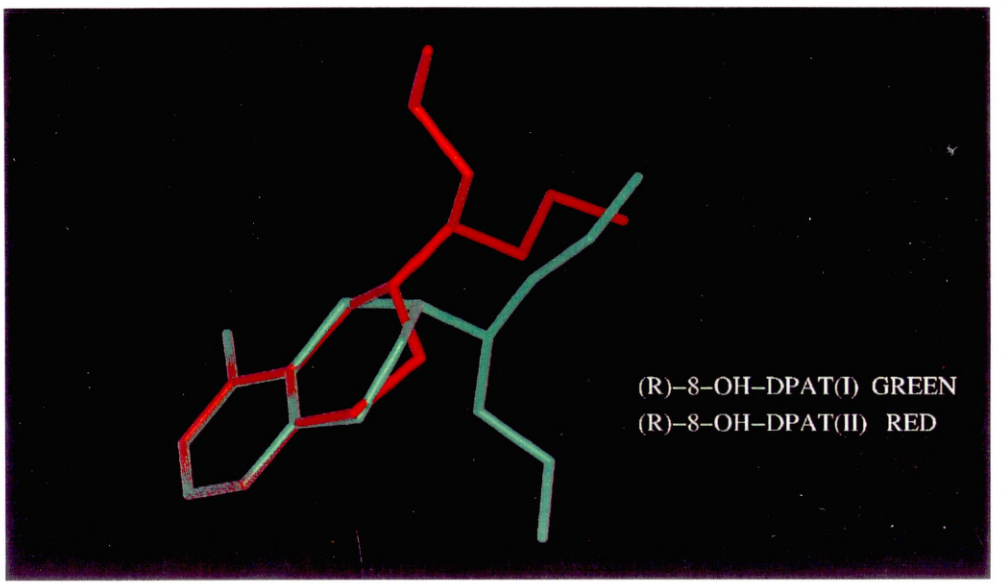

FIGURE 8
The two conformations of 8-OH-DPAT

complexes were energy minimised in exactly the same manner as for the 5-HT receptor complexes with the exception that 18 Å cutoffs were used due to the increased size of the ligand.

2.1.8.3 5-Carboxamidotryptamine and 5-Hydroxy-*N,N,N*-trimethyltryptamine

5-Carboxamidotryptamine (5-CT, 18) is a high affinity nonselective 5-HT receptor agonist[391] (Table 3). 5-Hydroxy-*N,N,N*-trimethyltryptamine (5-OH-TMT, 132) binds at 5-HT_{1A} sites with an affinity several hundred fold lower than 5-HT[392]. Both molecules were constructed within InsightII, 5-CT was protonated, partial charges were assigned and both molecules were energy minimised as previously described for 5-HT. For each molecule two minimum energy conformations having the C-3 substituent in a similar position to that of the optimised conformations of 5-HT were obtained. These were named 5-CT(A), 5-CT(B), 5-OH-TMT(A) and 5-OH-TMT(B).

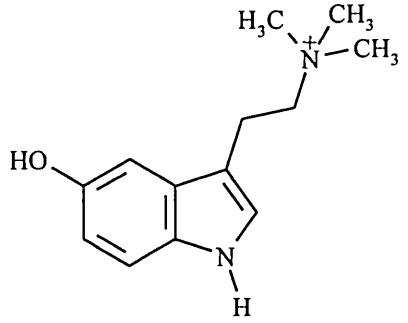

(132)

The two conformations of 5-CT were docked into all the 5-HT receptor models while 5-OH-TMT was docked only into the 5-HT_{1A} receptor model since there was no binding affinity data available for this compound at cloned 5-$HT_{1D\alpha}$ and 5-$HT_{1D\beta}$ receptors. All conformations were docked into the receptor models by superposition of the indole ring of the ligands onto the indole ring of

5-HT in the final energy minimised 5-HT receptor complexes. All the ligand receptor complexes were then energy minimised using exactly the same criteria as described for 8-OH-DPAT.

2.1.8.4 Sumatriptan

Sumatriptan (4) was constructed within InsightII, the molecule was protonated, and partial charges were assigned. Energy minimisation afforded two conformations A and B similar to those described for 5-HT. The C-5 substituent of sumatriptan contains three rotatable bonds (Figure 9) which will dictate the position of the substituent.

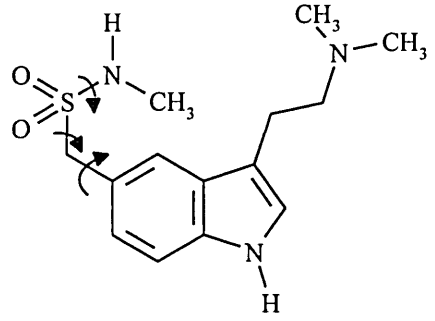

Figure 9 The three rotatable bonds of the C-5 substituent of sumatriptan

A conformational analysis was performed about these bonds using a 30° increment. Subsequent energy minimisation to an RMS gradient of less than 0.001 kcal/Å yielded two sets of thirteen minimum energy conformations differing in energy by 6.8 kcal/mol. The twenty-six conformers were docked into the 5-$HT_{1D\alpha}$ and 5-$HT_{1D\beta}$ receptor models by superposition of the indole ring of sumatriptan onto the indole ring of 5-HT in the final energy minimised 5-HT receptor complexes. Only the most promising conformations of the ligand from the sumatriptan 5-HT_{1D} receptor complexes were docked into the 5-HT_{1A} receptor model. All ligand receptor complexes were energy minimised as described previously for 8-OH-DPAT.

2.1.9 Small molecule modelling of thieno[2,3-b]pyridines

The thieno[2,3-b]pyridine analog (133) of 5-HT was constructed within InsightII, protonated and CVFF forcefield potential types and partial charges were assigned. The molecule was energy minimised to an RMS gradient of less than 0.001 kcal/Å. This resulted in two global minimum energy conformations[258] similar to 5-HT(A) and 5-HT(B), these were named THI(A) and THI(B) (Figure 10).

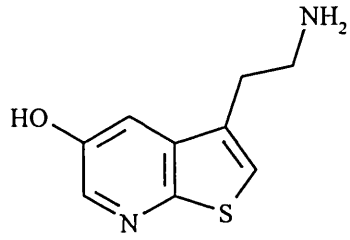

(133)

The thieno[2,3-b]pyridines were subjected to an RMS fitting procedure onto the respective conformation of 5-HT by means of superimposing the 6-membered rings, protonated amino groups, hydroxyl groups and a superposition of the thiophene sulfur of THI(A) and THI(B) onto the indole nitrogen of 5-HT. Additionally the technique of electrostatic fitting was also used. An electrostatic potential similarity function was calculated for the molecules under consideration using the Search_Compare module of InsightII. The thienopyridines THI(A) and THI(B) were aligned onto the 5-HT conformations 5-HT(A) and 5-HT(B) respectively by optimisation of the electrostatic potential similarity function. Thus the two molecules under consideration are overlapped in such a way as to maximise the similarity function. This resulted in a molecular alignment and a similarity score between -1 (maximum dissimilarity) and 1 (maximum similarity). A molecular volume comparison was also performed.

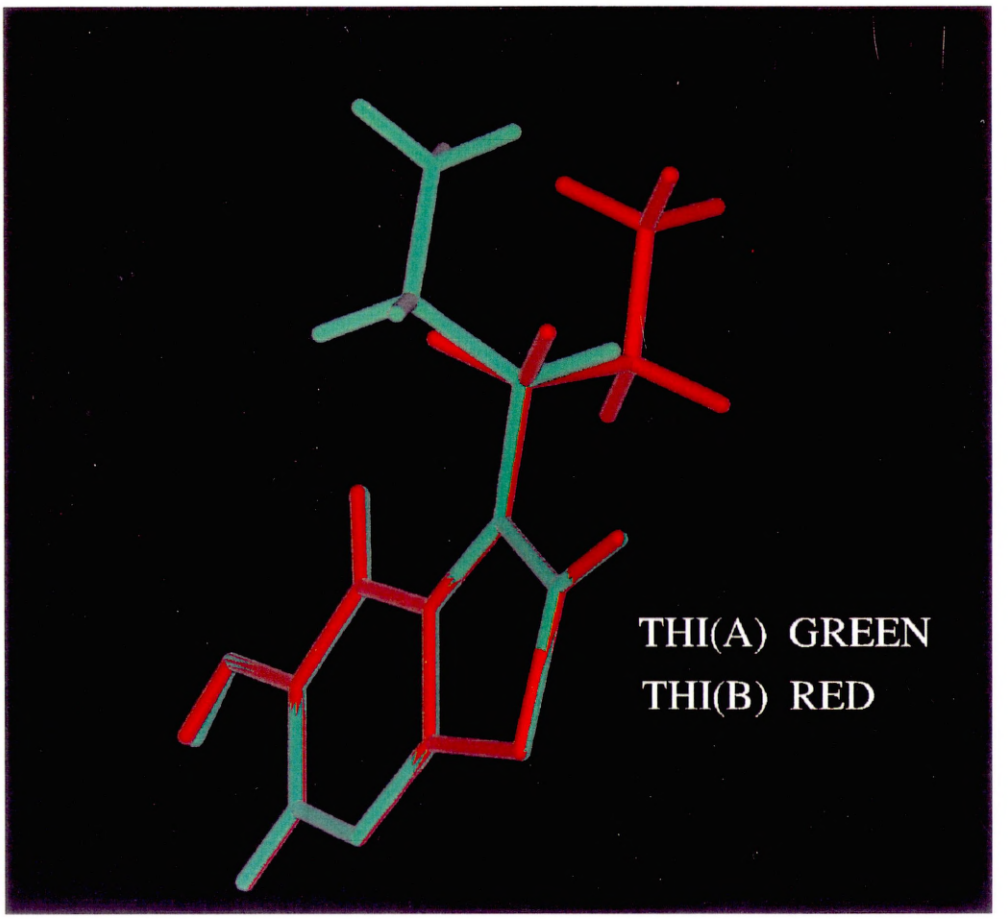

FIGURE 10
The two conformations of the thieno[2,3-b] pyridine analog of 5-HT

2.1.10 Thieno[2,3-b]pyridine receptor interactions

The two thieno[2,3-b]pyridine conformations THI(A) and THI(B) were docked into the 5-HT receptor models by superposition of the pyridine ring onto the phenyl ring of 5-HT in the final, energy minimised 5-HT receptor complexes. The resulting complexes were energy minimised following the same minimisation protocol as described for the 8-OH-DPAT receptor complexes.

2.1.11 Ligand design

In an attempt to identify possible regions within the 5-HT receptor models that may confer selectivity, use has been made of the ligand design program Ludi[395]. Ludi suggests how suitable molecular fragments from a fragment library may be positioned within an active site of a protein of interest. A receptor interaction score is calculated for each suggested fragment. Additionally Ludi can be used in link mode suggesting fragments which may be linked to existing ligands which are positioned within the binding site of the protein.

The energy minimised receptor complexes of 5-HT, 5-CT and THI were used as starting points for Ludi fragment searches. All searches were performed in link mode looking for potential fragments to add to the existing ligands. All suggestions were studied and checked for their viability. Some of the more interesting suggestions of ligands were docked into the final, energy minimised 5-HT receptor complex and energy minimised as described previously for 8-OH-DPAT.

2.2 DISCUSSION

2.2.1 The modelling procedure

A number of assumptions have been made during the modelling procedure, most notably the use of bacteriorhodopsin coordinates as a template. At present the bacteriorhodopsin coordinates are the only high resolution data available for any seven transmembrane helix protein[119]. Since it is known that the GPCRs are seven helical proteins it is a reasonable assumption that bacteriorhodopsin is a suitable starting place for modelling the 5-HT receptors. If, or when, full transmembrane coordinates of the GPCR rhodopsin become available the 5-HT receptors could be remodelled using a homology approach from a sequence alignment of the 5-HT receptors with rhodopsin. There is however no guarantee that the exact arrangement of α-helices in the 5-HT receptors is identical to that of rhodopsin.

The transmembrane helices of the 5-HT receptors were identified from the hydrophobicity analysis and sequence conservation data. The rotational position of each helix was determined from helical wheel projections which allowed the modelling of the 5-HT_{1A} receptor by superimposing the helices of the 5-HT_{1A} receptor onto the template of bacteriorhodopsin. The 5-HT_{1D} receptors were then modelled using the prototype 5-HT_{1A} receptor model as a template. The modelling procedure may seem a little crude but without high resolution coordinates of the 5-HT receptors or any homologous protein it is believed that the procedure utilised resulted in models that are as accurate as any that have been described in the literature. It was not the intention of this study to create the "perfect" 5-HT receptor model but merely to produce a model that is qualitatively useful and could be used as a guide in the rational design of novel drugs.

The complexity and lack of knowledge of the entire 5-HT receptor system render the modelling procedure very difficult. Only the seven transmembrane helices of the 5-HT receptors were modelled (Figure 11). The loop and terminal regions were not modelled since there is too much uncertainty over the conformation of these domains, and in any case ligand binding of the cationic amine neurotransmitters is believed to involve the transmembrane helices only[84]. No lipid bilayer or internal water molecules were included in the models to save computational time and because it is still not entirely clear whether or not water molecules are present in the transmembrane cleft. All minimisations of the complete receptor models therefore have been performed with the backbone atoms fixed in position. This is obviously unrealistic but in the absence of the loop regions and the lipid bilayer the positions of the α-helices must be constrained to preserve the overall topology of the receptor models.

It is further believed that molecular dynamics simulations of GPCR models without modelling the loops, terminal domains, lipid bilayer and solvent are unrealistic. Any attempts to account quantitatively for ligand binding and signal transduction using models of this type must be viewed with scepticism.

2.2.2 Agonist receptor complexes

Amino acid residues of the 5-HT receptors will be referred to by their three letter code followed by the respective position of the residue in the helix followed finally by the helix number in parenthesis.

2.2.2.1 The 5-HT receptor complex

The results from the extensive docking studies of the 5-HT conformations were analysed in terms of ligand receptor interactions and relevance towards the

experimental data available. Given the limitations of the modelling approach and the forcefield used, the overall topology of the receptor binding site was considered to be the most important aspect of the models. Hence the final results obtained and presented are not necessarily the most energetically favourable orientations of the ligand within the binding site but they did prove to be the most feasible in terms of the experimental data reported in the literature.

The observed 5-HT binding pocket was found to be in a similar position for both conformations of 5-HT at the 5-HT_{1A} (Figure 12), 5-$HT_{1D\alpha}$ (Figure 13) and 5-$HT_{1D\beta}$ (Figure 14) receptor models. The 5-HT molecule is positioned approximately 15 Å into the central cleft from the extracellular opening and is surrounded by helices 3, 4, 5 and 6. It is also conceivable that helix 7 may contribute to the binding of some agonists. The aromatic indole ring of 5-HT is anchored by two conserved aromatic residues TRP9(H4) and PHE18(H6) which lie below the plane (towards the cytoplasm) of the indole ring and create favourable perpendicular interactions with the ligand.

The protonated amine of 5-HT forms an ionic interaction with the carboxylate anion of the important aspartate residue of helix 3 ASP10(H3) with a mean NH--OC distance of 2.01 Å. The ion pair is further stabilised from the interactions of the protonated amine function with three neighbouring aromatic residues PHE/TRP6(H3), PHE17(H6) and TRP14(H6). This type of stabilisation has been observed in the crystal structures of some globular proteins[396].

The 5-hydroxyl group of 5-HT can accept a hydrogen bond from THR6(H5) with a mean OH--O distance of 1.93 Å. This residue is mutated for a serine in the 5-HT_2 subtype of receptors. In the case of the 5-HT_{1D} receptors it is also possible that the oxygen of the hydroxyl group of 5-HT can accept an additional

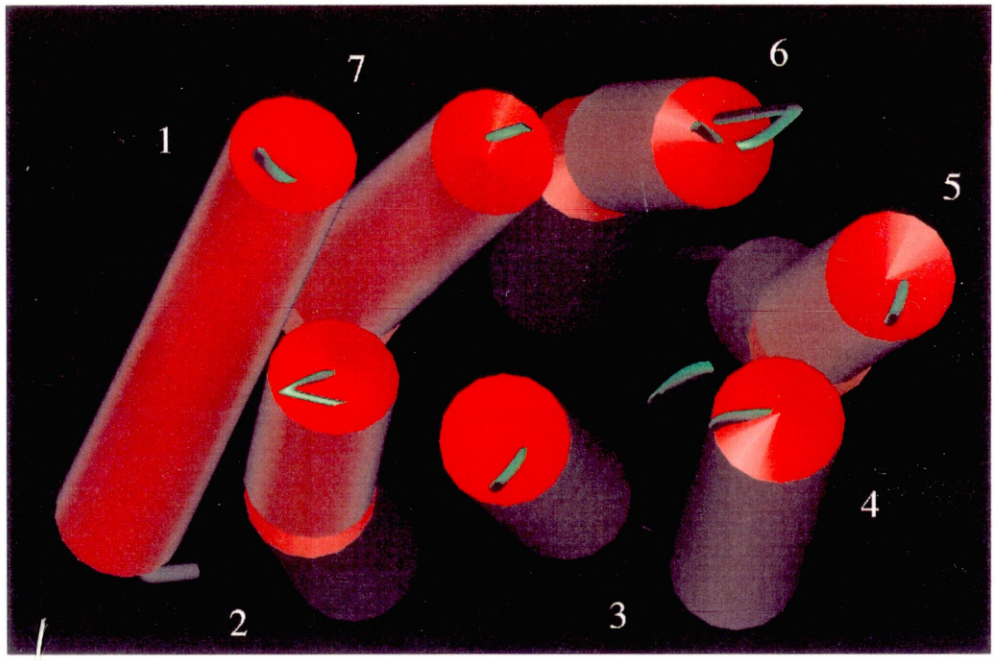

FIGURE 11
The seven helices of the 5-HT receptor models viewed from the extracellular surface

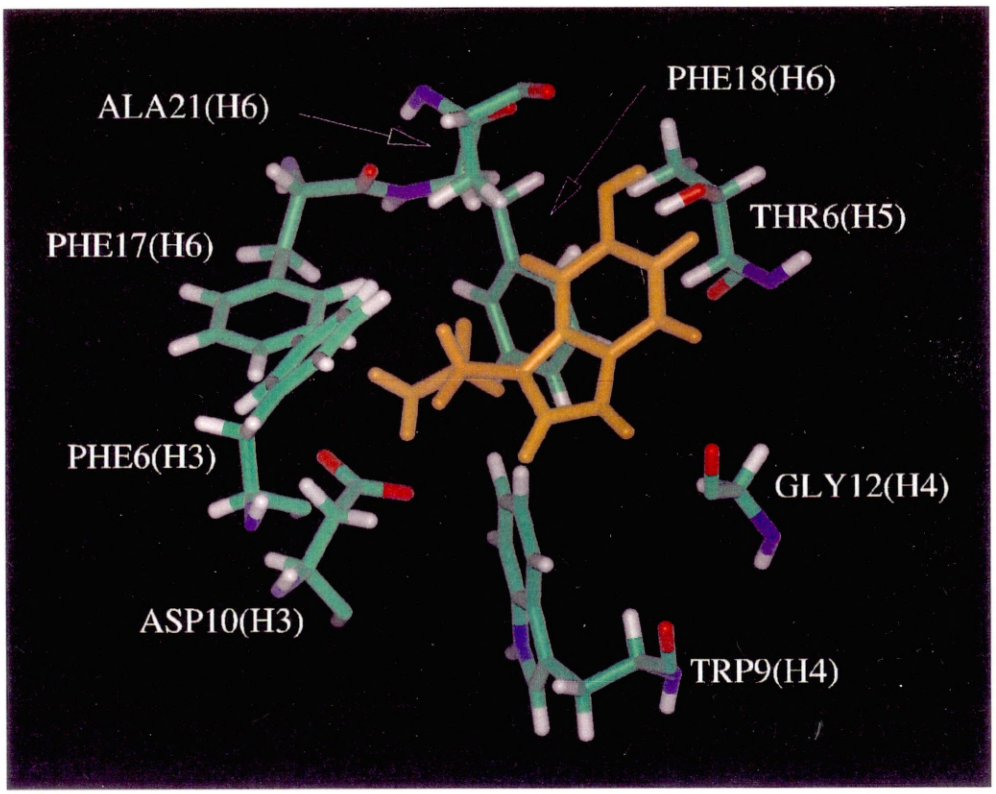

FIGURE 12
5-HT(A) In the 5-HT$_{1A}$ receptor agonist binding site

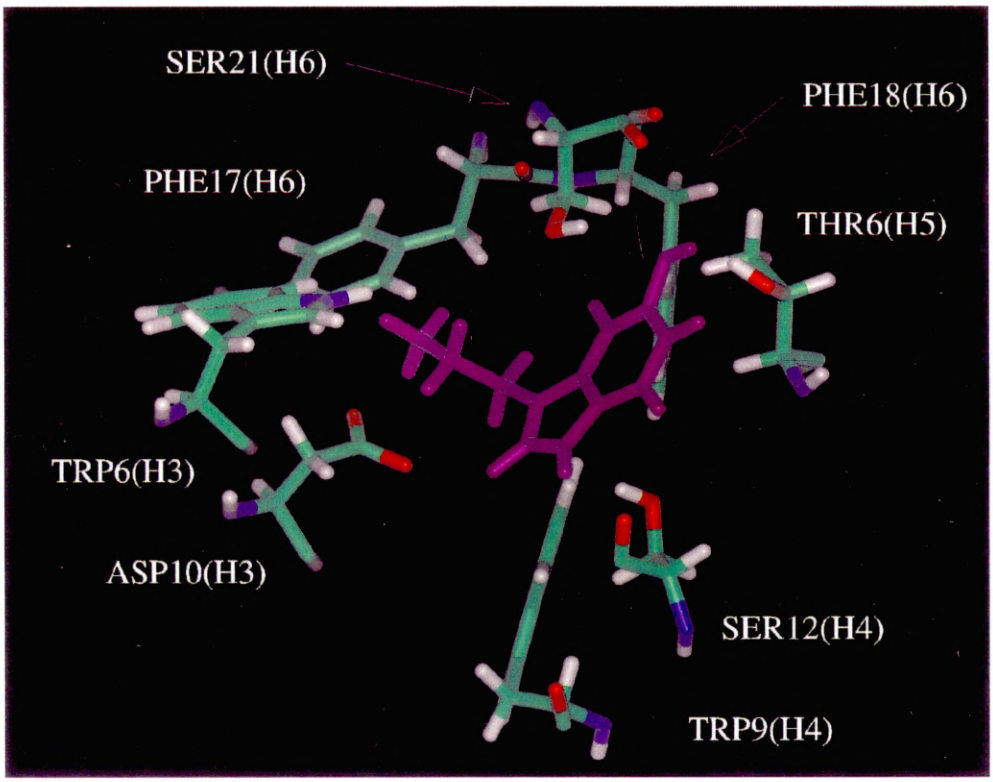

FIGURE 13

5-HT(B) In the 5-$HT_{1D\alpha}$ receptor agonist binding site

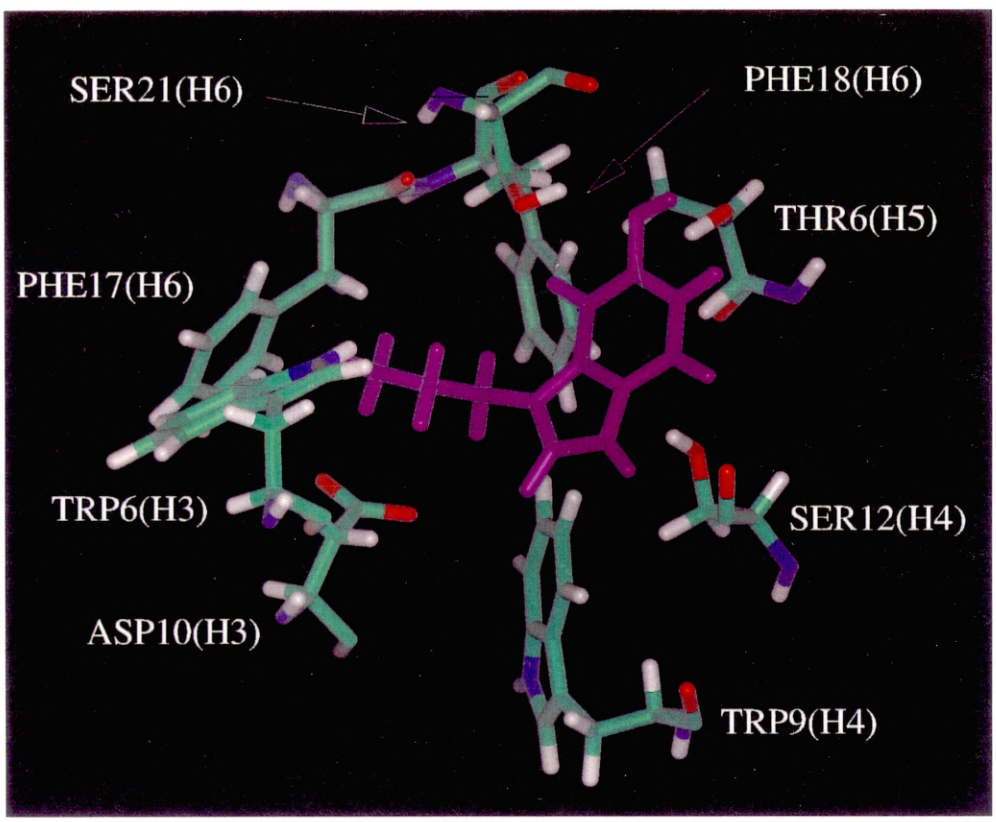

FIGURE 14

5-HT(B) In the 5-HT$_{1D\beta}$ receptor agonist binding site

hydrogen bond from SER21(H6) although the mean hydrogen bond angle (O--H--O) of 114° is not ideal. This residue is mutated for an alanine residue in the 5-HT_{1A} receptor.

An unusual interaction was discovered between the indole N-H group of 5-HT and SER12(H4) of the 5-HT_{1D} receptor models. The hydroxyl group of SER12(H4) is below the plane of the indole ring and directly underneath the 5-membered pyrrole moiety thus the serine residue cannot accept a hydrogen bond from the indole ring. The indole ring cannot act as a good hydrogen bond acceptor since the lone pair of electrons associated with the indole nitrogen is used in maintaining the aromaticity of the indole ring. This therefore prompts the hypothesis that the hydroxyl group of the serine residue interacts in a charge transfer complex with the π-electrons of the indole ring. The mean distance from the hydroxyl group to the centroid of the 5-membered ring is 2.49 Å. This type of interaction has previously been reported[236] in a model of the β_2-adrenergic receptor. The alternatives to this hypothesis are that the indole N-H can donate a hydrogen bond to the backbone carbonyl of SER12(H4) or that the 5-HT binding site is inaccurate. In the 5-HT_{1A} receptor model the serine residue is mutated for glycine and the indole N-H of 5-HT can interact with the backbone of GLY12(H4). This interaction however is thought to be of minor importance for agonist binding at the 5-HT_{1A} receptor for reasons that will be discussed in section 2.2.2.2.

It has also become apparent that both conformations of the ligand 5-HT(A) and 5-HT(B) can be accommodated within the binding site with minimum steric clashing between receptor and ligand. A closer inspection taking into account the relative ligand receptor interaction energies (Table 4) indicates that the 5-HT_{1A} receptor model has a distinct preference for conformation A of 5-HT.

This is in direct contrast to the 5-HT_{1D} receptor models which show greater (less positive) interaction energies with 5-HT(B) i.e. conformation B.

Ligand	Receptor model	Interaction Energy (kcal/mol)
5-HT(A)	5-HT_{1A}	0.0
5-HT(B)	5-HT_{1A}	17.3
5-HT(A)	5-$HT_{1D\alpha}$	5.1
5-HT(B)	5-$HT_{1D\alpha}$	0.0
5-HT(A)	5-$HT_{1D\beta}$	3.3
5-HT(B)	5-$HT_{1D\beta}$	0.0

Table 4 Relative interaction energies of 5-HT(A) and 5-HT(B) with the receptor models

2.2.2.2 The 8-OH-DPAT receptor complex

Within the 5-HT_{1A} receptor model both conformations of the ligand, 8-OH-DPAT(I) and 8-OH-DPAT(II) can be accommodated in the agonist binding site (Figure 15) which was identified for 5-HT. The *n*-propyl substituents are surrounded by the hydrophobic residues PHE17(H6) and PHE6(H3) which appear to adjust their conformations slightly to allow ligand binding. The residues TRP14(H6), ILE7(H3) and ILE5(H7) also form interactions with the *n*-propyl substituents but are not shown in Figure 15.

The protonated amino group forms an ion pair with ASP10(H3) and the hydroxyl group can accept a hydrogen bond from THR6(H5). Calculation of the ligand receptor interaction energies (Table 5) have demonstrated that 8-OH-

DPAT(II) forms a more energetically favourable ligand receptor complex. This is consistent with 8-OH-DPAT(II) being the global minimum energy conformation of the ligand.

Ligand	Receptor model	Interaction Energy (kcal/mol)
8-OH-DPAT(I)	5-HT_{1A}	14.1
8-OH-DPAT(II)	5-HT_{1A}	0.0

Table 5 Relative interaction energies of 8-OH-DPAT(I) and 8-OH-DPAT(II) with the 5-HT_{1A} receptor model

The results for the docking of 8-OH-DPAT into the 5-HT_{1D} receptor models presented quite a different story (Figure 16). Both conformations of 8-OH-DPAT in the 5-$HT_{1D\alpha}$ and 5-$HT_{1D\beta}$ receptor models have moved down the central cleft towards the cytoplasm by 1-2 Å. This has been attributed to steric repulsion between one of the bulky *n*-propyl groups with the larger tryptophan residue, TRP6(H3). This residue is conserved in all of the 5-HT receptors of the present study with the exception of the 5-HT_{1A} receptor which has a phenylalanine residue which, with a slight adjustment of conformation can accommodate the *n*-propyl substituent quite easily.

Steric bumping was also observed between the aminotetralin ring of the ligand and SER12(H4) of the 5-HT_{1D} receptors. This residue is also conserved in all the 5-HT receptors examined in this work with the exception of the 5-HT_{1A} receptor where a glycine is found. Movement of the ligand as a result of this steric bumping at the 5-HT_{1D} receptors results in the hydrogen bond of the hydroxyl group of 8-OH-DPAT to THR6(H5) being altered. The hydroxyl

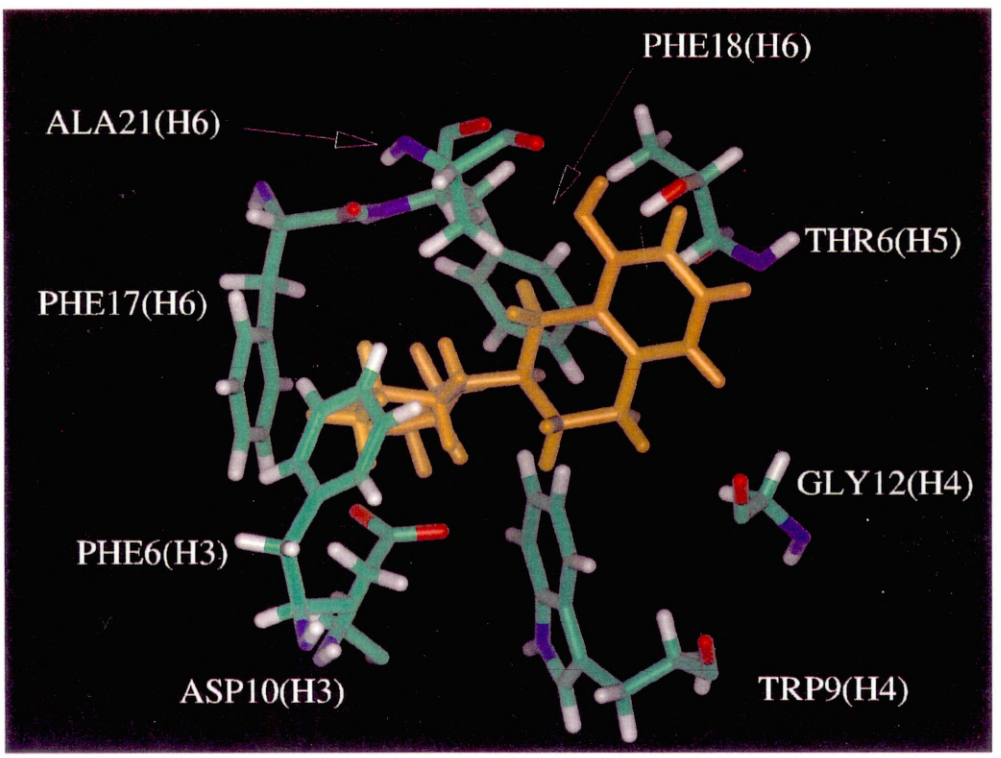

FIGURE 15
8-OH-DPAT(II) In the 5-HT_{1A} receptor agonist binding site

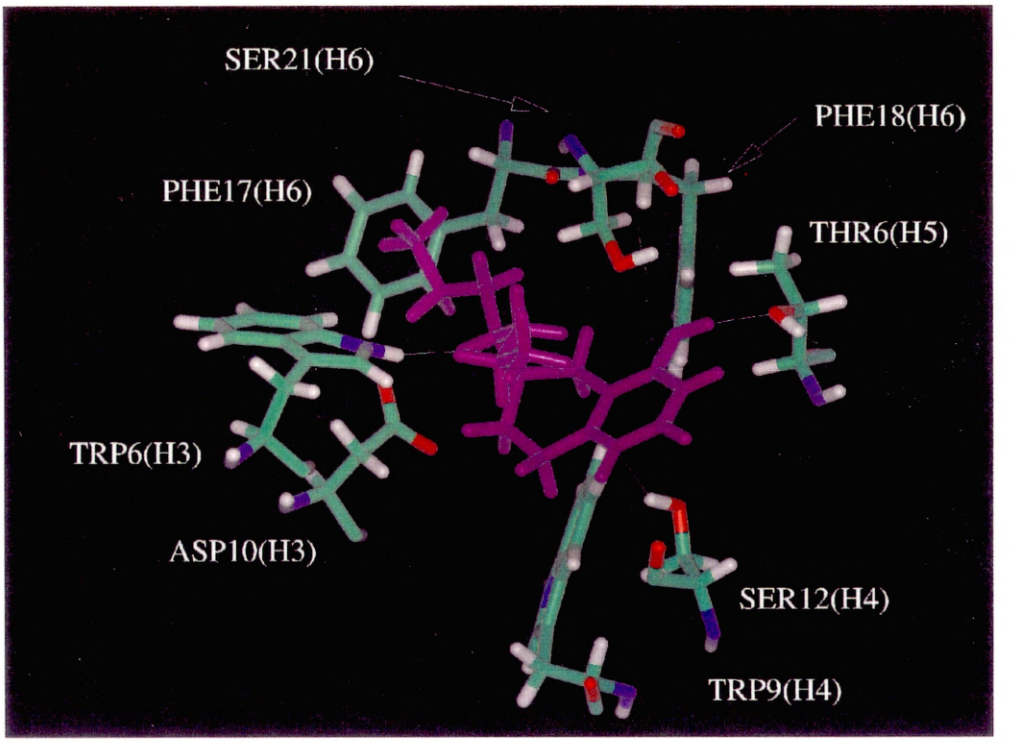

FIGURE 16
8-OH-DPAT(I) In the 5-$HT_{1D\alpha}$ receptor agonist binding site

group of the ligand now donates a hydrogen to the threonine residue instead of accepting a hydrogen as is observed for the 5-HT_{1A} receptor complex.

It is therefore suggested that SER/GLY12(H4) and TRP/PHE6(H3) play an important role in the fit and selectivity of 8-OH-DPAT at the 5-HT receptors. The steric bumping and tightness of fit of 8-OH-DPAT at the 5-HT_{1D} receptor models has led to unfavourable interactions and has caused the movement of the ligand within the agonist binding site. This may account for the selectivity of 8-OH-DPAT for the 5-HT_{1A} receptor.

Going back to the role of GLY/SER12(H4) it is clear that 8-OH-DPAT has no hydrogen bond donating group with the potential to interact with the backbone of GLY12(H4). It is therefore proposed that the interaction between the indole N-H of 5-HT which was observed in the complex of 5-HT with the 5-HT_{1A} receptor is not required for high affinity binding to the 5-HT_{1A} receptor and is probably of minimal importance.

2.2.2.3 The 5-CT receptor complex

5-Carboxamidotryptamine was accommodated in the 5-HT_{1A}, 5-$HT_{1D\alpha}$ and 5-$HT_{1D\beta}$ receptor models in a similar position to that observed for 5-HT (no figure shown). In all the receptor models the ion pair was formed between the protonated amine and ASP10(H3). The aromatic indole ring of the ligand was held in position by TRP9(H4) and PHE18(H6) and the carbonyl group of 5-CT was well positioned to accept a hydrogen bond from THR6(H5). Additionally, in the 5-HT_{1D} receptor models the carbonyl oxygen could accept a further hydrogen bond from SER21(H6).

The indole ring formed an interaction with SER12(H4) for the 5-HT_{1D} receptor complexes as previously described for 5-HT. The hydroxyl group of SER12(H4) is directly below the 5-membered pyrrole ring of the ligand, allowing the hydroxyl group to interact with the aromatic ring of the ligand. The indole N-H is also in a position to form a hydrogen bond with the backbone carbonyl of SER12(H4). Again, similar to the results for 5-HT, the 5-HT_{1A} receptor model exhibited greater interaction energy with 5-CT(A) and the 5-HT_{1D} receptor models showed a preference for 5-CT(B) (Table 6).

Ligand	Receptor model	Interaction Energy (kcal/mol)
5-CT(A)	5-HT_{1A}	0.0
5-CT(B)	5-HT_{1A}	30.7
5-CT(A)	5-$HT_{1D\alpha}$	5.1
5-CT(B)	5-$HT_{1D\alpha}$	0.0
5-CT(A)	5-$HT_{1D\beta}$	3.7
5-CT(B)	5-$HT_{1D\beta}$	0.0

Table 6 Relative interaction energies of 5-CT(A) and 5-CT(B) with the receptor models

2.2.2.4 The 5-OH-TMT receptor complex

Initial analysis of these complexes shows that both conformations of the ligand were accommodated in a similar position to that of 5-HT within the proposed binding site of the 5-HT_{1A} receptor model. A hydrogen bond was formed between THR6(H5) and the hydroxyl group of 5-OH-TMT but a closer inspection of the ligand binding site unearthed some additional findings.

For 5-OH-TMT(A), steric bumping between the methyl groups of the quaternary amine and the aromatic residues PHE17(H6) and PHE18(H6) causes the conformation of the C-3 sidechain of the ligand to become extended. In the case of 5-OH-TMT(B) steric bumping of the sidechain methyl groups with PHE17(H6) and ASP10(H3) was observed. This bumping results in a conformational change of the highly important aspartate residue causing the carboxylate anion to be directed away from the agonist binding site towards transmembrane helices 2 and 7.

The conformational changes described above result in the cationic amine group being positioned further away from the carboxylate anion of ASP10(H3) compared to the corresponding distance in the 5-HT - 5-HT_{1A} receptor model complexes (Table 7).

Ligand	Distance ligand-N^+---O-ASP10(H3) (Å)
5-OH-TMT(A)	5.18
5-OH-TMT(B)	4.38
5-HT(A)	3.01
5-HT(B)	2.93

Table 7 Protonated amine-ASP10(H3) distances for the 5-OH-TMT and 5-HT complexes with the 5-HT_{1A} receptor

This will undoubtedly lead to a significant decrease in the electrostatic interaction energy between 5-OH-TMT and ASP10(H3). In conclusion the results highlight the tightness of fit between 5-OH-TMT and the 5-HT_{1A} receptor. This tightness of fit has induced conformational changes in either the

ligand or the receptor leading to an increased distance and decreased electrostatic interaction energy between the ligand and the important aspartate residue of helix 3. This may explain the reduced binding affinity of 5-OH-TMT for the 5-HT_{1A} receptor when compared to 5-HT.

2.2.2.5 The sumatriptan receptor complex

Major conformational changes in both ligand and 5-HT_{1D} receptor models were observed for all but one of the sumatriptan C-5 substituent conformations. The exception occurred when the C-5 substituent was folded back across the indole ring moiety, thus enabling sumatriptan to be accommodated. This resulted in two conformations of sumatriptan, sumatriptan(A) and sumatriptan(B) dependant upon the conformation of the C-3 sidechain and similar to 5-HT(A) and 5-HT(B) respectively.

Both conformations of sumatriptan fit into the 5-$HT_{1D\alpha}$ and 5-$HT_{1D\beta}$ receptor models allowing the protonated amine group of sumatriptan to form an ion pair with ASP10(H3) (Figure 17). The indole ring is again anchored by the aromatic residues TRP9(H4) and PHE18(H6). There is however a minor reorganisation of the aromatic residues surrounding the protonated amine - ASP10(H3) ion pair. The sidechains of PHE17(H6), PHE2(H7) and PHE5(H7) all undergo a slight change in conformation to avoid steric bumping with the dimethylamino group of the ligand. The hydroxyl group of SER12(H4) is positioned directly below the 5-membered pyrrole ring of sumatriptan thus allowing the hydrogen of the hydroxyl to interact with the π-electrons of the aromatic system. An additional hydrogen bonding interaction is proposed between the indole N-H and the hydroxyl oxygen of SER16(H4) which is conserved in all the 5-HT receptors studied. One of the oxygens of the sulfone group can accept hydrogen bonds from both THR6(H5) and SER21(H6).

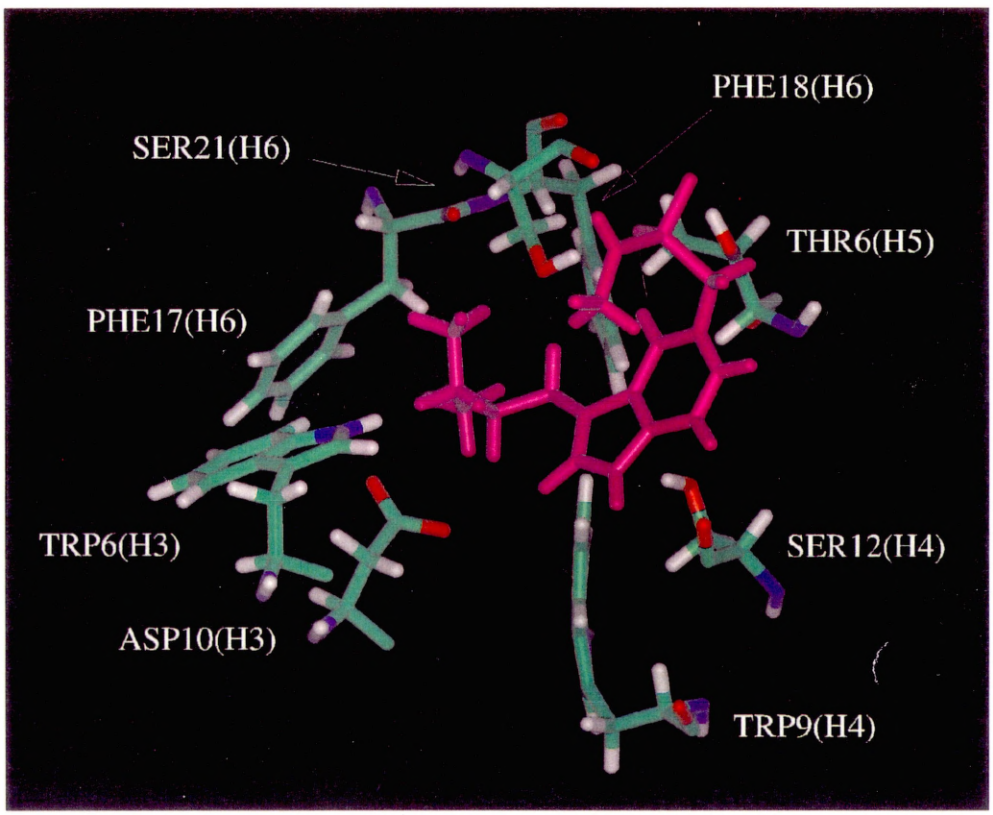

FIGURE 17
Sumatriptan(B) In the 5-$HT_{1D\beta}$ receptor agonist binding site

Examination of the interaction energies between the two conformations of sumatriptan and the 5-HT_{1D} receptor models showed results that were consistent with those for 5-HT and 5-CT. The 5-$HT_{1D\alpha}$ and 5-$HT_{1D\beta}$ receptor models have a preference for the sumatriptan(B) conformation (Table 8).

Ligand	Receptor model	Interaction Energy (kcal/mol)
Sumatriptan(A)	5-$HT_{1D\alpha}$	12.2
Sumatriptan(B)	5-$HT_{1D\alpha}$	0.0
Sumatriptan(A)	5-$HT_{1D\beta}$	20.2
Sumatriptan(B)	5-$HT_{1D\beta}$	0.0

Table 8 Relative interaction energies of sumatriptan(A) and sumatriptan(B) with the 5-HT_{1D} receptor models

The 5-HT_{1A} receptor model and sumatriptan complex showed quite contrasting results. The ion pair between the protonated amine and ASP10(H3) is formed and one of the sulfone oxygen atoms can maintain the hydrogen bond with THR6(H5). The 5-HT_{1A} receptor has an alanine residue at position 21 of helix 6 (serine in the case of 5-HT_{1D}), but this residue does not allow the C-5 substituent of sumatriptan to be held in position and thus stabilise the conformation of the ligand. The nonpolar alanine residue ALA21(H6) does not interact favourably with the polar sidechain of sumatriptan. As a result the ligand has repositioned itself within the central cleft causing some conformational changes in the aromatic residues TRP14(H6) and PHE17(H6) which are in the vicinity of the cationic amine. The inability of ALA21(H6) of the 5-HT_{1A} receptor to hold sumatriptan in the folded conformation and to

stabilise the "active" conformation of the ligand may contribute to the decreased affinity of sumatriptan for the 5-HT_{1A} receptor.

2.2.3 Evaluation of the binding site

2.2.3.1 Consistency with mutagenesis data

The agonist binding site presented within this study for the three 5-HT receptor models is consistent with the limited mutagenesis data available. ASP10(H3) is known[104] to be crucial in the binding of high affinity agonists at the 5-HT_{1A} receptor. Mutation of THR6(H5) has also been shown[104] to have a critical effect on the binding of agonists to the 5-HT_{1A} receptor. In the models developed both of these residues have been shown to have essential roles. The aspartate residue forms an ion pair with the cationic amine group which is characteristic of all 5-HT receptor agonists and the threonine residue donates a hydrogen bond to the agonist.

Mutagenesis studies[104] have also implicated the serine residue SER5(H5) in the binding of agonists to the 5-HT_{1A} receptor. The 5-HT receptor models however show no direct interaction between any of the studied agonists and SER5(H5). Mutation of the equivalent residue[397] in the β_2-adrenergic receptor, SER203-ALA resulted in the absence of normally processed receptor protein[94]. It is therefore possible that the SER5(H5) residue of the 5-HT_{1A} and 5-HT_{1D} receptors may play a similar role or be involved in maintaining the conformation of the receptor.

The conserved phenylalanine residue PHE18(H6) is one of the aromatic residues in the models which anchors the aromatic ring moiety present in all 5-HT receptor agonists and has been shown for the 5-HT_{2A} receptor to be important in agonist binding[108]. It is therefore plausible that since this residue is conserved

in all the 5-HT receptors studied it will play a similar important role in the binding of agonists to the 5-HT_{1A} and 5-HT_{1D} receptors.

Of the remaining residues that have been shown from the models to participate directly in agonist binding there is no available mutagenesis data for the 5-HT_1 subtype of receptors. These amino acid residues such as ALA/SER21(H6) and the residues of helix 4 may well be worthy of mutation studies. Nevertheless the presented models do seem highly feasible because of their compatibility with the limited mutagenesis data.

2.2.3.2 The binding of 5-HT, 5-CT, 5-OH-TMT and 8-OH-DPAT

The receptor models can account for the high affinity binding of 5-CT and 5-HT as a result of the comfortable accommodation of these ligands within the central cleft of the 5-HT_{1A} and 5-HT_{1D} receptor models. The decreased affinity of 5-OH-TMT for the 5-HT_{1A} receptor is explained by steric bumping between the ligand and the 5-HT_{1A} receptor model. This causes conformational changes which increase the distance between the cationic nitrogen of 5-OH-TMT and the important aspartate residue of helix 3, ASP10(H3). The increase in interatomic distance is accompanied by a decrease in the electrostatic energy between the ligand and ASP10(H3) thus explaining the decreased affinity of 5-OH-TMT for the 5-HT_{1A} receptor.

The 5-HT_{1A} selective agonist 8-OH-DPAT is one of the few 5-HT receptor full agonists that does not contain an indole ring. The 5-HT_{1A} receptor however has no residue with the potential to interact with the pyrrole moiety of the indole ring since a glycine residue is found at position 12 on helix 4 (GLY12(H4)). All the other 5-HT receptors in this study have a serine residue at this position which can cause steric bumping with the tetralin ring structure of 8-OH-DPAT. The

5-HT_{1A} receptor model also has a phenylalanine residue PHE6(H3) which is directly above (towards the extracellular space) the aspartate residue ASP10(H3). PHE6(H3) can adjust its conformation slightly to tolerate one of the bulky *n*-propyl groups of 8-OH-DPAT. The phenylalanine residue is only present in the 5-HT_{1A} receptor and occupies a lesser volume than the tryptophan residue TRP6(H3) observed for the other 5-HT receptors. Therefore the fact that the 5-HT_{1A} receptor is the only 5-HT receptor of the present study that has the GLY12(H4) and PHE6(H3) residues whereas the others have SER12(H4) and TRP6(H3) may explain why 8-OH-DPAT is one of the few selective 5-HT receptor agonists.

2.2.3.3 The role of THR6(H5)

One of the many interesting questions encountered in this study was the role of the hydroxyl group of 5-HT. The hydroxyl group almost certainly participates in a hydrogen bond with the receptor, but does it accept or donate a hydrogen bond?

It has been demonstrated[398] that the hydroxyl group of 5-HT may be replaced by a methoxy group without any significant loss of binding affinity for the 5-HT_{1A} receptor. The 8-hydroxy group of 8-OH-DPAT has also been replaced by a methoxy, thiomethyl or carboxamido group without loss of 5-HT_{1A} receptor binding affinity[398].

The 5-HT_{1D} receptors show a similar pattern. Replacement of the hydroxyl group of 5-HT for methoxy resulted in a slight decrease in binding affinity for bovine 5-HT_{1D} sites[65] (5-HT K_i=2.2 nM, 5-MeOT K_i=4.1 nM). *O*-Alkyl derivatives of 5-HT are also known to bind with high affinity to the 5-$HT_{1D\beta}$ receptor[68].

Therefore the replacement of the hydrogen atom of the hydroxyl group of 5-HT_{1A} and 5-HT_{1D} receptor agonists by other functional groups appears to have very little effect upon the binding affinities of the compounds. This suggests that the C-5 substituent of 5-HT and equivalent substituent of other 5-HT receptor agonists normally acts as a hydrogen bond acceptor during agonist binding at the 5-HT_{1A} and 5-HT_{1D} receptors. The presented models are entirely consistent with this hypothesis since all the modelled agonists can accept a hydrogen bond from THR6(H5). It is noted that an assumption has been made that all the 5-HT receptor agonists occupy the same binding pocket and bind in a similar manner.

2.2.3.4 The binding of sumatriptan

The binding of sumatriptan to the 5-HT receptor models has some important implications. Sumatriptan can fit into the agonist binding site of the 5-HT_{1D} receptor models when the C-5 substituent is folded back across the indole ring moiety. It appears likely that the amino acid residues SER21(H6) and THR6(H5) can hold the amino-sulfone group in position by hydrogen bonding. Mutation of SER21(H6) to alanine as observed for the 5-HT_{1A} receptor model can create unfavourable interactions between the small nonpolar alanine residue and the polar C-5 substituent of sumatriptan. This may contribute to the reduced affinity of sumatriptan for the 5-HT_{1A} receptor.

Although there is no mutagenesis data available for residue 21 of helix 6 there are two literature reports[152,207] of the participation of this residue in ligand binding at the 5-HT receptor models. The equivalent residue of the 5-HT_{2C} receptor, ASN21(H6) has been reported[152] to form a hydrogen bond with the hydroxyl group of 5-HT in a similar manner to the results presented in this

study. The same residue has also been implicated[207] from sequence analysis in the binding of 5-CT to the 5-HT_1 receptor subtype. Therefore it does appear to be possible that residue 21 of helix 6 is a major player in the binding of some compounds at the 5-HT receptors and would be a suitable candidate for mutagenesis experiments.

When discussing the binding of sumatriptan to the 5-HT_{1D} receptors the involvement of THR6(H7) cannot be ignored. It has been shown by a number of independent research groups that the mutation of THR6(H7)-ASN (asparagine is found in the 5-HT_{1A} and rodent 5-HT_{1B} receptors) decreases the affinity for sumatriptan by 5-15 fold[110-112]. This could imply a direct role for THR6(H7) in sumatriptan binding.

Analysing the models developed during this study, the threonine residue was found to be a distance of 8-10 Å away from the ligand. The threonine can however form a hydrogen bond to the backbone carbonyl of PHE2(H7) but the asparagine residue of the 5-HT_{1A} receptor cannot. Furthermore it is particularly interesting that the threonine residue is directly above the glycine residue GLY9(H7) which is conserved in the serotonergic, adrenergic, dopaminergic and histamine receptors[397]. The glycine residue may act as a helical hinge allowing the helix to kink during ligand binding but unfortunately this cannot be shown in the present model since the backbone atoms were fixed during minimisations. Therefore the conformational changes of PHE17(H6), PHE2(H7) and PHE5(H7) that accompany sumatriptan binding to the 5-HT_{1D} receptors may affect the conformation of helix 7. Any induced movement of helix 7 can be stabilised by a hydrogen bond between THR6(H7) and the backbone of PHE2(H7). There is no equivalent hydrogen bond observed for the 5-HT_{1A} receptor model thus any changes in the conformation of the helix around THR6(H7) will not be stabilised.

This proposal of the function of THR6(H7) is supported by Smolyar and Osman[173] who studied the interactions of sumatriptan with the 5-$HT_{1D\alpha}$ receptor, although the sumatriptan binding site of these workers differs considerably from that of the present study.

It can be postulated that THR6(H7) plays a direct role in sumatriptan binding either by hydrogen bonding or in a steric capacity. However at present there is not enough experimental data available to prove any of these hypotheses. The possibility of a direct role for THR6(H7) has arisen from the rhodopsin[121] derived models of the GPCRs. In these models it is believed that helix 7 is closer to the agonist binding site and helix 4 plays a less prominent role. It has been further stated[152] that bacteriorhodopsin based models ignore the importance of residues upon helix 7.

To test this hypothesis helix 7 of the 5-HT_{1D} receptor models developed in this study was translated into the central cleft in closer proximity to helices 2 and 3 and in a position similar to that of the helix in rhodopsin derived models. Although the calculated distance between THR6(H7) and sumatriptan decreased, it was still in the region of 4-5 Å. This renders the possibility of a direct hydrogen bond unlikely. It is also worth noting that of all the transmembrane helices of the 5-HT receptors the seventh helix is undoubtedly the most conserved and therefore is less likely to be important in the selectivity of ligands at the 5-HT receptors. Thus the findings of this study appear to support the hypothesis that THR6(H7) plays an indirect role in the binding and selectivity of sumatriptan.

In summary, two amino acid residues have been identified from the receptor models as having a major effect upon sumatriptan selectivity at the 5-HT_{1D}

receptors. The polar SER21(H6) residue forms favourable interactions with the amino-sulfone group of sumatriptan and THR6(H7) can play an indirect role stabilising any agonist induced conformational changes of the receptor.

2.2.3.5 The receptor bound conformation of 5-HT, 5-CT and sumatriptan

The results of energy minimisation demonstrated that both global minimum energy conformations of 5-HT and similar conformations of 5-CT and sumatriptan can occupy the proposed agonist binding site. This suggests two possible explanations.

The ligand binding process may allow the conformation of the flexible C-3 substituent of the ligand to fluctuate between minimum energy conformations during ligand binding and receptor activation. Obviously the static nature of the receptor models make this impossible to demonstrate however the calculated *in vacuo* energy barrier between the two global minimum energy conformations of 5-HT is low and of the order of 6 kcal/mol.

Alternatively the different conformations A and B may interact preferentially with the 5-HT_{1A} and 5-HT_{1D} receptors respectively. The interaction energies of the 5-HT, 5-CT and sumatriptan complexes have consistently shown that conformation B is preferred at the 5-HT_{1D} receptor models and conformation A is preferred at the 5-HT_{1A} receptor model. A similar hypothesis has been proposed[60] where, if the orientation of the ethylamine substituent of 5-HT receptor agonists was in an "easterly" direction relative to the indole ring this would confer high affinity binding for the 5-HT_{1D} receptors. If the sidechain was orientated in a "northerly" direction, high affinity for the 5-HT_{1A} receptor would be observed. Although these conformations are different from

conformations A and B presented in this study, the feasibility of the situation is highlighted.

The two explanations given above would have very different consequences upon the design of selective drugs for the 5-HT_1 subtype of receptors. If the 5-HT_1 receptors have a preference for different conformations of the characteristic C-3 sidechain of agonists this would allow the design of conformationally restricted molecules which may have improved 5-HT receptor selectivity. On the other hand the alternative hypothesis would be of no significant help in the design of new drugs.

2.2.3.6 Comparison with published models

The identified agonist binding site for the 5-HT receptor models has a certain degree of similarity to the models of Hibert's group[153-163]. Both models incorporate the aspartate of helix 3 and THR6(H5) but the aromatic residues anchoring the aromatic ring of the agonists differ and no mention has been made by this group of ALA/SER21(H6).

The 5-HT_{1A} receptor model was also compared to the model of the 5-HT_{1A} receptor from the 7TM database at EMBL in Heidelberg[214]. Although the exact lengths of the α-helices differ by a few residues the relative positions of the important amino acid residues are similar.

In summary although the presented models have a degree of similarity to some of the published 5-HT receptor models, this is the first work which correlates the modelling procedure and detailed ligand receptor interactions of agonists at the human 5-HT_{1A}, 5-$HT_{1D\alpha}$ and 5-$HT_{1D\beta}$ receptors.

2.2.3.7 Extrapolation of the models to other 5-HT receptors

Molecular models of the 5-ht$_{1E}$, 5-ht$_{1F}$, 5-HT$_{2A}$ and 5-HT$_{2C}$ receptors have not been constructed in this study but the models of the 5-HT$_{1A}$ and 5-HT$_{1D}$ receptors can be used in conjunction with the sequence alignment (Figure 4) to discuss possible agonist binding to these receptors. The glutamate residue GLU21(H6) of the 5-ht$_{1E}$ and 5-ht$_{1F}$ receptors may form unfavourable interactions with the amide group of 5-CT but not the hydroxyl group of 5-HT. This could account for the low affinity of 5-CT at the cloned 5-ht$_{1E}$ and 5-ht$_{1F}$ receptors[379]. This assumes that tryptamine compounds such as 5-HT bind to these receptors in a similar manner to ligand binding at the 5-HT$_{1A}$ and 5-HT$_{1D}$ receptors.

The binding of sumatriptan results in an intriguing anomaly. The 5-ht$_{1E}$ receptor has a threonine residue at position 6 of helix 7 and the 5-ht$_{1F}$ receptor has an alanine residue at this position. One would consequently expect that the 5-ht$_{1E}$ receptor would exhibit high affinity for sumatriptan and the 5-ht$_{1F}$ receptor low affinity for the ligand. However this is not the case and the exact opposite is true, sumatriptan binds with high affinity to the 5-ht$_{1F}$ receptor and low affinity to the 5-ht$_{1E}$ receptor[379]. This suggests that there are other unidentified factors contributing to the binding of sumatriptan at these receptors possibly a different mode of binding or the involvement of additional, as yet unidentified amino acid residues. From the sequence alignment the only residues that the 5-HT$_{1D}$ and 5-ht$_{1F}$ receptors have in common that are absent from the 5-HT$_{1A}$ and 5-ht$_{1E}$ receptors are ILE11(H3) and LEU11(H7). One or both of these residues may have an effect upon the binding of sumatriptan to the 5-ht$_{1E}$ and 5-ht$_{1F}$ receptors.

For the 5-HT_2 subtype of receptors, residue 21 of helix 6 is asparagine and this residue may force the nearby serine residue of helix 5 SER6(H5) to adopt a certain conformation with the hydroxyl group in a different position to the hydroxyl group of the threonine residue in the 5-HT_1 subtype of receptors. This would change the directionality of the hydrogen bond accepted by the ligand, thus creating a slightly different binding site. This issue of hydrogen bond directionality between the 5-HT_1 and 5-HT_2 subtypes has already been suggested[399,400] from the synthesis and pharmacological evaluation of conformationally constrained analogs of the natural neurotransmitter where the C-5 hydrogen bond acceptor function is constrained in a 6-membered ring. The slight changes in ligand binding site could perhaps allow 5-HT and other agonists to be orientated further into the cleft away from ASN21(H6) possibly allowing the indole N-H group to be in the vicinity of GLY5(H5) or SER/ALA9(H5). The latter residue is known to be important in the binding of some agonists to the 5-HT_{2A} and 5-HT_{2C} receptors[106,107,190].

Therefore although the 5-ht_{1E}, 5-ht_{1F}, 5-HT_{2A} and 5-HT_{2C} receptors have not been modelled a picture of the probable agonist binding sites can be proposed based on the models developed during this study which appear to be consistent with some of the available experimental data.

2.2.3.8 Antagonists, partial agonists and signal transduction

The binding of antagonists and partial agonists has not been investigated during this study but it is probable that the β-adrenoceptor antagonists such as (-)-propranolol (11) could interact with the 5-HT_{1A} receptor model by occupying the pocket between helices 1, 2, 3 and 7. The amino group could form an ion pair with ASP10(H3) and the hydroxyl group and ether oxygen can

participate in hydrogen bonds with ASN6(H7) in a similar manner to that recently described[172].

The 5-HT_{1A} partial agonists such as buspirone[398] (134) can conceivably occupy both the agonist and β-adrenoceptor antagonist binding pockets with one of the piperazine nitrogens forming an ion pair with ASP10(H3). These hypotheses are sheer speculation and unlike the agonists, partial agonists and antagonists are structurally diverse and may occupy different regions of the receptor and interact with different amino acid residues.

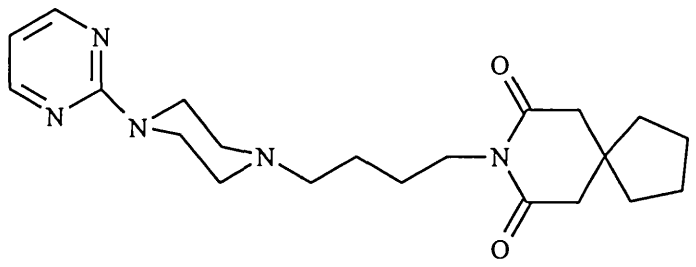

(134)

No attempt whatsoever has been made to rationalise the signal transduction process. In order to study this, one would need to analyse the dynamics trajectories of receptor models with bound agonists, partial agonists and antagonists. It is thought that without the explicit inclusion of the loops, terminal domains, lipid bilayer and any solvent into the models that any attempt to rationalise signal transduction would be very crude and potentially misleading.

2.2.4 Thienopyridine small molecule modelling

As anticipated there was a high degree of similarity between the thieno[2,3-b]pyridine analogs of 5-HT, THI(A) and THI(B) with the neurotransmitter conformations 5-HT(A) and 5-HT(B) (Table 9).

Thienopyridine	5-HT	RMS Fit (Å)	Electrostatic Fit (score)
THI(A)	5-HT(A)	0.182	0.999
THI(B)	5-HT(B)	0.182	0.999

Table 9 RMS and electrostatic similarity comparisons of 5-HT and THI

The RMS fit (Figure 18) indicated an excellent superposition between the two molecules with both the hydroxyl oxygen and protonated nitrogen in identical positions. The only minor difference being the position of the sulfur atom of the thieno[2,3-b]pyridine as compared with the indole N-H group of 5-HT. Molecular volumes were calculated (Table 10) and it was observed that they were similar for the 5-HT and thieno[2,3-b]pyridine conformations however the thiophene ring of the thieno[2,3-b]pyridine occupies a slightly greater volume than the pyrrole ring of 5-HT.

Ligand	Volume ($Å^3$)
5-HT(A)	142.51
5-HT(B)	143.26
THI(A)	149.66
THI(B)	149.07

Table 10 Molecular volumes of 5-HT and THI

Furthermore, molecular volume differences using the RMS superposition were calculated (Table 11). The difference in volumes accounted for approximately 10% of the volume occupied by the thieno[2,3-b]pyridine and this was attributed to the overlap around the indole N-H and thiophene sulfur.

Thienopyridine	5-HT	Alignment	Volume difference ($Å^3$)
THI(A)	5-HT(A)	RMS	14.96
THI(B)	5-HT(B)	RMS	15.03
THI(A)	5-HT(A)	Electrostatic	20.06
THI(B)	5-HT(B)	Electrostatic	15.74

Table 11 Aligned molecular volume differences between THI and 5-HT

The electrostatic similarity scores (Table 9) indicate virtually identical electrostatic potentials. The molecular alignment (Figure 19) however is certainly not as good as that observed in the RMS fitting. The C-3 ethylamino sidechains of the molecules are superimposed very well but this is at the expense of the aromatic rings. It appears that the electrostatic fitting procedure is dominated by the large positive electrostatic potential associated with the protonated amino groups. This has resulted in an excellent alignment of the C-3 substituents but a poorer alignment of the aromatic rings and hydroxyl groups. Molecular volume difference analysis using the electrostatic alignment (Table 11) has shown that the difference in volumes has increased for conformation A and is essentially unchanged for conformation B in comparison to the volume differences from the RMS alignment. The main areas of difference are surrounding the hydroxyl groups and the sulfur atoms of the thieno[2,3-b]pyridine conformations.

This small molecule modelling has therefore acted as an initial guide and has highlighted the similarities between the thieno[2,3-b]pyridine analog of 5-HT and 5-HT. There are however small differences in occupied volume, mainly surrounding the 5-membered rings which may or may not be of importance.

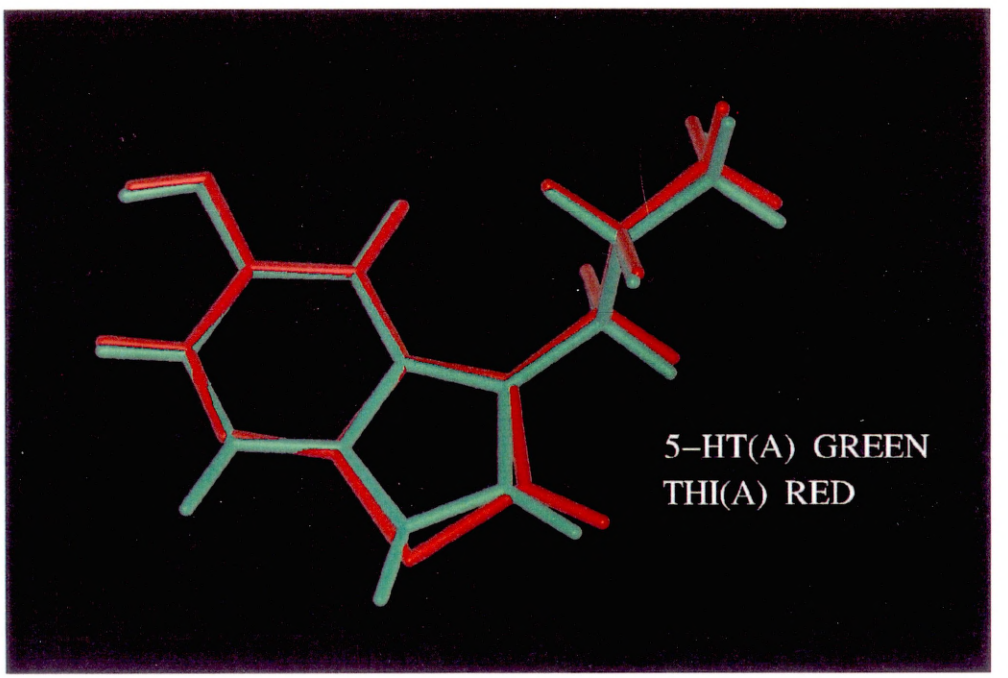

FIGURE 18
RMS Superposition of 5-HT(A) and THI(A)

FIGURE 19
Electrostatic superposition of 5-HT(B) and THI(B)

Nevertheless due to the similarity with 5-HT, the thieno[2,3-b]pyridine analog of 5-HT is a suitable candidate for ligand receptor modelling studies and synthesis.

2.2.5 Thieno[2,3-b]pyridine receptor interactions

The two conformations of the thieno[2,3-b]pyridine analog of 5-HT can be accommodated easily within the agonist binding site of all the 5-HT receptor models (Figure 20). The thieno[2,3-b]pyridine ring can occupy the same position as the indole ring of 5-HT interacting with PHE18(H6) and TRP9(H4). The protonated amine can form an ion pair with ASP10(H3) and the hydroxyl group can accept a hydrogen bond from THR6(H5). In the 5-HT_{1D} receptor complexes, the ligand can form an additional interaction between the hydroxyl group and SER21(H6). The serine residue SER12(H4) of the 5-HT_{1D} receptors can interact with the electron rich thiophene ring in the same manner as the residue can interact with the 5-membered pyrrole ring of 5-HT. Obviously the thiophene ring cannot participate in a hydrogen bond to the backbone carbonyl of SER12(H4) but it is not known how important this interaction is. If the interaction is unimportant, the thieno[2,3-b]pyridine would be expected to have equal affinity for the 5-HT_{1A} and 5-HT_{1D} receptors. On the other hand if the interaction is indeed important one would expect a higher affinity of the compound for the 5-HT_{1A} receptor since a hydrogen bond donating group at this position is definitely not essential for high affinity 5-HT_{1A} receptor binding.

Looking at the ligand receptor interaction energies (Table 12) it is again apparent that the 5-HT_{1A} receptor has a preference for THI(A) which is the equivalent of conformation A of 5-HT. The 5-HT_{1D} receptor models have a preference for conformation B i.e. THI(B).

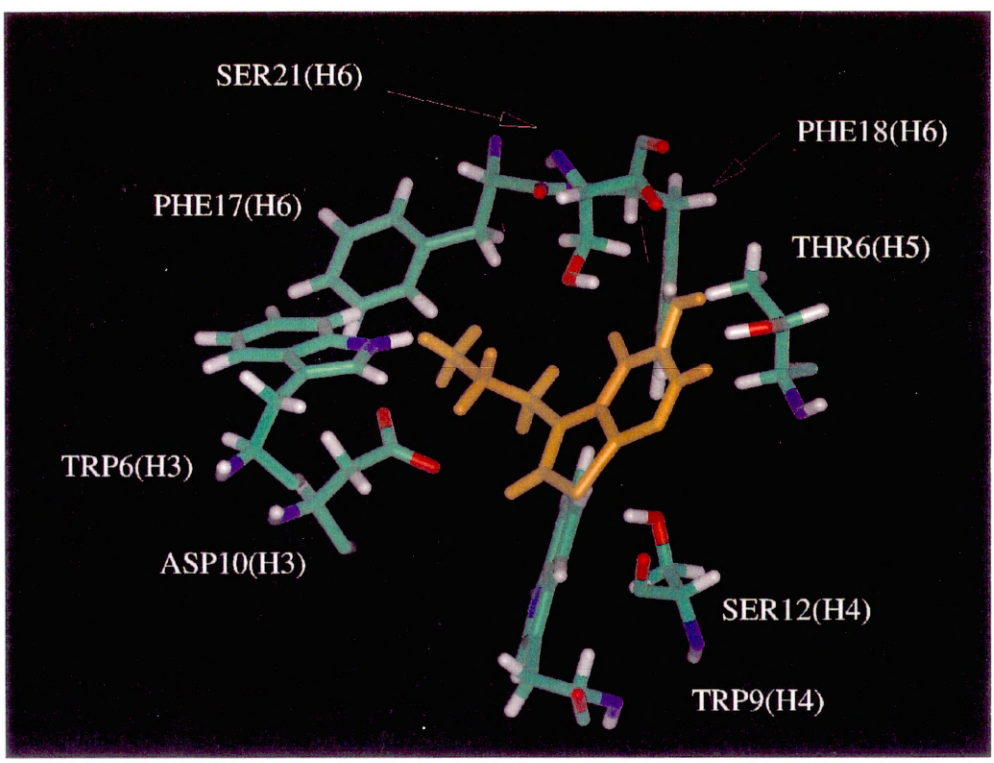

FIGURE 20
THI(B) In the 5-HT$_{1D\alpha}$ receptor agonist binding site

Ligand	Receptor model	Interaction Energy (kcal/mol)
THI(A)	5-HT_{1A}	0.0
THI(B)	5-HT_{1A}	16.3
THI(A)	5-$HT_{1D\alpha}$	4.3
THI(B)	5-$HT_{1D\alpha}$	0.0
THI(A)	5-$HT_{1D\beta}$	0.8
THI(B)	5-$HT_{1D\beta}$	0.0

Table 12 Relative interaction energies of THI(A) and THI(B) with the receptor models

These results further demonstrate that the thieno[2,3-b]pyridine analog of 5-HT can occupy the proposed agonist binding sites of the 5-HT_{1A}, 5-$HT_{1D\alpha}$ and 5-$HT_{1D\beta}$ receptor models. It therefore seems appropriate that this molecule be considered as an initial target for synthesis. Biological evaluation of this compound could then aid a better understanding of the requirements for agonist binding at the 5-HT_{1A} and 5-HT_{1D} receptors.

2.2.6 Ligand design and receptor selectivity

2.2.6.1 Suggestions of ligands

Many fragments that could be added to 5-HT, 5-CT or the thienopyridine analog of 5-HT were suggested using Ludi[395] (for a brief overview of Ludi see section 2.1.11). Only the fragments that occurred exclusively for one receptor model or those which were suggested many times for different ligands are discussed in the following sections. The most intriguing results were obtained exclusively for the 5-$HT_{1D\alpha}$ receptor where in many cases aromatic or alkyl groups were

suggested either at the C-5 or C-6 position of the aromatic rings of the ligand. One such suggestion was structure (135). It is proposed that the pyridine ring can occupy a similar region of the receptor model to the C-5 sidechain of sumatriptan.

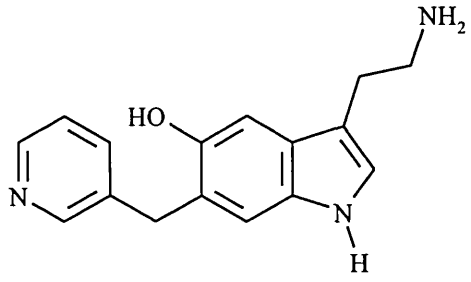

(135)

Suggestions that were common for all three receptor models included substitutions of the ethylamino sidechain with an (R)-hydroxyl group e.g. (136) with the hydroxyl group potentially forming interactions with either ASP10(H3) or SER12(H4).

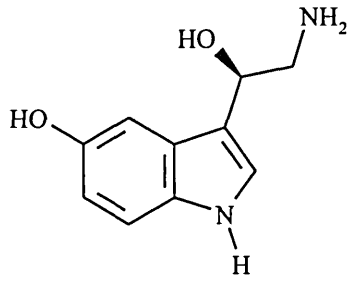

(136)

The incorporation of the C-5 hydrogen bonding acceptor into a 5 or 6 membered ring as observed in the structure (137) was another frequent suggestion allowing the new ring to be positioned between transmembrane helices 5 and 6. Similarly the constrained structure (138) allows the ring embedded nitrogen to interact with SER21(H6) of the 5-HT_{1D} receptors.

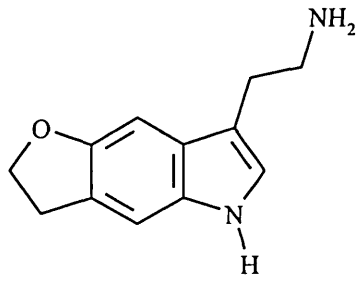

(137)

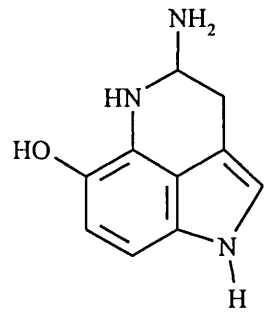

(138)

There was no significant difference between the fragments suggested for the indole compounds 5-HT and 5-CT compared to the fragments suggested for the thieno[2,3-b]pyridine. The new potential ligands described above are all shown as indole compounds but could have equally been shown as the thieno[2,3-b]pyridine analogs.

2.2.6.2 Discussion and validation of the structures devised via Ludi

The fragments suggested by Ludi were compared to the vast experimental binding affinity data available for the 5-HT_{1A} and 5-HT_{1D} receptor sites. This permitted the feasibility of the suggestions to be assessed and also proved useful in the validation of the binding site.

Similar compounds to (135) have previously been examined for 5-HT receptor binding affinity. It was discovered[62] that the conformationally restricted compound (139) exhibited a 21 fold selectivity for 5-HT_{1D} sites over the 5-HT_{1A} site.

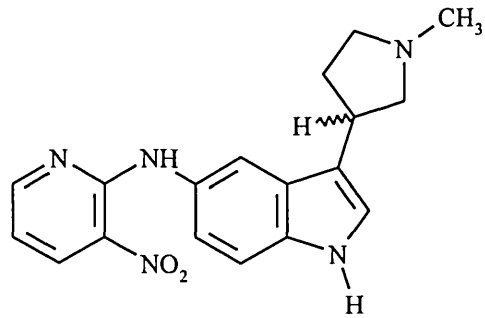

(139)

The same authors[400] have also studied compounds where the hydrogen bond acceptor is part of a 6-membered ring. The dihydropyrano[2,3-f]indole (140) however did not have an appreciable affinity for 5-HT_{1A} or 5-HT_{1D} receptor sites. Thus thieno[2,3-b]pyridine analogs of (137) would not appear to be suitable candidates to pursue.

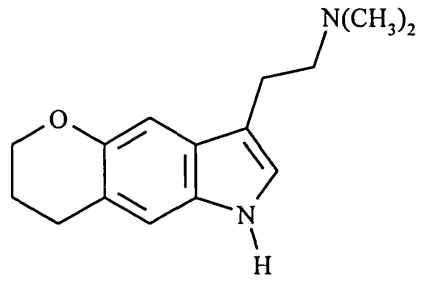

(140)

LY197206 (141) is a high affinity 5-HT_{1A} receptor ligand[401] which is similar to structure (138). Therefore compounds that are similar to the structures devised using Ludi are known 5-HT receptor agonists. This further validates the agonist binding sites proposed in this study.

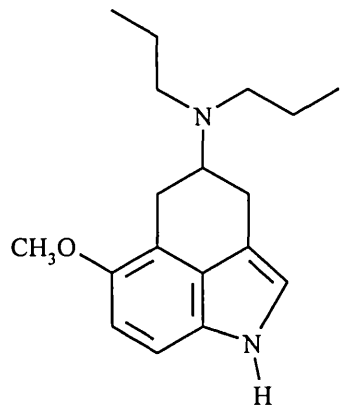

(141)

2.2.6.3 Receptor ligand interactions of compound (135)

Clearly, due to time constraints, all the suggested fragments could not be evaluated for ligand receptor interactions. As (135) was the only ligand suggested for one specific subtype of receptor, it was decided to study the receptor interactions of this molecule.

Compound (135) was constructed within InsightII, atom potential types and partial charges were assigned according to the CVFF forcefield and the amino nitrogen was protonated. Energy minimisation afforded two minimum energy conformations of (135) similar to conformations A and B of 5-HT. A conformational analysis was performed around the three rotatable bonds (Figure 21) at 30^{o} increments. Subsequent energy minimisation to an RMS gradient of less than 0.001 kcal/Å yielded two sets of four suitable minimum energy structures differing in energy by 5.9 kcal/mol. These were docked into the 5-HT_{1A}, 5-$HT_{1D\alpha}$ and 5-$HT_{1D\beta}$ receptor models in a position equivalent to 5-HT at the respective receptor models. The ligand receptor complexes were energy minimised as described previously for the 8-OH-DPAT receptor complex.

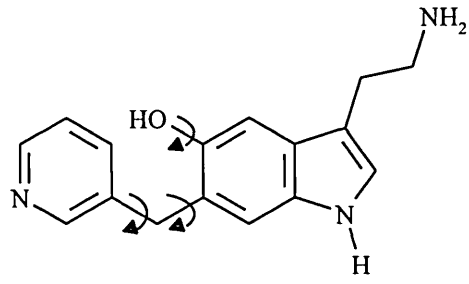

Figure 21 The three rotatable bonds of (135)

Compound (135) was found to be accommodated at the 5-$HT_{1D\alpha}$ receptor model occupying a position similar to sumatriptan at the same receptor model (Figure 22). The protonated amine could interact with ASP10(H3) and the indole nucleus was anchored by TRP9(H4) and PHE18(H6). Interaction with SER12(H4) was also possible. The hydroxyl group accepted a hydrogen bond from THR6(H5) and interacted with SER21(H6). Additionally the nitrogen of the pyridine ring could accept a hydrogen bond from THR2(H5) however this residue is conserved in all the 5-HT_1 subtype of receptors.

More interestingly when the same molecule was docked into the 5-$HT_{1D\beta}$ receptor model and energy minimised all the interactions described for the 5-$HT_{1D\alpha}$ receptor were maintained except the hydrogen bond between the pyridine ring of (135) and THR2(H5). The pyridine ring bumped with PHE20(H4) (LEU for 5-$HT_{1D\alpha}$) causing a reorientation of the pyridine ring and a conformational change in PHE20(H4) resulting in no hydrogen bond formation.

Similarly at the 5-HT_{1A} receptor model, (135) can interact with ASP10(H3), THR6(H5), TRP9(H4) and PHE18(H6) but due to steric hindrance between the pyridine ring and MET20(H4) both the ligand and the residue have to change their positions. Thus no interaction is observed between (135) and THR2(H5). The pyridine ring can therefore cause steric bumping with residue 20 of helix 4 of the 5-HT_{1A} and 5-$HT_{1D\beta}$ receptor models causing both the pyridine ring and the offending residue to change conformation preventing hydrogen bond formation. If this change in conformation is unfavourable (135) may have a higher affinity for the 5-$HT_{1D\alpha}$ subtype over the remaining 5-HT_1 receptors.

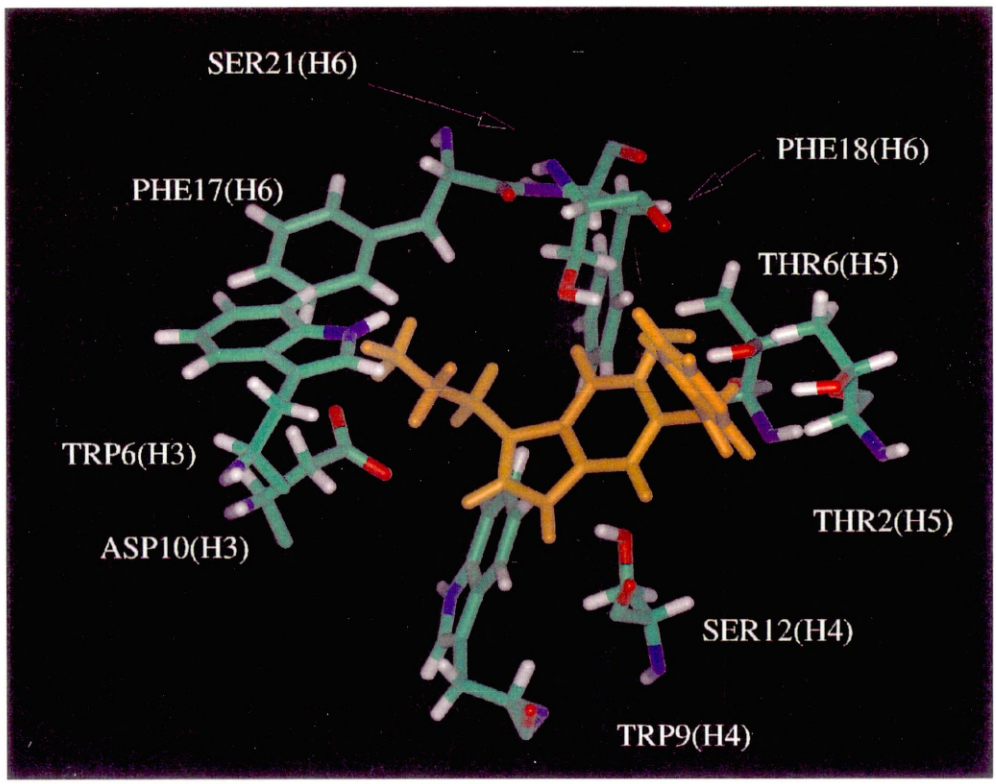

FIGURE 22
Compound (135)(B) In the 5-$HT_{1D\alpha}$ receptor agonist binding site

2.2.7 Receptor selectivity

The preceding section has highlighted one of the few amino acid residues within the vicinity of the agonist binding pocket that is different for the 5-HT_{1A}, 5-$HT_{1D\alpha}$ and 5-$HT_{1D\beta}$ receptors i.e. MET/LEU/PHE20(H4). In the design of more selective agonists, residues which differ between receptors must be identified and used to suggest ligands that might increase receptor selectivity. It is therefore possible that ligands which may interact with the various amino acids positioned at residue 20 helix 4 can improve the selectivity for one of the 5-HT_{1D} receptors.

From analysis of the sequence alignment, several alternative residues which differ between the 5-HT_{1D} receptors can be proposed. Possible candidates include ILE/VAL1(H3), LEU/VAL2(H3), ILE/PHE5(H3), ILE/LEU18(H3) and LEU/ILE19(H3). Of these helix 3 residues only LEU/VAL2(H3) and ILE/LEU18(H3) are within the central cleft but both are conserved mutations that are too far away from the proposed agonist binding site to have an effect.

THR/VAL3(H4), ILE/LEU7(H4), ALA/VAL10(H4), ILE/PHE11(H4), CYS/SER14(H4), ILE/LEU17(H4) and LEU/PHE20(H4) are the residues that differ between the 5-HT_{1D} receptors on helix 4 but only the previously identified LEU/PHE20(H4) is within the central cleft close to the agonist binding site. The potential effects of this residue on selectivity have already been discussed. No suitable helix 5 residues were found but LEU/MET24(H6) is directed towards the central cleft above the important SER21(H6) residue. However the distance between LEU/MET24(H6) and the protonated amine of 5-HT in the energy minimised 5-HT_{1D} receptor complexes is approximately 10 Å and is probably too distant from the agonist binding site. Helix 7 is almost identical for the 5-$HT_{1D\alpha}$ and 5-$HT_{1D\beta}$ receptors except for the first and last

residues. The former being a conserved LEU/ILE substitution and the latter is too distant from the binding site.

Thus from a consideration of the sequence alignment and correlating this with the 3-dimensional receptor models, volumes of the surrounding agonist binding site which may confer selectivity can be identified. In the case of the 5-$HT_{1D\alpha}$ and 5-$HT_{1D\beta}$ receptors the most promising volume of difference is that above the aromatic ring of 5-HT in the region of LEU/PHE20(H4). It may be possible that agonists can be designed and synthesised with larger C-5 or C-6 substituents which demonstrate a higher binding affinity for the 5-$HT_{1D\alpha}$ receptor over the 5-$HT_{1D\beta}$ receptor. These agonists would certainly be desirable in the determination of the exact mode of action of antimigraine drugs.

It has also been observed from the models developed in this study that the 5-HT_{1D} receptors may prefer one conformation of the ligand and the 5-HT_{1A} receptor a different conformation of the ligand. Agonists could then be designed and synthesised that incorporate these features by conformationally constraining the ethylamine sidechain of 5-HT which then may exhibit 5-HT_{1A}/5-HT_{1D} receptor selectivity.

Many research groups have studied extensively the effect of substitution of the indole ring, in particular at the C-5 position[53,56-58] mainly addressing the issue of 5-HT_{1D}/5-HT_{1A} receptor selectivity. All the known indole agonists which have high affinity for the cloned 5-$HT_{1D\beta}$ receptor also have a high affinity for the cloned 5-$HT_{1D\alpha}$ receptor. The question therefore to be answered is that, given the high degree of sequence homology between the 5-$HT_{1D\alpha}$ and 5-$HT_{1D\beta}$ receptors, are selective agonists possible? Selective antagonists can probably be found since antagonists tend to interact with the receptors in different manners, interacting with different residues, but agonists all appear to

interact with the same residues thus questioning the whole possibility of selective agonists.

2.2.8 Conclusions

The agonist binding site of the human 5-HT_{1A}, 5-$HT_{1D\alpha}$ and 5-$HT_{1D\beta}$ receptors has been identified with a high degree of certainty from the bacteriorhodopsin derived molecular models of these receptors. The agonist binding site has been studied not in terms of energies, but in a more qualitative sense, accounting for the binding of some known agonists.

The thieno[2,3-b]pyridine (133) analog of 5-HT has been identified from both small molecule modelling and ligand receptor modelling as a potential bio-isostere for 5-HT (the attempted synthesis of this compound is dealt with in chapter 3).

The entire concept of receptor selectivity has been considered using sequence analysis and the ligand design program Ludi to identify features of the models and ligand receptor interactions which may confer selectivity. Two such features have been identified which may help the design and synthesis of 5-HT receptor agonists with selectivity for one of the 5-HT_{1D} receptor subtypes.

3 SYNTHETIC CHEMISTRY DISCUSSION

3.1 SYNTHESIS AND REACTIONS OF 3-CARBOETHOXY-2-METHYL-THIOTHIENO[2,3-B]PYRIDINE

From modelling of the analogs of 5-HT (133) within the agonist binding site, the thieno[2,3-b]pyridine (133) was identified as an initial synthetic target. Methodology for the synthesis of thieno[2,3-b]pyridines has already been developed at the University of Abertay, Dundee[249-251,402] and it was therefore decided to use this route to prepare 3-carboethoxy-2-methylthiothieno[2,3-b] pyridine[251,402] (70a). It was the intention of this work to reduce the 3-carboethoxy group to the hydroxymethyl derivative which could be substituted by a nitrile function increasing the chain length by one carbon atom. Reduction of the nitrile would afford the amine and the methylthio group could be removed and functionality would then be introduced into the C-5 position in an electrophilic substitution reaction [Scheme 30].

Alternatively, the methylthio group could be removed prior to conversion of the C-3 carboethoxy substituent of (70a) to the hydroxymethyl derivative. Thieno[2,3-b]pyridine compounds with a hydrogen bond acceptor at the C-5 position such as (133) could then be evaluated for biological activity at the 5-HT receptors. If these compounds are active the implications upon receptor selectivity studied in section 2.2.7 would be used to suggest additional synthetic targets.

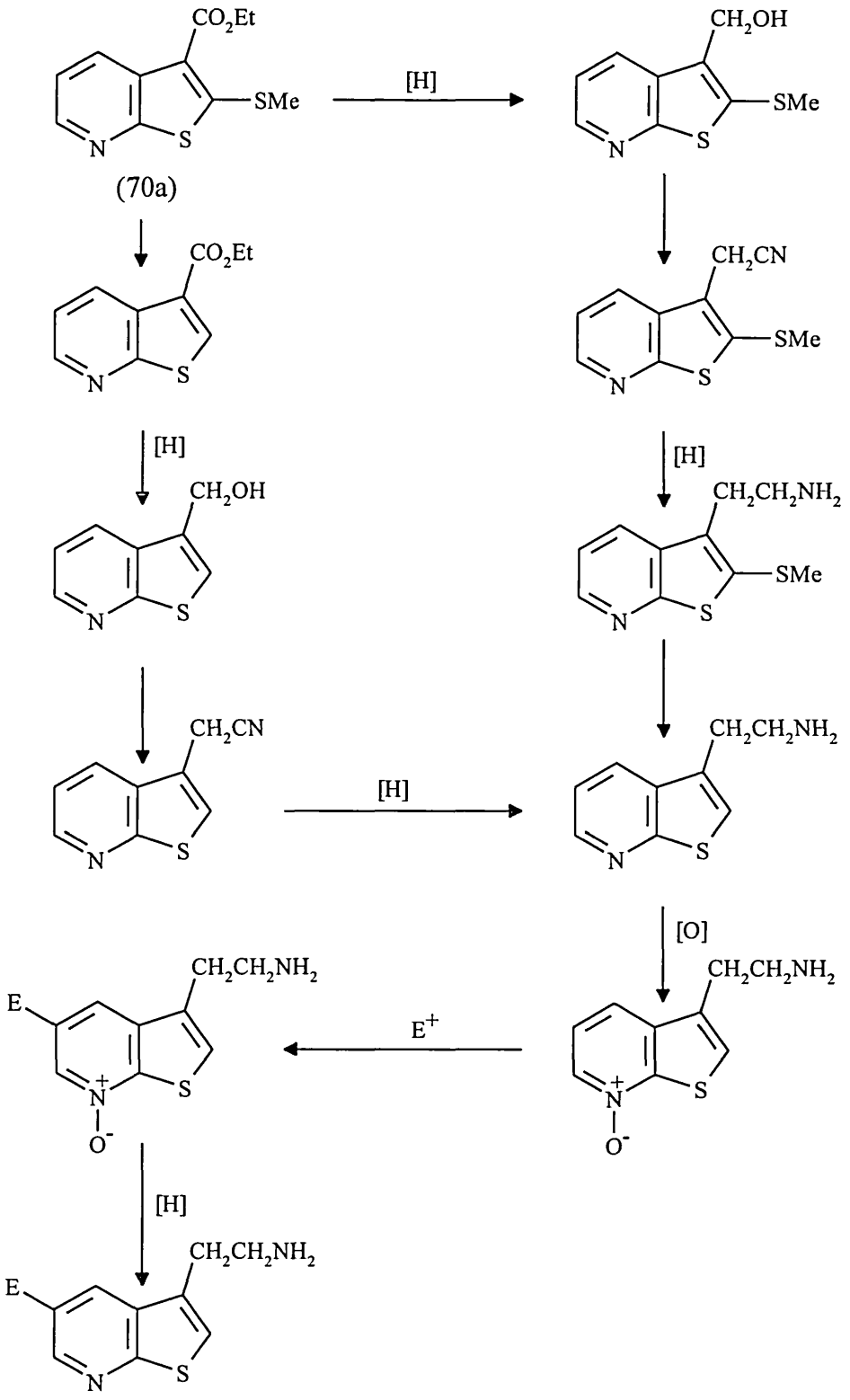

[Scheme 30]

Ethyl 3-pyridylacetate-1-oxide (143) had originally been prepared[251] in 55% yield from the reaction of ethyl 3-pyridylacetate (142) with hydrogen peroxide and glacial acetic acid. In an attempt to improve this moderate yield (142) was stirred at room temperature with magnesium monoperoxyphthalate (MMPP). MMPP is a newer reagent which is stable at ambient temperatures and has been shown to oxidise alkenes, ketones, sulfides, sulfoxides and pyridines in high yields[403]. Due to the solubility of the product (143) in water an aqueous work-up procedure to remove the phthalic acid by-product had to be avoided. Thus a work-up procedure was developed where solid reagents were added directly to the reaction mixture, solid sodium metabisulfite to destroy any excess oxidising agent and solid potassium carbonate to neutralise the acid by-product. Removal of the solids by filtration followed by evaporation of the filtrate afforded the required product (143) also in 55% yield (identified from its ir spectrum and melting point[404]).

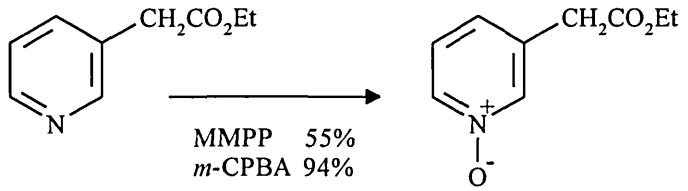

(142) (143)

Due to the failure to improve the yield of (143) using MMPP an alternative oxidising agent was sought. The oxidation was thus attempted at room temperature using *m*-chloroperoxybenzoic acid (*m*-CPBA) in dichloromethane. A similar solid reagent work-up procedure was used and ethyl 3-pyridylacetate-1-oxide (143) was isolated in a much improved 94% yield.

When ethyl 3-pyridylacetate-1-oxide (143) was refluxed in phosphoryl chloride tlc indicated that three major products had formed. Column chromatography

however only allowed the exclusive separation of the most polar component which was identified as ethyl 4-chloro-3-pyridylacetate (144) (20% yield) on the comparison of its ir spectrum with that of an authentic sample[251].

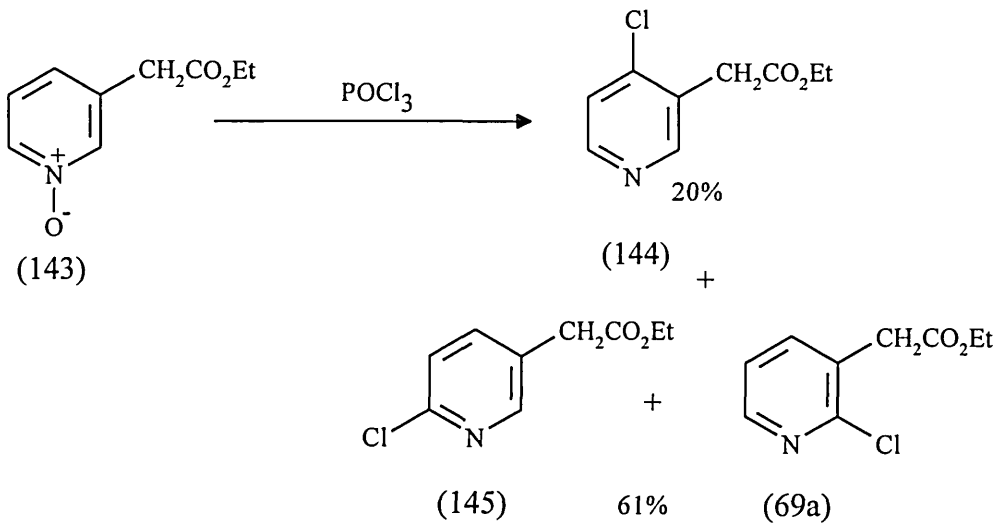

The two less polar compounds were obtained substantially as a mixture (61% yield) presumably consisting of ethyl 2-chloro-5-pyridylacetate (145) and ethyl 2-chloro-3-pyridylacetate (69a). Further attempts to separate these compounds by column chromatography with a variety of solvent mixtures also failed. Therefore the mixture was stirred at room temperature with MMPP for 24 h and after work-up the resulting oil was chromatographed on silica to afford firstly 47% of the unoxidised mixture of (145) and (69a). Also isolated was ethyl 2-chloro-5-pyridylacetate-1-oxide (146) in 6% yield. The ^{1}H nmr spectrum showed a double doublet at 6.97 δ corresponding to the C-4 proton of the pyridine ring coupling with the C-3 and C-6 protons. The C-3 and C-6 protons were both observed as doublets at 7.25 δ and 8.07 δ respectively, coupling with the C-4 proton only. The ir spectrum indicated the presence of the N-oxide function (1275 cm^{-1}) thus confirming that the product was the 2,5-disubstituted pyridine-1-oxide (146).

Ethyl 2-chloro-3-pyridylacetate-1-oxide (147) was also isolated in 9% yield. The infrared spectrum of (147) again confirmed the presence of the N-oxide function (1250 cm^{-1}) and the ^1H nmr spectrum showed a multiplet at 7.11 δ characteristic of the C-5 and C-4 protons of a pyridine-1-oxide and a multiplet at 8.18 δ which was assigned to the C-6 proton. All of which is consistent with the proposed structure (147).

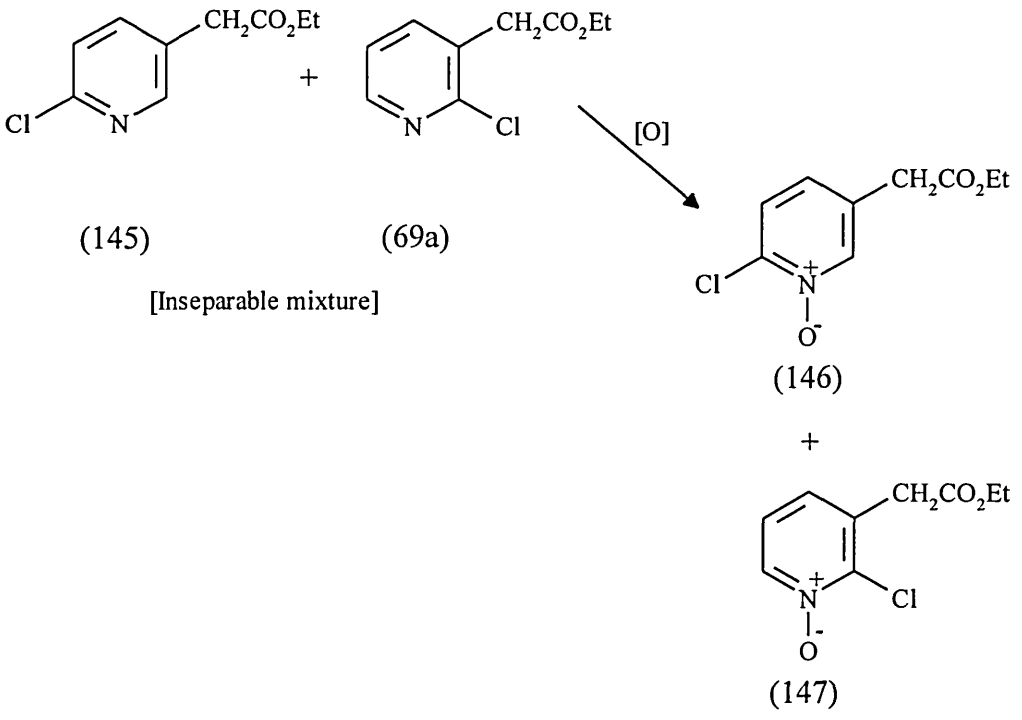

(145) (69a)

[Inseparable mixture]

(146)

+

(147)

Reagent	(146) %	(147) %	(145) + (69a) %
MMPP	6	9	47
m-CPBA	42	56	0

Oxidation with MMPP was obviously unsatisfactory, therefore the remaining mixture of (145) and (69a) was oxidised with the stronger oxidising agent *m*-CPBA. Room temperature oxidation of (145) and (69a) with *m*-CPBA followed by solid reagent work-up and column chromatography afforded (146) in 42% yield and (147) in 56% yield. The low yields observed with using MMPP can be

attributed to a combination of steric hindrance caused by the chloro group α to the nitrogen and the -I effect of the chloro group rendering the pyridine nitrogen less nucleophilic. Thus to effect the oxidation reaction a stronger oxidising agent had to be used.

Ethyl 2-chloro-3-pyridylacetate-1-oxide (147) was then treated with base and heated with carbon disulfide at 70 ^{o}C for 1.5 h [Scheme 31]. After cooling to room temperature the reaction was quenched with methyl iodide, stirred for a further 1.5 h at room temperature then poured onto ice/water and extracted with ethyl acetate. The resulting solid was chromatographed to afford a white solid in 17% yield. The ir spectrum of the product showed the presence of an ester (1690 cm^{-1}) and N-oxide (1240 cm^{-1}) functional groups. The ^{1}H nmr spectrum showed no singlet corresponding to the methylene protons of the acetate ester as observed for the starting material (147), but the presence of a two proton quartet and a three proton triplet at 4.38 δ and 1.44 δ respectively suggested an ethyl ester. A three proton singlet was observed at 2.72 δ which was assigned to a methylthio group and the downfield protons were indicative of a 2,3-disubstituted pyridine-1-oxide. The compound was assigned the structure of 3-carboethoxy-2-methylthiothieno[2,3-b]pyridine-7-oxide (148) and the molecular ions of 270 (M+H) and 254 [(M+H)-O] further corroborated this finding. The mechanism of this reaction[251] has already been discussed in section 1.2.3.5.

Deoxygenation of compound (148) at ice temperature with phosphorus tribromide in DMF afforded 3-carboethoxy-2-methylthiothieno[2,3-b]pyridine (70a) in 80% yield [Scheme 31]. The ir spectrum showed no peak associated with the N-O stretch of a pyridine-N-oxide and the ^{1}H nmr spectrum was identical to that of an authentic sample of (70a) as described in the literature[251].

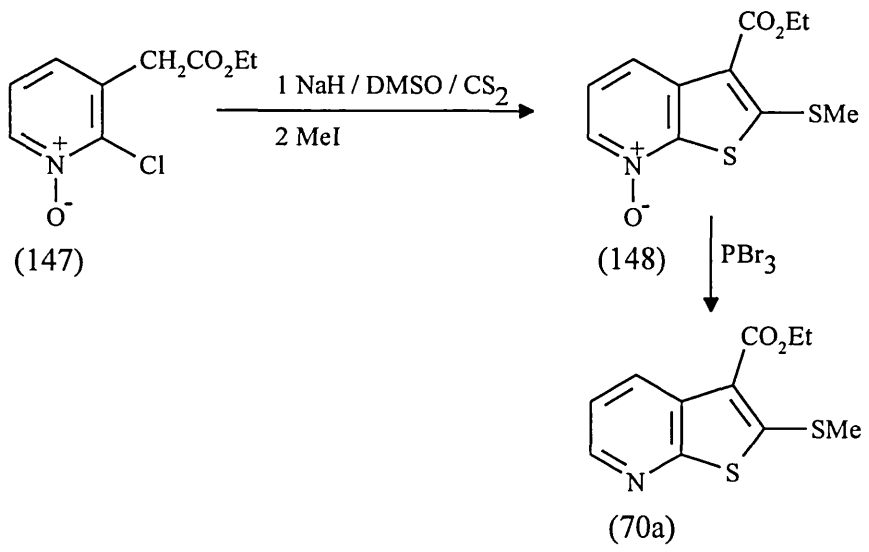

(147) (148) (70a)

[Scheme 31]

Furthermore, ethyl 2-chloro-3-pyridylacetate[402] (69a) was cyclised under the same conditions as described for ethyl 2-chloro-3-pyridylacetate-1-oxide (147) to afford compound (70a) directly in 67% yield. This is a significant improvement on the literature reported yield[251] of 36%.

The ester group of 3-carboethoxy-2-methylthiothieno[2,3-b]pyridine (70a) was reduced to the primary alcohol (149) with lithium aluminium hydride in diethyl ether. Excess lithium aluminium hydride was destroyed by the careful addition of water and 2N sulfuric acid in a 5:2 volumetric ratio. This allowed the extraction of the product into diethyl ether. Subsequent removal of solvent and column chromatography gave 3-hydroxymethyl-2-methylthiothieno[2,3-b] pyridine (149) in 50% yield. The product was identified from the absence of a carbonyl stretch and the presence of a broad O-H stretch peak in the ir spectrum. The ^{1}H nmr spectrum showed no evidence of the characteristic quartet and triplet of an ethyl ester however a broad one proton singlet at 3.05 δ and a two proton singlet at 4.89 δ were observed and accounted for the hydroxyl and C-3 methylene protons respectively. The three proton singlet at 2.50 δ was assigned to the methylthio protons. Three double doublets were observed downfield

corresponding to the pyridine ring protons which is typical of a 2,3-disubstituted pyridine. The C-6 proton is the furthest downfield resonating at 8.38 δ and coupling with the C-4 proton (J=1.7 Hz) and the C-5 proton (J=4.5 Hz). The C-4 proton is observed at 8.06 δ and couples with the C-5 (J=8.1 Hz) and the C-6 proton. This is further downfield than is normally associated with a pyridine γ proton due to the deshielding effect of the thiophene ring. The C-5 proton is the least downfield of the aromatic protons at 7.20 δ. The LC mass spectrum gave molecular ions of 212 (M+H) and 197 [(M+H)-CH_3] and the microanalytical figures were consistent with the structure of (149).

(70a) (149)

When the reaction was attempted in THF the yields of (149) were inconsistent ranging from 20-70% possibly due to the poorer solubility of lithium aluminium hydride in THF.

Classical methods for the conversion of an alcohol to a nitrile[405] involve a two step procedure where the hydroxyl group is converted to a good leaving group such as a halide or sulfonate ester. This is followed by nucleophilic displacement of that group by the cyanide anion, however some undesirable side reactions can occur. A direct one step method for the conversion of alcohols to nitriles in high yields has been published[406]. The alcohol is treated with two equivalents of sodium cyanide and chlorotrimethylsilane and a catalytic amount of sodium iodide in a DMF/acetonitrile mixture. For example[406] benzyl alcohol was converted to benzylcyanide in 98% yield [Equation 8].

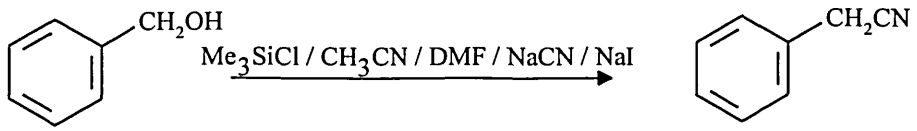

[Equation 8]

3-Hydroxymethyl-2-methylthiothieno[2,3-b]pyridine (149) was therefore heated at 60 °C with chlorotrimethylsilane, sodium cyanide and a catalytic amount of sodium iodide in a 1:1 mixture of DMF/acetonitrile. After 5 h tlc indicated that only starting material and baseline material was present so heating was continued for a further 14 h. Subsequent work-up yielded a small return of what was identified as unreacted starting material and the reaction was therefore abandoned. At this stage it was envisaged that the methylthio group may be interfering with the reaction and preventing the formation of the crucial intermediate (150) by steric hindrance or by reaction with chlorotrimethylsilane. It was therefore decided to look at possible methods of removing the methylthio group.

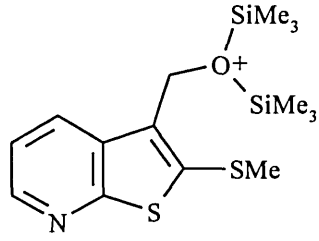

(150)

There are many methods available for the cleavage of carbon-sulfur bonds[407,408]. The most common being the use of Raney nickel. There are however known problems associated with the use of Raney nickel; it is pyrophoric and must be kept wet; the reactivity of Raney nickel varies from one batch to another; and reactions using it may not be reproducible. In a typical laboratory procedure the compound of interest is treated with a 5-10 fold excess of Raney nickel in ethanol at 20-80 °C. With respect to this work the overriding

problem is that the Raney nickel would also desulfurise the thiophene ring of the thieno[2,3-b]pyridines so an alternative method was sought.

Alkali metal liquid ammonia reductions are also well known and reactions with thienyl sulfides have been described[408] but instead of yielding the unsubstituted thiophene, the bond between the sulfur atom and the sp^3 hybridised carbon is cleaved[408] [Equation 9]. A subsequent literature search unearthed a publication on the synthesis of thiasteroids where a methylthio group was removed in the presence of a thiophene ring [Equation 10] using Raney nickel in acetone[409]. The acetone will react with the catalyst to give isopropyl alcohol, deactivating the catalyst prior to reaction with the thiophene compound. This method was thus used in an attempt to remove the methylthio group from the thieno[2,3-b]pyridines (70a) and (149).

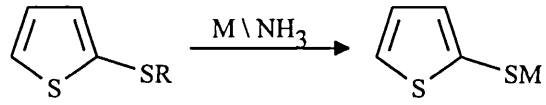

M = Alkali Metal
R = Alkyl group

[Equation 9]

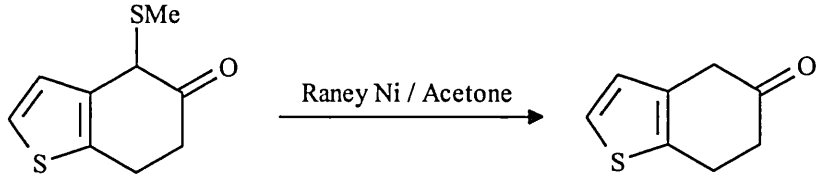

58%

[Equation 10]

3-Hydroxy-2-methylthiothieno[2,3-b]pyridine (149) was refluxed with an excess of Raney nickel in acetone for 1 h. The Raney nickel was removed by gravity filtration, the solvent was dried and removed to give an oil which tlc showed to be a complex mixture of five components. Column chromatography afforded the

two major components but in very low yields. The ^1H nmr spectrum of the least polar compound (2% yield) was identical to that of unreacted (149). The more polar compound was obtained as only a trace but the ^1H nmr spectrum showed the presence of the three double doublets at 8.54 δ, 8.14 δ and 7.29 δ which are consistent with a thieno[2,3-b]pyridine ring. A two proton singlet at 4.89 δ corresponded to the methylene protons of the C-3 substituent but no singlet was observed at 2.50 δ for the methylthio group, instead a downfield one proton singlet at 7.69 δ appeared which is typical of a C-2 proton of a thiophene ring. Although due to the low yield of the compound no ir spectrum, mass spectrum or microanalysis was obtained the compound was believed to be 3-hydroxymethylthieno[2,3-b]pyridine (151) on the strength of the ^1H nmr spectrum. Any attempts to repeat this reaction in the hope of obtaining an improved yield of (151) gave low yields of complex mixtures.

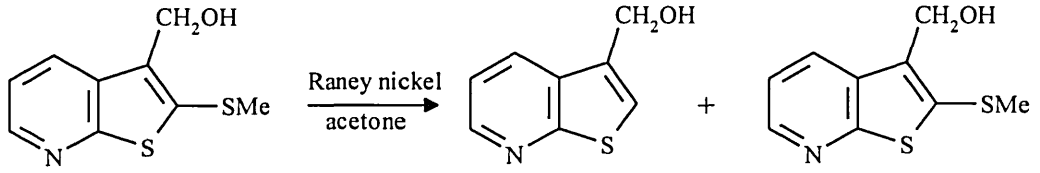

(149) (151) trace (149) 2%

The same reaction conditions were applied to 3-carboethoxy-2-methylthiothieno[2,3-b]pyridine (70a) and again only a trace amount of a mixture of products was isolated. The ^1H nmr spectrum of the mixture indicated that the major component was a thieno[2,3-b]pyridine but the low yield prevented the reaction being taken any further.

Instead of using deactivated Raney nickel, 3-hydroxy-2-methylthiothieno[2,3-b] pyridine (149) was stirred with an excess of Raney nickel in ethanol at -10 ^oC, tlc indicated that no reaction had taken place thus the reaction mixture was allowed to warm to room temperature and stirred for a further 2 h. Work-up

afforded 30 mg of an oil but tlc and ^1H nmr indicated a complex mixture of products so the reaction was not pursued any further due to the low yield.

Interestingly, however, 3-cyano-2-methylthiothieno[2,3-b]pyridine[250,251] (70c) did undergo reaction with Raney nickel in acetone to give the required product 3-cyanothieno[2,3-b]pyridine (152) in 98% yield. Compound (152) was identified from the ^1H nmr spectrum showing the three double doublets of a 2,3-substituted pyridine and a one proton singlet at 8.19 δ caused by the C-2 proton of the thieno[2,3-b]pyridine ring. No upfield signals corresponding to methyl protons were observed. The liquid chromatography mass spectrum gave a molecular ion of 161 (M+H) and microanalysis figures were consistent with the proposed structure (152).

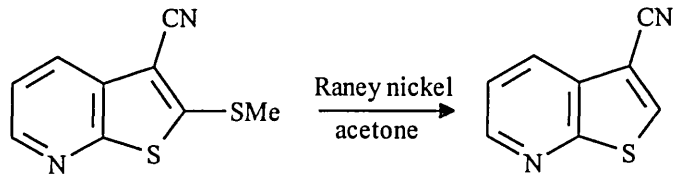

(70c) (152)

When this reaction was repeated the 98% yield was not reproducible and a mixture of products was obtained. It became apparent during the reactions of the thieno[2,3-b]pyridines with deactivated Raney nickel that large excesses of the reagent were required and the reactions only proceeded when there was very little solvent in the reaction vessel. When the reactions did take place complex mixtures were obtained which contained unreacted starting material and required product in yields that were too low to allow the isolation and purification of these compounds. The reaction of (70c) with deactivated Raney nickel did produce the required product (152) in almost quantitative yield. It was therefore thought that the smaller nitrile group may allow reaction to take place however it was subsequently proved that this was a one-off and the reaction was certainly

not reproducible. In conclusion the attempted removal of the methylthio group with Raney nickel was not reproducible thus it was decided to take this approach no further.

3.2 SYNTHESIS AND REACTIONS OF 3-CARBOMETHOXY-5-CYANOTHIENO[2,3-B]PYRIDINE AND (E)-ETHYL-3-(5-CYANO-THIENO[2,3-B]PYRIDIN-3-YL)PROP-2-ENOATE

Due to the failure in removing the methylthio group from the thieno[2,3-b]pyridine (149) synthesised using CS_2 methodology a new synthetic route to thieno[2,3-b]pyridines was sought. In general, the majority of methods to thieno[2,3-b]pyridines from preformed pyridine rings lead to 2,3-disubstituted thieno[2,3-b]pyridines (section 1.2.3) but as we have already seen in the preceding section substitution at the C-2 position is undesirable. The synthesis of thieno[2,3-b]pyridines from preformed thiophene rings in a Skraup type reaction and its variations on the other hand can afford non highly substituted thieno[2,3-b]pyridines in variable yields. The general reaction involves the cyclisation of a 2-aminothiophene salt with a 1,3-dicarbonyl, α,β–unsaturated carbonyl compound or an equivalent compound with two electrophilic carbon atoms separated by a methylene spacer which can be substituted if desired. The thiophene compound contributes two carbon atoms and the nitrogen of the pyridine ring and the carbonyl compound provides the three remaining carbon atoms of the ring.

Such an approach has been reported[271,272] (see section 1.2.2.2) for the synthesis of 3,5-disubstituted thieno[2,3-b]pyridines in good yields from reduction of 2-nitrothiophenes followed by cyclisation with 3,3-dimethoxy-2-formylpropionitrile sodium salt.

It was therefore envisaged that this approach could be used to prepare thieno[2,3-b]pyridine analogs of 5-HT [Scheme 32]. Thieno[2,3-b]pyridine (153) could be hydrogenated and hydrolysed to the saturated carboxylic acid. Conversion to the *t*-BOC protected amine would then allow the C-5 substituent to be converted into many other functional groups.

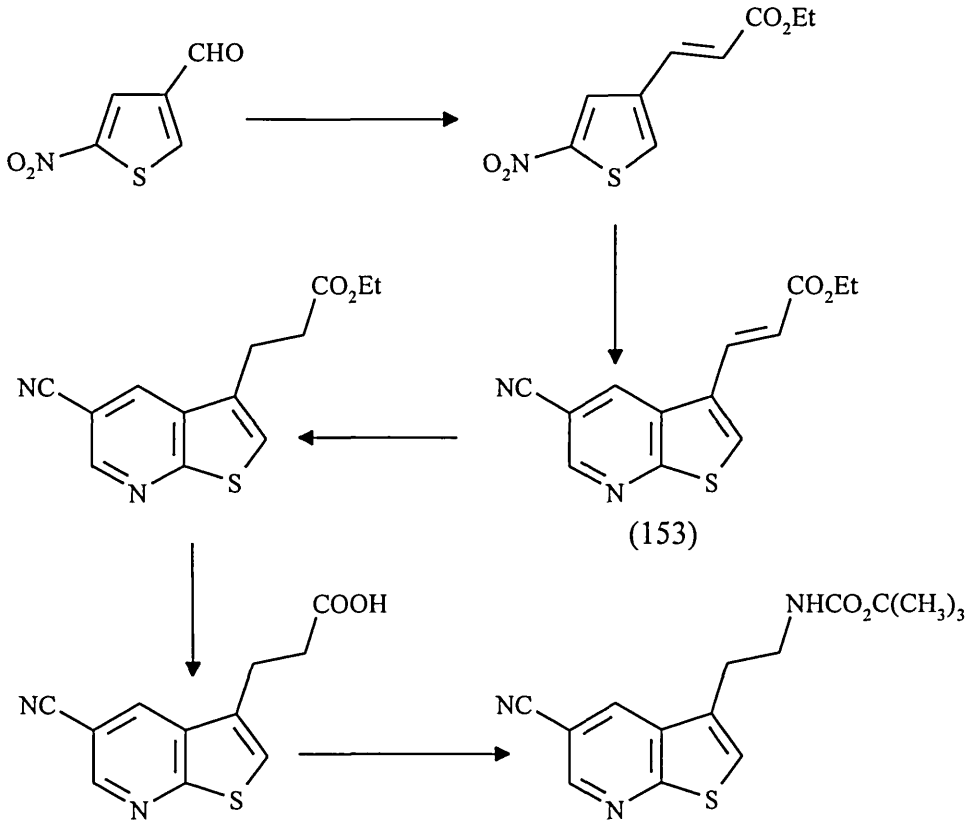

[Scheme 32]

3,3-Dimethoxy-2-formylpropionitrile sodium salt (155) was prepared according to the literature procedure[272] from reaction of 3,3-dimethoxypropionitrile (154) with sodium hydride and methyl formate in dry diethyl ether at room temperature.

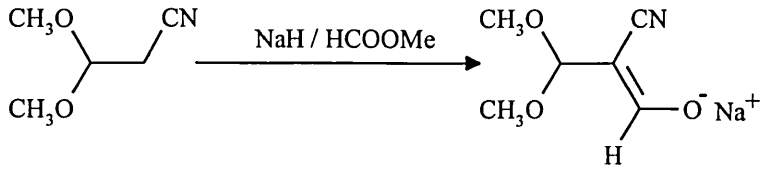

(154) (155)

The required [Bis(4-carboxythienyl-2-ammonium)]hexachlorostannate(IV) (157) was prepared from the reduction of 2-nitrothiophene-4-carboxylic acid (156) with powdered tin metal at 40 ^{o}C in concentrated hydrochloric acid [Scheme 33]. If the reaction temperature is allowed to rise to over 50 ^{o}C no (157) is isolated and only decomposition products are obtained. Compound (157) was characterised from the ^{1}H nmr spectrum showing the presence of the two thiophene protons as one proton singlets at 6.59 δ and 7.46 δ.

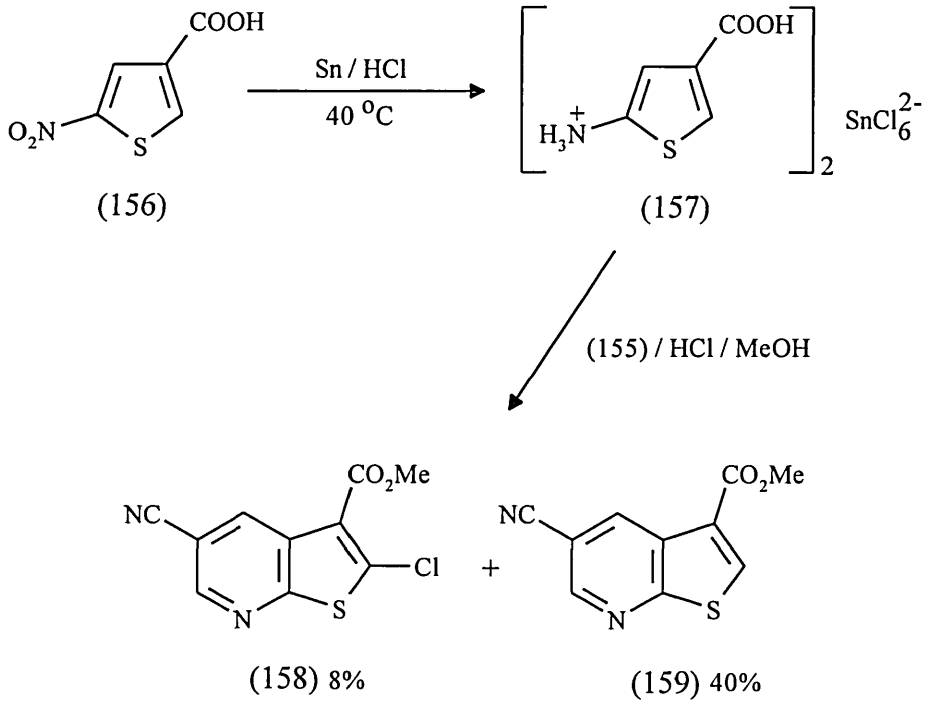

[Scheme 33]

The cyclisation of (157) with 3,3-dimethoxy-2-formylpropionitrile sodium salt (155) and concentrated hydrochloric acid in methanol proceeded smoothly over

24 h [Scheme 33]. Subsequent work-up afforded a mixture of two components which were separated by column chromatography. The ir spectrum of the least polar compound (8% yield) indicated the presence of a nitrile group at 2233 cm^{-1} and an ester group at 1727 cm^{-1}. The ^{1}H nmr spectrum exhibited the expected pattern for the pyridine ring protons, two doublets at 8.77 δ and 8.96 δ each integrating to one proton and corresponding to the C-4 and C-6 protons respectively. The small coupling constant of J=1.8 Hz is characteristic of coupling between the α and γ protons of a pyridine ring. A three proton singlet at 4.06 δ suggested a methyl ester attached directly to the thiophene ring at the C-3 position however there was no downfield singlet corresponding to a proton attached to the thiophene ring. The proton decoupled ^{13}C nmr spectrum showed three carbon atoms with bonded hydrogen of which the carbon of the methyl ester was assigned the most upfield peak at 52.4 δ. The C-4 carbon was observed at 136.0 δ and the C-6 carbon at 148.7 δ. There were additionally seven other peaks of a lesser magnitude which could not be assigned unambiguously. The compound was obviously not the required 3-carbomethoxy-5-cyanothieno[2,3-b]pyridine (159) but a 2-substituted derivative of (159). The mass spectrum gave a molecular ion of 253 which is consistent with the C-2 substituent being a chloro group and the compound was therefore identified as 3-carbomethoxy-2-chloro-5-cyanothieno[2,3-b]pyridine (158). The microanalytical data was consistent with structure (158).

The more polar compound isolated in 40% yield also showed the presence of a nitrile and an ester group in the ir spectrum. The ^{1}H nmr spectrum was almost identical to that of (158) except a one proton singlet was seen at 8.56 δ which was assigned to the C-2 proton of the thiophene ring. Therefore the compound was identified as the expected product 3-carbomethoxy-5-cyanothieno[2,3-b]pyridine (159). The mass spectrum and microanalysis data were also consistent with this compound.

Although the yield of (159) is lower than that reported in the literature[271,272] the presence of 3-carbomethoxy-2-chloro-5-cyanothieno[2,3-b]pyridine (158) had previously not been reported. The mechanism of formation of (159) probably proceeds by hydrolysis of 3,3-dimethoxy-2-formylpropionitrile sodium salt (155) to the 1,3-dialdehyde (160) followed by nucleophilic attack of the amino group of the thiophene. Cyclisation can then occur with the loss of water. It is not known when the esterification of the carboxylic acid takes place [Scheme 34].

The formation of (158) probably results from electrophilic attack of chlorine onto the formed 3-carbomethoxy-5-cyanothieno[2,3-b]pyridine (159). Similar chlorinations have been observed in the synthesis of quinolines and in the tin/hydrochloric acid reduction of 3-nitrothieno[3,2-b]pyridine[343] [Equation 11]. There was no evidence from the ^{1}H nmr spectrum of any chlorinated by-product in the tin/hydrochloric acid reduction of (156) to (157) therefore the mechanism of the reaction probably proceeds from Lewis acid catalysed electrophilic substitution of chlorine into the C-2 position of the thieno[2,3-b]pyridine ring of (159). Typical chlorinations are effected by chlorine gas which may or may not be present but reactions of this type are known to proceed in the presence of Lewis acid catalyst alone[410]. This reaction could be investigated further by subjecting (159) to the same reaction conditions used in the cyclisation step.

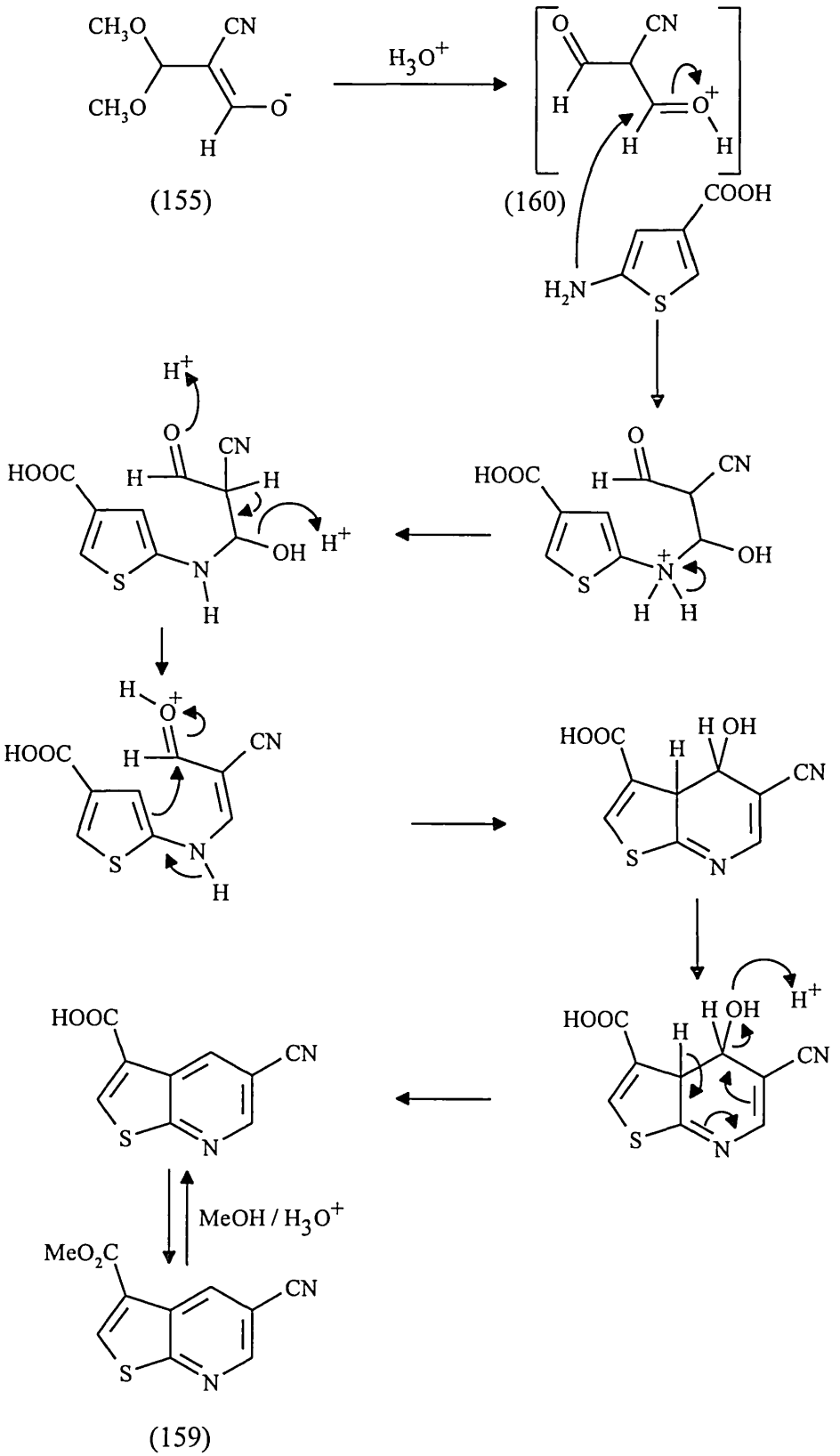
CH3O
CN
CH3O
O-
H
H3O+
(155)
(160)
COOH
H2N
S
HOOC
H+
OH
N
H
MeOH / H3O+
MeO2C

[Scheme 34]

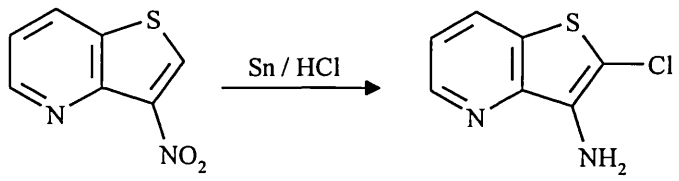

[Equation 11]

The Horner-Wadsworth-Emmons reaction is an important variation of the well known Wittig reaction and is frequently used because of its versatility and mild reaction conditions. A phosphonate ester deprotonated by base, attacks the carbonyl group of an aldehyde or ketone. Syn-elimination of the intermediate betaine affords alkenes in good yields [Equation 12].

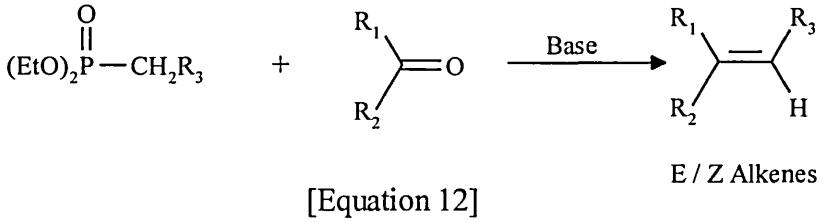

[Equation 12]

When R_3=CO_2Et, α,β-unsaturated esters are formed with the E isomer predominating. It has been reported[411] that the reaction between triethylphosphonoacetate and benzaldehyde in a two phase system using phase transfer catalysis results in the exclusive formation of the E isomer of ethyl cinnamate[411] [Equation 13].

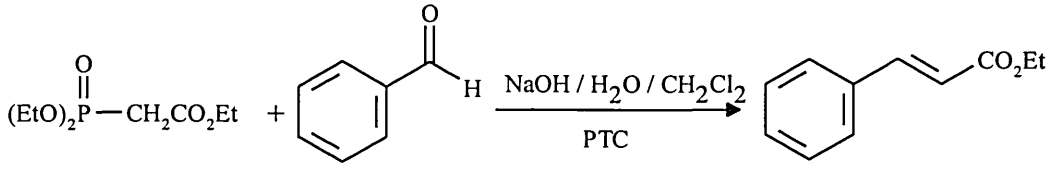

[Equation 13]

2-Nitrothiophene-4-carboxaldehyde (161) and triethylphosphonoacetate were stirred for 7 days in a two phase system of toluene and aqueous potassium carbonate in the presence of a phase transfer catalyst (Method A).

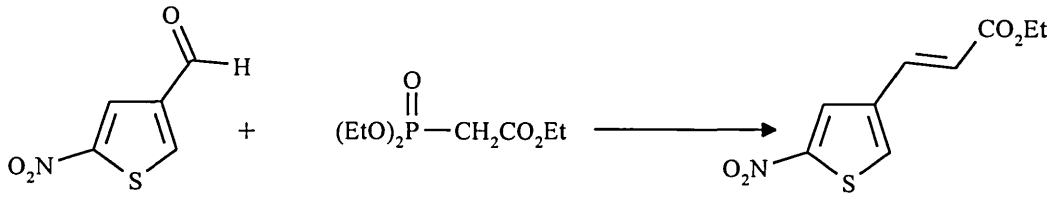

(161) (162)

Method	(162) %	Unreacted (161) %
A	34	6
B	71	20
C	62	20

Separation of the two phases of the resulting dark emulsion proved almost impossible thus a 10% solution of hydrochloric acid was added. The toluene layer could then be separated and the aqueous phase was extracted with ethyl acetate. Even after the addition of the hydrochloric acid the separation and extraction still proved tedious due to the dark colouration of the mixture and involved the use of large volumes. Combination of the organic washings and removal of solvent afforded a dark solid which tlc showed to consist of two components and a considerable amount of baseline material which were separated by column chromatography. The ir spectrum of the major, less polar component showed peaks at 1700 and 1639 cm^{-1} which correspond to the carbonyl group of a conjugated ester and a carbon-carbon double bond respectively. Furthermore, the two absorbances at 1509 and 1337 cm^{-1} were representative of a nitro group. The ^1H nmr spectrum indicated the presence of an ethyl ester from the mutually coupling three proton triplet at 1.32 δ and the

two proton quartet at 4.25 δ (J=7.2 Hz). The two doublets at 8.04 δ and 7.58 δ each integrating to one proton and coupling with each other (J=1.9 Hz) are typical of the C-5 and C-3 protons of a 2,4-disubstituted thiophene ring. The one proton doublets at 6.31 δ and 7.51 δ accounted for the hydrogens of a carbon-carbon double bond. The large vinylic coupling constant of J=16.2 Hz implied that the geometry of the double bond is trans (E). Of the two doublets the most downfield signal at 7.51 δ was assigned to the ArC<u>H</u>=CHCO$_2$Et proton due to the strong deshielding effect from the aromatic thiophene ring and the doublet at 6.31 δ was assigned to the ArCH=C<u>H</u>CO$_2$Et proton. Therefore the ^{1}H nmr and ir spectra confirmed that the product was the expected (E)-ethyl-3-(2-nitro-4-thienyl)prop-2-enoate (162) obtained in 34% yield. The mass spectrum shows no molecular ion but the most abundant peak at 198 is consistent with the loss of an ethyl group from the molecular ion. The microanalysis data is consistent with structure (162).

Unreacted 2-nitrothiophene-4-carboxaldehyde (161) was also isolated in 6% yield but there was no evidence of the formation of the Z isomer of (162). The low yield of the required product (162) and the problems encountered during the tedious extraction of the product prompted an investigation into the use of other methods for the preparation of (162).

The Horner-Wadsworth-Emmons variation of the Wittig reaction using triethylphosphonoacetate has also been reported[412] using just aqueous potassium carbonate without organic solvent or phase transfer catalyst to give high yields and E stereoselectivity of the alkene. A two phase solid-liquid reaction of aldehydes with triethylphosphonoacetate and potassium carbonate in THF has also been reported[413] again giving almost exclusively the E alkene.

Thus, in method B, a mixture of (161) and triethylphosphonoacetate was stirred at room temperature for 3 h in an aqueous solution of potassium carbonate. Ethyl acetate extraction of the reaction mixture proved less troublesome than in method A and subsequent column chromatography afforded (162) in a much improved 71% yield and unreacted starting material (161) in 20% yield. Again there was no evidence for the presence of the Z isomer from the ^{1}H nmr spectrum of the isolated compound.

In method C a mixture of (161), triethylphosphonoacetate and solid potassium carbonate was stirred in THF for 24 h at room temperature in the absence of a phase transfer catalyst. No extraction was required as the insoluble by-products were removed by filtration. Removal of the solvent and column chromatography of the crude solid afforded (162) in 62% yield and unreacted (161) in 20% yield. Again there was no evidence of the Z isomer of (162).

Thus method B was used in subsequent synthesis of (162). Although the work-up still involves an extraction, the extraction is more facile than that of method A and the yield of (162) is better than both methods A and C. The higher yields of (162) in methods B and C may be attributed to the product being contaminated with less of the dark baseline material which was observed in method A and rendered the isolation of (162) very difficult. This and the use of a phase transfer catalyst could have been detrimental to the isolated yield in method A. Attempts to force the reaction to completion (method B) using longer reaction times only made the extraction step more tedious due to the formation of more baseline material.

(E)-Ethyl-3-(2-nitro-4-thienyl)prop-2-enoate (162) was then reduced carefully at 40 ^{o}C with tin in concentrated hydrochloric acid to the tin double salt [bis((E)-ethyl-3-(2-ammonium-4-thienyl)prop-2-enoate)]hexachlorostannate(IV)

(163). The ir spectrum confirmed the presence of an amine from the absorbance bands at 3568, 3472 and 3288 cm^{-1}. The peaks at 1706 and 1638 cm^{-1} are typical of a conjugated ester. No ^1H nmr was obtained due to decomposition of the product in hexadeuterodimethylsulfoxide.

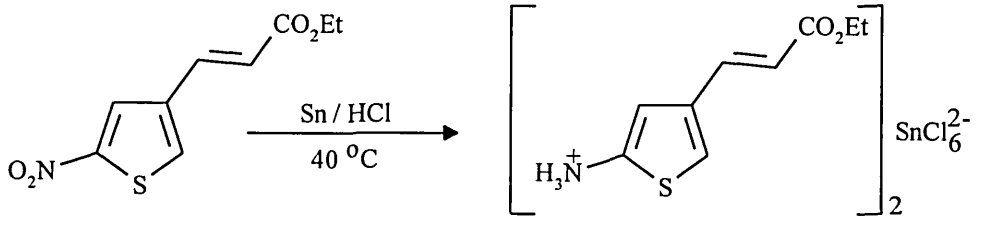

(162) (163)

Compound (163) was refluxed with 3,3-dimethoxy-2-formylpropionitrile sodium salt (155) and concentrated hydrochloric acid in ethanol. The reaction was monitored by tlc and after 4 h no more product appeared to be formed thus the solvent was removed from the deep blue reaction mixture and replaced by water. Extraction into ethyl acetate and removal of the solvent gave a dark oil which consisted of two major products, several minor components and a large amount of coloured baseline material (by tlc). Column chromatography afforded a white solid in 12% overall yield from (162). The ir spectrum showed peaks at 2234, 1731 and 1636 cm^{-1} confirming the presence of a nitrile, ester and carbon-carbon double bond respectively. The ^1H nmr spectrum looked quite similar to that of compound (162). A quartet at 4.33 δ and a triplet at 1.40 δ indicated an ethyl ester. The two single proton doublets at 6.65 δ and 7.85 δ with a coupling constant of J=16 Hz correspond to the vinylic protons. The aromatic protons were observed further downfield than in (162) at 8.48 δ and 8.80 δ and these represent the C-4 and C-6 protons of a substituted thieno[2,3-b]pyridine ring. There was no evidence of the C-2 proton of the thiophene ring suggesting that the compound was a 2,3,5-substituted thieno[2,3-b]pyridine. The mass spectrum gave a molecular ion at 293 (M+H) which confirmed that the C-2 substituent

was a chloro group and the compound was (E)-ethyl-3-(2-chloro-5-cyanothieno[2,3-b]pyridin-3-yl)prop-2-enoate (164). The microanalysis figures are consistent with this structure.

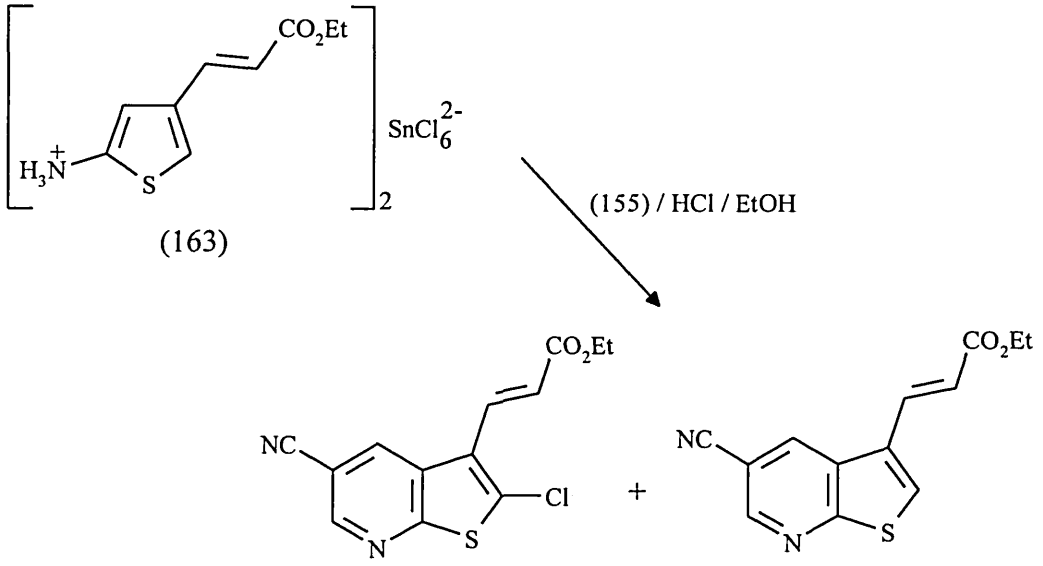

(163) (164) (153)

The more polar compound isolated in 18% yield from (162) showed almost identical ir and ^{1}H nmr spectra to that of (164). However a one proton singlet appears in the ^{1}H nmr spectrum at 7.93 δ suggesting that the thieno[2,3-b] pyridine ring is unsubstituted at the C-2 position and the compound is the required product (E)-ethyl-3-(5-cyanothieno[2,3-b]pyridin-3-yl)prop-2-enoate (153). The molecular ion of 259 (M+H) and microanalysis figures were consistent with structure (153).

The low yield of (153) compared to the yield of 3-carbomethoxy-5-cyanothieno[2,3-b]pyridine (159) is particularly disappointing. Throughout the synthesis of (153) large amounts of a blue polymeric tar formed which hampered the work-up procedure. It was therefore hoped that the cyclisation reaction could be modified to reduce the production of the tar and increase the yield of (153). It was originally thought that the ester function of (163) may be more susceptible to nucleophilic attack by the amine group of another molecule of (163) leading

to tar formation. To investigate this (E)-ethyl-3-(2-nitro-4-thienyl)prop-2-enoate (162) was hydrolysed at room temperature with 4.8M sodium hydroxide solution in ethanol. Acidic work-up afforded (E)-3-(2-nitro-4-thienyl)prop-2-enoic acid (165) in 82% yield [Scheme 35]. The product was confirmed as (165) from the spectral data. The ir spectrum shows a broad O-H stretch at 3110 cm^{-1} and a C=O stretch at 1686 cm^{-1}. The ^1H nmr spectrum also showed no protons corresponding to an ethyl ester but did show the expected aromatic and vinylic protons.

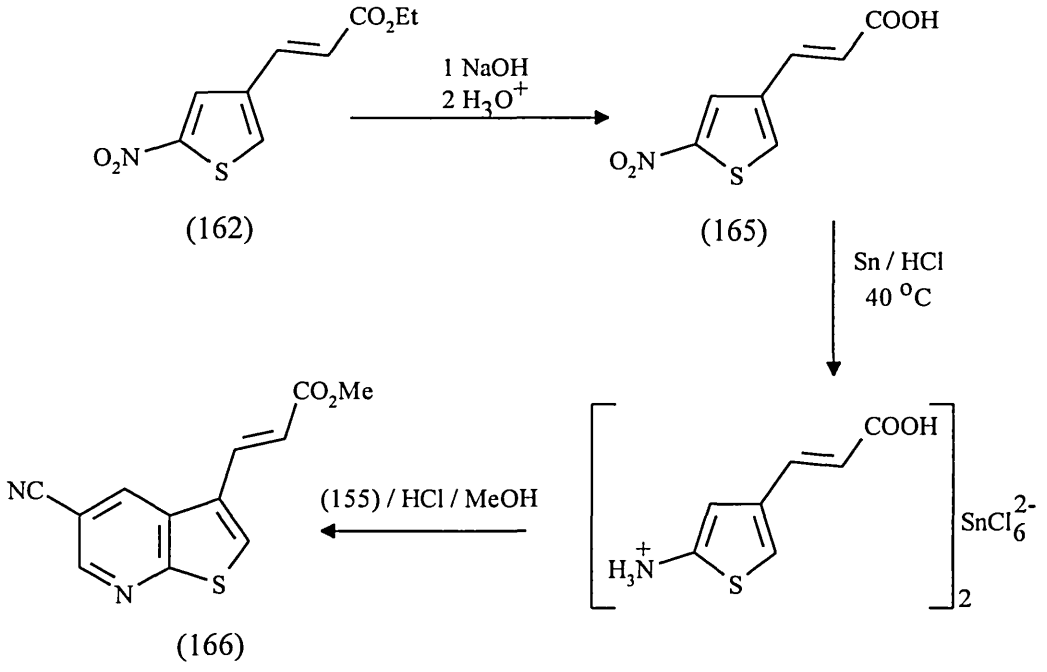

[Scheme 35]

Reduction of (165) with tin and hydrochloric acid afforded a crude solid which was reacted immediately with 3,3-dimethoxy-2-formylpropionitrile sodium salt (155) and concentrated hydrochloric acid in methanol. Subsequent work-up yielded a solid which tlc indicated to consist of one major product and several minor components. Only the major product was isolated by column chromatography in 10% overall yield from (165). The ir spectrum of the product exhibited peaks corresponding to a nitrile and conjugated ester. The ^1H nmr

spectrum was similar to that of (153) but showed no protons indicative of an ethyl ester, however a three proton singlet at 3.86 δ was consistent with the compound being the methyl ester. The compound was identified as (E)-methyl-3-(5-cyanothieno[2,3-b]pyridin-3-yl)prop-2-enoate (166) and confirmed by the molecular ion of 245.1 (M+H) from the liquid chromatography mass spectrum [Scheme 35].

The low yield of this reaction implies that the ester group of (163) is probably not reacting with the amino group of the same compound to give polymers and that this hypothesis is not the reason for the low yield of (153) from (163). Therefore attempts were made to selectively hydrogenate the carbon-carbon double bond of (E)-ethyl-3-(2-nitro-4-thienyl)prop-2-enoate (162) prior to cyclisation.

The catalytic hydrogenation of olefins is well known[414], but for thiophene compounds high pressures are generally required. Catalytic hydrogenation has also been reported[415] using a hydrogen source such as ammonium formate with a palladium on carbon catalyst. For example ethyl cinnamate was converted to ethyl 3-phenylpropionate in 92% yield[415] [Equation 14].

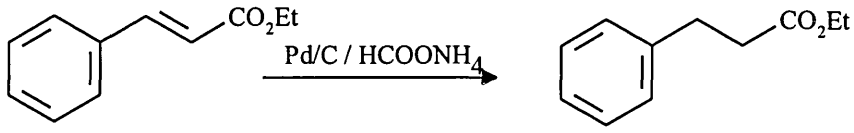

[Equation 14]

Sodium borohydride - cuprous chloride in methanol has also been utilised[416] in the conjugate reduction of α,β-unsaturated esters. Optimised reaction conditions using ten equivalents of borohydride gave a quantitative yield of ethyl 3-phenylpropionate from ethyl cinnamate[416].

The attempted hydrogenation of (E)-ethyl-3-(2-nitro-4-thienyl)prop-2-enoate (162) with palladium on carbon and ammonium formate in refluxing glacial acetic acid failed and only unreacted starting material was recovered. Compound (162) was then stirred with cuprous chloride in methanol. An excess of sodium borohydride was added portionwise over 30 minutes, the mixture was stirred for a further 30 minutes then partitioned between diethyl ether and water. Evaporation of the solvent from the organic phase afforded a brown solid which turned red on exposure to the atmosphere. It was postulated that the nitro group had been reduced to the primary amine giving the 2-aminothiophene which is notoriously unstable. The attempted hydrogenation of (162) was therefore not pursued any further.

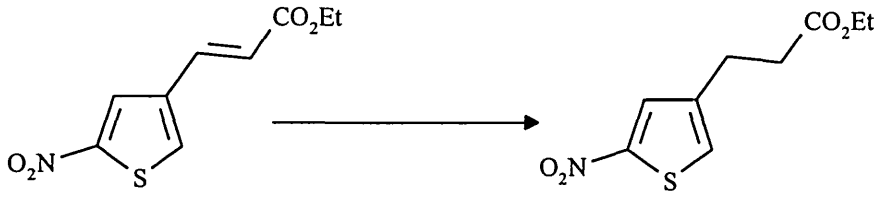

(162)

In a further effort to improve the overall yield of (153) the cyclisation of (163) was attempted in concentrated sulfuric acid. The work-up procedure was altered and after removal of the ethanol the residue was basified with concentrated ammonia solution. The extraction stage with diethyl ether was cleaner and any of the insoluble blue baseline material was removed by filtration through a bed of Celite. The required product (153) was isolated after column chromatography in 14% yield. Additionally isolated was (162) in 17% yield arising from contamination of the hexachlorostannate salt (163) with compound (162).

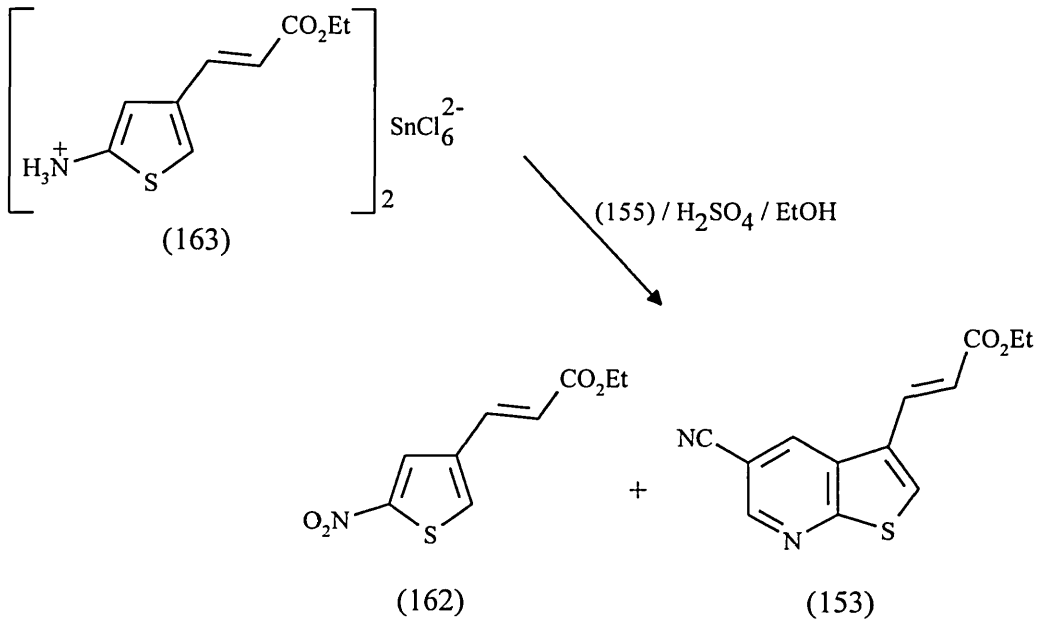

It is also very interesting that there was no evidence of (E)-ethyl-3-(2-chloro-5-cyanothieno[2,3-b]pyridin-3-yl)prop-2-enoate (164) being formed in this reaction. This could suggest that the concentrated hydrochloric acid plays a crucial role in the formation of (164) from (163) and confirms that the chlorinated derivative (164) is synthesised in the cyclisation step. By changing the acid from hydrochloric acid to sulfuric acid the yield of (153) from (162) was not improved. Likewise hydrolysis of the ester group of (162) to the carboxylic acid (165) prior to reduction and cyclisation also offered no improvement. It therefore seems plausible that the introduction of an α,β-unsaturated ester sidechain at the C-4 position of 2-nitrothiophene renders the tin salt of the amino compound to be highly unstable in the harsh reaction conditions used for cyclisation. This probably leads to decomposition and/or polymerisation of (163) producing large amounts of the blue tar.

One final attempt to improve the yield of (153) also failed. Compound (162) was heated at 40 ^{o}C in ethanol with tin(II) chloride.2H_2O. When tlc had indicated that all the starting material had reacted a suspension of 3,3-dimethoxy-2-formylpropionitrile sodium salt (155) and concentrated

hydrochloric acid were added and the reaction mixture was refluxed for 48 h. Work-up afforded an oil which was chromatographed to give only 3% of (153).

Summarising, although the desired compound (153) has been synthesised the yields were much lower than expected. This has been accounted for by the instability of the crucial tin salt intermediate (163) which decomposes and/or polymerises in the harsh cyclisation conditions.

The hydrogenation of (E)-ethyl-3-(5-cyanothieno[2,3-b]pyridin-3-yl)prop-2-enoate (153) was then studied. Attempted catalytic hydrogenation at atmospheric pressure under a hydrogen atmosphere failed and only unreacted (153) was recovered in 89% yield.

When ten equivalents of sodium borohydride was added portionwise over a period of 30 minutes to a suspension of (153) and cuprous chloride (1.5 equivalents) at ice temperature followed by stirring for a further 1 h a dark brown suspension formed. Ethyl acetate was added and the reaction mixture was washed with water and brine. Evaporation of the solvent gave a solid which was chromatographed upon silica gel to give a single product. The ir spectrum confirmed the presence of the nitrile and ester groups but no peak at around 1640 cm^{-1} was observed suggesting that the olefinic bond had indeed been hydrogenated. This was confirmed from the ^{1}H nmr spectrum when the two doublets at 6.49 δ and 7.81 δ seen in the ^{1}H nmr spectrum of (153) were missing and replaced by two proton triplets at 2.77 δ and 3.20 δ coupling with each other (J=7.2 Hz). The mass spectrum gave a molecular ion of 261 (M+H) and the product was identified as ethyl-3-(5-cyanothieno[2,3-b]pyridin-3-yl)propanoate (167) (55% yield). The microanalytical data was also consistent with the molecular formula of $C_{13}H_{12}N_2O_2S$.

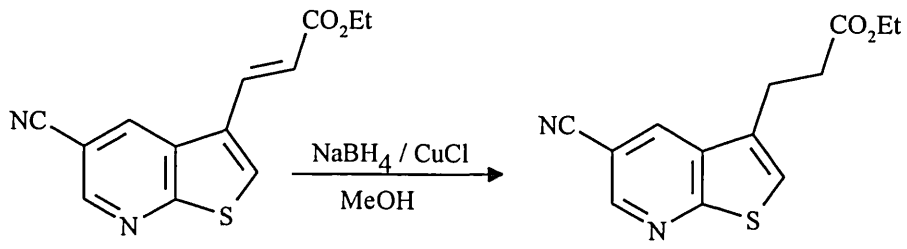

(153) (167)

The moderate yield of (167) prompted a decrease in the amount of sodium borohydride used in the reaction. When six equivalents of sodium borohydride was used under exactly the same reaction conditions tlc indicated the reaction mixture contained one component with the same R_f value as that of the starting material, and some baseline material. Chromatography afforded 72% of a white solid however the ^1H nmr spectrum demonstrated that the solid was in fact a mixture of (153) and (167) in almost equal proportions. All attempts to separate (153) and (167) by column chromatography were unsuccessful due to the two compounds having very similar R_f values on silica gel.

The conjugate reduction of (153) was further attempted using a 10% palladium on carbon catalyst and ammonium formate as a hydrogen donor. Refluxing the reaction mixture in glacial acetic acid followed by work-up and column chromatography gave the required product (167) in 30% yield. There was no evidence of any unreacted starting material (153) in the ir and ^1H nmr spectra of the product.

To study the conversion of the C-3 sidechain of ethyl-3-(5-cyanothieno[2,3-b]pyridin-3-yl)propanoate (167) to a protected ethylamine, 3-carbomethoxy-5-cyanothieno[2,3-b]pyridine (159) was used as a test compound prior to attempting the reactions with (167) [Scheme 36].

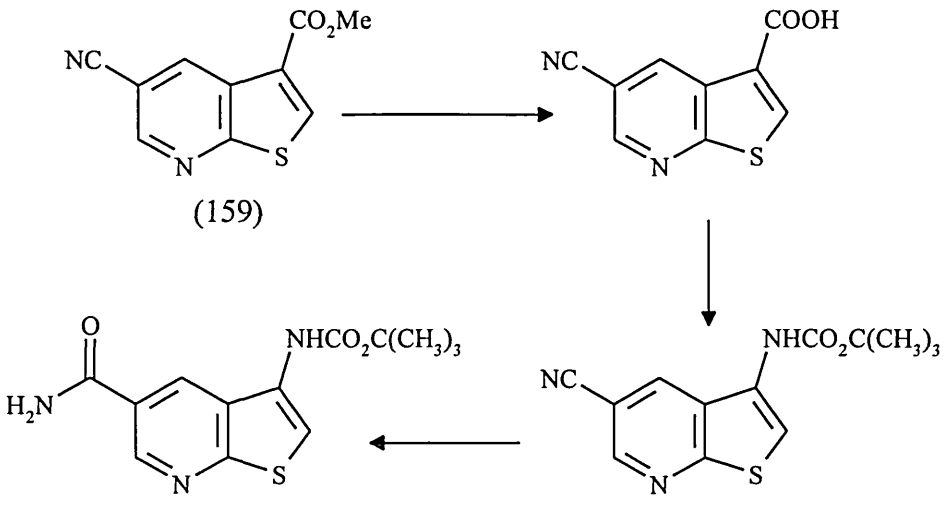

[Scheme 36]

The hydrolysis of esters is normally a straight forward procedure carried out using acid or base catalysis with the latter normally being the method of choice. In this instance a problem arises due to the presence of a nitrile group which could possibly also be hydrolysed to the amide or carboxylic acid, however the reaction normally requires higher temperatures than that required for ester hydrolysis.

A mild and efficient method for the cleavage of carboxylic esters has been reported[417] in the literature using iodotrimethylsilane prepared *in situ* from chlorotrimethylsilane and sodium iodide in acetonitrile. Alkyl and aryl esters were shown[417] to undergo facile cleavage to the intermediate trimethylsilylcarboxylate which can be hydrolysed to the carboxylic acid [Scheme 37].

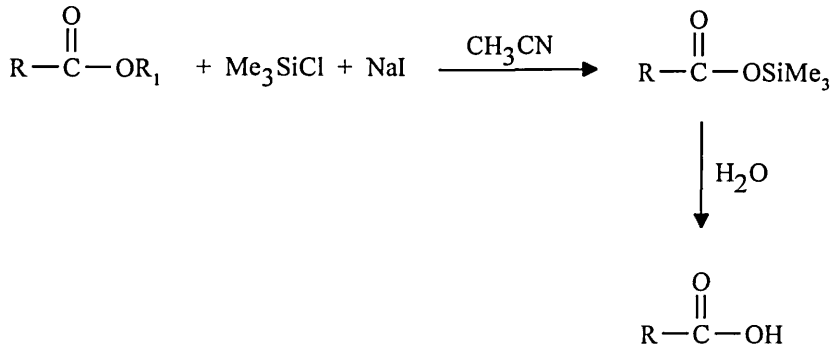

[Scheme 37]

A solution of chlorotrimethylsilane, sodium iodide and 3-carbomethoxy-5-cyanothieno[2,3-b]pyridine (159) in dry acetonitrile was refluxed for 48 h but tlc indicated that only starting material was present. Subsequent work-up afforded only unreacted (159) in 60% yield.

The hydrolysis was then attempted using a slight excess of 2M sodium hydroxide solution at room temperature in methanol. After stirring for 24 h tlc showed no starting material was present so the methanol was removed, the residue was acidified to pH=3 and the resulting white precipitate was filtered. The ir spectrum of the product confirmed the presence of a carboxylic acid from the C=O stretch at 1706 cm^{-1} and the characteristic broad O-H stretch at around 3000 cm^{-1}. Furthermore the sharp peak at 2235 cm^{-1} confirmed that the nitrile group was intact. The ^{1}H nmr spectrum showed no upfield protons whatsoever. The one proton singlet at 8.90 δ is further downfield than is normally expected for the C-2 proton of a thieno[2,3-b]pyridine but this could be attributed to the strong deshielding effect of a C-3 carboxylic acid group and the use of hexadeuterodimethylsulfoxide as solvent for the recording of the spectrum. An unresolved signal at 9.05 δ integrating to two protons is evidence of the C-4 and C-6 protons of the ring. The LC-mass spectrum showed a molecular ion of 203 (M-1) and the most abundant peak at 159 is attributed to the loss of the carboxylic acid group from the molecular ion. The product was therefore

confirmed as 5-cyanothieno[2,3-b]pyridine-3-carboxylic acid (168) obtained in 68% yield. Due to the low solubility of (168) in almost all common solvents a sample of sufficient purity for microanalysis was not obtained.

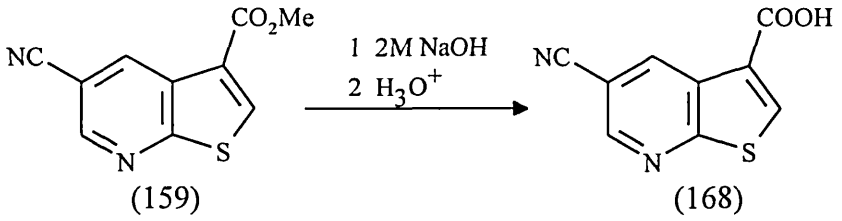

(159) (168)

The pyrolysis of acyl azides to isocyanates is the Curtius rearrangement. If the reaction is performed in water or alcohol the products formed are amines and urethanes respectively. The reaction is therefore an extremely valuable method for the preparation of amines and their protected derivatives.

Acyl azides can be prepared relatively easily from carboxylic acids by the formation of an acid chloride[418] or mixed anhydride[419-425] followed by nucleophilic substitution by an azide anion. Problems often occur due to the high reactivity of the acid chloride and the preferred method is usually via the mixed anhydride intermediate.

The conversion of carboxylic acids to urethanes can be alternatively accomplished directly using the reagent diphenylphosphorylazide (DPPA)[426-428] [Equation 15].

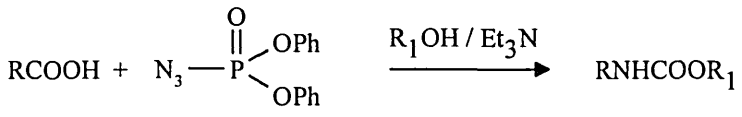

[Equation 15]

The reaction is thought to proceed by the transfer of the azide group of DPPA to the carbonyl carbon of the carboxylic acid. Typically an equimolar mixture of the carboxylic acid, DPPA and triethylamine is heated in the presence of *t*-butanol to afford the *t*-BOC protected amine in high yield.

5-Cyanothieno[2,3-b]pyridine-3-carboxylic acid (168) was refluxed with DPPA and triethylamine in *t*-butanol for 18 h. The solvent was removed and the residue was dissolved in ethyl acetate and washed with saturated sodium hydrogen carbonate solution then brine. Evaporation of the ethyl acetate afforded a low yield of a complex mixture of products which were inseparable by column chromatography. When the aqueous washings were acidified and extracted with ethyl acetate unreacted (168) was obtained almost quantitatively thus proving the reaction was unsuccessful.

Thieno[2,3-b]pyridine (168) was however converted to the acyl azide using the mixed anhydride route [Scheme 38]. After stirring (168) with triethylamine and ethyl chloroformate in acetone for 3 h sodium azide was added and the reaction mixture stirred for a further 2.5 h. Work-up and purification by column chromatography gave a quantitative yield of 3-azidocarbonyl-5-cyanothieno[2,3-b]pyridine (169). The ir spectrum showed two sharp peaks at 2232 and 2181 cm^{-1} corresponding to nitrile and azide groups respectively; a carbonyl stretch was also observed at 1694 cm^{-1}. The ^{1}H nmr spectrum was very similar to that of the starting material (168), with three downfield signals. A one proton singlet at 8.65 δ was assigned to the C-2 proton and the two single proton doublets at 8.84 δ and 9.18 δ are typical of the C-4 and C-6 protons of a thieno[2,3-b]pyridine ring respectively. The microanalysis figures are also consistent with (169) for carbon, hydrogen and sulfur, however the figure for nitrogen is lower than the expected figure; this is quite common in acyl azides due to decomposition through loss of nitrogen gas.

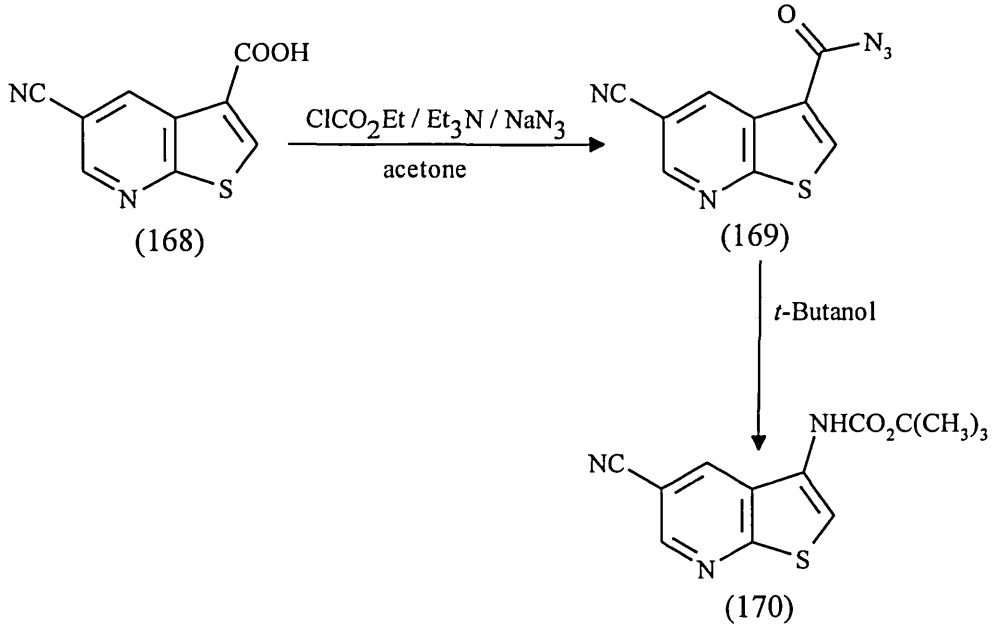

[Scheme 38]

Compound (169) was then refluxed in *t*-butanol until tlc had indicated that no unreacted (169) remained. Evaporation of the solvent and purification by column chromatography afforded a white solid in 68% yield. The ir spectrum showed peaks at 3276 and 3174 cm^{-1} consistent with the N-H stretch of a urethane. Furthermore the peak at 2231 cm^{-1} confirmed the nitrile group was still present but there was no evidence of any azide. The ^1H nmr spectrum showed a large singlet at 1.61 δ integrating to nine protons which can only be indicative of a *t*-butyl group. A broad singlet at 6.83 δ was caused by the exchangeable urethane proton. The three signals for the aromatic protons were most interesting, as expected the C-6 proton was the furthest downfield and was observed as a clear doublet with a coupling constant of J=1.85 Hz typical of the coupling between the C-6 and C-4 protons of a thieno[2,3-b]pyridine. The C-4 and C-2 protons were observed as broad one proton singlets at 8.26 δ and 7.75 δ respectively. This unexpected line broadening in the ^1H nmr spectrum can possibly be explained by the presence of the urethane N-H group which may interfere with the relaxation mechanism[429]. The mass spectrum gave a

molecular ion at 276 (M+H) and the microanalytical data is consistent with the assigned structure of 3-[(*t*-butoxycarbonyl)amino]-5-cyanothieno[2,3-b]pyridine (170) [Scheme 38].

Hydrolysis of the nitrile function of (170) was effected by stirring with concentrated ammonia and hydrogen peroxide in ethanol at room temperature for 24 h. Removal of solvent and recrystallisation of the resulting solid gave a quantitative yield of a product which according to tlc was pure. The most notable feature of the ir spectrum of the compound was the disappearance of the sharp peak associated with the nitrile function. A carbonyl C=O stretch was observed at 1668 cm^{-1}. Peaks at 3418, 3211 and 3060 cm^{-1} imply an amide and urethane function. The product was thus identified as 3-[(*t*-butoxycarbonyl)amino]-5-carboxamidothieno[2,3-b]pyridine (171). The ^1H nmr spectrum was consistent with the structure (171).

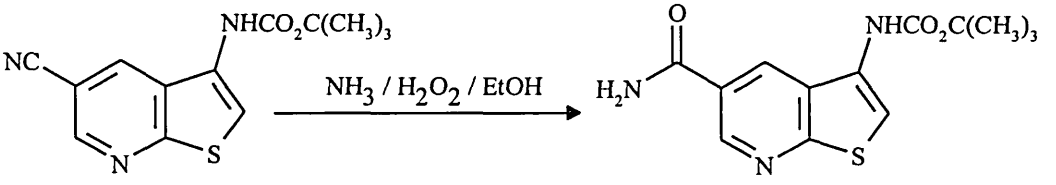

(170) (171)

It has therefore proved possible to convert 3-carbomethoxy-5-cyanothieno[2,3-b]pyridine (159) to the *t*-BOC protected amines (170) and (171) in good yield. The experience gained in studying these reactions was used for similar reactions of ethyl-3-(5-cyanothieno[2,3-b]pyridin-3-yl)propanoate (167) in an attempt to synthesise potential bio-isosteres of 5-HT.

As an aside the chlorinated thieno[2,3-b]pyridine (158) was refluxed with guanidine hydrochloride and sodium hydride in DMF in an effort to prepare the tricyclic thieno[2,3-b]pyridine (172) which has an amino function in a similar

region to that of the amino group of 5-HT. The reaction mixture was poured onto ice/water and extracted with ethyl acetate affording only unreacted starting material (158).

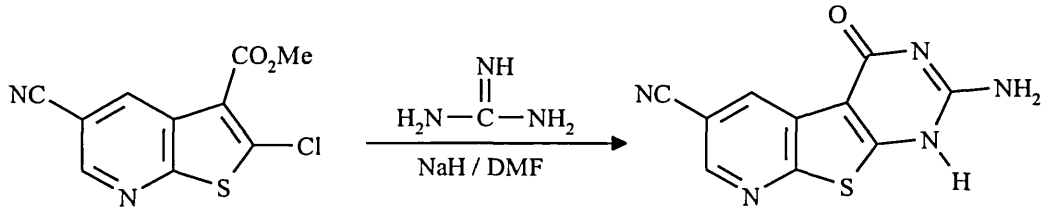

(158) (172)

The base catalysed hydrolysis of ethyl-3-(5-cyanothieno[2,3-b]pyridin-3-yl)propanoate (167) afforded an excellent yield of a yellow solid. Purification of the substance however proved to be very difficult due to the poor solubility of the solid in almost all solvents. When the product was dissolved in aqueous base and precipitation induced by the addition of acid the purity was not improved. The ir spectrum showed a broad absorption band at 3439 cm^{-1} and a carbonyl C=O stretch at 1717 cm^{-1} which is consistent with a non-conjugated carboxylic acid. Furthermore the sharp peak at 2232 cm^{-1} confirms that the nitrile group is still intact. No ^{1}H nmr spectrum was obtained due to the poor solubility of the compound but from the ir spectrum the product was assumed to consist of mainly 3-(5-cyanothieno[2,3-b]pyridin-3-yl)propanoic acid (173).

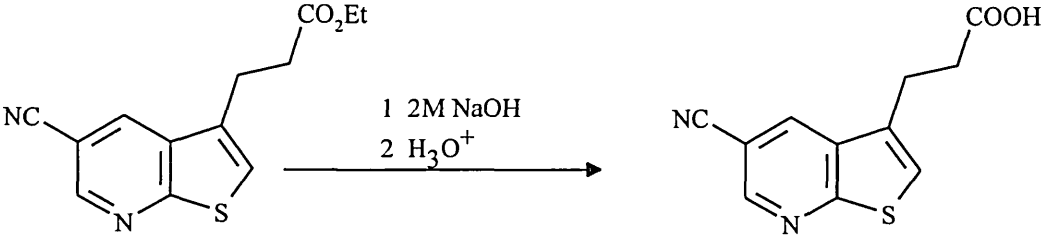

(167) (173)

When (173) was stirred with triethylamine and ethyl chloroformate in acetone followed by the addition of sodium azide the ir of the isolated crude product

indicated the presence of an azide group from the strong absorption at around 2100 cm^{-1}. Purification of the crude product by column chromatography however afforded a solid (37% yield) which was confirmed as ethyl-3-(5-cyanothieno[2,3-b]pyridin-3-yl)propanoate (167).

The formation of (167) from (173) was unexpected but tlc of the starting material (173) showed that there were no nonpolar components present therefore formation of (167) cannot be accounted for by the presence of unreacted (167) from the hydrolysis reaction. It is possible however that in the reaction the mixed anhydride formed undergoes nucleophilic attack by the azide anion to give the required acyl azide, carbon dioxide and the ethoxide anion. The ethoxide anion could subsequently displace the azide group from the acyl azide to afford the isolated product (167) [Scheme 39].

Since the ir spectrum of the crude solid exhibited a strong azide peak it was postulated that the required azide is present in the reaction mixture either as a minor product or as an intermediate in the reaction to form the ester (167). Therefore the crude solid of the reaction was taken up directly in *t*-butanol and refluxed. However, tlc indicated that no reaction was taking place so the solvent was removed and the crude solid was refluxed in *o*-xylene in the presence of *t*-butanol. When the *o*-xylene was removed tlc indicated a complex mixture of components and the ir spectrum suggested possibly a urethane but the ^1H nmr spectrum confirmed that the major component was (167).

The attempted synthesis of the intermediate azide via the acid chloride also failed. Thieno[2,3-b]pyridine (173) was refluxed with thionyl chloride for 24 h, the thionyl chloride was removed and the crude product was stirred in acetone with sodium azide for 5 h. Work-up and column chromatography afforded low

yields of two components but the ir spectra of both indicated the absence of the nitrile function and the reaction was abandoned.

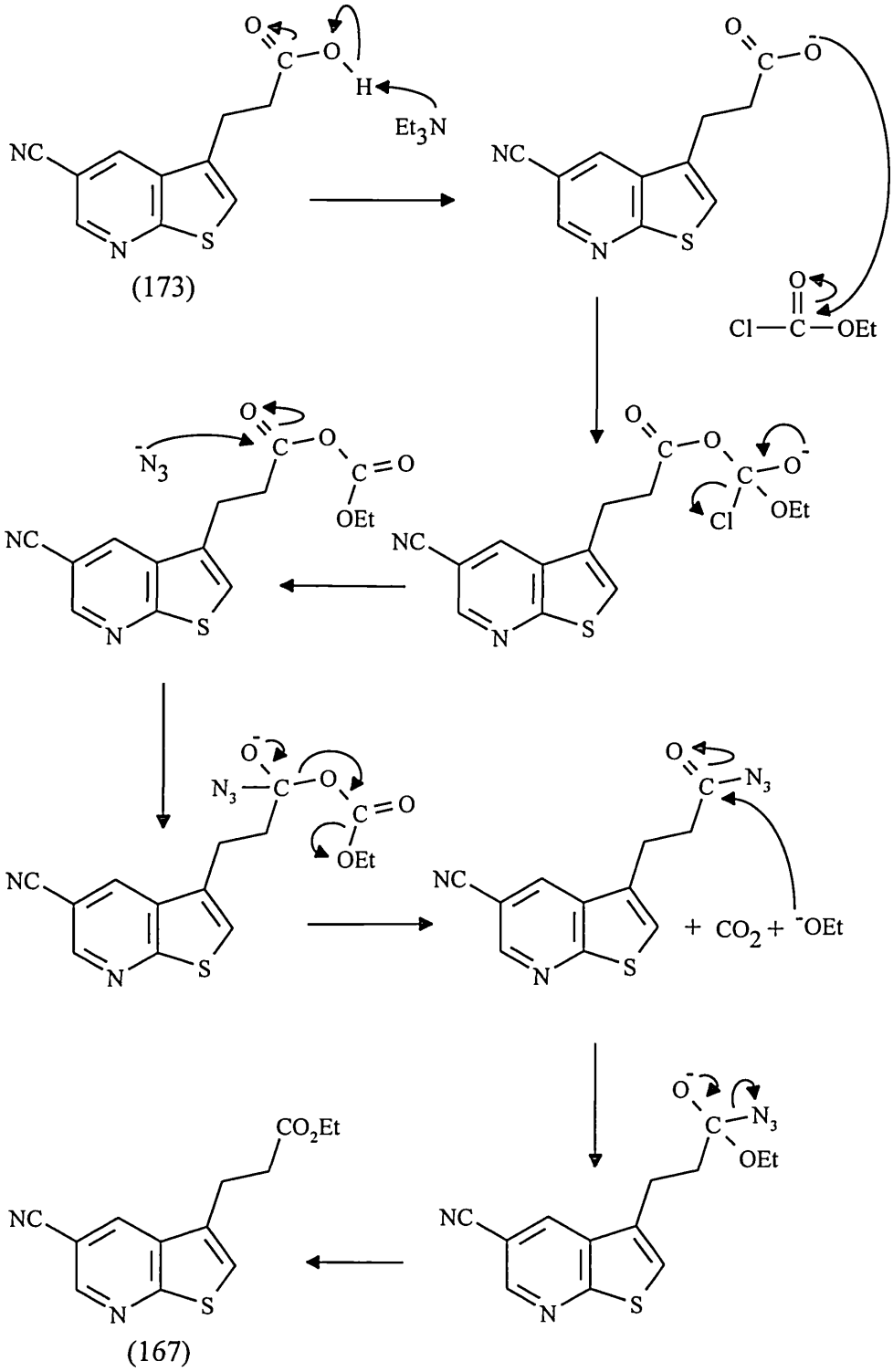

[Scheme 39]

The conversion of (173) to the *t*-BOC protected amine (174) was also attempted in one step by refluxing (173) with DPPA and triethylamine in *t*-butanol but the ir spectrum of the crude product suggested that the nitrile group was no longer present and the ^1H nmr spectrum indicated that no protons corresponding to a thieno[2,3-b]pyridine ring were present.

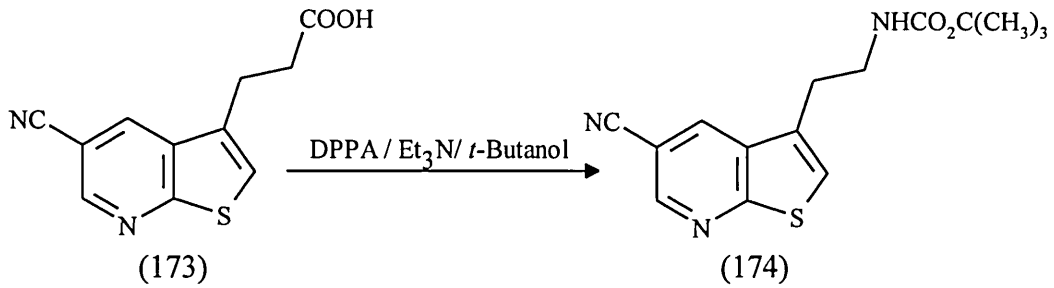

(173) (174)

The problems encountered in the attempted synthesis of the *t*-BOC protected amine derivative have prompted an investigation into alternative methods for the synthesis of the required compound.

The Gabriel reaction is a widely used method for the synthesis of amines[430]. The reaction of an alkyl halide with potassium phthalimide forms a protected amine which upon treatment with potassium hydroxide solution or hydrazine can be converted to the primary amine [Scheme 40].

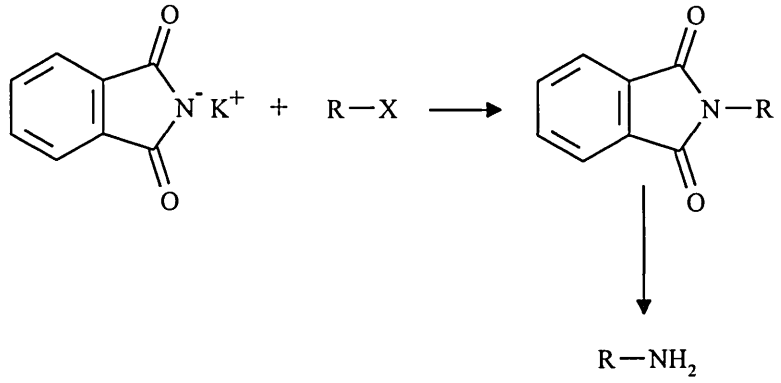

[Scheme 40]

Thus if the carboxylic acid (173) could be chain shortened by the Hunsdiecker reaction to the halide (175) the Gabriel reaction would afford one of the synthetic target compounds.

Using a modified procedure[431] for the Hunsdiecker reaction lead tetraacetate and lithium chloride were heated at 80 °C for 3 h with a suspension of crude 3-(5-cyanothieno[2,3-b]pyridine)propanoic acid (173) in dry toluene. The reaction mixture was partitioned between diethyl ether and sodium hydrogen carbonate. The organic phase was dried and solvent removed to afford a low yield of a solid which ^{1}H nmr indicated to be a complex mixture of components. Thus the reaction was pursued no further due to the low yield and complex mixture. Acidification and extraction of the aqueous phase into ethyl acetate yielded unreacted (173). The low solubility of the starting material (173) in toluene may have prevented the reaction from proceeding.

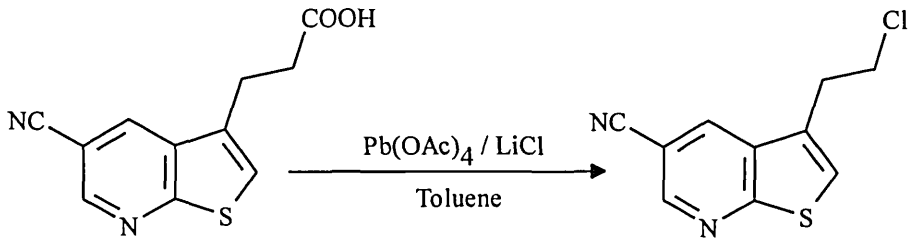

(173) (175)

A further alternative synthetic route to amines is the Hofmann rearrangement[432]. A primary amide is treated with sodium hydroxide and bromine to afford an isocyanate which upon hydrolysis would give a primary amine [Scheme 41].

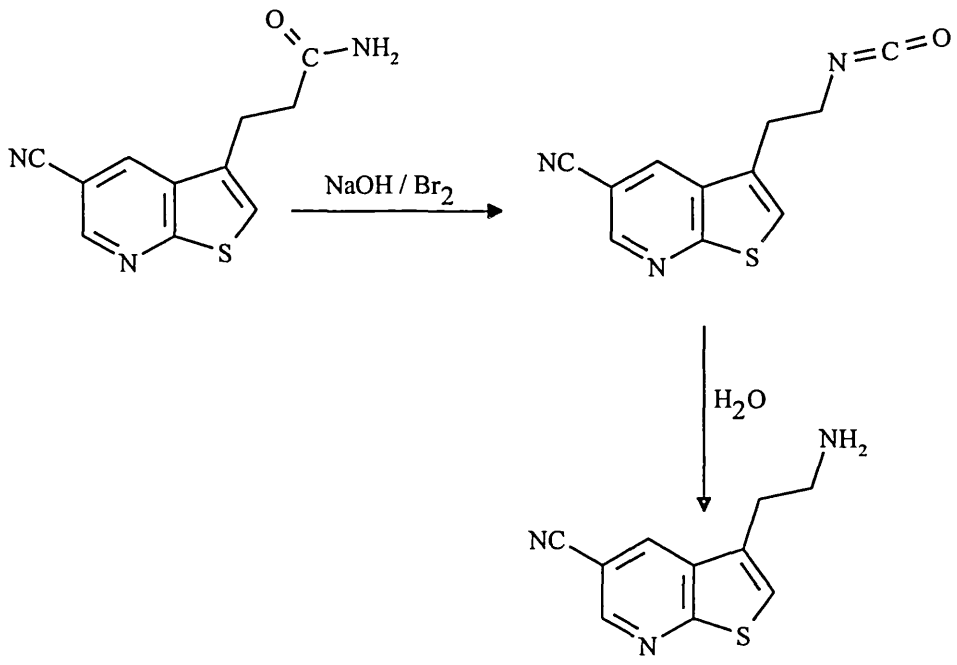

[Scheme 41]

The ester (167) was refluxed with concentrated ammonia in ethanol until tlc indicated that no unreacted (167) remained. The ir spectrum of the isolated crude product suggested that the nitrile function was still present and a carbonyl C=O stretch at 1684 cm^{-1} suggested an amide. A mixture of sodium hydroxide solution and bromine was added to the crude product and the reaction mixture was heated at 90 ^{o}C for 3 h. After work-up the crude product was dissolved in dry diethyl ether and hydrogen chloride gas was bubbled through the ether solution. The precipitated solid darkened probably due to decomposition on exposure to air. The ^{1}H nmr spectrum provided no evidence whatsoever of any thieno[2,3-b]pyridine. Thus if the required product was formed it had decomposed prior to the recording of the ^{1}H nmr spectrum.

In a final effort (E)-3-(2-nitro-4-thienyl)prop-2-enoic acid (165) was stirred with triethylamine, ethyl chloroformate and sodium azide. The ir spectrum of the intermediate product indicated a peak corresponding to an azide group. This crude product was refluxed in *t*-butanol; removal of solvent and purification by

column chromatography afforded (E)-1-[(*t*-butoxycarbonyl)amino]-2-(2-nitro-4-thienyl)ethene (176) in 28% yield. The ir spectrum exhibited an amide N-H stretch at 3354 cm^{-1} and C=O stretch at 1700 cm^{-1}. The peak at 1654 cm^{-1} was attributed to the carbon-carbon double bond and the nitro group caused peaks at 1499 and 1326 cm^{-1}. The ^1H nmr spectrum was consistent with a 2,4-substituted thiophene. The nine proton singlet at 1.25 δ confirmed the *t*-butyl group and the vinylic protons were observed as two doublets at 6.61 δ and 5.82 δ (J=14.6 Hz). The molecular ion of 269 (M-1) is consistent with the assigned structure (176).

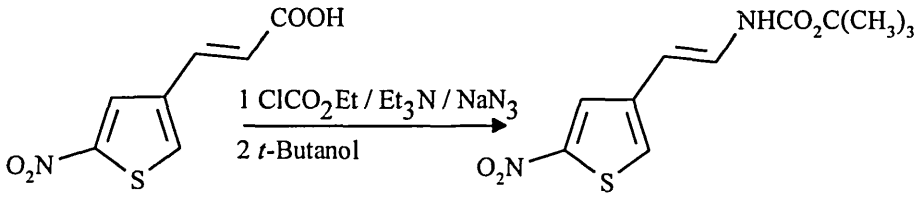

(165) (176)

Attempted tin hydrochloric acid reduction of (176) followed by cyclisation with 3,3-dimethoxy-2-formylpropionitrile sodium salt (155) afforded a low yield of a complex mixture possibly containing a thieno[2,3-b]pyridine but inseparable by column chromatography. The failure of this reaction is probably due to the cleavage of the amine protecting group in the harsh reaction conditions followed by reaction of the resulting enamine.

Unfortunately time constraints did not allow the synthesis of the required thieno[2,3-b]pyridine analogs of 5-HT. Although 3-carbomethoxy-5-cyanothieno[2,3-b]pyridine (159) could however be converted to the protected amine derivatives (170) and (171) the attempted route from (E)-ethyl-3-(5-cyanothieno[2,3-b]pyridin-3-yl)prop-2-enoate (153) has proved to be unsuccessful. This may be due to the carbonyl function of (153) not being directly attached to the aromatic rings. The synthesis of (153) from the thiophene precursor is low yielding and involves a tedious work-up and

purification routine. Although (153) could be converted to the hydrogenated compound (167) any further attempts at reactions have generally afforded low yields, mixed products and decomposition. Therefore it has been concluded that this route is definitely not the best method for the synthesis of the desired compounds and alternative methods must be investigated.

4 CONCLUSIONS AND FUTURE WORK

4.1 CONCLUSIONS

Molecular models of the human 5-HT_{1A}, 5-$HT_{1D\alpha}$ and 5-$HT_{1D\beta}$ receptors have been constructed using the heptahelical structure of bacteriorhodopsin as an initial template. The probable agonist binding site of the receptor models has been identified and validated by the docking of several known agonists. The models account for the high affinity of 5-HT and 5-CT, the 5-HT_{1A} receptor selectivity of (R)-8-OH-DPAT, the 5-HT_{1D} receptor selectivity of sumatriptan and the low 5-HT_{1A} receptor affinity of 5-OH-TMT.

The possibility of a thieno[2,3-b]pyridine analog of 5-HT acting as a bio-isostere for 5-HT has been investigated. Small molecule similarity studies and ligand receptor modelling have confirmed this possibility. Therefore compound (133) and similar thieno[2,3-b]pyridine derivatives which can accept a hydrogen bond at the C-5 position were identified as synthetic target compounds.

The ligand design program Ludi was used to provide further suggestions of possible synthetic targets and proved valuable in the identification of a receptor volume that may confer selectivity between the 5-$HT_{1D\alpha}$ and 5-$HT_{1D\beta}$ receptors.

The models are consistent with most of the available experimental data for the 5-HT receptors. Even so, as with all GPCR models, the models must be treated with caution. They are qualitatively useful in studying the requirements for ligand binding and in the design of new ligands but they are certainly not "real". One of the major dangers of GPCR modelling is that the modellers actually believe that their models are true. There will be inaccuracies in the models

which may only be eliminated or minimised upon the availability of further experimental data.

The major disappointment of this work was that a thieno[2,3-b]pyridine analog of 5-HT could not be synthesised and isolated. Nevertheless in the attempts to synthesise compounds of this type a number of novel thieno[2,3-b]pyridines were prepared en route. Using methodology developed at the University of Abertay Dundee 3-carboethoxy-2-methylthiothieno[2,3-b]pyridine (70a) was synthesised and reduced to the hydroxymethyl derivative however the removal of the methylthio group in the presence of a thiophene ring proved troublesome. The attempted synthesis of (174) via (E)-ethyl-3-(5-cyanothieno[2,3-b]pyridin-3-yl)prop-2-enoate (153) likewise proved problematic due to low yields, tedious work-ups and complex reaction mixtures. The key intermediate azide could not be synthesised from the carboxylic acid so alternative routes to (174) were attempted without success.

The unfortunate consequence of this work is that no biological activity data for the synthetic targets was obtained. This would have been used as feedback in an effort to improve the models and to provide a greater understanding of the requirements for 5-HT receptor binding.

4.2 SUGGESTIONS OF FUTURE WORK

On the modelling front it would be relatively easy to model many more agonists, partial agonists and antagonists in order to study how these compounds might interact with the receptor models. However it has been said[433] "more calculations do not validate calculations" and thus studying more compounds is probably not worthwhile investigating.

One of the more interesting points to arise from the models was the possible role of SER12(H4) interacting with the electron rich indole ring of some compounds in the 5-HT_{1D} receptor models. This could be further investigated. The preference of different conformations of the ethylamine sidechain of tryptamines for different 5-HT receptors could also be investigated further, studying the synthesis and 5-HT receptor affinities of conformationally constrained compounds similar to known 5-HT receptor agonists. The 5-ht_{1E} and 5-ht_{1F} receptors could also be modelled but again these models would only act as a potentially useful guide in the rational design of novel drugs.

The main thrust must therefore be on the synthetic chemistry. Thieno[2,3-b]pyridine analogs of 5-HT need to be synthesised and isolated. A more in depth investigation into the removal of the methylthio group of (70a) could be studied. Alternatively a possible synthetic route is described below [Scheme 42].

In scheme 42 the hexachlorostannate salt (25) of 2-aminothiophene is reacted with 3,3-dimethoxy-2-formylpropionitrile sodium salt (155) to give the thieno[2,3-b]pyridine (177). Monohalogenation as described in the literature[342] should occur at the C-3 position. Displacement of the halogen in a lithium - halogen exchange reaction and reaction of the lithiated compound with 2-bromoethylamine (the amine function of 2-bromoethylamine may need to be protected) should afford the desired thieno[2,3-b]pyridine (178). Subsequent manipulation of the nitrile group could then take place and the thieno[2,3-b]pyridine analogs of 5-HT could be evaluated for biological activity at the 5-HT receptors.

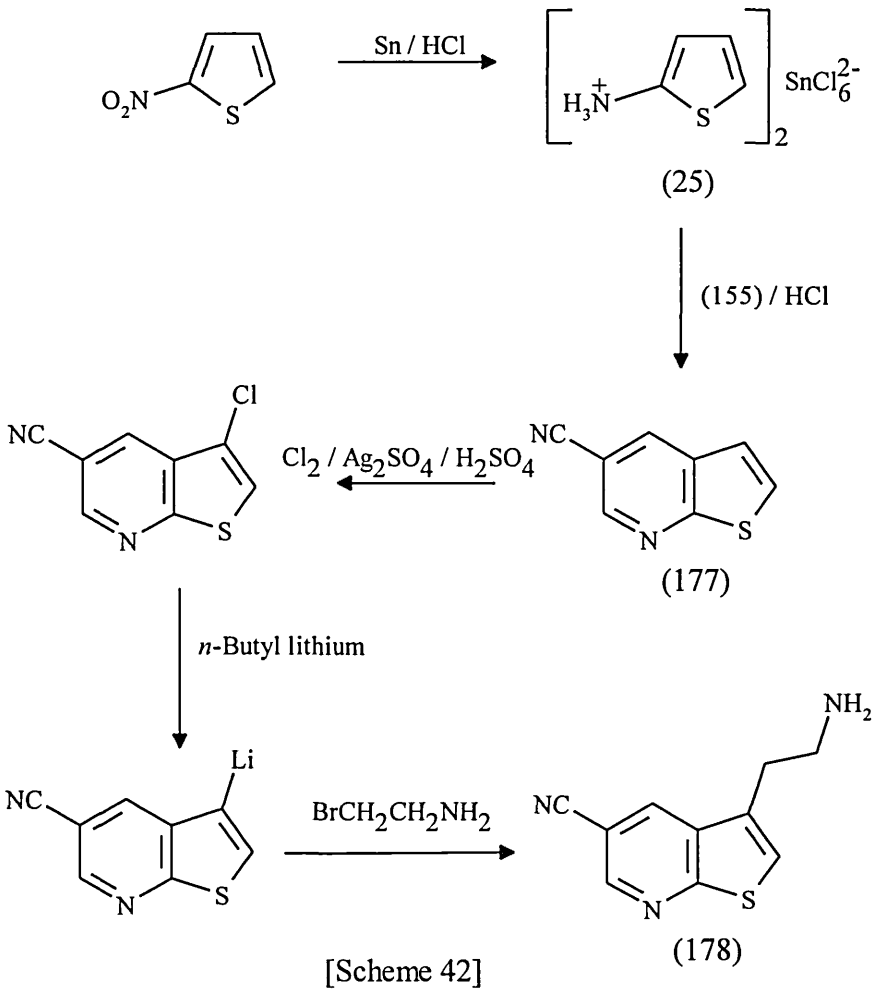
Sn / HCl
(25)
(155) / HCl
(177)
$Cl_2 / Ag_2SO_4 / H_2SO_4$
n-Butyl lithium
$BrCH_2CH_2NH_2$
(178)

[Scheme 42]

5 EXPERIMENTAL

Infrared spectra were recorded on a Perkin-Elmer 1600 FT-IR spectrophotometer. NMR spectra were recorded using tetramethylsilane as reference on a Jeol PMX 60si or a Bruker AMX 360 spectrometer. Melting points were determined with an Electrothermal melting point apparatus and are uncorrected. Column chromatography was performed using the method of Still[434] with Silica gel 60, 220-440 mesh, particle size 0.035-0.070 mm, purchased from Fluka. Reactions were monitored by thin layer chromatography on Merck DC-Alufolien Kieselgel 60 F_{254} (Merck #5554) plates which were visualised under ultraviolet irradiation. Mass spectra, LC-mass spectra and microanalysis were provided by Glaxo-Wellcome Medicines Research, Stevenage. Reagent quality solvents were used unless otherwise stated. Petroleum ether refers to the fraction of petroleum boiling in the range 60-80 ^{o}C. Raney nickel was purchased ready to use from Fluka.

Ethyl 3-pyridylacetate-1-oxide (143)

a) Oxidation of ethyl 3-pyridylacetate (142) with magnesium monoperoxy-phthalate.

Ethyl 3-pyridylacetate (142) (1.0 g, 6.05 mmol) was added dropwise to a solution of magnesium monoperoxyphthalate (3.02 g, 6.10 mmol) in ethanol (25 ml). The reaction mixture was stirred at room temperature for 2.5 h. Excess oxidising agent was destroyed by the addition of solid sodium metabisulfite (wet starch/iodide paper). Solid potassium carbonate was then added and any insoluble solids were removed by filtration. The solvent was removed *in vacuo* to afford a solid which was recrystallised from toluene to give ethyl 3-

pyridylacetate-1-oxide (143) as a white solid (0.60 g, 55%), mp 94-96 °C (literature[404] 97-98 °C); ν_{max}(KBr)/cm^{-1} 1733, 1271.

b) Oxidation of ethyl 3-pyridylacetate (142) with *m*-chloroperoxybenzoic acid.

m-Chloroperoxybenzoic acid (70%) (16.41 g, 95 mmol) was added to a solution of ethyl 3-pyridylacetate (142) (10.0 g, 60 mmol) in dichloromethane (70 ml). The mixture was stirred at room temperature for 7 days. When no oxidising agent remained (wet starch/iodide paper) solid potassium carbonate was added and any insoluble solids were removed by filtration. The solvent was removed *in vacuo* to give a solid which was recrystallised from toluene affording ethyl 3-pyridylacetate-1-oxide (143) (10.27 g, 94%) as a white solid identical (tlc, ir) to a sample prepared in (a).

Reaction of ethyl 3-pyridylacetate-1-oxide (143) with phosphoryl chloride[251]

Ethyl 3-pyridylacetate-1-oxide (143) (12.67 g, 69.9 mmol) was refluxed in phosphoryl chloride (150 ml) for 3 h. The phosphoryl chloride was removed *in vacuo* and the residue poured onto ice/water (150 ml), neutralised with 2M ammonium chloride solution and extracted with ethyl acetate (3 x 150 ml). The combined organic extracts were dried over magnesium sulfate and the solvent removed *in vacuo* to afford an oil. The oil was dissolved in a little dichloromethane and chromatographed on silica gel. Gradient elution with petroleum ether/ethyl acetate (5-50%) afforded a mixture of ethyl 2-chloro-5-pyridylacetate (145) and ethyl 2-chloro-3-pyridylacetate (69a) (8.54 g, 61%). Also isolated was ethyl 4-chloro-3-pyridylacetate[251] (144) (2.82 g, 20%) as an oil; ν_{max}/cm^{-1}1737. No boiling point was obtained due to decomposition.

Oxidation of the mixture of ethyl 2-chloro-5-pyridylacetate (145) and ethyl 2-chloro-3-pyridylacetate (69a)

(a) Oxidation with magnesium monoperoxyphthalate.

Magnesium monoperoxyphthalate (13.54 g, 24.6 mmol) was added to a mixture of ethyl 2-chloro-5-pyridylacetate (145) and ethyl 2-chloro-3-pyridylacetate (69a) (8.94 g, 44.8 mmol) in ethanol (50 ml). The reaction mixture was stirred at room temperature for 24 h. Solid sodium metabisulfite was added to destroy any excess oxidising agent. The ethanol was removed *in vacuo* and replaced with dichloromethane (100 ml). The dichloromethane solution was washed with saturated sodium hydrogen carbonate solution, dried over magnesium sulfate and the solvent removed *in vacuo* to give an oil which was chromatographed on silica gel. Gradient elution with petroleum ether/ethyl acetate (10-100%) afforded the unoxidised mixture of (145) and (69a) as an oil (4.20 g, 47%). Also isolated was ethyl 2-chloro-5-pyridylacetate-1-oxide[402] (146) (0.59 g, 6%) as a white solid, mp 104-105 ^{o}C; ν_{max}(KBr)/cm^{-1} 1710, 1275; δ_H($CDCl_3$) 1.20 (t, 3H, J=6 Hz, CH_3), 3.47 (s, 2H, CH_2CO_2), 4.03 (q, 2H, J=6 Hz, CO_2CH_2), 6.97 (dd, 1H, J=2 & 8 Hz, H-4), 7.25 (d, 1H, J=8 Hz, H-3) and 8.07 (d, 1H, J=2 Hz, H-6); MS m/z 216 (M+H), 200 [(M+H)-O]. Further elution afforded ethyl 2-chloro-3-pyridylacetate-1-oxide[402] (147) (0.86 g, 9%) as a white solid, mp 59-60 ^{o}C; ν_{max}(KBr)/cm^{-1} 1700, 1250; δ_H($CDCl_3$) 1.24 (t, 3H, J=6 Hz, CH_3), 3.74 (s, 2H, CH_2CO_2), 4.14 (q, 2H, J=6 Hz, CO_2CH_2), 7.11 (m , 2H, H-4 & H-5) and 8.18 (m, 1H, H-6); MS m/z 216 (M+H), 200 [(M+H)-O].

(b) Oxidation with *m*-chloroperoxybenzoic acid[402].

m-Chloroperoxybenzoic acid (70%) (14.49 g, 62.7 mmol) was added to a mixture of ethyl 2-chloro-5-pyridylacetate (145) and ethyl 2-chloro-3-

pyridylacetate (69a) (4.20 g, 21 mmol) in dichloromethane (80 ml). The reaction mixture was stirred at room temperature for 3 days. Excess oxidising agent was destroyed by the addition of solid sodium metabisulfite. Solid potassium carbonate was then added and any insoluble solids were removed by filtration. The filtrate was dried over magnesium sulfate and the solvent removed *in vacuo* to give a brown oil which was chromatographed on silica gel. Gradient elution with petroleum ether/ethyl acetate (75-100%) gave ethyl 2-chloro-5-pyridylacetate-1-oxide (146) (1.91 g 42%) as a white solid which was identical (tlc, ir, mp) to an authentic sample of (146) prepared in (a). Further elution afforded ethyl 2-chloro-3-pyridylacetate-1-oxide (147) (2.54 g, 56%) as a white solid which was identical (tlc, ir, mp) to an authentic sample of (147) prepared in (a).

3-Carboethoxy-2-methylthiothieno[2,3-b]pyridine-7-oxide (148)[402]

Sodium hydride (0.6 g, 25 mmol) was added portionwise to a stirred solution of ethyl 2-chloro-3-pyridylacetate-1-oxide (147) (2.39 g, 11 mmol) and carbon disulfide (0.93 g, 12.2 mmol) in DMSO (30 ml) under nitrogen. The reaction mixture was stirred at room temperature for 1 h then at 70 ^{o}C for 1.5 h, cooled and methyl iodide (3.5 g, 25 mmol) was added and stirring continued at room temperature for a further 1.5 h. The reaction mixture was poured onto ice/water (200 ml) and extracted with ethyl acetate (3 x 100 ml). The combined extracts were dried over magnesium sulfate and the solvent removed *in vacuo* to yield a solid which was then dissolved in a little dichloromethane and chromatographed on silica gel. Gradient elution with petroleum ether/ethyl acetate (50-100%) afforded 3-carboethoxy-2-methylthiothieno[2,3-b]pyridine-7-oxide (148) (0.5 g, 17%) as a white solid, mp 158-159 ^{o}C; ν_{max}(KBr)/cm^{-1} 3025, 2950, 1690, 1240; δ_H($CDCl_3$) 1.44 (t, 3H, J=7.2 Hz, CH_3), 2.72 (s, 3H, SCH_3), 4.38 (q, 2H,

J=7.2 Hz, CO_2CH_2), 7.22 (dd, 1H, J=6.2 & 7.6 Hz, H-5) and 8.20 (m, 2H, H-4 & H-6); MS m/z 270 (M+H), 254 [(M+H)-O].

3-Carboethoxy-2-methylthiothieno[2,3-b]pyridine (70a)

a) Deoxygenation of 3-carboethoxy-2-methylthiothieno[2,3-b]pyridine-7-oxide (148).

Phosphorus tribromide (0.8 ml, 8.42 mmol) was added dropwise at ice temperature to a solution of 3-carboethoxy-2-methylthiothieno[2,3-b]pyridine-7-oxide (148) (0.4 g, 1.5 mmol) in DMF (15 ml). The reaction mixture was stirred for 5 minutes, saturated sodium hydrogen carbonate solution (20 ml) was added and the aqueous phase was extracted with ethyl acetate (3 x 35 ml). The combined organic extracts were washed with brine then dried over magnesium sulfate. The solvent was removed *in vacuo* to give a solid which was recrystallised from ethyl acetate to afford 3-carboethoxy-2-methylthiothieno[2,3-b]pyridine[251] (70a) (0.3 g, 80%) as a white solid, mp 108-110 ^oC; $\nu_{max}(KBr)/cm^{-1}$ 1695; $\delta_H(CDCl_3)$ 1.46 (t, 3H, J=7.1 Hz, CH_3), 2.66 (s, 3H, SCH_3), 4.44 (q, 2H, J=7.1 Hz, CO_2CH_2), 7.29 (dd, 1H, J=4.65 & 8.26 Hz, H-5), 8.41 (dd, 1H, J=1.65 & 4.65 Hz, H-4) and 8.51 (dd, 1H, J=1.65 & 8.26 Hz, H-6).

(b) Cyclisation of ethyl 2-chloro-3-pyridylacetate (69a)[251].

Sodium hydride (0.53 g, 22 mmol) was added portionwise to a stirred solution of ethyl 2-chloro-3-pyridylacetate[402] (69a) (2.02 g, 10.1 mmol) and carbon disulfide (0.85 g, 11 mmol) in DMSO (25 ml) under nitrogen. The reaction mixture was stirred at room temperature for 1 h then at 70 ^oC for 1.5 h, cooled and methyl iodide (3.15 g, 22 mmol) was added and stirring continued at room

temperature for a further 1.5 h. The reaction mixture was poured onto ice/water (150 ml) and extracted with ethyl acetate (3 x 75 ml). The combined extracts were dried over magnesium sulfate and the solvent removed *in vacuo* to yield a yellow solid. The solid was dissolved in a little dichloromethane and chromatographed on silica gel. Gradient elution with petroleum ether/ethyl acetate (0-50%) afforded 3-carboethoxy-2-methylthiothieno[2,3-b]pyridine (70a) (1.72 g, 67%) as a white solid which was identical (tlc, ir, ^{1}H nmr) to an authentic sample[251].

3-Hydroxymethyl-2-methylthiothieno[2,3-b]pyridine (149)

3-Carboethoxy-2-methylthiothieno[2,3-b]pyridine (70a) (1.16 g, 4.57 mmol) in diethyl ether (20 ml) was added dropwise under nitrogen to a suspension of lithium aluminium hydride (0.22 g, 5.95 mmol) in diethyl ether (60 ml). The reaction mixture was refluxed for 48 h. Water (10 ml) and 2N sulfuric acid (4 ml) was added and the diethyl ether phase was separated. The aqueous phase was extracted with a further 2 x 50 ml of diethyl ether. The combined extracts were dried over sodium sulfate and the solvent removed *in vacuo* to give a yellow oil which was dissolved in dichloromethane and chromatographed on silica gel. Elution with cyclohexane/ethyl acetate (40%) afforded 3-hydroxymethyl-2-methylthiothieno[2,3-b]pyridine (149) (0.48 g, 50%), a white solid, mp 92-93 ^{o}C (Found: C, 50.94; H, 4.27; N, 6.52. $C_9H_9NOS_2$ requires C, 51.16; H, 4.29; N, 6.63%); ν_{max}(KBr)/cm^{-1} 3197, 1380; δ_H($CDCl_3$) 2.50 (s, 3H, CH_3), 3.05 (br s, 1H, OH), 4.89 (s, 2H, CH_2), 7.20 (dd, 1H, J=4.5 & 8.1 Hz, H-5), 8.06 (dd, 1H, J=1.7 & 8.1 Hz, H-4) and 8.38 (dd, 1H, J=1.7 & 4.5 Hz, H-6); LC-MS m/z 212 (M+H), 197 [(M+H)-CH_3].

Attempted reaction of 3-hydroxymethyl-2-methylthiothieno[2,3-b]pyridine (149) with chlorotrimethylsilane, sodium iodide and sodium cyanide

3-Hydroxymethyl-2-methylthiothieno[2,3-b]pyridine (149) (0.30 g, 1.4 mmol) was added to a mixture of chlorotrimethylsilane (0.31 g, 2.8 mmol), sodium cyanide (0.14 g, 2.8 mmol) and sodium iodide (0.002 g) in dry acetonitrile (5 ml) and dry DMF (5 ml). The reaction mixture was heated at 60 ^{o}C under nitrogen for 19 h, poured onto ice/water (50 ml) and extracted with diethyl ether (3 x 50 ml). The organic extracts were combined, dried over magnesium sulfate and the solvent removed *in vacuo* to afford an oil (0.02 g) which tlc and ir confirmed as unreacted (149). The reaction was not pursued any further.

Reaction of 3-hydroxymethyl-2-methylthiothieno[2,3-b]pyridine (149) with Raney nickel

3-Hydroxymethyl-2-methylthiothieno[2,3-b]pyridine (149) (0.25 g, 1.18 mmol) in acetone (10 ml) was added, under nitrogen, to a suspension of Raney nickel (3 g) in acetone (60 ml). The reaction mixture was refluxed for 1 h, the Raney nickel was removed by gravity filtration and the filtrate was dried over sodium sulfate. The solvent was removed *in vacuo* to give a yellow oil which was chromatographed on silica gel. Elution with cyclohexane/ethyl acetate (20%) afforded unreacted 3-hydroxymethyl-2-methylthiothieno[2,3-b]pyridine (149) (0.005 g, 2%) which was identical (^{1}H nmr) to an authentic sample prepared above. Further elution afforded 3-hydroxymethylthieno[2,3-b]pyridine (151) (trace); $\delta_H(CDCl_3)$ 4.89 (s, 2H, CH_2), 7.29 (dd, 1H, J=4.5 & 8.1 Hz, H-5), 7.69 (s, 1H, H-2), 8.14 (dd, 1H, J=1.75 & 8.1 Hz, H-4) and 8.54 (dd, 1H, J=1.75 & 4.5 Hz, H-6). No mp, ir or microanalysis was obtained due to the low yield of (151).

Reaction of 3-carboethoxy-2-methylthiothieno[2,3-b]pyridine (70a) with Raney nickel

3-Carboethoxy-2-methylthiothieno[2,3-b]pyridine (70a) (0.05 g, 0.2 mmol) was added to a suspension of Raney nickel (0.5 g) in acetone (20 ml). The reaction mixture was refluxed under nitrogen for 24 h after which time the Raney nickel was removed by gravity filtration and the filtrate was dried over sodium sulfate. The solvent was removed *in vacuo* to afford an oil (0.002 g) which tlc and ^{1}H nmr showed to be a mixture of products thus the reaction was taken no further.

Reaction of 3-hydroxymethyl-2-methylthiothieno[2,3-b]pyridine (149) with Raney nickel in ethanol

3-Hydroxymethyl-2-methylthiothieno[2,3-b]pyridine (149) (0.18 g, 0.85 mmol) was added to a suspension of Raney nickel (3 g) in ethanol (50 ml) under nitrogen at -10 ^{o}C. The reaction mixture was allowed to warm to room temperature and stirred for 2 h. The Raney nickel was removed by gravity filtration and the filtrate was dried over magnesium sulfate. The solvent was removed *in vacuo* to afford an oil (0.03 g) which ^{1}H nmr indicated to be a mixture of unidentifiable products.

3-Cyanothieno[2,3-b]pyridine (152)

3-Cyano-2-methylthiothieno[2,3-b]pyridine[250,251] (70c) (0.5 g, 2.42 mmol) in acetone (20 ml) was added under nitrogen to a suspension of Raney nickel (5 g) in acetone (100 ml). The reaction mixture was refluxed for 7 h, the Raney nickel was removed by gravity filtration and the filtrate was dried over sodium sulfate. The solvent was removed *in vacuo* to give a yellow solid which was dissolved in cyclohexane and chromatographed on silica gel. Elution with cyclohexane/ethyl

acetate (20%) afforded 3-cyanothieno[2,3-b]pyridine (152) (0.38 g, 98%) as a white solid, mp 107-108 °C (Found: C, 59.42; H, 2.77; N, 17.08. $C_8H_4N_2S$ requires C, 59.98; H, 2.52; N, 17.49%); ν_{max}(KBr)/cm^{-1} 2226; δ_H($CDCl_3$) 7.48 (dd, 1H, J=4.5 & 8.2 Hz, H-5), 8.19 (s, 1H, H-2), 8.26 (dd, 1H, J=1.9 & 8.2 Hz, H-4) and 8.70 (dd, 1H, J=1.9 & 4.5 Hz, H-6); LC-MS m/z 161 (M+H).

3,3-Dimethoxy-2-formylpropionitrile sodium salt (155)[272]

Sodium hydride (1.5 g, 63 mmol) and anhydrous methyl formate (6.85 ml, 110 mmol) were added to a solution of 3,3-dimethoxypropionitrile (154) (6.25 ml, 55 mmol) in dry diethyl ether (75 ml). The reaction mixture was stirred under nitrogen at room temperature for 72 h. The precipitated solid was filtered and washed with diethyl ether to afford 3,3-dimethoxy-2-formylpropionitrile sodium salt[272] (155) (6.64 g, 73%) as an off white solid; ν_{max}(KBr)/cm^{-1} 3447, 2209, 1596. The crude product was used without further purification and hence no ^{1}H nmr spectrum was obtained.

Cyclisation of 2-nitrothiophene-4-carboxylic acid (156)

Tin powder (6.58 g, 55 mmol) was added portionwise at 40 °C under nitrogen to a suspension of 2-nitrothiophene-4-carboxylic acid (156) (3.0 g, 17 mmol) in concentrated hydrochloric acid (60 ml). Once all the tin had reacted the yellow solution was cooled and the resulting precipitate was filtered off. The filtrate was concentrated *in vacuo* and a further crop of [bis(4-carboxythienyl-2-ammonium)]hexachlorostannate(IV)[271] (157) (4.43 g, 83%) was obtained as a yellow solid; δ_H(d_6 DMSO) 6.59 (s, 1H, H-3) and 7.46 (s, 1H, H-5).

A solution of (157) (3.95 g, 6.37 mmol) and concentrated hydrochloric acid (14.4 ml) in methanol (150 ml) was added under nitrogen to a suspension of 3,3-dimethoxy-2-formylpropionitrile sodium salt (155) (2.33 g, 14 mmol) and concentrated hydrochloric acid (1.4 ml) in methanol (50 ml). The reaction mixture was refluxed for 24 h, solvent was removed *in vacuo*, replaced by water (50 ml) and extracted with ethyl acetate (3 x 75 ml). The combined organic extracts were dried over magnesium sulfate and the solvent removed *in vacuo* to afford a solid which was dissolved in dichloromethane and chromatographed on silica gel. Elution with petroleum ether/ethyl acetate (20%) afforded 3-carbomethoxy-2-chloro-5-cyanothieno[2,3-b]pyridine (158) (0.25 g, 8%) as a white solid, mp 141-142 ^{o}C (Found: C, 47.57; H, 1.89; N, 11.16; S, 12.66. $C_{10}H_5N_2O_2SCl$ requires C, 47.53; H, 1.99; N, 11.09; S, 12.69%); ν_{max}(KBr) /cm^{-1} 2233, 1727; δ_H($CDCl_3$) 4.06 (s, 3H, CH_3), 8.77 (d, 1H, J=1.8 Hz, H-4) and 8.96 (d, 1H, J=1.8 Hz, H-6); δ_C($CDCl_3$, 62.9 MHz) 52.4 (CH_3), 136.0 (C-4) and 148.7 (C-6); MS m/z 253 (M+H). Further elution afforded 3-carbomethoxy-5-cyanothieno[2,3-b]pyridine[271] (159) (1.12 g, 40%) as a white solid, mp 121-122 ^{o}C (Found: C, 54.96; H, 2.50; N, 12.85. $C_{10}H_6N_2O_2S$ requires C, 55.04; H, 2.77; N, 12.84%); ν_{max}(KBr)/cm^{-1} 2231, 1723; δ_H($CDCl_3$) 3.99 (s, 3H, CH_3), 8.56 (s, 1H, H-2), 8.81 (d, 1H, J=1.8 Hz, H-4) and 9.11 (d, 1H, J=1.8 Hz, H-6).

(E)-Ethyl-3-(2-nitro-4-thienyl)prop-2-enoate (162)

Method A: 2-nitrothiophene-4-carboxaldehyde (161) (5.0 g, 31.8 mmol), triethylphosphonoacetate (7.8 g, 35 mmol) and tetrabutylammonium hydrogen sulfate (0.1 g) in toluene (100 ml) were added to a solution of potassium carbonate (29 g, 0.2 mol) in water (100 ml). The reaction mixture was stirred at room temperature under nitrogen for 7 days. 10% Hydrochloric acid solution was then added and the organic phase was separated. The aqueous phase was

extracted with a further 2 x 200 ml of ethyl acetate, the combined extracts dried over sodium sulfate and the solvent was removed *in vacuo* to afford a dark solid. The solid was dissolved in dichloromethane and chromatographed on silica gel. Elution with petroleum ether/ethyl acetate (20%) afforded (E)-ethyl-3-(2-nitro-4-thienyl)prop-2-enoate (162) (2.48 g, 34%) as a pale yellow solid, mp 104 ^{o}C (Found: C, 47.51; H, 4.02; N, 6.17; S, 13.90. $C_9H_9NO_4S$ requires C, 47.57; H, 3.99; N, 6.16; S, 14.11%); ν_{max}(KBr)/cm^{-1} 3074, 1700, 1639, 1509, 1337; δ_H($CDCl_3$) 1.32 (t, 3H, J=7.2 Hz, CH_3), 4.25 (q, 2H, J=7.2 Hz, CH_2), 6.31 (d, 1H, J= 16.2 Hz, =$CHCO_2$), 7.51 (d, 1H, J=16.2 Hz, ArCH=), 7.58 (d, 1H, J=1.9 Hz, H-3) and 8.04 (d, 1H, J=1.9 Hz, H-5); MS m/z 198 (M-CH_2CH_3). Further elution gave unreacted 2-nitrothiophene-4-carboxaldehyde (161) (0.30 g, 6%) as an orange solid which was identical (tlc, ir) to an authentic sample.

Method B: A mixture of 2-nitrothiophene-4-carboxaldehyde (161) (5.0 g, 31.8 mmol), triethylphosphonoacetate (8.56 g, 38.2 mmol) and water (50 ml) was added at ice temperature to a solution of potassium carbonate (8.79 g, 63 mmol) in water. The reaction was stirred under nitrogen at room temperature for 3 h, a further 200 ml of water was added and then extracted with ethyl acetate (3 x 200 ml). The combined organic extract was dried over magnesium sulfate and the solvent removed *in vacuo* to afford a dark solid which was chromatographed on silica gel. Elution with petroleum ether/ethyl acetate (20%) afforded (E)-ethyl-3-(2-nitro-4-thienyl)prop-2-enoate (162) (5.1 g, 71%) as a pale yellow solid which was identical (tlc, ir, ^{1}H nmr) to a sample prepared using method A. Further elution gave unreacted 2-nitrothiophene-4-carboxaldehyde (161) (1.01 g, 20%) as an orange solid which was identical (tlc, ir) to an authentic sample.

Method C: 2-nitrothiophene-4-carboxaldehyde (161) (0.2 g, 1.27 mmol) and triethylphosphonoacetate (0.34 g, 1.53 mmol) was added to potassium carbonate (0.35 g, 2.54 mmol) in dry THF (20 ml). The reaction mixture was stirred under

nitrogen at room temperature for 24 h. Any insoluble solids were removed by filtration and the filtrate was evaporated *in vacuo* to afford a yellow solid. The solid was dissolved in dichloromethane and chromatographed on silica gel. Elution with petroleum ether/ethyl acetate (20%) afforded (E)-ethyl-(2-nitro-4-thienyl)prop-2-enoate (162) (0.18 g, 62%) as a pale yellow solid identical (tlc, ir, ^{1}H nmr) to a sample prepared using method A. Also eluted was unreacted 2-nitrothiophene-4-carboxaldehyde (161) (0.04 g, 20%) as an orange solid identical (tlc and ir) to an authentic sample.

[Bis((E)-ethyl-3-(2-ammonium-4-thienyl)prop-2-enoate)]hexachlorostannate(IV) (163)

Tin powder (4.35 g, 36.6 mmol) was added portionwise at 40 ^{o}C under nitrogen to a suspension of (E)-ethyl-3-(2-nitro-4-thienyl)prop-2-enoate (162) (3.0 g, 22 mmol). Once all the tin had reacted the reaction mixture was cooled and the precipitate was filtered. The filtrate was concentrated *in vacuo* and a further crop of [bis((E)-ethyl-3-(2-ammonium-4-thienyl)prop-2-enoate)]hexachloro-stannate(IV) (163) (7.60 g, 95%) was obtained as a yellow solid; ν_{max}(KBr) /cm^{-1} 3568, 3472, 3288, 3191, 2920, 1706, 1638. No ^{1}H nmr spectrum was obtained due to decomposition in solution.

Cyclisation of [bis((E)-ethyl-3-(2-ammonium-4-thienyl)prop-2-enoate)]hexa-chlorostannate(IV) (163)

(a) Cyclisation in concentrated hydrochloric acid.

A suspension of [bis((E)-ethyl-3-(2-ammonium-4-thienyl)prop-2-enoate)]hexa-chlorostannate(IV) (163) (7.60 g, 10.4 mmol) and concentrated hydrochloric acid (27.5 ml) in ethanol (80 ml) was added under nitrogen to a suspension of

3,3-dimethoxy-2-formylpropionitrile sodium salt (155) (4.02 g, 24.2 mmol) in ethanol (30 ml). The reaction mixture was refluxed for 4 h, the solvent was removed *in vacuo*, replaced by water (400 ml) and extracted with ethyl acetate (3 x 200 ml). The combined organic extracts were dried over magnesium sulfate and the solvent removed *in vacuo* to afford a dark oil which was dissolved in dichloromethane and chromatographed on silica gel. Elution with petroleum ether/ethyl acetate (20%) afforded (E)-ethyl-3-(2-chloro-5-cyano-thieno[2,3-b]pyridin-3-yl)prop-2-enoate (164) [0.80 g, 12% from (162)] as a white solid, mp 145-147 ^{o}C (Found: C, 53.20; H, 2.90; N, 9.56; S, 10.84. $C_{13}H_9N_2O_2SCl$ requires C, 53.34; H, 3.10; N, 9.57; S, 10.95%); ν_{max}(KBr) /cm^{-1} 2234, 1731, 1636; δ_H($CDCl_3$) 1.40 (t, 3H, J=7.2 Hz, CH_3), 4.33 (q, 2H, J=7.2 Hz, CO_2CH_2), 6.65 (d, 1H, J=16 Hz, =$CHCO_2$), 7.85 (d, 1H, J=16 Hz, ArCH=), 8.48 (d, 1H, J=1.9 Hz, H-4) and 8.80 (d, 1H, J=1.9 Hz, H-6); MS m\z 293 (M+H). Further elution afforded (E)-ethyl-3-(5-cyanothieno[2,3-b]pyridin-3-yl)prop-2-enoate (153) [1.02 g, 18% from (162)] as a white solid, mp 135-136 ^{o}C (Found: C, 60.12; H, 3.98; N, 10.69; S, 12.12. $C_{13}H_{10}N_2O_2S$ requires C, 60.45; H, 3.90; N, 10.85; S, 12.41%); ν_{max}(KBr)/cm^{-1} 2238, 1716, 1639; δ_H($CDCl_3$) 1.23 (t, 3H, J=7.2 Hz, CH_3), 4.29 (q, 2H, J=7.2 Hz, CO_2CH_2), 6.49 (d, 1H, J=16 Hz, =$CHCO_2$), 7.81 (d, 1H, J=16 Hz, ArCH=), 7.93 (s, 1H, H-2), 8.52 (d, 1H, J=1.75 Hz, H-4) and 8.81 (d, 1H, J=1.75 Hz, H-6); MS m/z 259 (M+H).

(b) Cyclisation in concentrated sulfuric acid.

A suspension of [bis((E)-ethyl-3-(2-ammonium-4-thienyl)prop-2-enoate)]hexa-chlorostannate(IV) (163) (1.63 g, 2.24 mmol) and concentrated sulfuric acid (1.04 g) in ethanol (30 ml) was added under argon to a suspension of 3,3-dimethoxy-2-formylpropionitrile sodium salt (155) (0.89 g, 5.3 mmol) in ethanol (5 ml). The reaction mixture was refluxed for 22 h and solvent was removed *in*

vacuo. The residue was poured onto ice/water (300 ml), neutralised with concentrated ammonia solution and extracted with diethyl ether (3 x 100 ml). The combined ether extracts were filtered through Celite to remove any insoluble material, dried over magnesium sulfate and solvent removed *in vacuo* to afford a brown oil. The oil was dissolved in dichloromethane and chromatographed on silica gel. Elution with petroleum ether/diethyl ether (50%) afforded (E)-ethyl-3-(2-nitro-4-thienyl)prop-2-enoate (162) (0.21 g, 17%) identical (tlc, ir) to an authentic sample. Further elution afforded (E)-ethyl-3-(5-cyanothieno[2,3-b]pyridin-3-yl)prop-2-enoate (153) [0.16 g, 14% from (162)] as a white solid which was identical (tlc, ir, ^{1}H nmr) to a sample of (153) prepared in (a).

(E)-3-(2-nitro-4-thienyl)prop-2-enoic acid (165)

Sodium hydroxide solution (1 ml, 4.8M) was added dropwise to a solution of (E)-ethyl-3-(2-nitro-4-thienyl)prop-2-enoate (162) (1.0 g, 4.4 mmol) in ethanol (30 ml). The reaction mixture was stirred at room temperature under nitrogen for 8 h until tlc had indicated that no starting material remained. The ethanol was removed *in vacuo* and replaced by water (10 ml). The aqueous solution was extracted with ethyl acetate (3 x 50 ml), acidified to a pH of 4 with 2M hydrochloric acid solution, saturated with sodium chloride and extracted with THF (3 x 75 ml). The combined THF washings were dried over magnesium sulfate and the solvent removed *in vacuo* to afford a solid. The solid was recrystallised from ethanol/dichloromethane to give (E)-3-(2-nitro-4-thienyl)prop-2-enoic acid (165) (0.72 g, 82%) as a yellow solid; ν_{max}(KBr) /cm^{-1} 3110 br, 1686, 1628, 1501, 1338; δ_H(d_6 DMSO) 6.49 (d, 1H, J=16.8 Hz, =CHCO$_2$), 7.50 (d, 1H, J=16.8 Hz, ArCH=), 8.24 (s, 1H, H-3) and 8.43 (s, 1H, H-5). In spite of several attempts at recrystallisation the product was not of sufficient purity for melting point or microanalysis.

(E)-Methyl-3-(5-cyanothieno[2,3-b]pyridin-3-yl)prop-2-enoate (166)

Tin powder (1.96 g, 16 mmol) was added portionwise at 40 ^{o}C under nitrogen to a stirring suspension of (E)-3-(2-nitro-4-thienyl)prop-2-enoic acid (165) (1.03 g, 5.2 mmol) in concentrated hydrochloric acid (30 ml). Once all the tin had reacted the hydrochloric acid was removed *in vacuo* to afford a brown solid (3.43 g). A suspension of the solid and concentrated hydrochloric acid (5.5 ml) in methanol (70 ml) was added to a suspension of 3,3-dimethoxy-2-formylpropionitrile sodium salt (155) (0.89 g, 5.35 mmol) in methanol (20 ml). The reaction mixture was refluxed for 24 h, the methanol was removed *in vacuo* and replaced by water (200 ml). The aqueous mixture was extracted with ethyl acetate (3 x 100 ml), the combined extracts were dried over magnesium sulfate and the solvent removed *in vacuo* to give a yellow solid. The solid was chromatographed on silica gel. Elution with petroleum ether/ethyl acetate (20%) afforded (E)-methyl-3-(5-cyanothieno[2,3-b]pyridin-3-yl)prop-2-enoate (166) (0.12 g, 10%) as a white solid, mp 202-204 ^{o}C; ν_{max}(KBr)/cm^{-1} 2230, 1717, 1635; δ_H($CDCl_3$) 3.86 (s, 3H, CH_3), 6.54 (d, 1H, J=16 Hz, =$CHCO_2$), 7.86 (d, 1H, J=16 Hz, ArCH=), 8.05 (s, 1H, H-2), 8.56 (d, 1H, J=1.75 Hz, H-4) and 8.85 (d, 1H, J=1.75 Hz, H-6); LC-MS m/z 245.1 (M+H).

Attempted hydrogenation of (E)-ethyl-3-(2-nitro-4-thienyl)prop-2-enoate (162)

(a) Reaction with palladium on carbon and ammonium formate.

5% Palladium on carbon (0.1 g) and ammonium formate (0.2 g, 4.3 mmol) were added under nitrogen to a solution of (E)-ethyl-3-(2-nitro-4-thienyl)prop-2-enoate (162) (0.25 g, 1.1 mmol) in glacial acetic acid (5 ml). The reaction mixture was refluxed for 2 h, diethyl ether (20 ml) was added and filtered

through Celite. The organic solution was washed with water (30 ml) and 2M sodium hydroxide solution (30 ml) then dried over magnesium sulfate. The solvent was removed *in vacuo* to give a solid which was recrystallised from ethanol to afford unreacted (E)-ethyl-3-(2-nitro-4-thienyl)prop-2-enoate (162) (0.20 g, 80%) as a pale yellow solid which was identical (tlc, ^{1}H nmr, ir) to an authentic sample.

(b) Reaction with sodium borohydride and copper(I) chloride.

Sodium borohydride (0.47 g, 12.4 mmol) was added portionwise over a period of 0.5 h at ice temperature under nitrogen to a suspension of copper(I) chloride (0.24 g, 2.42 mmol) and (E)-ethyl-3-(2-nitro-4-thienyl)prop-2-enoate (162) (0.25 g, 1.1 mmol) in methanol (10 ml). Stirring was continued for a further 0.5 h, diethyl ether (50 ml) was added and the organic solution was washed with water (2 x 50 ml) then dried over magnesium sulfate. The solvent was removed *in vacuo* to afford a brown solid (0.1 g) which decomposed on exposure to the atmosphere and the ^{1}H nmr spectrum indicated that no aromatic protons were present.

<u>One step synthesis of (E)-ethyl-3-(5-cyanothieno[2,3-b]pyridin-3-yl)prop-2-enoate (153)</u>

Tin(II) chloride.2H_2O (0.74 g, 3.3 mmol) was added portionwise at 40 ^{o}C under nitrogen to a solution of (E)-ethyl-3-(2-nitro-4-thienyl)prop-2-enoate (162) (0.15 g, 0.66 mmol) in ethanol (10 ml). Heating at 40 ^{o}C was continued until tlc indicated that no starting material remained. A suspension of 3,3-dimethoxy-2-formylpropionitrile sodium salt (155) (0.12 g, 0.72 mmol) and concentrated hydrochloric acid (0.7 ml) in ethanol (10 ml) was then added and the reaction mixture was refluxed for 48 h. The ethanol was removed *in vacuo* and replaced

by water (100 ml). The aqueous solution was extracted with ethyl acetate (3 x 100 ml), the combined organic extracts were dried over magnesium sulfate and the solvent removed *in vacuo* to give an oil. The oil was chromatographed on silica gel using a gradient elution with petroleum ether/ethyl acetate (0-50%) to afford (E)-ethyl-3-(5-cyanothieno[2,3-b]pyridin-3-yl)prop-2-enoate (153) (0.005 g, 3%) identical (tlc, ^{1}H nmr) to an authentic sample of (153).

Attempted hydrogenation of (E)-ethyl-3-(5-cyanothieno[2,3-b]pyridin-3-yl)prop-2-enoate (153)

(a) Catalytic hydrogenation.

A suspension of (E)-ethyl-3-(5-cyanothieno[2,3-b]pyridin-3-yl)prop-2-enoate (153) (0.09 g, 0.35 mmol) and 10% palladium on carbon (0.02 g) in dry ethanol (20 ml) was stirred under hydrogen gas at atmospheric pressure for 1.5 h. The hydrogen gas source was removed and the reaction flask was purged with argon. The reaction mixture was filtered through Celite, the ethanol was removed *in vacuo* and the crude solid was recrystallised from ethanol to afford unreacted (E)-ethyl-3-(5-cyanothieno[2,3-b]pyridin-3-yl)prop-2-enoate (153) (0.08 g, 89%) identical (tlc, ^{1}H nmr, ir) to an authentic sample.

(b) Reaction with sodium borohydride and copper(I) chloride.

Sodium borohydride (0.37 g, 9.7 mmol) was added portionwise over a period of 0.5 h at ice temperature under nitrogen to a suspension of copper(I) chloride (0.14 g, 1.4 mmol) and (E)-ethyl-3-(5-cyanothieno[2,3-b]pyridin-3-yl)prop-2-enoate (153) (0.25 g, 0.97 mmol) in methanol (20 ml). Stirring was continued for a further 1 h then ethyl acetate (100 ml) was added. The organic solution was washed with water (50 ml) and brine (50 ml), dried over magnesium sulfate

and the solvent removed *in vacuo* to give a brown solid which was dissolved in a little dichloromethane and chromatographed on silica gel. Elution with petroleum ether/ethyl acetate (20%) afforded ethyl-3-(5-cyanothieno[2,3-b]pyridin-3-yl)propanoate (167) (0.14 g, 55%) as a white solid, mp 102-103 ^{o}C (Found: C, 59.96; H, 4.80; N, 10.46; S, 12.17. $C_{13}H_{12}N_2O_2S$ requires C, 59.98; H, 4.65; N, 10.76; S, 12.32%); ν_{max}(KBr)/cm^{-1} 3055, 2235, 1736; δ_H($CDCl_3$) 1.25 (t, 3H, J=7.2 Hz, CH_3), 2.77 (t, 2H, J=7.2 Hz, CH_2CO_2), 3.20 (t, 2H, J=7.2 Hz, $ArCH_2$), 4.15 (q, 2H, J=7.2 Hz, CO_2CH_2), 7.40 (s, 1H, H-2), 8.33 (d, 1H, J=1.92 Hz, H-4) and 8.80 (d, 1H, J=1.92 Hz, H-6); MS m/z 261 (M+H); LC-MS m/z 261.1 (M+H).

(c) Reaction with palladium on carbon and ammonium formate.

10% Palladium on carbon (0.13 g) and ammonium formate (0.13 g, 2.4 mmol) were added under nitrogen to a solution of (E)-ethyl-3-(5-cyanothieno[2,3-b] pyridin-3-yl)prop-2-enoate (153) (0.2 g, 0.77 mmol) in glacial acetic acid (5 ml). The reaction mixture was refluxed for 2 h, diethyl ether (100 ml) was added and filtered through Celite. The organic solution was washed with water (50 ml) and 2M sodium hydroxide solution (50 ml) then dried over magnesium sulfate. The solvent was removed *in vacuo* to give a yellow solid. The solid was chromatographed on silica gel. Elution with petroleum ether/diethyl ether (50%) afforded ethyl-3-(5-cyanothieno[2,3-b]pyridin-3-yl)propanoate (167) (0.06 g, 30%) as a white solid identical (tlc, ^{1}H nmr, ir) to an authentic sample obtained from method (b) above.

Attempted reaction of 3-carbomethoxy-5-cyanothieno[2,3-b]pyridine (159) with sodium iodide and chlorotrimethylsilane

Sodium iodide (0.27 g, 1.8 mmol) and chlorotrimethylsilane (0.33 g, 3 mmol) were added to a solution of 3-carbomethoxy-5-cyanothieno[2,3-b]pyridine (159) (0.20 g, 0.9 mmol) in dry acetonitrile (20 ml). The reaction mixture was refluxed for 48 h then poured onto ice/water (50 ml) and extracted with diethyl ether (3 x 100 ml). The combined ether extracts were dried over magnesium sulfate and the solvent was removed *in vacuo* to afford unreacted 3-carbomethoxy-5-cyanothieno[2,3-b]pyridine (159) (0.12 g, 60%) as a yellow solid identical (tlc, ^{1}H nmr) to an authentic sample.

5-cyanothieno[2,3-b]pyridine-3-carboxylic acid (168)

3-Carbomethoxy-5-cyanothieno[2,3-b]pyridine (159) (0.69 g, 3.16 mmol) and 2M sodium hydroxide solution (2 ml) in methanol (30 ml) was stirred at room temperature under nitrogen for 24 h until tlc showed no starting material remained. The methanol was removed *in vacuo* and the residue was dissolved in water (30 ml). 2M Hydrochloric acid solution was added dropwise and the white precipitate was filtered to afford 5-cyanothieno[2,3-b]pyridine-3-carboxylic acid (168) (0.47 g, 68%) as a white solid, mp >250 ^{o}C; ν_{max}(KBr) /cm^{-1} 3127, 3079, 2922, 2578, 2235, 1706; δ_H(d_6 DMSO) 8.90 (s, 1H, H-2) and 9.05 (m, 2H, H-4 & H-6); LC-MS m/z 203 (M-1), 159 (M-CO_2H). A suitable sample for microanalysis could not be prepared due to solubility problems however LC-MS indicated the presence of a single pure product.

Reaction of 5-cyanothieno[2,3-b]pyridine-3-carboxylic acid (168) with diphenyl-phosphorylazide

A solution of 5-cyanothieno[2,3-b]pyridine-3-carboxylic acid (168) (0.08 g, 0.39 mmol), diphenylphosphorylazide (0.22 g, 0.78 mmol) and triethylamine (0.08 g, 0.78 mmol) in dry *t*-butanol was refluxed under nitrogen for 18 h. The reaction mixture was cooled and the *t*-butanol was removed *in vacuo*. The residue was dissolved in ethyl acetate (50 ml) and washed with saturated sodium hydrogen carbonate solution (50 ml) and brine (50 ml). The organic phase was dried over magnesium sulfate and the solvent removed *in vacuo* to afford a yellow oil (0.006 g) which tlc indicated to be a complex mixture of components. The aqueous washings were acidified with 2M hydrochloric acid and extracted with ethyl acetate (3 x 50 ml). The combined extracts were dried over magnesium sulfate and the solvent removed *in vacuo* to afford a solid (0.08 g) which ^{1}H nmr indicated to consist mainly of unreacted 5-cyanothieno[2,3-b]pyridine-3-carboxylic acid (168).

3-Azidocarbonyl-5-cyanothieno[2,3-b]pyridine (169)

Ethyl chloroformate (0.27 g, 2.49 mmol) was added dropwise under argon to a stirred solution of 5-cyanothieno[2,3-b]pyridine-3-carboxylic acid (168) (0.39 g, 1.91 mmol) and triethylamine (0.23 g, 2.27 mmol) in acetone (20 ml) at ice temperature. The reaction mixture was stirred for 3 h then a solution of sodium azide (0.21 g, 3.23 mmol) in water (2 ml) was added. Stirring was continued for a further 2.5 h then the mixture was poured onto ice/water (20 ml) and extracted with dichloromethane (3 x 50 ml). The combined organic extracts were dried over magnesium sulfate and the solvent removed *in vacuo* to afford a solid which was chromatographed on silica gel. Elution with petroleum ether/ethyl acetate (20%) afforded 3-azidocarbonyl-5-cyanothieno[2,3-b]pyridine (169)

(0.44 g, 100%) as a white solid, mp 137-138 °C d (Found: C, 46.96; H, 1.29; N, 29.65; S, 13.76. $C_9H_3N_5OS$ requires C, 47.16; H, 1.32; N, 30.55; S, 13.99%); ν_{max}(KBr)/cm^{-1} 2232, 2181, 1694; δ_H($CDCl_3$) 8.65 (s, 1H, H-2), 8.84 (d, 1H, J=1.95 Hz, H-4) and 9.18 (d, 1H, J=1.95 Hz, H-6).

3-[(*t*-Butoxycarbonyl)amino]-5-cyanothieno[2,3-b]pyridine (170)

3-Azidocarbonyl-5-cyanothieno[2,3-b]pyridine (169) (0.28 g, 1.22 mmol) was refluxed in dry *t*-butanol for 10 h under nitrogen until tlc indicated no starting material remained. The solvent was removed *in vacuo* to afford a brown solid which was dissolved in a little dichloromethane and chromatographed on silica gel. Elution with petroleum ether/ethyl acetate (20%) afforded 3-[(*t*-butoxycarbonyl)amino]-5-cyanothieno[2,3-b]pyridine (170) (0.23 g, 68%) as a white solid, mp 199-201 °C d (Found: C, 56.64; H, 4.66; N, 15.15; S, 11.51. $C_{13}H_{13}N_3O_2S$ requires C, 56.71; H, 4.76; N, 15.26; S, 11.65%); ν_{max}(KBr) /cm^{-1} 3276, 3174, 2231, 1689, 1563; δ_H($CDCl_3$) 1.61 (s, 9H, 3 x CH_3), 6.83 (s, 1H, NH), 7.75 (s br, 1H, H-2), 8.26 (s br, 1H, H-4) and 8.80 (d, 1H, J=1.85 Hz, H-6); MS m/z 276 (M+H).

3-[(*t*-Butoxycarbonyl)amino]-5-carboxamidothieno[2,3-b]pyridine (171)

3-[(*t*-Butoxycarbonyl)amino]-5-cyanothieno[2,3-b]pyridine (170) (0.1 g, 0.36 mmol), concentrated ammonia solution (1 ml, sg 0.88) and 30% hydrogen peroxide solution (0.07 g) were stirred in ethanol (20 ml) at room temperature under nitrogen for 24 h. The solvent was removed *in vacuo* to afford a solid which was recrystallised from methanol/water to afford 3-[(*t*-butoxycarbonyl)amino]-5-carboxamido-thieno[2,3-b]pyridine (171) (0.11 g, 100%) as a white solid, mp 206-207 °C; ν_{max}(KBr)/cm^{-1} 3418, 3211, 3060, 2984, 1668; δ_H(d_6 acetone) 1.52 (s, 9H, 3 x CH_3), 5.62 (s, 1H, NH-CO_2), 7.82

(s br, 1H, H-2), 9.01 (s br, 1H, H-4) and 9.08 (d, 1H, J=1.85 Hz, H-6); MS m/z 294 (M+H); LC-MS 294.2 (M+H).

Reaction of 3-carbomethoxy-2-chloro-5-cyanothieno[2,3-b]pyridine (158) with guanidine hydrochloride

3-Carbomethoxy-2-chloro-5-cyanothieno[2,3-b]pyridine (158) (0.03 g, 0.118 mmol), guanidine hydrochloride (0.012 g, 0.13 mmol) and sodium hydride (0.006 g, 0.26 mmol) were refluxed in DMF (2 ml) under nitrogen for 4 h. The reaction mixture was poured onto ice/water (40 ml) and extracted with ethyl acetate (3 x 50 ml). The combined organic extracts were dried over magnesium sulfate and the solvent removed *in vacuo* to give a solid (0.02 g) which was identical (tlc, ^{1}H nmr) to unreacted 3-carbomethoxy-2-chloro-5-cyanothieno[2,3-b]pyridine (158).

Hydrolysis of ethyl-3-(5-cyanothieno[2,3-b]pyridin-3-yl)propanoate (167)

2M Sodium hydroxide solution (2 ml) was added dropwise to a solution of ethyl-3-(5-cyanothieno[2,3-b]pyridin-3-yl)propanoate (167) (0.53 g, 2.03 mmol) in ethanol (20 ml) under nitrogen. The reaction mixture was stirred at room temperature for 24 h until tlc had indicated that no starting material remained. The ethanol was removed *in vacuo* and replaced by water (50 ml). The aqueous solution was acidified with 2M hydrochloric acid and the precipitated solid (0.5 g) was filtered. Any attempts to purify the solid failed due to poor solubility in all common solvents; ν_{max}(KBr)/cm^{-1} 3439-2586 br, 2232, 1717. No ^{1}H nmr spectrum was obtained due to the solubility problems and the product was assumed to be crude 3-(5-cyanothieno[2,3-b]pyridin-3-yl)propanoic acid (173).

Reaction of 3-(5-cyanothieno[2,3-b]pyridin-3-yl)propanoic acid (173) with triethylamine, ethyl chloroformate and sodium azide

Ethyl chloroformate (0.27 g, 2.49 mmol) was added dropwise under nitrogen to a stirred solution of crude 3-(5-cyanothieno[2,3-b]pyridin-3-yl)propanoic acid (173) (0.29 g, 1.25 mmol) and triethylamine (0.25 g, 2.47 mmol) in acetone (20 ml) at room temperature. The reaction mixture was stirred at room temperature for 2 h then a solution of sodium azide (0.16 g, 2.49 mmol) in water (1 ml) was added and stirring continued for a further 2 h. Dichloromethane (20 ml) was added and any insoluble solids were removed by filtration. The filtrate was washed with water (2 x 30 ml), dried over magnesium sulfate and the solvent removed *in vacuo* to give a solid. Chromatography on silica gel eluting with petroleum ether/ethyl acetate (20%) afforded a white solid (0.12 g, 37%) which was identical (tlc, ^{1}H nmr) to an authentic sample of ethyl-3-(5-cyanothieno[2,3-b]pyridin-3-yl)propanoate (167).

Attempted Curtius rearrangement of 3-(5-cyanothieno[2,3-b]pyridin-3-yl)propanoic acid (173) without characterising the intermediate

Ethyl chloroformate (0.34 g, 3.2 mmol) was added under nitrogen to a solution of 3-(5-cyanothieno[2,3-b]pyridin-3-yl)propanoic acid (173) (0.37 g, 1.6 mmol) and triethylamine (0.32 g, 3.2 mmol) in acetone (30 ml) at room temperature. The reaction mixture was stirred for 2 h then a solution of sodium azide (0.17 g, 2.7 mmol) in water (1 ml) was added and stirring continued for a further 2 h. Dichloromethane (50 ml) was added and any insoluble solids were removed by filtration. The filtrate was washed with water (2 x 30 ml), dried over magnesium sulfate and the solvent removed *in vacuo* to afford a brown solid. The solid, without further purification, was refluxed under nitrogen in dry *t*-butanol (20 ml) for 2 h. The *t*-butanol was removed *in vacuo* and replaced by a mixture of *o*-

xylene (15 ml) and *t*-butanol (5 ml) and reflux was continued for a further 17 h. Solvents were removed *in vacuo* to afford an oil which tlc indicated to be a complex mixture of products. The oil was dissolved in dichloromethane and chromatographed on silica gel. Elution with petroleum ether/ethyl acetate (10%) afforded a brown solid (0.028 g) which ^{1}H nmr indicated was mainly ethyl-3-(5-cyanothieno[2,3-b]pyridin-3-yl)propanoate (167).

Attempted reaction of 3-(5-cyanothieno[2,3-b]pyridin-3-yl)propanoic acid (173) with thionyl chloride and sodium azide

3-(5-Cyanothieno[2,3-b]pyridin-3-yl)propanoic acid (173) (0.35 g, 1.53 mmol) and thionyl chloride (50 ml) were refluxed under nitrogen for 24 h. The thionyl chloride was evaporated *in vacuo* and replaced by acetone (20 ml). Sodium azide (0.1 g, 1.53 mmol) was added and the reaction mixture was stirred at room temperature under nitrogen for 5 h. The acetone was removed *in vacuo* and the crude solid was dissolved in dichloromethane (100 ml), washed with water (50 ml) and brine (50 ml). The organic phase was dried over magnesium sulfate and the dichloromethane was removed *in vacuo* to afford a solid which was chromatographed on silica gel. Elution with petroleum ether/ethyl acetate (10%) afforded two compounds but the infrared spectra of both showed no peaks indicative of a nitrile group.

Reaction of 3-(5-cyanothieno[2,3-b]pyridin-3-yl)propanoic acid (173) with diphenylphosphoryl azide

A solution of 3-(5-cyanothieno[2,3-b]pyridin-3-yl)propanoic acid (173) (0.1 g, 0.43 mmol) and triethylamine (0.09 g, 0.9 mmol) in *t*-butanol (6 ml) was heated at 50 ^{o}C for 1 h under nitrogen. Diphenylphosphoryl azide (0.13 g, 0.47 mmol) was added and the reaction mixture was refluxed for 18 h, cooled to room

temperature and stirred for a further 24 h. Saturated sodium hydrogen carbonate solution (50 ml) was added and the mixture was extracted with ethyl acetate (3 x 50 ml). The combined organic extracts were dried over magnesium sulfate and the solvent removed *in vacuo* to afford a viscous oil. The oil was dissolved in dichloromethane and chromatographed on silica gel using a gradient elution with petroleum ether/ethyl acetate (0-40%) to afford a brown oil (0.01 g). ^{1}H nmr indicated that no thieno[2,3-b]pyridine was present.

Attempted synthesis of 3-(2-chloroethyl)-5-cyanothieno[2,3-b]pyridine (175)

Lead tetraacetate (0.19 g, 0.44 mmol) and lithium chloride (0.018 g, 0.44 mmol) were added at room temperature under argon to a suspension of 3-(5-cyanothieno[2,3-b]pyridin-3-yl)propanoic acid (173) (0.3 g, 1.29 mmol) in dry toluene (4 ml). The reaction mixture was heated at 80 ^{o}C for 3 h, diethyl ether (50 ml) was then added and the solution was washed with saturated sodium hydrogen carbonate solution (2 x 50 ml). The ether solution was then dried over magnesium sulfate and the solvent removed *in vacuo* to afford a solid (0.015 g). The ^{1}H nmr spectrum indicated a mixture of products thus the reaction was taken no further. The aqueous washings were acidified with 6M hydrochloric acid and extracted with ethyl acetate (2 x 200 ml), the organic extracts were dried over magnesium sulfate and the solvent removed *in vacuo* to afford a solid (0.08 g) which ir indicated to be unreacted crude (173).

Attempted Hofmann rearrangement

A solution of ethyl-3-(5-cyanothieno[2,3-b]pyridin-3-yl)propanoate (167) (0.1 g, 0.38 mmol), sodium cyanide (2 mg), concentrated ammonia solution (25 ml, sg 0.88) and ethanol (25 ml) was refluxed for 24 h until tlc indicated that no starting material remained. The solvent was removed *in vacuo*, replaced by brine (20

ml) and the reaction mixture was extracted with THF (3 x 50 ml). The combined organic extracts were dried over magnesium sulfate and the solvent removed *in vacuo* to afford an oil (0.14 g). The infrared spectrum of the crude product indicated the presence of a nitrile and amide; ν_{max}/cm^{-1} 2238, 1684.

Bromine (0.015 ml) was added at ice temperature to a solution of sodium hydroxide (0.06 g, 1.4 mmol) in water (2 ml). This mixture was then added to the crude amide prepared above (0.14 g) and the reaction mixture was heated at 90 ^{o}C for 3 h. Brine was added and the aqueous phase was extracted with THF (4 x 10 ml), the THF extracts were dried over magnesium sulfate and the THF was removed *in vacuo* and replaced with dry diethyl ether (10 ml). Dry hydrogen chloride gas was bubbled through the ether solution which afforded a solid which darkened on exposure to air. The ^{1}H nmr spectrum of the solid indicated that no thieno[2,3-b]pyridine was present.

(E)-1-[(*t*-butoxycarbonyl)amino]-2-(2-nitro-4-thienyl)ethene (176)

Ethyl chloroformate (0.25 g, 2.34 mmol) was added under nitrogen at ice temperature to a solution of (E)-3-(2-nitro-4-thienyl)prop-2-enoic acid (165) (0.39 g, 1.95 mmol) and triethylamine (0.23 g, 2.34 mmol) in acetone (30 ml). The reaction mixture was stirred for 1 h then sodium azide (0.21 g, 3.3 mmol) was added and stirring was continued for a further 1 h. Water (100 ml) was added and the reaction mixture was extracted with diethyl ether (3 x 50 ml), the combined extracts were dried over magnesium sulfate and the solvent removed *in vacuo* to afford a pale yellow solid (0.15 g); $\nu_{max}(KBr)/cm^{-1}$ 3102, 2144, 1684, 1498, 1347. The solid was refluxed in dry *t*-butanol under nitrogen for 4 h. The solvent was then removed *in vacuo* to give an orange solid which was chromatographed on silica gel. Elution with petroleum ether/ethyl acetate (20%) afforded (E)-1-[(*t*-butoxycarbonyl)amino]-2-(2-nitro-4-thienyl)ethene (176)

(0.15 g, 28%) as an orange solid, mp 144-146 °C; ν_{max}(KBr)/cm^{-1} 3354, 3083, 1700, 1654, 1499, 1326; δ_H($CDCl_3$) 1.25 (s, 9H, 3 x CH_3), 5.82 (d, 1H, J=14.6 Hz, ArCH=), 6.61 (d, 1H, J=14.6 Hz, =CH-N), 7.11 (d, 1H, J=1.7 Hz, H-3) and 7.86 (d, 1H, J=1.7 Hz, H-5); MS m/z 269 (M-1).

Attempted cyclisation of (E)-1-[(*t*-butoxycarbonyl)amino]-2-(2-nitro-4-thienyl) ethene (176)

Tin powder (0.12 g, 1.0 mmol) was added portionwise over 0.5 h to a suspension of (E)-1-[(*t*-butoxycarbonyl)amino]-2-(2-nitro-4-thienyl)ethene (176) (0.15 g, 0.55 mmol) in concentrated hydrochloric acid (5 ml) at 40 °C under nitrogen. The reaction mixture was stirred until no unreacted tin remained. 3,3-Dimethoxy-2-formylpropionitrile sodium salt (155) (0.11 g, 0.66 mmol) and ethanol (50 ml) were then added and the reaction mixture was refluxed for 16 h. The solvent was removed *in vacuo* and replaced by water (50 ml). Concentrated ammonia solution was added to neutralise the acid and the aqueous mixture was extracted with ethyl acetate (3 x 100 ml). The combined extracts were dried over magnesium sulfate and the solvent was removed *in vacuo* to afford a brown solid (0.14 g) which tlc indicated to be a complex mixture of products which were inseparable by column chromatography.

6 REFERENCES

1 Rapport MM, Green AA, Page IH *Science* 1948, **108**, 329-330.

2 Rapport MM *J. Biol. Chem.* 1949, **180**, 961-969.

3 Erspamer V, Ghiretti F *J. Physiol.* 1951, **115**, 470-481.

4 Erspamer V *Pharmacol. Rev.* 1954, **6**, 425-487.

5 Erspamer V, Asero B *Nature* 1952, **169**, 800-801.

6 Hamlin KE, Fischer FE *J. Am. Chem. Soc.* 1951, **73**, 5007-5008.

7 Twarog BM, Page IH *Am. J. Physiol.* 1953, **175**, 157-161.

8 Welsh JH *Federation Proc.* 1954, **13**, 162-163.

9 Dourish CT *Obesity Research* 1995, **3**, Suppl 4, 449S-462S.

10 Saxena PR *In Migraine a Spectrum of Ideas,* Ed Sandler M, Collins G, Oxford University Press 1990, 182-190.

11 Barrett JE, Vanover KE *Psychopharmacology* 1993, **112**, 1-12.

12 Ohuoha DC, Hyde TM, Kleinman JE *Psychopharmacology* 1993, **112**, S5-S15.

13 Leonard BE *Int. Clinical Psychopharmacology* 1994, **9**, Suppl 1 , 7-17.

14 Gaddum JH, Picarelli ZP *Br. J. Pharmacol.* 1957, **12**, 323-328.

15 Peroutka SJ, Snyder SH *Mol. Pharmacol.* 1979, **16**, 687-699.

16 Julius D *Annu. Rev. Neurosci.* 1991, **14**, 335-360.

17 Hartig PR, Adham N, Zgombick J, Weinshank R, Branchek T *Drug Dev. Res.* 1992, **26**, 215-224.

18 Shih JC, Yang W, Chen K, Gallaher T *Pharmacol. Biochem. Behavior* 1991, **40**, 1053-1058.

19 Peroutka SJ *Synapse* 1994, **18**, 241-260.

20 Boess FG, Martin IL *Neuropharmacology* 1994, **33**, 275-317.

21 Teitler M, Herrick-Davis K *Critical Rev. Neurobiol.* 1994, **8**, 175-188.

22 Peroutka SJ *Annu. Rev. Neurosci.* 1988, **11**, 45-60.

23 Hibert MF, Mir AK, Fozard JR *In Comprehensive Medicinal Chemistry* Ed Emmett JC, Pergamon Press 1990, **3**, 567-600.

24 Zifa E, Fillion G, *Pharmacol. Rev.* 1992, **44**, 401-458.

25 Saxena PR *Pharmac. Ther.* 1995, **66**, 339-368.

26 Hoyer D, Clarke DE, Fozard JR, Hartig PR, Martin GR, Mylecharane EJ, Saxena PR, Humphrey PPA *Pharmacol. Rev.* 1994, **46**, 157-203.

27 Weinshank RL, Zgombick JM, Macchi MJ, Branchek TA, Hartig PR *Proc. Natl. Acad. Sci. USA* 1992, **89**, 3630-3634.

28 Adham N, Romanienko P, Hartig P, Weinshank RL, Branchek T *Mol. Pharmacol.* 1992, **41**, 1-7.

29 Hoyer D, Martin GR *Behavioural Brain Res.* 1996, **73**, 263-268.

30 Hartig PR, Hoyer D, Humphrey PPA, Martin GR *TiPS* 1996, **17**, 103-105.

31 Kimball RW, Friedman AP, Vallejo E *Neurology* 1960, **10**, 107-111.

32 Anthony M, Lance JW *Arch. Neurol.* 1967, **16**, 544-552.

33 Lance JW *Eur. Neurol.* 1991, **31**, 279-281.

34 Silberstein SD *Headache* 1994, **34**, 408-417.

35 Fozard JR, Gray JA *TiPS* 1989, **10**, 307-309.

36 Callaham M, Raskin N *Headache* 1986, **26**, 168-171.

37 Humphrey PPA, Feniuk W, Perren MJ, Oxford AW, Coates IH, Butina D, Brittain RT, Jack D *Br. J. Pharmacol.* 1987, **92**, 616P.

38 Humphrey PPA, Feniuk W, Perren MJ, Connor HE, Oxford AW, Coates IH, Butina D *Br. J. Pharmacol.* 1988, **94**, 1123-1132.

39 Oxford AW *Contemporary Organic Synthesis* 1995, **2**, 35-41.

40 Doenicke A, Brand J, Perrin VL *The Lancet* 1988, **1**, 1309-1311.

41 Peroutka SJ, McCarthy BG *Eur. J. Pharmacol.* 1989, **163**, 133-136.

42 McCarthy BG, Peroutka SJ *Headache* 1989, **29**, 420-422.

43 Perren MJ, Feniuk W, Humphrey PPA *Br. J. Pharmacol.* 1991, **102**, 191-197.

44 Miller KJ, King A, Demchyshyn L, Niznik H, Teitler M *Eur. J. Pharmacol. (Mol. Pharmacol. Sect.)* 1992, **227**, 99-102.

45 Demchyshyn L, Sunahara RK, Miller K, Teitler M, Hoffman BJ, Kennedy JL, Seeman P, Van Tol HHM, Niznik HB *Proc. Natl. Acad. Sci. USA* 1992, **89**, 5522-5526.

46 Cushing DJ, Baez M, Kursar JD, Schenck K, Cohen ML *Life Sciences* 1994, **54**, 1671-1680.

47 Humphrey PPA, Feniuk W *TiPS* 1991, **12**, 444-446.

48 Humphrey PPA, Goadsby PJ *Cephalalgia* 1994, **14**, 401-410.

49 Moskowitz MA, Cutrer FM *Annu. Rev. Med.* 1993, **44**, 145-154.

50 Peroutka SJ *Neurology* 1993, **43** (Suppl 3), S34-S38.

51 Rebeck GW, Maynard KI, Hyman BT, Moskowitz MA *Proc. Natl. Acad. Sci. USA* 1994, **91**, 3666-3669.

52 Hamel E, Fan E, Linville D, Ting V, Villemure J-G, Chia L-S *Mol. Pharmacol.* 1993, **44**, 242-246.

53 Glen RC, Martin GR, Hill AP, Hyde RM, Woollard PM, Salmon JA, Buckingham J, Robertson AD *J. Med. Chem.* 1995, **38**, 3566-3580.

54 Goadsby PJ, Edvinsson L *Headache* 1994, **34**, 394-399.

55 Ferrari MD, Saxena PR *Eur. J. Neurology* 1995, **2**, 5-21.

56 Beer MS, Stanton JA, Bevan Y, Heald A, Reeve AJ, Street LJ, Matassa VG, Hargreaves RJ, Middlemiss DN *Br. J. Pharmacol.* 1993, **110**, 1196-1200.

57 Street LJ, Baker R, Castro JL, Chambers MS, Guiblin AR, Hobbs SC, Matassa VG, Reeve AJ, Beer MS, Middlemiss DN, Noble AJ, Stanton AJ, Scholey K, Hargreaves RJ *J. Med. Chem.* 1993, **36**, 1529-1538.

58 Chen C-y, Lieberman DR, Larsen RD, Reamer RA, Verhoeven TR, Reider PJ *Tet. Lett.* 1994, **35**, 6981-6984.

59 *Drugs of the Future* 1995, **20**, 676-679.

60 King FD, Brown AM, Gaster LM, Kaumann AJ, Medhurst AD, Parker SG, Parsons AA, Patch TL, Raval P *J. Med. Chem.* 1993, **36**, 1918-1919.

61 Macor JE, Blank DH, Post RJ, Ryan K *Tet. Lett.* 1992, **33**, 8011-8014.

62 Macor JE, Blank DH, Fox CB, Lebel LA, Newman ME, Post RJ, Ryan K, Schmidt AW, Schulz DW, Koe BK *J. Med. Chem.* 1994, **37**, 2509-2512.

63 Perez M, Fourrier C, Sigogneau I, Pauwels PJ, Palmier C, John GW, Valentin J-P, Halazy S *J. Med. Chem.* 1995, **38**, 3602-3607.

64 Perez M, Pauwels P, Palmier C, John GW, Valentin J-P, Halazy S *Bioorg. Med. Chem. Lett.* 1995, **5**, 663-666.

65 Glennon RA, Ismaiel AM, Chaurasia C, Teitler M *Drug Dev. Res.* 1991, **22**, 25-36.

66 Glennon RA, Hong S-S, Dukat M, Teitler M, Davis K *J. Med. Chem.* 1994, **37**, 2828-2830.

67 Hong S-S, Dukat M, Teitler M, Herrick-Davis K, McCallum K, Kamboj R, Glennon RA *Med. Chem. Res.* 1995, **5**, 690-699.

68 Glennon RA, Hong S-S, Bondarev M, Law H, Dukat M, Rakhit S, Power P, Fan E, Kinneau D, Kamboj R, Teitler M, Herrick-Davis K, Smith C *J. Med. Chem.* 1996, **39**, 314-322.

69 Neer EJ *Cell* 1995, **80**, 249-257.

70 Rens-Domiano S, Hamm HE *Faseb J.* 1995, **9**, 1059-1066.

71 Noel JP, Hamm HE, Sigler P *Nature* 1993, **366**, 654-663.

72 Lambright DG, Sondek J, Bohm A, Skiba NP, Hamm HE, Sigler PB *Nature* 1996, **379**, 311-319.

73 Sondek J, Bohm A, Lambright DG, Hamm HE, Sigler PB *Nature* 1996, **379**, 369-374.

74 Ovchinnikov YuA, Abdulaev NG, Feigina MYu, Artamonov ID, Zolotarev AS, Kostina MB, Bogachuk AS, Moroshnikov AI, Martinov VI, Kudelin AB *Bioorg. Khim.* 1982, **8**, 1011-1014.

75 Nathans J, Hogness DS *Proc. Natl. Acad. Sci. USA* 1984, **81**, 4851-4855.

76 Dratz EA, Hargrave PA *TiBS* 1983, **8**, 128-131.

77 Findlay JBC, Pappin DJC *Biochem. J.* 1986, **238**, 625-642.

78 Applebury ML, Hargrave PA *Vision Res.* 1986, **26**, 1881-1895.

79 Hargrave PA, McDowell JH, Curtis DR, Wang JK, Juszczak E, Fong S-L, Rao JKM, Argos P *Biophys. Struct. Mech.* 1983, **9**, 235-244.

80 Henderson R, Unwin PNT *Nature* 1975, **257**, 28-32.

81 Pappin DJC, Eliopoulos E, Brett M, Findlay JBC *Int. J. Biol. Macromol.* 1984, **6**, 73-76.

82 Engelman DM, Henderson R, McLachlan AD, Wallace BA *Proc. Natl. Acad. Sci. USA* 1980, **77**, 2023-2027.

83 Dixon RAF, Kobilka BK, Strader DJ, Benovic JL, Dohlman HG, Frielle T, Bolanowski MA, Bennett CD, Rands E, Diehl RE, Mumford RA, Slater EE, Sigal IS, Caron MG, Lefkowitz RJ, Strader CD *Nature* 1986, **321**, 75-79.

84 Dixon RAF, Sigal IS, Rands E, Register RB, Candelore MR, Blake AD, Strader CD *Nature* 1987, **326**, 73-77.

85 Strader CD, Sigal IS, Register RB, Candelore MR, Rands E, Dixon RAF *Proc. Natl. Acad. Sci. USA* 1987, **84**, 4384-4388.

86 Dohlman HG, Bouvier M, Benovic JL, Caron MG, Lefkowitz RJ *J. Biol. Chem.* 1987, **262**, 14282-14288.

87 Dixon RAF, Sigal IS, Candelore MR, Register RB, Scattergood W, Rands E, Strader CD *EMBO J.* 1987, **6**, 3269-3275.

88 Dohlman HG, Caron MG, Lefkowitz RJ *Biochemistry* 1987, **26**, 2657-2664.

89 Strader CD, Dixon RAF, Cheung AH, Candelore MR, Blake AD, Sigal IS *J. Biol. Chem.* 1987, **262**, 16439-16443.

90 Lefkowitz RJ, Caron MG *J. Biol. Chem.* 1988, **263**, 4993-4996.

91 Strader CD, Sigal IS, Candelore MR, Rands E, Hill WS, Dixon RAF *J. Biol. Chem.* 1988, **263**, 10267-10271.

92 Frielle T, Daniel KW, Caron MG, Lefkowitz RJ *Proc. Natl. Acad. Sci. USA* 1988, **85**, 9494-9498.

93 Wang H-y, Lipfert L, Malbon CC, Bahouth S *J. Biol. Chem.* 1989, **264**, 14424-14431.

94 Strader CD, Candelore MR, Hill WS, Sigal IS, Dixon RAF *J. Biol. Chem.* 1989, **264**, 13572-13578.

95 Dohlman HG, Caron MG, DeBlasi A, Frielle T, Lefkowitz RJ *Biochemistry* 1990, **29**, 2335-2342.

96 Strader CD, Sigal IS, Dixon RAF *Faseb J.* 1989, **3**, 1825-1832.

97 Ostrowski J, Kjelsberg MA, Caron MG, Lefkowitz RJ *Annu. Rev. Pharmacol. Toxicol.* 1992, **32**, 167-183.

98 Kobilka B *Annu. Rev. Neurosci.* 1992, **15**, 87-114.

99 Dixon RAF, Strader CD, Sigal IS *Annu. Rep. Med. Chem.* 1988, **23**, 221-233.

100 Jackson T *Pharmac. Ther.* 1991, **50**, 425-442.

101 Savarese TM, Fraser CM *Biochem. J.* 1992, **283**, 1-19.

102 Kobilka BK, Frielle T, Collins S, Yang-Feng T, Kobilka TS, Francke U, Lefkowitz RJ, Caron MG *Nature* 1987, **329**, 75-79.

103 Fargin A, Raymond JR, Lohse MJ, Kobilka BK, Caron MG, Lefkowitz RJ *Nature* 1988, **335**, 358-360.

104 Ho BY, Karschin A, Branchek T, Davidson N, Lester HA *FEBS Lett.* 1992, **312**, 259-262.

105 Wang CD, Gallaher TK, Shih JC *Mol. Pharmacol.* 1993, **43**, 931-940.

106 Kao H-T, Adham N, Olsen MA, Weinshank RL, Branchek TA, Hartig PR *FEBS Lett.* 1992, **307**, 324-328.

107 Johnson MP, Loncharich RJ, Baez M, Nelson DL *Mol. Pharmacol.* 1994, **45**, 277-286.

108 Choudhary MS, Craigo S, Roth BL *Mol. Pharmacol.* 1993, **43**, 755-761.

109 Guan X-M, Peroutka SJ, Kobilka BK *Mol. Pharmacol.* 1992, **41**, 695-698.

110 Oksenberg D, Marsters SA, O'Dowd BF, Jin H, Havlik S, Peroutka SJ, Ashkenazi A *Nature* 1992, **360**, 161-163.

111 Metcalf MA, McGuffin RW, Hamblin MW *Biochemical Pharmacology* 1992, **44**, 1917-1920.

112 Parker EM, Grisel DA, Iben LG, Shapiro RA *J. Neurochem.* 1993, **60**, 380-383.

113 Adham N, Tamm JA, Salon JA, Vaysse J-J, Weinshank RL, Branchek TA *Neuropharmacology* 1994, **33**, 387-391.

114 Chanda PK, Minchin MCW, Davis AR, Greenberg L, Reilly Y, McGregor WH, Bhat R, Lubeck MD, Mizutani S, Hung PP *Mol. Pharmacol.* 1993, **43**, 516-520.

115 Buck F, Meyerhof W, Werr H, Richter D *Biochem. Biophys. Res. Comm.* 1991, **178**, 1421-1428.

116 Choudhary MS, Craigo S, Roth BL *Mol. Pharmacol.* 1992, **42**, 627-633.

117 Branchek T *Med. Chem. Res.* 1993, **3**, 287-296.

118 Roth BL, Choudhary MS, Craigo S *Med. Chem. Res.* 1993, **3**, 297-305.

119 Henderson R, Baldwin JM, Ceska TA, Zemlin F, Beckmann E, Downing KH *J. Mol. Biol.* 1990, **213**, 899-929.

120 Henderson R, Schertler GFX *Phil. Trans. R. Soc. Lond.* 1990, **B 326**, 379-389.

121 Schertler GFX, Villa C, Henderson R *Nature* 1993, **362**, 770-772.

122 Baldwin JM *EMBO J.* 1993, **12**, 1693-1703.

123 Hoflack J, Trumpp-Kallmeyer S, Hibert M *TiPS* 1994, **15**, 7-9.

124 Unger VM, Schertler GFX *Biophysical. J.* 1995, **68**, 1776-1786.

125 Schertler GFX, Hargrave PA *Proc. Natl. Acad. Sci. USA* 1995, **92**, 11578-11582.

126 Grigorieff N, Ceska TA, Downing KH, Baldwin JM, Henderson R *J. Mol. Biol.* 1996, **259**, 393-421.

127 Kyte J, Doolittle RF *J. Mol. Biol.* 1982, **157**, 105.

128 Ijzerman AP, van Vlijmen HWTh *J. Computer-Aided Molecular Design* 1988, **2**, 43-53.

129 van Vlijmen HWTh, Ijzerman AP *J. Computer-Aided Molecular Design* 1989, **3**, 165-174.

130 Mitchell TJ, Tute MS, Webb GA *J. Computer-Aided Molecular Design* 1989, **3**, 211-223.

131 Venter JC, Fraser CM, Kerlavage AR, Buck MA *Biochemical Pharmacology* 1989, **38**, 1197-1208.

132 Attwood TK, Eliopoulos EE, Findlay JBC *Gene* 1991, **96**, 153-159.

133 Findlay J, Eliopoulos E *TiPS* 1990, **11**, 492-499.

134 Findlay JBC, Donnelly D *In GTPases in Biology II*, Springer Verlag 1994, 17-31.

135 Findlay JBC, Donnelly D, Bhogal N, Hurrell C, Attwood TK *Biochem. Soc. Trans.* 1993, **21**, 869-873.

136 Attwood TK, Findlay JBC *Protein Engineering* 1993, **6**, 167-176.

137 Donnelly D, Overington JP, Ruffle SV, Nugent JHA, Blundell TL *Protein Science* 1993, **2**, 55-70.

138 Attwood TK, Findlay JBC *Protein Engineering* 1994, **7**, 195-203.

139 Donnelly D, Findlay JBC, Blundell TL *Receptors and Channels* 1994, **2**, 61-78.

140 Donnelly D, Cogdell RJ *Protein Engineering* 1993, **6**, 629-635.

141 Bhogal N, Donnelly D, Findlay JBC *J. Biol. Chem.* 1994, **269**, 27269-27274.

142 Donnelly D, Findlay JBC *Current Opinion in Structural Biology* 1994, **4**, 582-589.

143 Saunders J, Findlay JBC *Biochem. Soc. Symp.* 1990, **57**, 81-90.

144 Saunders J *Drug Design and Discovery* 1993, **9**, 213-220.

145 Dahl SG, Edvardsen Ø, Sylte I *Eur. J. Pharmacol.* 1990, **183**, 14.

146 Dahl SG, Edvardsen Ø, Sylte I *Proc. Natl. Acad. Sci. USA* 1991, **88**, 8111-8115.

147 Dahl SG, Edvardsen Ø, Sylte I *Therapie* 1991, **46**, 453-459.

148 Edvardsen Ø, Sylte I, Dahl SG *Mol. Brain Res.* 1992, **14**, 166-178.

149 Sylte I, Edvardsen Ø, Dahl SG *Protein Engineering* 1993, **6**, 691-700.

150 Kristiansen K, Edvardsen Ø, Dahl SG *Med. Chem. Res.* 1993, **3**, 370-385.

151 Sylte I, Edvardsen Ø, Dahl SG *Protein Engineering* 1996, **9**, 149-160.

152 Kristiansen K, Dahl SG *Eur. J. Pharmacol.* 1996, **306**, 195-210.

153 Trumpp-Kallmeyer S, Bruinvels A, Hoflack J, Hibert M *Neurochem. Int.* 1991, **19**, 397-406.

154 Hibert MF, Trumpp-Kallmeyer S, Bruinvels A, Hoflack J *Mol. Pharmacol.* 1991, **40**, 8-15.

155 Hibert MF, Trumpp-Kallmeyer S, Bruinvels AT, Hoflack J *Therapie* 1991, **46**, 445-451.

156 Trumpp-Kallmeyer S, Hoflack J, Bruinvels A, Hibert M *J. Med. Chem.* 1992, **35**, 3448-3462.

157 Hibert MF, Hoflack J, Trumpp-Kallmeyer S, Bruinvels AT *Médicine/Sciences* 1993, **9**, 31-40.

158 Hibert MF, Trumpp-Kallmeyer S, Hoflack J, Bruinvels A *TiPS* 1993, **14**, 7-12.

159 Huggins JP, Trumpp-Kallmeyer S, Hibert MF, Hoflack JM, Fanger BO, Jones CR *Eur. J. Pharmacol. (Mol. Pharmacol. Sect.)* 1993, **245**, 203-214.

160 Trumpp-Kallmeyer S, Hoflack J, Hibert M *In The Tachykinin Receptors,* Ed Buck SH, Humana Press 1994, 237-255.

161 Hoflack J, Hibert MF, Trumpp-Kallmeyer S, Bidart J-M *Drug Design and Discovery* 1993, **10**, 157-171.

162 Hoflack J, Trumpp-Kallmeyer S, Hibert M *In 3D QSAR in Drug Design,* Ed Kubinyi H, ESCOM 1993, 355-372.

163 Hibert M, Hoflack J, Trumpp-Kallmeyer S, Paquet J-L, Leppik R, Barberis C, Mouillac B, Chini B, Jard S *Eur. J. Med. Chem.* 1995, **30**, 189s-199s.

164 Chini B, Mouillac B, Ala Y, Balestre M-N, Trumpp-Kallmeyer S, Hoflack J, Elands J, Hibert M, Manning M, Jard S, Barberis C *EMBO J.* 1995, **14**, 2176-2182.

165 Mouillac B, Chini B, Balestre M-N, Elands J, Trumpp-Kallmeyer S, Hoflack J, Hibert M, Jard S, Barberis C *J. Biol. Chem.* 1995, **270**, 25771-25777.

166 Westkaemper RB, Glennon RA *Phamacol. Biochem. Behavior* 1991, **40**, 1019-1031.

167 Glennon RA, Westkaemper RB *In Trends in Receptor Research,* Ed Angeli P, Gulini U, Quaglia W, Elsevier 1992, 185-207.

168 Westkaemper RB, Glennon RA *Med. Chem. Res.* 1993, **3**, 317-334.

169 Westkaemper RB, Glennon RA *In Hallucinogens: An Update,* US Government Print Office 1994, 263-283.

170 Choudhary MS, Sachs N, Uluer A, Glennon RA, Westkaemper RB, Roth BL *Mol. Pharmacol.* 1995, **47**, 450-457.

171 Glennon RA, Westkaemper RB *Drug News and Perspectives* 1993, **6**, 390-405.

172 Glennon RA, Dukat M, Westkaemper RB, Ismaiel AM, Izzarelli DG, Parker EM *Mol. Pharmacol.* 1996, **49**, 198-206.

173 Smolyar A, Osman R *Mol. Pharmacol.* 1993, **44**, 882-885.

174 Perlman JH, Laakkonen L, Osman R, Gershengorn MC *J. Biol. Chem.* 1994, **269**, 23383-23386.

175 Perlman JH, Laakkonen L, Osman R, Gershengorn MC *Mol. Pharmacol.* 1995, **47**, 480-484.

176 Perlman JH, Laakkonen LJ, Guarnieri F, Osman R, Gershengorn MC *Biochemistry* 1996, **35**, 7643-7650.

177 Laakkonen LJ, Guarnieri F, Perlman JH, Gershengorn MC, Osman R *Biochemistry* 1996, **35**, 7651-7663.

178 Nordvall G, Hacksell U *J. Med. Chem.* 1993, **36**, 967-976.

179 Malmberg Å, Nordvall G, Johansson AM, Mohell N, Hacksell U *Mol. Pharmacol.* 1994, **46**, 299-312.

180 Hedberg MH, Johansson AM, Nordvall G, Yliniemelä A, Li HB, Martin AR, Hjorth S, Unelius L, Sundell S, Hacksell U *J. Med. Chem.* 1995, **38**, 647-658.

181 Kask K, Berthold M, Kahl U, Nordvall G, Bartfai T *EMBO J.* 1996, **15**, 236-244.

182 Weinstein H, Osman R *Neuropsychopharmacology* 1990, **3**, 397-409.

183 Pardo L, Ballesteros JA, Osman R, Weinstein H *Proc. Natl. Acad. Sci. USA* 1992, **89**, 4009-4012.

184 Ballesteros JA, Weinstein H *Biophysical J.* 1992, **62**, 107-109.

185 Zhang D, Weinstein H *J. Med. Chem.* 1993, **36**, 934-938.

186 Zhang D, Weinstein H *Med. Chem. Res.* 1993, **3**, 357-369.

187 Luo X, Zhang D, Weinstein H *Protein Engineering* 1994, **7**, 1441-1448.

188 Sealfon SC, Chi L, Ebersole BJ, Rodic V, Zhang D, Ballesteros JA, Weinstein H *J. Biol. Chem.* 1995, **270**, 16683-16688.

189 Almaula N, Ebersole BJ, Zhang D, Weinstein H, Sealfon SC *J. Biol. Chem.* 1996, **271**, 14672-14675.

190 Almaula N, Ebersole BJ, Ballesteros JA, Weinstein H Sealfon SC *Mol. Pharmacol.* 1996, **50**, 34-42.

191 Zhou W, Flanagan C, Ballesteros JA, Konvicka K, Davidson JS, Weinstein H, Millar RP, Sealfon SC *Mol. Pharmacol.* 1994, **45**, 165-170.

192 Zhou W, Rodic V, Kitanovic S, Flanagan CA, Chi L, Weinstein H, Maayani S, Millar RP, Sealfon SC *J. Biol. Chem.* 1995, **270**, 18853-18857.

193 Bramblett RD, Panu AM, Ballesteros JA, Reggio PH *Life Sciences* 1995, **56**, 1971-1982.

194 Ballesteros JA, Weinstein H *In Methods in Neurosciences,* Ed Sealfon SC, Academic Press 1995, **25**, 366-428.

195 Taylor EW, Agarwal A *FEBS Lett.* 1993, **325**, 161-166.

196 Agarwal A PhD Thesis, University Georgia, Athens, USA 1993.

197 Moereels H, Janssen PAJ *Med. Chem. Res.* 1993, **3**, 335-343.

198 Moereels H, Leysen JE *Receptors and Channels* 1993, **1**, 89-97.

199 Dijkstra GDH, Tulp MThM, Hermkens PHH, van Maarseveen JH, Scheeren HW, Kruse CG *Rec. Trav. Chim. Pays-Bas* 1993, **112**, 131-136.

200 Kuipers W, van Wijngaarden I, Ijzerman AP *Drug Design and Discovery* 1994, **11**, 231-249.

201 Kuipers W, van Wijngaarden I, Kruse CG, Amstel MTHV, Tulp MThM, Ijzerman AP *J. Med. Chem.* 1995, **38**, 1942-1954.

202 Höltje H-D, Briem H *In QSAR: Rational Approaches to the Design of Bioactive Compounds,* Ed Silipo C, Vittoria A, Elsevier 1991, 245-252.

203 Höltje H-D, Jendretzki UK *Arch. Pharm. (Weinheim)* 1995, **328**, 577-584.

204 Rippmann F, Boettcher H *7TM* 1993, **1**.

205 Rippmann F *7TM* 1994, **4**.

206 Rippmann F *In Membrane Protein Models,* Ed Findlay JBC, Bios 1996, 91-104.

207 Kuipers W, Oliveira L, Paiva ACM, Rippmann F, Sander C, Vriend G, Ijzerman AP *In Membrane Protein Models,* Ed Findlay JBC, Bios 1996, 27-45.

208 MaloneyHuss K, Lybrand TP *J. Mol. Biol.* 1992, **225**, 859-871.

209 Lybrand TP *In Membrane Protein Models,* Ed Findlay JBC, Bios 1996, 145-159.

210 Kontoyianni M, Lybrand TP *Med. Chem. Res.* 1993, **3**, 407-418.

211 Kontoyianni M, Lybrand TP *Perspectives in Drug Discovery and Design* 1993, **1**, 291-300.

212 Cronet P, Sander C, Vriend G *Protein Engineering* 1993, **6**, 59-64.

213 Oliveira L, Paiva ACM, Vriend G *J. Computer-Aided Molecular Design* 1993, **7**, 649-658.

214 For details of the "7TM" database e-mail the message "HELP" to TM7@EMBL-Heidelberg.DE

215 Oliveira L, Paiva ACM, Sander C, Vriend G *TiPS* 1994, **15**, 170-172.

216 Vriend G *7TM* 1993, **3**.

217 Grötzinger J, Engels M, Jacoby E, Wollmer A, Straßburger W *Protein Engineering* 1991, **4**, 767-771.

218 Röper D, Jacoby E, Krüger P, Engels M, Grötzinger J, Wollmer A, Straßburger W *J. Receptor Research* 1994, **14**, 167-186.

219 Röper D, Krüger P, Grötzinger J, Wollmer A, Straßburger W *Receptors and Channels* 1995, **3**, 97-106.

220 Benedetti PGD, Menziani MC, Fanelli F, Cocchi M *J. Mol. Struct. (Theochem)* 1993, **285**, 147-153.

221 Fanelli F, Menziani MC, Carotti A, Benedetti PGD *Bioorganic & Medicinal Chemistry* 1994, **2**, 195-211.

222 Fanelli F, Menziani MC, Cocchi M, Leonardi A, Benedetti PGD *J. Mol. Struct. (Theochem)* 1994, **314**, 265-276.

223 Fanelli F, Menziani MC, Cocchi M, Benedetti PGD *J. Mol. Struct. (Theochem)* 1995, **333**, 49-69.

224 Fanelli F, Menziani MC, Benedetti PGD *Bioorganic & Medicinal Chemistry* 1995, **3**, 1465-1477.

225 Fanelli F, Menziani MC, Benedetti PGD *Protein Engineering* 1995, **8**, 557-564.

226 Hutchins C *Endocrine J.* 1994, **2**, 7-23.

227 Herzyk P, Hubbard RE *Biophysical J.* 1995, **69**, 2419-2442.

228 Blaney FE, Tennant M *In Membrane Protein Models,* Ed Findlay JBC, Bios 1996, 161-176.

229 Ijzerman AP, van Galen PJM, Jacobson KA *Drug Design and Discovery* 1992, **9**, 49-67.

230 Ijzerman AP, van der Wenden EM, van Galen PJM, Jacobson KA *Eur. J. Pharmacol. (Mol. Pharmacol. Sect.)* 1994, **268**, 95-104.

231 van Galen PJM, van Bergen AH, Gallo-Rodriguez C, Melman N, Olah ME, Ijzerman AP, Stiles GL, Jacobson KA *Mol. Pharmacol.* 1994, **45**, 1101-1111.

232 Dudley MW, Peet NP, Demeter DA, Weintraub HJR, Ijzerman AP, Nordvall G, van Galen PJM, Jacobson KA *Drug Dev. Res.* 1993, **28**, 237-243.

233 Alkorta I, Du P *Protein Engineering* 1994, **7**, 1231-1238.

234 Mirzadegan T, Humblet C, Ripka WC, Colmenares LU, Liu RSH *Photochemistry and Photobiology* 1992, **56**, 883-893.

235 Mirzadegan T, Liu RSH *Prog. Retinal Res.* 1992, **11**, 57-74.

236 Lewell XQ *Drug Design and Discovery* 1992, **9**, 29-48.

237 Strosberg AD, Camoin L, Blin N, Maigret B *Drug Design and Discovery* 1993, **9**, 199-211.

238 Yamamoto Y, Kamiya K, Terao S *J. Med. Chem.* 1993, **36**, 820-825.

239 Livingstone CD, Strange PG, Naylor LH *Biochem. J.* 1992, **287**, 277-282.

240 Teeter MM, Froimowitz M, Stec B, DuRand CJ *J. Med. Chem.* 1994, **37**, 2874-2888.

241 Singer MS, Shepherd GM *NeuroReport* 1994, **5**, 1297-1300.

242 Timms D, Wilkinson AJ, Kelly DR, Broadley KJ, Davies RH *Int. J. Quantum Chem.: Quantum Biol. Symp.* 1992, **19**, 197-215.

243 Brann MR, Klimkowski VJ, Ellis J *Life Sciences* 1993, **52**, 405-412.

244 Kyle DJ, Chakravarty S, Sinsko JA, Stormann TM *J. Med. Chem.* 1994, **37**, 1347-1354.

245 Underwood DJ, Strader CD, Rivero R, Patchett AA, Greenlee W, Prendergast K *Chemistry and Biology* 1994, **1**, 211-221.

246 Mahmoudian M *J. Mol. Graphics* 1994, **12**, 22-28.

247 Schwartz TW, Hjorth SA, Elling C, Nielsen SM, Gether U, Rosenkilde MM, Zoffmann S, den Hollander R, Schambye HT, Perlmann S, van Vijk B *Eur. J. Pharmaceutical Sciences* 1994, **2**, 85-87.

248 Schwartz TW, Rosenkilde MM *TiPS* 1996, **17**, 213-216.

249 Dunn AD, Norrie R *J. Prakt. Chem.* 1992, **334**, 483-486.

250 Bremner DH, Dunn AD, Wilson KA *Synthesis* 1992, 528-530.

251 Wilson KA PhD Thesis, Dundee Institute of Technology 1993.

252 King FD *In Medicinal Chemistry Principles and Practice,* Ed King FD, Royal Society of Chemistry 1994, 206-225.

253 Cannon JG *In Burgers Medicinal Chemistry and Drug Discovery,* Ed Wolff ME, Wiley 1995, **1**, 783-802.

254 Martin-Smith M, Reid ST *J. Medicinal and Pharmaceutical Chemistry* 1959, **1**, 507-564.

255 Nobles WL, Blanton CD *J. Pharmaceutical Sciences* 1964, **53**, 115-129.

256 Chakrabarti JK, Horsman L, Hotten TM, Pullar IA, Tupper DE, Wright FC *J. Med. Chem.* 1980, **23**, 878-884.

257 Ward TJ *Current Opinion in Therapeutic Patents* 1993, 417-423.

258 Wishart G, Ringan NS Unpublished Results.

259 Pailer M, Jiresch W *Monatshefte für Chemie* 1969, **100**, 121-131.

260 Steinkopf W, Lützkendorf G *Chemiker-Zeitung* 1912, **36**, 379.

261 Steinkopf W, Lützkendorf G *Justus Liebigs Ann. Chem.* 1914, 45-49.

262 Schneller SW *Int. J. Sulfur Chem.* 1972, **B7**, 309-317.

263 Barker JM *Adv. Heterocycl. Chem.* 1977, **21**, 65-118.

264 Klemm LH *Heterocycles* 1981, **15**, 1285-1308.

265 Paronikyan EG, Noravyan AS, Vartanyan SA *Khim.-Farm. Zh.* 1987, **21**, 536-545.

266 Zhiryakov VG, Abramenko PI *Zh. Vsesoyuz. Obshch. D.T. Mendeleeva* 1960, **5**, 707-708.

267 Klemm LH, Klopfenstein CE, Zell R, McCoy DR, Klemm RA *J. Org. Chem.* 1969, **34**, 347-354.

268 Emerson WS, Holly FW, Klemm LH *J. Am. Chem. Soc.* 1941, **63**, 2569-2570.

269 Abramenko PI *Khim. Geterotsikl. Soedin.* 1971, **7**, 468-470.

270 Zhiryakov VG, Abramenko PI *Khim. Geterotsikl. Soedin.* 1965, **1**, 334-341.

271 Benoit R, Duflos J, Dupas G, Bourguignon J, Queguiner G *J. Heterocyclic Chem.* 1989, **26**, 1595-1600.

272 Benoit R, Dupas G, Bourguignon J, Queguiner G *Synthesis* 1987, 1124-1126.

273 Raich WJ, Hamilton CS *J. Am. Chem. Soc.* 1957, **79**, 3800-3804.

274 Corral C, Madroñero R, Ulecia N *Afinidad* 1978, **35**, 129-133.

275 Shvedov VI, Kharizomenova IA, Grinev AN *Khim. Geterotsikl. Soedin.* 1974, **10**, 58-60.

276 Shvedov VI, Kharizomenova IA, Grinev AN USSR Patent 364613, 1973.

277 Schäfer H, Gewald K, Hartmann H *J. Prakt. Chem.* 1974, **316**, 169-172.

278 Schäfer H, Bartho B, Gewald K *Z. Chem.* 1973, **13**, 294.

279 Rajappa S, Advani BG *Indian J. Chem.* 1974, **12**, 1-3.

280 Biere H, Seelen W *Liebigs Ann. Chem.* 1976, 1972-1981.

281 Pedersen EB, Carlsen D *Tetrahedron* 1977, **33**, 2089-2092.

282 Lalezari I *J. Heterocyclic Chem.* 1979, **16**, 603-604.

283 Barker JM, Huddleston PR, Holmes D *J. Chem. Res. M* 1985, 2501-2523.

284 Khan MA, Guarçoni AE *J. Heterocyclic Chem.* 1977, **14**, 807-812.

285 Gilis PM, Haemers A, Bollaert W *Eur. J. Med. Chem.* 1978, **13**, 265-269.

286 Gilis PM, Haemers A, Bollaert W *Eur. J. Med. Chem.* 1980, **15**, 185-188.

287 Gewald K, Schäfer H, Sattler K *Monatshefte für Chemie* 1979, **110**, 1189-1196.

288 Meth-Cohn O, Narine B *Tet. Lett.* 1978, **23**, 2045-2048.

289 Meth-Cohn O, Narine B, Tarnowski B *J. Chem. Soc. Perkin 1* 1981, 1531-1536.

290 Meth-Cohn O *Heterocycles* 1993, **35**, 539-557.

291 Koenigs E, Geisler H *Ber.* 1924, **57B**, 2076-2079.

292 Chichibabin AE, Woroshtzow NN *Ber.* 1933, **66B**, 364-372.

293 Duffin GF, Kendall JD *J. Chem. Soc.* 1951, 734-739.

294 Schneller SW, Clough FW *J. Heterocyclic Chem.* 1974, **11**, 975-977.

295 Schneller SW, Clough FW *Heterocycles* 1975, **3**, 135-138.

296 Beugelmans R, Bois-Choussy M, Boudet B *Tetrahedron* 1983, **39**, 4153-4161.

297 Niess R, Eilingsfeld H West German Patent 2241 717, 1974.

298 Quintela JM, Soto JL *Anales de Quimica* 1984, **80**, 268-272.

299 Shvedov VI, Sycheva TP, Sakovich TV *Khim. Geterotsikl. Soedin.* 1979, **10**, 1331-1335.

300 Gewald K, Hentschel M, Illgen U *J. Prakt. Chem.* 1974, **316**, 1030-1036.

301 Tornetta B, Guerrera F, Ronsisvalle G *Annali di Chimica* 1974, **64**, 833-842.

302 Guerrera F, Siracusa MA, Tornetta B *Farmaco.-Ed. Sc.* 1976, **31**, 21-30.

303 Youssefyeh RD, Brown RE, Wilson J, Shah U, Jones H, Loev B, Khandwala A, Leibowitz MJ, Sonnino-Goldman P *J. Med. Chem.* 1984, **27**, 1639-1643.

304 Hassan KHM, El-Dean AMK, Youssef MSK, Atta FM, Abbady MS *Phosphorus, Sulfur and Silicon* 1990, **47**, 283-289.

305 Attaby FA, Ibrahim LI, Eldin SM, El-Louh AKK *Phosphorus, Sulfur and Silicon* 1992, **73**, 127-135.

306 El-Dean AMK *Phosphorus, Sulfur and Silicon* 1994, **90**, 85-93.

307 Martani A, Fravolini A, Schiaffella F, Orzalesi G, Selleri R, Volpato I *Boll. Chim. Farm.* 1975, **114**, 590-597.

308 Krauze AA, Bomika ZA, Shestopalov AM, Rodinovskaya LA, Pelcher YuÉ, Dubur GYa, Sharanin YuA, Promonenkov VK *Khim. Geterotsikl. Soedin.* 1981, **3**, 377-382.

309 Sharanin YuA, Promonenkov VK, Shestopalov AM *Zh. Org. Khim.* 1982, **18**, 630-640.

310 Litvinov VP, Sharanin YuA, Rodinovskaya LA, Shestopalov AM, Mortikov VYu, Promonenkov VK *Izv. Akad. Nauk SSSR Ser. Khim.* 1984, **12**, 2760-2765.

311 Sharanin YuA, Shestopalov AM, Promonenkov VK *Zh. Org. Khim.* 1984, **20**, 2012-2020.

312 Shestopalov AM, Promonenkov VK, Sharanin YuA, Rodinovskaya LA, Sharanin SYu *Zh. Org. Khim.* 1984, **20**, 1517-1538.

313 Rodinovskaya LA, Promonenkov VK, Sharanin YuA, Shvedov VI, Shestopalov AM, Litvinov VP, Mortikov VYu *Zh. Org. Khim.* 1985, **21**, 1578-1580.

314 Shestopalov AM, Sharanin YuA *Zh. Org. Khim.* 1984, **20**, 1991-2002.

315 Sharanin YuA, Shestopalov AM *Zh. Org. Khim.* 1984, **20**, 1539-1553.

316 Litvinov VP, Apyonova YeA, Sharanin YuA, Bogdanov VS, Nefedov OM *Sulfur Letters* 1985, **3**, 107-116.

317 Sharanin YuA, Shestopalov AM, Mortikov VYu, Melenchuk SN, Promonenkov VK, Zolotarev BM, Litvinov VP *Izv. Akad. Nauk SSSR Ser. Khim.* 1986, **1**, 153-159.

318 Nesterov VN, Rodinovskaya LA, Litvinov VP, Sharanin YuA, Shestopalov AM, Mortikov VYu, Shvedov VI, Shklover VE, Struchkov YuT *Izv. Akad. Nauk SSSR Ser. Khim.* 1988, **1**, 140-145.

319 Rodinovskaya LA, Sharanin YuA, Shestopalov AM, Litvinov VP *Khim. Geterotsikl. Soedin.* 1988, **6**, 805-812.

320 Litvinov VP, Sharanin YuA, Rodinovskaya LA, Nesterov VN, Shklover VE, Struchkov YuT *Chemica Scripta* 1989, **29**, 327-332.

321 Klokol GV, Sharanin YuA, Promonenkov VK, Litvinov VP, Bogdanov VS, Nesterov VN, Shklover VE, Struchkov YuT, Kamernitskii AV *Zh. Org. Khim.* 1989, **25**, 1788-1798.

322 Sharanin YuA, Goncharenko MP, Shestopalov AM, Litvinov VP, Turov AV *Zh. Org. Khim.* 1991, **27**, 1996-2008.

323 Sharanin YuA, Shestopalov AM, Litvinov VP, Klokol GV, Mortikov VYu, Demerkov AS *Zh. Org. Khim.* 1988, **24**, 854-861.

324 Krauze AA, Liepin'sh ÉÉ, Pelcher YuÉ, Dubur GYa *Khim. Geterotsikl. Soedin.* 1987, **1**, 124-128.

325 Gewald K, Hentschel M East German Patent 105 805, 1974.

326 Encinas MJR, Seoane C, Soto JL *Liebigs Ann. Chem.* 1984, 213-222.

327 Vieweg H, Leistner S, Wagner G *Pharmazie* 1988, **43**, 358-359.

328 Elgemeie GEH, Elfahham HA, Nabey HA *Bull. Chem. Soc. Jpn.* 1988, **61**, 4431-4433.

329 Elgemeie GEH, Ramiz MMM *Phosphorus, Sulfur and Silicon* 1989, **46**, 95-98.

330 Awad IMA, Abdel-Rahman AE, Bakhite EA *Phosphorus, Sulfur and Silicon* 1991, **61**, 305-318.

331 Hassan KHM, El-Dean AMK, Youssef MSK, Atta FM, Abbady MS *Phosphorus, Sulfur and Silicon* 1990, **47**, 181-189.

332 Briel D, Dumke S, Wagner G, Olk B *J. Chem. Res. S* 1991, 178-179.

333 Becher J, Dreier C, Frandsen EG, Wengel AS *Tetrahedron* 1978, **34**, 989-991.

334 Klemm LH, McCoy DR *J. Heterocyclic Chem.* 1969, **6**, 73-75.

335 Smith RE, Boatman S, Hauser CR *J. Org. Chem.* 1968, **33**, 2083-2085.

336 Cossey AL, Harris RLN, Huppatz JL, Phillips JN *Aust. J. Chem.* 1976, **29**, 1039-1050.

337 Lok WN, Ward AD *Aust. J. Chem.* 1978, **31**, 617-625.

338 Sakamoto T, Kondo Y, Watanabe R, Yamanaka H *Chem. Pharm. Bull.* 1986, **34**, 2719-2724.

339 Taylor EC, Macor JE *Tet. Lett.* 1985, **26**, 2419-2422.

340 Taylor EC, Macor JE *J. Org. Chem.* 1987, **52**, 4280-4287.

341 Alunni S, Clementi S, Klemm LH *J. Chem. Soc. Perkin 2* 1976, 1135-1139.

342 Klemm LH, Merrill RE, Lee FHW, Klopfenstein CE *J. Heterocyclic Chem.* 1974, **11**, 205-209.

343 Klemm LH, Zell R, Barnish IT, Klemm RA, Klopfenstein CE, McCoy DR *J. Heterocyclic Chem.* 1970, **7**, 373-379.

344 Klemm LH, Lund H *J. Heterocyclic Chem.* 1973, **10**, 871-872.

345 Barker JM, Huddleston PR, Holmes D *J. Chem. Res. M* 1986, 1063-1090.

346 Klemm LH, Zell R *J. Heterocyclic Chem.* 1968, **5**, 773-778.

347 Klemm LH, Bajer M *J. Heterocyclic Chem.* 1979, **16**, 1289-1291.

348 Meth-Cohn O, Narine B, Tarnowski B, Hayes R, Keyzad A, Rhouati S, Robinson A *J. Chem. Soc. Perkin 1* 1981, 2509-2517.

349 Klemm LH, Merrill RE *J. Heterocyclic Chem.* 1974, **11**, 355-361.

350 Klemm LH, Barnish IT, Zell R *J. Heterocyclic Chem.* 1970, **7**, 81-89.

351 Klemm LH, Lu JJ, Greene DS, Boisvert W *J. Heterocyclic Chem.* 1987, **24**, 1467-1472.

352 Klemm LH, Muchiri DR, Anderson M, Salbador W, Ford J *J. Heterocyclic Chem.* 1994, **31**, 261-263.

353 Klemm LH, Wang J, Sur SK *J. Heterocyclic Chem.* 1990, **27**, 1537-1541.

354 Klemm LH, Mathur SB, Zell R, Merrill RE *J. Heterocyclic Chem.* 1971, **8**, 931-935.

355 Klemm LH, Merrill RE *J. Heterocyclic Chem.* 1972, **9**, 293-298.

356 Klemm LH, Hartling R *J. Heterocyclic Chem.* 1976, **13**, 1197-1200.

357 Klemm LH, Muchiri DR *J. Heterocyclic Chem.* 1983, **20**, 213-217.

358 Klemm LH, Muchiri DR, Louris JN *J. Heterocyclic Chem.* 1984, **21**, 1135-1140.

359 Klemm LH, Sur SK, Louris JN, Tran LK, Yee S, Hamilton SR *J. Heterocyclic Chem.* 1990, **27**, 1721-1725.

360 Klemm LH, Hsin W *J. Heterocyclic Chem.* 1975, **12**, 1183-1186.

361 Schneller SW, Clough FW, Hardee LE *J. Heterocyclic Chem.* 1976, **13**, 273-275.

362 Tsuchiya T, Enkaku M, Okajima S *Chem. Pharm. Bull.* 1981, **29**, 3173-3180.

363 Bruno JJ, Molony BA *In New Drugs Annual: Cardiovascular Drugs,* Ed Scriabine A, Raven 1983, 295-316.

364 Bruno JJ *Thrombosis Research* 1983, Suppl 4, 59-67.

365 Savi P, Herbert JM, Pflieger AM, Dol F, Delebassee D, Combalbert J, Defreyn G, Maffrand JP *Biochemical Pharmacology* 1992, **44**, 527-532.

366 Schrör K *Drugs* 1995, **50**, 7-28.

367 Andersen PH, Nielsen EB, Scheel-Krüger J, Jansen JA, Hohlweg R *Eur. J. Pharmacol.* 1987, **137**, 291-292.

368 Andersen PH, Jansen JA *Eur. J. Pharmacol. (Mol. Pharmacol. Sect.)* 1990, **188**, 335-347.

369 Schneider CS, Weber KH, Daniel H, Bechtel WD, Boeke-Kuhn K *J. Med. Chem.* 1984, **27**, 1150-1155.

370 New JS, Christopher WL, Yevich JP, Butler R, Schlemmer RF, VanderMaelen CP, Cipollina JA *J. Med. Chem.* 1989, **32**, 1147-1156.

371 Labelle M, Gareau Y, Dufresne C, Lau CK, Belley M, Jones TR, Leblanc Y, McAuliffe M, McFarlane CS, Metters KM, Ouimet N, Perrier H, Rochette C, Sawyer N, Slipetz D, Xiang YB, Wang Z, Pickett CB, Ford-Hutchinson AW, Young RN, Zamboni RJ *Bioorg. Med. Chem. Lett.* 1995, **5**, 2551-2556.

372 Hamblin MW, Metcalf MA *Mol. Pharmacol.* 1991, **40**, 143-148.

373 Hamblin MW, Metcalf MA, McGuffin RW, Karpells S *Biochem. Biophys. Res. Comm.* 1992, **184**, 752-759.

374 Levy FO, Gudermann T, Perez-Reyes E, Birnbaumer M, Kaumann AJ, Birnbaumer L *J. Biol. Chem.* 1992, **267**, 7553-7562.

375 Mochizuki D, Yuyama Y, Tsujita R, Komaki H, Sagai H *Biochem. Biophys. Res. Comm.* 1992, **185**, 517-523.

376 Levy FO, Gudermann T, Birnbaumer M, Kaumann AJ, Birnbaumer L *FEBS Lett.* 1992, **296**, 201-206.

377 Zgombick JM, Schechter LE, Macchi M, Hartig PR, Branchek TA, Weinshank RL *Mol. Pharmacol.* 1992, **42**, 180-185.

378 McAllister G, Charlesworth A, Snodin C, Beer MS, Noble AJ, Middlemiss DN, Iversen LL, Whiting P *Proc. Natl. Acad. Sci. USA* 1992, **89**, 5517-5521.

379 Adham N, Kao H-T, Schechter LE, Bard J, Olsen M, Urquhart D, Durkin M, Hartig PR, Weinshank RL, Branchek TA *Proc. Natl. Acad. Sci. USA* 1993, **90**, 408-412.

380 Saltzman AG, Morse B, Whitman MM, Ivanshchenko Y, Jaye M, Felder S *Biochem. Biophys. Res. Comm.* 1991, **181**, 1469-1478.

381 InsightII Version 2.3.0, Biosym/MSI 9685 Scranton Road, San Diego, CA 92121-2777.

382 Dayhoff MO, Schwartz RM, Orcutt BC *In Atlas of Protein Sequence and Structure,* Ed Dayhoff MO, Washington: Nat. Biomed. Res. Found 1978, **5**, Suppl 3, 342-354.

383 Devereux J, Haeberli P, Smithies O *Nucleic Acids Res.* 1984, **12**, 387-395, as implemented in the GCG software at University of Wisconsin, Biotechnology Center, 1710 University Ave., Madison, Wisconsin 53705.

384 von Heijne G *J. Mol. Biol.* 1991, **218**, 499-503.

385 Polinsky A, Goodman M, Williams KA, Deber CM *Biopolymers* 1992, **32**, 399-406.

386 Dauber-Osguthorpe P, Roberts VA, Osguthorpe DJ, Wolff J, Genest M, Hagler AT *Proteins: Structure Function and Genetics* 1988, **4**, 31-47.

387 Discover Version 2.9.5, Biosym/MSI 9685 Scranton Road, San Diego, CA 92121-2777, USA.

388 Arvidsson L-E, Hacksell U, Nilsson JLG, Hjorth S, Carlsson A, Lindberg P, Sanchez D, Wikström H *J. Med. Chem.* 1981, **24**, 921-923.

389 Middlemiss DN, Fozard JR *Eur. J. Pharmacol.* 1983, **90**, 151-153.

390 Cornfield LJ, Lambert G, Arvidsson L-E, Mellin C, Vallgårda J, Hacksell U, Nelson DL *Mol. Pharmacol.* 1991, **39**, 780-787.

391 Van Wijngaarden I, Tulp MThM, Soudijn W *Eur. J. Pharmacol. (Mol. Pharmacol. Sect.)* 1990, **188**, 301-312.

392 Glennon RA, Peroutka SJ, Dukat M *In Serotonin: Molecular Biology, Receptors and Functional Effects,* Ed Fozard JR, Saxena PR, Birkhäuser 1991, 186-191.

393 Karlsson A, Pettersson C, Sundell S, Arvidsson L-E, Hacksell U *Acta Chem. Scand.* 1988, **B 42**, 231-236.

394 Johansson AM, Nilsson JLG, Karlén A, Hacksell U, Sanchez D, Svensson K, Hjorth S, Carlsson A, Sundell S, Kenne L *J. Med. Chem.* 1987, **30**, 1827-1837.

395 Ludi Version 2.3 Biosym/MSI 9685 Scranton Road, San Diego, CA 92121-2777, USA.

396 Verdonk ML, Boks GJ, Kooijman H, Kanters JA, Kroon J *J. Computer-Aided Molecular Design* 1993, **7**, 173-182.

397 Probst WC, Snyder LA, Schuster DI, Brosius J, Sealfon SC *DNA and Cell Biology* 1992, **11**, 1-20.

398 Glennon RA *Drug Dev. Res.* 1992, **26**, 251-274.

399 Macor JE, Newman ME *Tet. Lett.* 1991, **32**, 3345-3348.

400 Macor JE, Fox CB, Johnson C, Koe BK, Lebel LA, Zorn SH *J. Med. Chem.* 1992, **35**, 3625-3632.

401 Nelson DL *Phamacol. Biochem. Behavior* 1991, **40**, 1041-1051.

402 Sturrock KR, Bremner DH Unpublished Results.

403 Brougham P, Cooper MS, Cummerson DA, Heaney H, Thompson N *Synthesis* 1987, 1015-1016.

404 Tan R, Taurins A *Tet. Lett.* 1965, **31**, 2737-2744.

405 Katz RB, Mitchell MB, Sammes PG *Tetrahedron* 1989, **45**, 1801-1814.

406 Davis R, Untch KG *J. Org. Chem.* 1981, **46**, 2987-2988.

407 Caubère P, Coutrot P *In Comprehensive Organic Synthesis*, Pergamon 1993, **8**, 835-870.

408 Belen'kii LI *In Chemistry of Organosulfur Compounds*, Ellis Horwood 1990, 193-228.

409 Takahata H, Hara M, Tomiguchi A, Yamazaki T, Castle RN *J. Heterocyclic Chem.* 1980, **17**, 403-404.

410 Nonhebel DC *J. Chem. Soc.* 1963, 1216-1220.

411 Piechucki C *Synthesis* 1974, 869-870.

412 Villieras J, Rambaud M, Graff M *Tet. Lett.* 1985, **26**, 53-56.

413 Texier-Boullet F, Foucaud A *Synthesis* 1979, 884-885.

414 Hudlický M *Reductions in Organic Chemistry*, Ellis Horwood 1984.

415 Ram S, Spicer LD *Synthetic Comm.* 1992, **22**, 2683-2690.

416 Narisada M, Horibe I, Watanabe F, Takeda K *J. Org. Chem.* 1989, **54**, 5308-5313.

417 Olah GA, Narang SC, Gupta BGB, Malhotra R *J. Org. Chem.* 1979, **44**, 1247-1251.

418 Lwowski W *In Azides and Nitrenes*, Ed Scriven EFV, Academic Press 1984, 205-246.

419 Weinstock J *J. Org. Chem.* 1961, **26**, 3511.

420 Finkelstein J, Chiang E, Vane FM, Lee J *J. Med. Chem.* 1966, **9**, 319-323.

421 Kaiser C, Weinstock J *Organic Synthesis* 1971, **51**, 48-52.

422 Binder D, Habison G, Noe CR *Synthesis* 1977, 255-256.

423 Overman LE, Taylor GF, Petty CB, Jessup PJ *J. Org. Chem.* 1978, **43**, 2164-2167.

424 Jessup PJ, Petty CB, Roos J, Overman LE *Organic Synthesis* 1979, **59**, 1-9.

425 Wheeler TN, Ray J *J. Org. Chem.* 1987, **52**, 4875-4877.

426 Shioiri T, Ninomiya K, Yamada S *J. Am. Chem. Soc.* 1972, **94**, 6203-6205.

427 Eaton PE, Shankar BKR, Price GD, Pluth JJ, Gilbert EE, Alster J, Sandus O *J. Org. Chem.* 1984, **49**, 185-186.

428 Shishido K, Shitara E, Komatsu H, Hiroya K, Fukumoto K, Kametani T *J. Org. Chem.* 1986, **51**, 3007-3011.

429 Sanders JKM, Hunter BK *Modern NMR Spectroscopy*, Oxford University Press 1993.

430 Bailey PD, Morgan KM *Organonitrogen Chemistry*, Oxford University Press 1996.

431 de Laszlo SE, Williard PG *J. Am. Chem. Soc.* 1985, **107**, 199-203.

432 Wallis ES, Lane JF *Organic Reactions* 1946, **3**, 267-306.

433 Hibert MF Membrane Protein Models: Experiment, Theory and Speculation, Leeds UK, March 1994.

434 Still WC, Kahn M, Mitra A *J. Org. Chem.* 1978, **43**, 2923-2925.